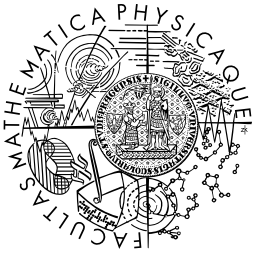

FACULTY
OF MATHEMATICS
AND PHYSICS
Charles University

DOCTORAL THESIS

Mgr. Jakub Zahumenský

Characterization of native and heterologously expressed membrane transporters in yeast using fluorescent probes

Institute of Physics of Charles University

Supervisor of the doctoral thesis:	doc. RNDr. Dana Gášková, CSc.
Study programme:	Physics
Study branch:	Biophysics, Chemical and Macromolecular Physics

Prague 2017

I declare that I carried out this doctoral thesis independently, and only with the cited sources, literature and other professional sources.

I understand that my work relates to the rights and obligations under the Act No. 121/2000 Sb., the Copyright Act, as amended, in particular the fact that the Charles University has the right to conclude a license agreement on the use of this work as a school work pursuant to Section 60 subsection 1 of the Copyright Act.

In ..... date ..... signature of the author

Title: Characterization of native and heterologously expressed membrane transporters in yeast using fluorescent probes

Author: Mgr. Jakub Zahumenský

Institute: Institute of Physics of Charles University

Supervisor: doc. RNDr. Dana Gášková, CSc., Institute of Physics of Charles University

Abstract: Yeast plasma membrane transporters play crucial roles in many cellular processes, including detoxification and build-up and maintenance of the plasma membrane potential ($\Delta\Psi$). The former development of the diS-$C_3(3)$ fluorescence assay by the Biophysics Group of the Institute of Physics, Charles University, enabled us to conveniently study both, including their changes, using a simple fluorescent probe diS-$C_3(3)$.

Many studies carried out on both animal and yeast cells have revealed that ethanol and other alcohols inhibit the functions of various membrane channels, receptors and solute transport proteins, and a direct interaction of alcohols with these membrane proteins has been proposed. Using the diS-$C_3(3)$ assay for multidrug-resistance pump inhibitors in a set of isogenic yeast *pdr5* and *snq2* deletion mutants we found that *n*-alcohols (from ethanol to hexanol) exhibit an inhibitory effect on both pumps, increasing with the length of the alcohol carbon chain. The inhibition is not connected with loss of plasma membrane structural or functional integrity and is fully reversible. This supports a notion that the inhibitory action does not necessarily involve only changes in the lipid matrix of the membrane but may entail a direct interaction of the alcohols with the pump proteins.

Tok1p is a highly specific yeast plasma membrane potassium channel with strong outward directionality. Its opening is induced by membrane depolarization. Although the biophysical properties of Tok1p are well-described, its potentially important physiological role is currently largely unexplored. We examined the Tok1p activity following chemically-induced depolarization by measuring $\Delta\Psi$ changes using the diS-$C_3(3)$ fluorescence assay and a *tok1* deletion mutant. We report that Tok1p channel opening in response to chemical stress does not depend solely on the extent of depolarization, but may also be negatively influenced by accompanying effects of the compound, e.g. interaction with plasma membrane or the channel itself, or cytosolic acidification. While ODDC-induced depolarization exhibits the cleanest Tok1p activation, restoring astonishing 75 % of lost $\Delta\Psi$, higher BAC concentrations reduce Tok1p activity.

Keywords: alcohols, diS-$C_3(3)$ fluorescence assay, membrane potential, multidrug resistance, potassium

Dedicated to Polly.

Either directly or indirectly a lot of people were involved in the path that lead me to writing my doctoral thesis. Some walked with me the whole way, some a part of it and some just crossed it somewhere in the middle. And of course, some paved parts of it before me. No matter their contribution, they are each of them very important.

First and foremost, I would like to thank my supervisor doc. RNDr. Dana Gášková, CSc. for her tremendous support and even more tremendous patience, a great deal of ideas and for never letting anything go unsolved. Apart from her importance as a guide and mentor, she also showed a huge heart and a human side that is rarely seen in supervisors. I am really lucky to have had such a great person for supervisor of both my master and doctoral thesis. My big thanks further go to my colleague Mgr. Iva Jančíková, who kept the lab running smoothly and helped with a lot of experiments and measurements crucial for this work. Also from our department, I would like to thank Prof. Mirek Plášek, CSc. for consultations, advice and contribution to the warm workplace atmosphere.

I would also like to thank Mgr. Tomáš Hendrych, PhD. for preparing the AD1-3 p_{TEF1}-YpHl mutant used in this study and for his habit of developing ways to make his life in the lab as easy as possible, which in turn made my life a lot easier (*Long live the lazy!*[1]). Tomáš was also always ready to offer advice and help when called upon, which I greatly appreciate. For preparation of the *tok1* mutant of the AD1-3 strain, I would like to thank Ing. Otakar Hlaváček, PhD. I know it was not easy, but it was definitely worth the effort.

For invaluable consultations I wish to give thanks to Ing. Karel Sigler, DrSc. His insights proved to be of great importance both in the process of interpretation of the data and designing of follow-up experiments, and in the preparation of the manuscripts of both scientific articles that form the basis of the doctoral thesis.

Furthermore, I would like to thank Prof. Dr. Milan Höfer for numerous consultations and willingness to listen to my, sometimes crazy, ideas. And of course for his never-failing support at conferences.

Last, but far from least, I wish to thank my wonderful parents who have always supported me no matter which way I chose to go, even if it was a road they would have not chosen themselves, or advised taking another. Now that this part of my way is almost concluded, I know I would have not been able to complete it without their love and support.

[1] Read: efficient.

Contents

Introduction

Every cell is divided from the surrounding area by a plasma membrane, enabling the cell to maintain different intracellular environment compared to its surroundings. This difference is essential for the existence of life. The processes taking place on/across the membrane are crucial for any living cell. These include the reception of a multitude of signals from the environment and neighbouring cells, but also transport of various compounds both in and out of the cells. The compounds transported through the membranes range from simple ions, such as hydrogen and potassium, to more complex organic molecules, such as sugars, amino acids or products of the cell's metabolism. Depending on their function and importance for the cell, the transported compounds can be divided into various categories, such as nutrients, toxic agents (both intrinsic and extrinsic) and those taking part in build-up of electrical gradients.

Living in an environment with a very complex chemical composition, cells have to defend themselves against a wide variety of potentially toxic agents. These do not necessarily originate in the environment, as the normal products of the cells metabolism can turn toxic if accumulated in higher amounts. There are also substances specifically designed to destroy cells, be it bacteria, yeast or tumour cells. Over the course of evolution, the needs of the cells to protect themselves gave rise to various defence mechanisms, including pump proteins that are able to directly export such harmful compounds out of the cells, giving rise to the phenomenon known as multidrug resistance (MDR). While being very useful for the cells themselves, the presence and activity of such proteins poses a serious problem in treatment of bacterial and yeast infections and also of cancer. The study of these proteins, and mechanisms that would enable us to inhibit them, is therefore crucial for fighting disease.

The basic laws of thermodynamics dictate that the total energy of a closed system is always conserved. It can be neither created nor destroyed, only converted to a different form. An example of such a conversion is the ATP hydrolysis-fuelled transport of protons out of the cell, creating a proton electrochemical gradient across the plasma membrane. In plants and fungi, the proton gradient (also called the proton-motive force) is a major part of the plasma membrane potential which can in turn be utilized as an energy source for the uptake of other ions and nutrients. The existence of membrane potential is tightly connected with the integrity of the plasma membrane and is essential for life. Its maintenance and regulation is therefore of primary interest to any cell.

Being the first line of cell defence, the plasma membrane is often the primary target of a wide range of chemical (and environmental) stressors. Apart from changing its properties, such as fluidity and permeability to substances (affecting both membrane potential and efficacy of drugs), the effect of such stressors may also include a change in the activity of membrane-bound enzymes, including those involved in mediating MDR as well as those responsible for the build-up and maintenance of membrane potential.

The main aim of the doctoral thesis was to study the activity of native and heterologously expressed membrane transporters involved in both multidrug resistance and membrane potential build-up and maintenance. Furthermore, we were interested in the effect of various compounds (i.e. chemical stressors) on both types of transporters. To this end, we deployed the diS-$C_3(3)$ fluorescence assay that had been developed by the Biophysics Group of the Institute of Physics, Charles University. This method had been proven to be appropriate for monitoring time-dependent changes in both membrane potential and activity of MDR pumps in response to chemical stressors. Early on into the research it became clear that the interesting phenomena we discovered in the context of the function of native transporters would deserve all of our attention and yield a great amount of interesting results. We have therefore opted to focus on the native transporters only and study their action thoroughly.

Chapter 1

Theoretical Introduction

1.1 Yeast *Saccharomyces cerevisiae* as a model eukaryotic organism

All living organisms share one important aspect - they are composed of cells, the most basic units of life. Depending on the complexity of their cells, namely the presence of a true nucleus, we distinguish between prokaryotic and eukaryotic organisms. While prokaryota are, without exception, unicellular organisms, eukaryota are predominantly, but not exclusively, multicellular complex organisms.

Among the simplest unicellular eukaryotic organisms is the baker's yeast *Saccharomyces cerevisiae* (*Phylum Ascomycota*) that has been known to the advantage of mankind for aeons and used in both baking and brewing. Being among the first discovered and isolated yeast species, it is also one of the best characterized. The yeast is non-pathogenic, easily manipulated and readily cultivated in media with wide range of pH, osmolarity and nutrient composition, exhibiting short duplication times under non-limiting nutrient conditions (ca. 2 hours). It is therefore not surprising that the yeast is widely used in industry in production of not only food and drink, but also in biotechnology, chemical industry and pharmacology, as well as in the production of biofuels (Volkov, 2015).

Adding to the list of advantages, *S. cerevisiae* is the first eukaryotic organism to have the whole genome sequenced (Cherry et al., 1997). It can exist in both diploid and haploid state and both can be exploited in very specific and relatively straightforward genetic manipulations and preparation of new mutant strains. In addition to chromosomal DNA, the yeast also contains a so-called 2 µm plasmid, which provides further means of genetic manipulation.

This easy manipulation makes yeast invaluable in the context of biomedical research. Certain yeast phenotypic deficiencies caused by a missing/non-functional protein can be rescued by the expression of a mammalian (e.g. human) homologue, providing insight into its function (for concrete examples consult Introduction in Volkov (2015)). Furthermore, since the fundamental processes in all eukaryotes are either same or very similar, study of yeast can bring useful insights into human physiology of the cell (Janderová and Bendová, 1999).

1.2 Yeast cell envelope

All living cells are defined by their outer envelope structures that give them shape and rigidity and provide the first line of defence against their environment. In contrast to mammals, the yeast cell envelope is made up of more than one constituent, namely the plasma membrane, cell wall and in certain cases also a capsule.

1.2.1 Capsule

The ∼3 µm thick capsule (in the case of *in vitro* cultures; Rivera et al. (1998)), representing the outermost layer of the cell envelope, is more common for bacteria than yeast. In fact, only a handful of yeast species, such as the opportunistic human pathogen *Cryptococcus neoformans*, form capsules (Bose et al., 2003), often giving rise to slimy colonies.

Capsules are made of radially oriented polysaccharides whose main building blocks are invariably mannose and glucuronic acid, accounting together with xylose for ∼90 % of the *C. neoformans* capsule saccharide content (Bose et al., 2003). Depending on the species, these are supplemented with other saccharides, such as glucose and galactose, in varying ratios. The polysaccharide structure is well-organized and stable and can be visualized microscopically after staining with an appropriate dye, e.g. India ink or Maneval's capsule stain.

The exact function of the capsules in yeast is presently unclear. It seems, however, that it might be involved in nutrient uptake under limiting conditions and may possibly help cells adhere to surfaces. Hence, it may be a factor in the formation of biofilms. The capsule is an important determinant in the pathogenicity of *C. neoformans*, helping the yeast bypass the immune response of the host (Bose et al., 2003). Furthermore, the thickness of the capsule varies in the approximate range of 8-20 µm depending on the type of infected tissue (Rivera et al., 1998). However, there is no general correspondence between the presence of capsule and pathogenicity of yeast, since *C. neoformans* is the only yeast exhibiting both attributes.

1.2.2 Cell wall

The cell wall, encapsulating the plasma membrane, is a 110-200 nm thick envelope structure (Dupres et al., 2010) that serves to protect the cell from mechanical and osmotic damage and is a major determinant of its morphology. Furthermore, it plays an indispensable role in both vegetative and sexual reproduction of yeast as well as sporulation and formation of biofilms. The cell wall is also involved in adhesion to other cells and communication with them. It is relatively permeable even for large molecules (smaller than 600 Da; Scherrer et al. (1974)), but the degree of permeability varies with growth phase and cultural conditions, being more porous in exponentially growing cells (de Nobel and Barnett, 1991).

The yeast cell wall shares certain similarities with the cell wall of bacteria and plants, as well as the extracellular matrix of mammalian cells. These include the negative charge of its surface and reliance on linked polysaccharides as the building blocks of its fibrous structure. Other characteristics of the cell wall from different species vary significantly (Fry, 1986; Cosgrove, 1997). For example, plant cell walls contain cellulose, while the yeast cell walls do not.

In *S. cerevisiae* the cell wall represents ∼15-30 % of the dry weight of a typical vegetative cell (Aguilar-Uscanga and François, 2003). The most abundant components of the cell wall are polysaccharides (∼70-85 % dry weight, Nguyen et al. (1998)), predominantly the fibrous β-1,3-glucan linked by the branched β-1,6-glucan (Kapteyn et al., 1996; Kollár et al., 1997), forming the fibrous scaffold of the cell wall. Its outer layer is the predominant localization site of highly (50-95 %) glycosylated mannoproteins (∼15-30 % dry weight; Nguyen et al. (1998)), Figure 1.1, which are involved in modulation of cell wall permeability (de Nobel et al., 1990; Zlotnik et al., 1984), cell adhesion, cell wall construction and remodelling etc. (Cabib and Arroyo, 2013). Furthermore, phosphorylation of the mannosyl side chains of mannoproteins gives yeast their negative surface charge.

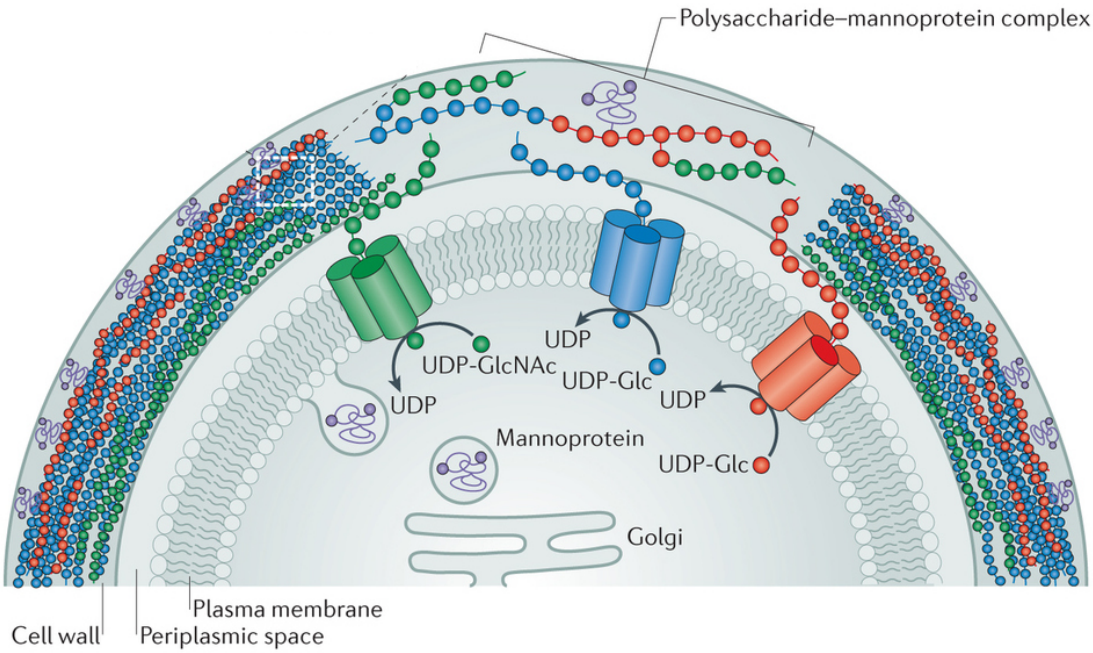

Figure 1.1: Schematic representation of cell wall assembly and spatial distribution of its components revealing its two-layer character. While chitin (green spheres) tends to occupy the inner region of the cell wall, β-1,6-glucan (red spheres) and mannoproteins (purple spheres connected with purple lines) are predominantly localized in its outer part. β-1,3-glucans (blue spheres) span the whole cell wall. Reprinted after cropping from Cabib and Arroyo (2013).

The third most abundant constituent of the cell wall is the *N*-acetylglucosamine polymer, chitin (∼1-2 % dry weight) that is linked to the glucans (Kollár

et al., 1997) and contributes to the insolubility of the cell wall (Hartland et al., 1994), being most abundant on its inner side (Zlotnik et al. (1984); Fig. 1.1). The amount of chitin increases in response to the presence of mating pheromones in the environment (Schekman and Brawley, 1979; Orlean et al., 1985), indicating that it plays an important role in yeast sexual proliferation. This is further supported by the fact that high amounts of chitin are to be found in the septum between the mother and daughter cell of budding yeast. As a result, the bud scars are also rich in chitin.

It has been shown that the various cell wall components are linked covalently to one another, forming a sort of lattice (Kollár et al., 1997). Their overall spacial distribution is depicted in Figure 1.1. While sharing some general characteristics, the actual composition of the cell wall depends on the yeast strain, carbon source and, for example, budding history of the cell.

In order to prevent cellular lysis, the rigidity and intactness of the cell wall needs to be maintained at all times. On the other hand, the structure needs to be dynamic enough to accommodate for the growth of the cell. This involves a constant breaking and reformation of bonds between the constituents of the cell wall, as well as their synthesis and breakdown. According to available data, the polysaccharide constituents are synthesized at the plasma membrane (Durán et al., 1975; Shematek et al., 1980), from precursors that are formed inside the cell and transported to the synthases, while the growing chain is being extruded simultaneously through the membrane into the periplasmic space (Fig. 1.1). This process has been studied extensively for chitin (Cabib et al., 1983) and seems to also be true for β-1,3-glucan. The mannoproteins are synthesized in the endoplasmic reticulum and Golgi apparatus, packed into vesicles and transported to the plasma membrane, where they are secreted into the periplasmic space (Orlean, 2012; Lesage and Bussey, 2006). It has been reported that up to a quarter (i.e. $\sim$1200, excluding essential genes) of all *S. cerevisiae* genes are involved in cell wall maintenance and synthesis (de Groot et al., 2001). Even if most of them are involved indirectly or only marginally, it is clear that the cell wall maintenance uses a significant amount of cellular energy.

The integrity and stability of the cell wall may be challenged by the application of various compounds, such as calcofluor white, Congo red, sodium dodecyl sulfate, aminoglycoside antibiotics, caffeine, and K1 killer toxin (Ram et al., 1994; Hampsey, 1997; Lussier et al., 1997; de Groot et al., 2001). The cell wall can also be enzymatically digested, e.g. by zymolyase or β-glucanase, to prepare spheroplasts, a technique widely used in cellular biology. The application of these stresses activates the cell wall integrity pathway (Levin, 2011).

1.2.3 Plasma membrane

The primary function of the plasma membrane is to serve as a permeability barrier for polar molecules and ions that separates the cytoplasm from the extracellular environment. The $\sim$7.5 nm thick structure is composed of complex polar lipids and proteins that form a bilayer due to the hydrophobic interactions among the

lipids and the hydrophilic interactions of their polar heads with the aqueous environment, Figure 1.2.

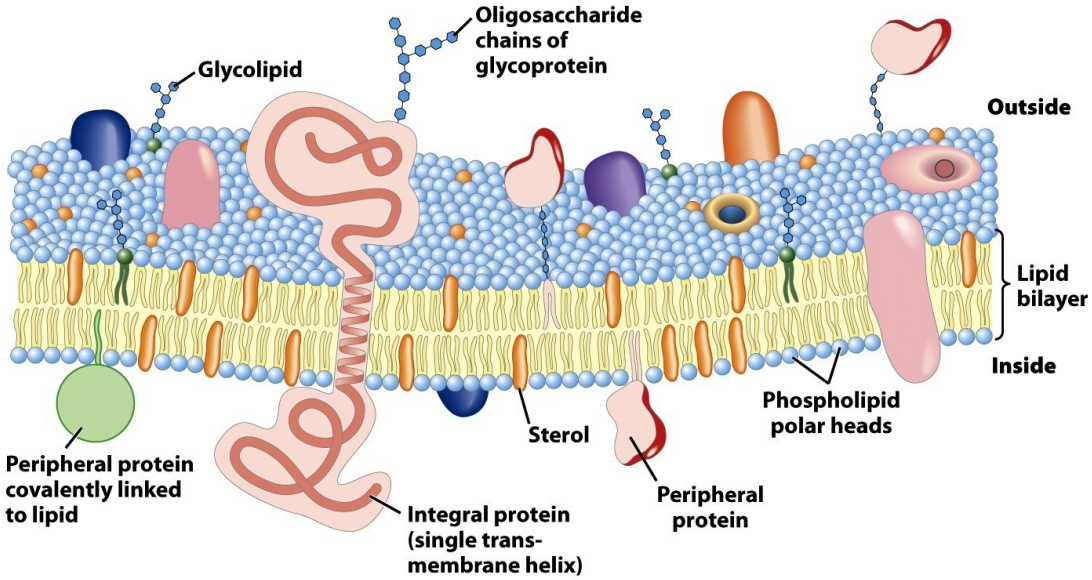

Figure 1.2: Schematic representation of the plasma membrane according to the fluid mosaic model. Reprinted from Nelson and Cox (2008).

The **lipid composition** of the plasma membrane is complex and tightly regulated, pointing to the importance of lipids in activity of membrane proteins. The major lipid classes forming the bilayer in yeast are phospholipids, sphingolipids and sterols.

Phospholipids generally consist of two hydrophobic fatty acid chains connected to a hydrophilic phosphate head by a glycerol molecule. The phosphate group is in certain cases modified by simple molecules, such as choline. The amphiphilic character of phospholipids is crucial in the formation of the plasma membrane bilayer. It is therefore not surprising that they are the most abundant plasma membrane lipids. Phospholipids in direct contact with the plasma membrane proteins seem to directly affect their function and activity (Yeagle, 1989), as has been reported for a chitin synthetase (Kang et al., 1984) and the Pma1p H^+-ATPase (Malpartida and Serrano, 1980). Indeed, it has been shown already by Serrano (1980) that in order to function properly, Pma1p needs to be in direct contact with lipids composed of negatively charged polar heads and unsaturated hydrophobic acyl chains.

Originally discovered in human brain tissue in 1884, *sphingolipids (glycosylceramides)* are abundant in plasma membranes of all eukaryotes, representing ∼30 % of their total lipid content (Patton and Lester, 1991). They are a class of lipids containing a backbone of sphingoid bases, a set of aliphatic amino alcohols, such as sphingosine. Like phospholipids, they also have two aliphatic chains. Presumably localized in the outer leaflet of the plasma membrane (Op den Kamp, 1979), sphingolipids have been proposed to play a role in the synthesis of the cell

wall, serving as anchors. They are also important in signal transduction across the plasma membrane (Hakomori, 1990) and intracellular protein trafficking and assembly (Skrzypek et al., 1997; Gaigg et al., 2005). Furthermore, sphingolipids are essential for growth at low pH, elevated temperatures and at high salt concentrations (Patton et al., 1992). In humans sphingolipids are involved in regulation of differentiation, apoptosis, inflammation and vasculogenesis. It has been shown that they also play a role in a wide range of diseases, e.g. diabetes, cancer, Alzheimer's disease etc. (Cowart and Obeid, 2007).

Sterols (steroid alcohols) are important determinants of rigidity of the plasma membrane, hence affecting the lateral movement and activity of membrane proteins. In contrast to higher eukaryotes, where cholesterol is the dominant type of sterol, the plasma membrane of yeast contains mainly ergosterol and zymosterol (Zinser et al., 1991). Yeasts not able to synthesize sterols rely on their high concentration in the environment (Rodriguez et al., 1985) to satisfy the need of the cell for specific sterols necessary for proliferation (Nes et al., 1993). Due to its effect on the plasma membrane rigidity, ergosterol also plays a critical role in ethanol tolerance in *S. cerevisiae* (Daum et al., 1998; Swan and Watson, 1998)

The nature and function of **membrane proteins** is rather diverse. The most abundant are without question various transport proteins, constituting ∼50 % of the total protein content of the plasma membrane (Serrano, 1991). This number does not include the Pma1p H^+-ATPase, however, an enzyme which by itself accounts for ∼50 % of membrane proteins in exponentially growing cells (Serrano, 1991). In lesser amounts are represented proteins involved in cell wall synthesis, signal transduction (Oehlen and Cross, 1994) and cytoskeleton anchorage (Barnes et al., 1990).

According to the nature of their association with the plasma membrane, we distinguish three types of membrane proteins:

- *Integral membrane proteins* span the whole bilayer and are stabilized in the membrane by the hydrophobic interactions of their trans-membrane domains (such as an α-helix) with the acyl chains of the membrane lipids. They are only removable by application of detergents and organic solvents.

- *Peripheral membrane proteins* are associated with the plasma membrane through electrostatic interactions and hydrogen bonding with hydrophilic domains of integral proteins and polar head-groups of membrane lipids. They can be removed rather easily by modifications of the electrostatic interactions, e.g. by modification of the ionic strength or pH.

- The last class are *amphitropic proteins* that can be found both in the cytosol and in association with membranes. Their localization is governed by their non-covalent interactions and their association with the membrane is often regulated, e.g. by a conformational change revealing a lipophilic domain or their binding to a lipid anchor, such as glycosylphosphatidylinositol (GPI), turning them in effect into peripheral proteins.

It had been believed for many years that the constituents of the plasma membrane are able to freely diffuse within the plane of the membrane (i.e. laterally), as well as undergo rotational and traverse motions (flip-flop; Singer and Nicolson (1972)). However, this view was proven incorrect when it was shown that the lateral movement of lipids in the *S. cerevisiae* plasma membrane is rather slow (Greenberg and Axelrod, 1993). Furthermore, the lateral movement of membrane proteins is hindered by their interaction with other membrane proteins, the cytoskeleton and the cell wall.

The plasma membrane displays two degrees of asymmetry - vertical (transmembrane) and lateral. The *vertical asymmetry* is the result of the action of various ATP-dependent plasma membrane proteins (flippases, floppases and scramblases) that catalyze the translocation of lipids from the outer to the inner leaflet (and vice versa). As a result, the inner layer of *S. cerevisiae* plasma membrane is enriched in phosphatidylethanolamine, phosphatidylinositol and phosphatidylserine (Cheng and Michels, 1991).

The *lateral asymmetry* is the result of the formation of areas that vary not only in their lipid and protein composition, but also overall structure and function. These are generally called microdomains. In the yeast *S. cerevisiae*, one such microdomain is the MCC (membrane compartment of the arginine permease Can1p; Malínská et al. (2003)), supported by a cytosolic protein complex called eisosome. Apart from microdomains, other structures have been detected, such as the detergent-resistant membranes (DRMs). While originally thought to originate in regions of the plasma membrane with distinct function, 10 years of intensive research failed to prove this view and it has been finally abandoned (Zurzolo et al., 2003). It is now generally believed that the DRMs are an artifact of the detergent-treatment of the cells. For an extensive and very detailed review of fungal plasma membrane domains and their physiological function consult Malínský et al. (2013).

Furthermore, in order to fully appreciate the complexity of the plasma membrane, one also needs to consider its dynamics in the terms of rapid turnover of lipids that is invariably connected with endocytosis and exocytosis. These two processes are responsible for the turnover of the area corresponding to that of the entire cell within 30 minutes. Moreover, there is another, less conspicuous, vesiculation and re-fusion process of unknown origin (possibly pinocytosis) that might actually be 20 times more rapid than endo- and exocytosis (Farge, 1995).

1.2.4 Protein-mediated transport across the plasma membrane

The significance of membrane transporters emerges from the realization that the plasma membrane, due to its lipid bilayer character, acts as a permeability barrier with a certain degree of selectivity, depending on the nature of the chemical species. Small hydrophobic molecules (e.g. O_2, CO_2, N_2 and benzene) readily diffuse through the membrane. Small electrically neutral polar molecules (e.g. H_2O, glycerol, ethanol) still diffuse, but not without a certain degree of difficulty. On

the other hand, polar molecules larger than 100-150 Da (e.g. monosaccharides and amino acids) pass only with a very low probability, and ions (e.g. H^+, Na^+, K^+, Ca^{2+}, etc.) are by themselves not able to diffuse through the plasma membrane at all (Fig. 1.3).

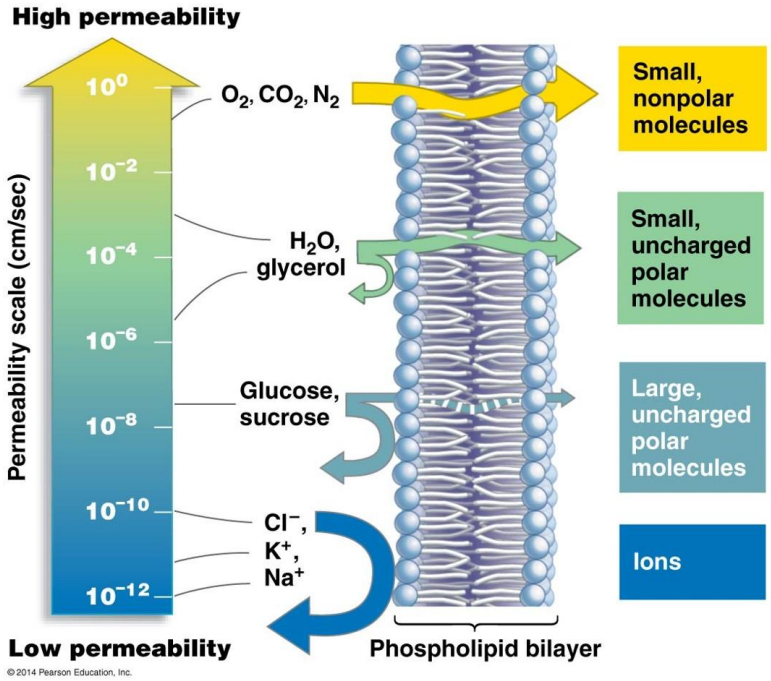

Figure 1.3: Overview of plasma membrane permeability for various types of chemical compounds, with approximate diffusion coefficients. Reprinted from www.studyblue.com.

Since many cellular processes are directly dependent on transport of substances through the membrane (nutrient uptake, efflux of metabolites and toxic compounds, membrane potential generation, etc.), it is essential that the plasma membrane contains proteins specialized in facilitating the transport of various substances.

Facilitated transport

Since the facilitated transport is directly dependent on the activity of specific proteins (transporters, translocases, permeases, channels etc.), there are several general rules that govern the transport. The transport rate is dependent on the concentration gradient of the substrate and can be described by the saturation Michaelis-Menten kinetics. While some of the transport-mediating proteins are highly selective for a narrow range of substrates, other are almost non-specific. Since the transport is connected with the conformational changes of proteins, it can, at least in theory, be inhibited by the action of an inhibitor, hindering such conformational changes.

Depending on the thermodynamics of the transport process, we distinguish two general categories of transporters, active and passive:

- **Active transporters** mediate the passage of substrates through the plasma membrane against their electrochemical gradients. Since this process is not thermodynamically favoured, it needs to be coupled to another from which it derives the necessary energy. Based on the source of energy we distinguish between primary and secondary active transporters:
  - **Primary active transporters** convert light or chemical energy into electrochemical energy. In yeast, where no light-powered transporters have been identified, hydrolysis of ATP is required to fuel the conformational changes leading to transport of substrates (Fig. 1.4(a)). Sometimes called "pumps", the enzymes are able to transport anything from ions through lipids and metabolites to small peptides. One of the most important active transporters in the yeast *S. cerevisiae* is the Pma1p H^+-ATPase that pumps protons out of the cytosol and hence helps maintain the cytosolic pH and membrane potential (Serrano, 1983). Other important examples of pumps are the ABC (ATP-binding cassette) proteins Snq2p and Pdr5p that play a crucial role in the pleiotropic drug resistance (Balzi and Goffeau, 1994; Balzi et al., 1994).
  - The activity of **secondary active transporters** is tightly linked to that of primary active transporters (Fig. 1.4(b)). Working without exception as cotransporters, they use the existing ion gradients (built up by the primary active transporters) to fuel the transport of other ions or small metabolites. For example, the uptake of potassium in *S. cerevisiae* via Trk1p is thought to be fueled by the electrochemical gradient of protons across the plasma membrane (Ko and Gaber, 1991) built predominantly by Pma1p.

- **Passive transporters** mediate facilitated diffusion of solutes through the plasma membrane down their electrochemical gradients. We distinguish between three classes of passive transporters, according to their *modus operandi*.
  - **Channels** open under certain circumstances and enable the passage of ions or small molecules down their electrochemical gradients. The activity of these channels can be gated (regulated) by membrane potential, mechanical stress, pH or other physical and/or chemical qualities of the environment, membrane or cytosol. In the yeast *S. cerevisiae* one such channel is the voltage-gated K^+-specific Tok1p (Bertl et al., 1993), whose opening is also modulated by cytosolic pH (Lesage et al., 1996; Bertl et al., 1998) and mechanical stress (Gustin, 1988).
  - Another type of passive transporters are the members of the **major facilitator superfamily** (MFS). These are believed to be working

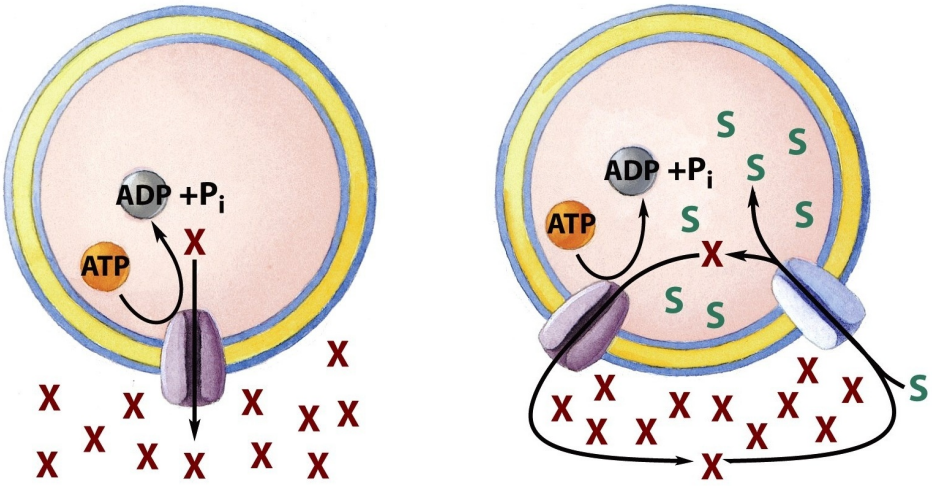

(a) Primary active transport (b) Secondary active transport

Figure 1.4: Schematic depiction of the two types of active transport. (a) Substrate X is transported out of the cell/organelle via primary active transport, which creates an electrochemical gradient of X across the membrane. **(b)** The electrochemical gradient of X is used to fuel the influx of substrate S via secondary active transport. Reprinted from Nelson and Cox (2008).

generally in the "rocker-switch" fashion, exposing only either the exracellular or intracellular binding site to the environment at any given time. The Hxtp sugar transporters of *S. cerevisiae* form a subfamily of MFS proteins (van der Rest et al., 1995; Boles and Hollenberg, 1997).

– Though not native to the cell and not necessarily of peptide character, the last group of diffusion mediators are **ionophores** that can work either as carriers or as pore-forming agents. While the specificity of the pores can be quite wide (gramicidin A forms channels and facilitates diffusion of Na^+, K^+ and H^+) to non-existent (as is the case of some antibiotics), the carriers are often specific for a single ion species (e.g. valinomycin for K^+ and carbonyl cyanide *m*-chlorophenyl hydrazone for H^+). The two groups can be distinguished experimentally, since only the mobility of the carriers is affected by changing temperature (leading to changes in plasma membrane fluidity).

Another important aspect of protein-mediated transport is its stoichiometry. While **uniporters** transport a single substrate molecule per transport cycle (e.g. Pma1p), the activity of **cotransporters** involves the simultaneous/subsequent movement of two or more different substrates per cycle. Based on the relative direction of movement of said cotransported substrates, we differentiate between *symporters* (movement in the same direction; Trk1p, Pho89p) and *antiporters* (movement in opposite directions; Nha1p), Figure 1.5. It is readily deducible that the uniporters include passive transporters and primary active

transporters, while the cotransporters will be in majority represented by secondary active transporters.

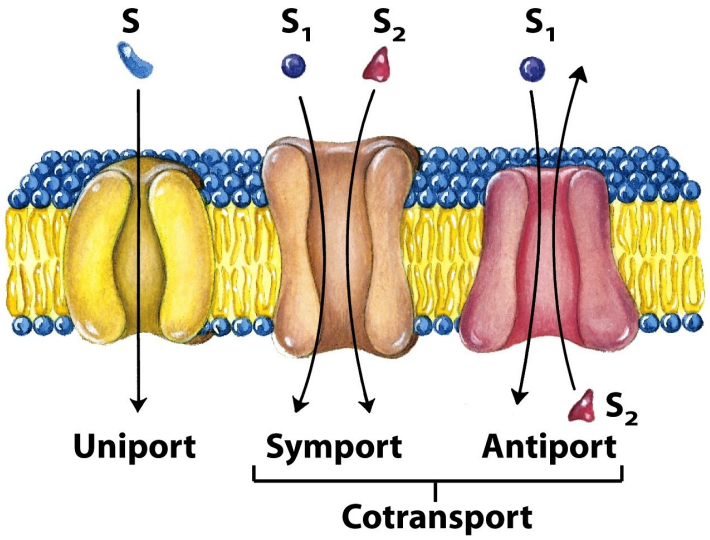

Figure 1.5: Schematic depiction of three general classes of transport systems based on stoichiometry. Transporters differ in the number of substrates transported and the direction in which each is transported. Reprinted from Nelson and Cox (2008).

Based on the impact of the transport on the distribution of electrical charge across the plasma membrane, we can further differentiate between **electrogenic** and **electoneutral** (electrosilent) transport.

1.3 Multidrug resistance in yeast *Saccharomyces cerevisiae*

All living organisms are constantly exposed to their environment, including potentially harmful substances. Over the course of time various mechanisms of defence against such xenobiotics (substances foreign to the cell) evolved. On the level of a single cell, these include the action of membrane-bound proteins that mediate the efflux of a wide range of structurally and chemically unrelated substances out of the cytosol either into the surroundings of the cell or into various intracellular compartments, out of reach of their targets. In order to make their way inside the cell, the xenobiotics need first cross the plasma membrane. It is therefore of great advantage that a big part of the transporters is localized here. Furthermore, there have been reports that at least some of the pumps are able to export xenobiotics directly from the plasma membrane, preventing them from ever reaching the cytoplasm (Prasad et al., 2002; Ernst et al., 2005).

While it is clear that the existence and activity of these pumps is of a great advantage for the cell and its ability to survive, their overexpression often gives rise to the so-called multidrug resistance (MDR) phenomenon. Cells exhibiting

MDR are often resistant to a wide range of chemicals, which poses a great complication in the treatment of diseases, including bacterial infections, mycoses and even cancer. Studying of these pumps and of ways to inhibit them is therefore of great medical importance.

The MDR pumps can be divided into two groups according to the type of energy they utilize for transport:

- Primary active transporters derive the energy for transport from the hydrolysis of ATP molecules. Such transporters form a big group called ABC (ATP-binding cassette) superfamily.
- Secondary active transporters, on the other hand, use the energy stores in the electrochemical gradients of ions, above all hydrogen, potassium and sodium. Hence, they work as cotransporters.

1.3.1 MDR pumps utilizing ATP

The primary active transporters contributing to MDR in yeast belong to one of the largest known paralogous protein families, the ATP-binding cassette (ABC) superfamily. According to our knowledge, ABC transporters are present and highly conserved in all organisms, from bacteria to man (Balzi and Goffeau, 1994). However, the number of ABC genes expressed varies with the organism, ranging from 70 in the *E. coli* genome (Linton and Higgins, 1998), through 30 in the case of yeast (Bauer et al., 1999; Decottignies and Goffeau, 1997; Taglicht and Michaelis, 1998) to around 50 in humans (Dean et al., 2001).

The chief function of ABC transporters is primary active transport of a wide range of substances across the plasma membrane. The transported molecules include ions, heavy metals, pigments, peptides, steroids, lipids and many others. While the prokaryotic ABC proteins are implicated in both uptake and export of compounds, no example of an uptake ABC protein has been reported in eukaryotes to this date. The substrate specificity of particular ABC transporters ranges from quite narrow to very wide, almost non-specific (Ernst et al., 2005). A highly conserved function of ABC proteins is detoxification of the cell and export of xenobiotics, including antibiotics, antimycotics and chemotherapeutical agents.

In humans, mutations of ABC genes are often the cause of various diseases, including cystic fibrosis (*CFTR* gene), Tangier disease, Dubin-Johnson syndrome, various sight disorders and adrenoleukodystrophy (Decottignies and Goffeau, 1997; Higgins and Linton, 2003). Furthermore, overexpression of P-glycoprotein, the product of the *MDR1* gene, often leads to tumour cells resistance against chemotherapy (Ames, 1986; Gottesman and Pastan, 1993).

The major ABC proteins contributing to multidrug resistance in yeast (in this case known under the term pleiotropic drug resistance; PDR) are the plasma membrane proteins Pdr5p, Snq2p and Yor1p. These pumps have different, but partially overlapping substrate specificities (Rogers et al., 2001) and are described in detail in section 1.3.3. Due to the high homology, the ABC transporters of *S. cerevisiae* are often used as a model to study the drug resistance in human

infectious diseases and cancer as well as screens for novel drugs for such (Sipos and Kuchler, 2006; Lamping et al., 2007).

Surprisingly, besides the transport of molecules across the plasma membrane, some ABC transporters have been reported to also act as receptors, sensors, proteases, channels, channel regulators and even signalling components (Higgins, 1995).

1.3.2 Molecular characteristics of ABC transporters

A typical ABC protein forms two transmembrane domains (TMD) and two nucleotide-binding domains (NBD). These two domain types usually alternate within the amino acid sequence, starting either with TMD or NBD. However, this is not a strict general rule, since also half-variants exist.

The NBD is of hydrophilic character and is essential for ATP hydrolysis and hence energization of the transport. It is formed by three peptide motives, Walker A and Walker B, which are present in all nucleotide-binding proteins (Walker et al., 1982), and of the ABC signature motive, unique to ABC transporters. This motive seems to be essential for the proper function of the ABC transporters, since mutations in its sequence often lead to loss of function of the transporter, leading to diseases, such as CFTR (Browne et al., 1996).

The TMD is lipophilic, constituting most often of 6 α-helices spanning the plasma membrane. Together, the α-helices form the translocation pore and binding site for the substrate, making it an important determinant of substrate specificity (Lage, 2003; Prasad and Panwar, 2004) which may, however, also be influenced by the NBD (Ernst et al., 2008).

1.3.3 Major yeast plasma membrane PDR transporters

Pdr5p (pleiotropic drug resistance) is a 1511 amino acids long ABC transporter (Balzi et al., 1994) whose functional unit is proposed to be a homodimer, Figure 1.6. It is the most extensively studied and best characterized of the yeast PDR proteins (Bauer et al., 1999; Ernst et al., 2005; Golin et al., 2007).

The *PDR5* gene is located on the right arm of chromosome XV, with its expression positively regulated by Pdr1p, Pdr3p (Balzi et al., 1987, 1994; Katzmann et al., 1994), Stb5p (Akache and Turcotte, 2002) and under heat shock conditions and oxidative stress also by Yap1p and Yap2p (Miyahara et al., 1996) transcription factors. Negative regulation is mediated by Rdr1p (Hellauer et al., 2002). While the *PDR1* and *PDR3* genes are partly redundant, the disruption of either leads to a drop in Pdr5p mRNA levels. Overexpression of Pdr5p, e.g. due to the *pdr1-3* point mutation in the transcription factor Pdr1p (Mahé et al., 1996), leads to pleiotropic drug resistance (Leppert et al., 1990; Bissinger and Kuchler, 1994; Hirata et al., 1994).

Basal expression of Pdr5p is the highest in the exponential growth phase, dropping rapidly during diauxic shift or when nutrients are limiting. There is almost no expression of the transporter in post-diauxic and stationary cells (Mamnun

Figure 1.6: Three-dimensional reconstruction of a Pdr5p dimer at 25-Å resolution in negative staining. Three regions are clearly differentiated: the first region corresponding to the lowest part of the volume has been attributed to the membrane embedded domains; the second region corresponds to four protruding segments that have been attributed to the stalks domains; the third region consists of four lobes that have been attributed to the nucleotide binding domains (NBDs). Arrows show the different orientations of the NBDs. Reprinted, including legend, from Ferreira-Pereira et al. (2003).

et al., 2004; Čadek et al., 2004; Maláč et al., 2005). Half-time of the protein is rather short, 45-90 minutes (Plemper et al., 1998; Egner et al., 1995; Ferreira-Pereira et al., 2003).

Substrates transported by Pdr5p include antimycin A, azoles, cycloheximide, cerulenin, chloramphenicol, dexametazone, erythromycin, estradiol and a wide range of other chemicals, unrelated neither structurally nor chemically (Leonard et al., 1994; Hirata et al., 1994; Kolaczkowski et al., 1996). Despite the wide range of its substrates, Pdr5p is not essential for the cell and *pdr5*Δ mutants, however drug- and salt-hypersensitive (Leppert et al., 1990; Miyahara et al., 1996), are fully viable. Even more so, deletion of the gene leads to more rapid growth of yeast cultures in the liquid media and higher overall mass (Hlaváček et al., 2009). The activity of the protein can be inhibited for example by fujimycin (FK506) (Kralli and Yamamoto, 1996) and by a group of compounds called enniatins (Hiraga et al., 2005).

Apart from mediating PDR, Pdr5p has also been reported to be involved in cation homeostasis of yeast under ionic stress conditions (Miyahara et al., 1996), to act as a phosphatidylethanolamine translocase, i.e. it plays a function in establishment of discrete plasma membrane microdomains (Decottignies et al., 1998; Pomorski et al., 2003; Kihara and Igarashi, 2004), and in quorum sensing for yeast populations growing in liquid culture (Hlaváček et al., 2009).

Snq2p (sensitivity to 4-nitroquinoline-N-oxide) is a 1501 amino acids long (Balzi and Goffeau, 1994) ABC transporter (Decottignies et al., 1995). Despite being the first identified yeast ABC transporter mediating PDR (Haase et al., 1992), it has been studied somewhat less extensively than its homologue Pdr5p, with which

it shares about 40 % identity of the amino acid sequence (Prasad and Panwar, 2004).

The expression of the *SNQ2* gene, located on chromosome IV, is positively regulated by Pdr1p, Pdr3p and Stb5p (Decottignies et al., 1995; Mahé et al., 1996; Cui et al., 1999; Akache and Turcotte, 2002) and also induced by the presence of drugs via Yrr1p and Yrm1p (Cui et al., 1998; Le Crom et al., 2002; Lucau-Danila et al., 2003) and by heat-shock via Yap1p and Yap2p (Miyahara et al., 1996; Bauer et al., 1999). In contrast to Pdr5p, the basal expression of Snq2p seems to be slightly elevated after the diauxic shift (Gasch et al., 2000).

The substrate specificity of Snq2p partly overlaps with that of Pdr5p and like its cousin is not essential for the cell. Its deletion, however, renders the cells sensitive to various metabolic inhibitors, including 4-nitroquinoline N-oxide (Servos et al., 1993; Cui et al., 1998), triaziquon, solfometuron-methyl, phenanthroline, staurosporine and fluphenazine. Snq2p can be inhibited specifically by erythrosine B and non-specifically by vanadate, Triton X-100 (Decottignies et al., 1995) and also by the protonophore CCCP (Hendrych et al., 2009).

Besides its role in PDR, Snq2p is also involved in the protection of yeast against photosensitizers that, when exposed to light of appropriate wavelength, produce singlet oxygen species (Ververidis et al., 2001) and, like Pdr5p, plays a role in quorum sensing in yeast populations growing in liquid culture (Hlaváček et al., 2009) and contributes to the maintenance of cationic homeostasis under ionic stress conditions. Disruption of the *SNQ2* gene leads to hypersensitivity to salts like NaCl, LiCl and $MnCl_2$ (Miyahara et al., 1996).

Yor1p (yeast oligomycin resistance) is a 1477 amino acids long ABC transporter. More specifically, it is the only yeast MRP (multidrug resistant protein)/CFTR (cystic fibrosis transmembrane conductance regulator) yeast protein located in the plasma membrane, as opposed to the rest that are located in the vacuolar membrane. Its ATPase activity is about 15-fold lower compared to Pdr5p (Decottignies et al., 1998).

The *YOR1* gene, located on chromosome VII, is a human MRP1 (30 %), CFTR (28 %) and yeast vacuolar Ycf1p homologue. Expression of the gene is positively regulated by Pdr1p (Balzi et al., 1987), Pdr3p (Delaveau et al., 1994), Pdr8p (Hikkel et al., 2003) and also by Yrr1p (Zhang et al., 2001) and Yrm1p (Lucau-Danila et al., 2003).

Yor1p mediates resistance of yeast cells to oligomycin (Katzmann et al., 1995), reveromycin A and aureobasidin A, and is important for detoxification of a wide range of organic anions (Cui et al., 1996) and cadmium by actively extruding cadmium-glutathione complexes out of the cytosol Nagy et al. (2006). Furthermore, like Pdr5p, Yor1p mediates efflux of rhodamine B (Cui et al., 1996; Decottignies et al., 1998) and is believed to act as a phosphatidylethanolamine translocase (Pomorski et al., 2003). The transporter may be inhibited by vanadate (Decottignies et al., 1998).

1.3.4 MDR pumps utilizing the electrochemical gradient

From the proteins utilizing electrochemical gradients to power the transport of xenobiotics, of highest importance are those belonging to the major facilitator superfamily (MFS). Besides contributing to MDR, these proteins transport a wide range of other compounds, both into and out of the cell, including oligosaccharides, amino acids, nucleotides and Krebs cycle metabolites (Marger and Saier, 1993). It is interesting to note that this class of proteins has been originally identified as sugar transporters, a function they exhibit in both prokaryotes (Kaback et al., 2001) and eukaryotes, including mammals (Mueckler et al., 1985).

1.4 Effect of alcohols on eukaryotes

Alcohols (in particular ethanol) have been long known to exhibit a wide range of effects on life and living organisms, from unicellular bacteria to high eukaryotes, including humans (Korpi et al., 1998; Möykkynen and Korpi, 2012). Interestingly, many molecular pathways sensitive to alcohol are conserved throughout species, such as mice, humans, worms and fruit flies (Dick and Foroud, 2002; Lewohl et al., 2011).

In lower organisms the most important effect of alcohols is their antimicrobial activity that is generally believed to be caused by membrane damage and protein denaturation with subsequent interference with metabolism and cell lysis. The most widely used alcohols for this purpose are ethanol and n-propanol which exhibit their effect against vegetative bacteria, viruses and fungi. The antimicrobial potency of alcohols is generally limited at concentrations below 50 %, while being optimal in the range 60-90 % (McDonnell and Russell, 1999).

Their mode of action on the molecular level, however, still remains subject to debate (Peoples et al., 1996). Alcohols were originally proposed to predominantly affect the lipid bilayer of membranes, including those of axons (Seeman, 1972; Franks and Lieb, 1978; Goldstein, 1984). However, direct alcohol-protein interactions have been observed in studies of the ligand- and voltage-gated neuronal channels (Li et al., 1994; Lovinger, 1997; Godden et al., 2001; Horishita and Harris, 2008), ion channels in non-excitable cells (Chanson et al., 1989; Hamada et al., 2005) and the soluble enzyme luciferase (Adey et al., 1975; Franks and Lieb, 1984, 1985).

Regardless of the nature of the interaction, however, the end result is always modification of protein activity. At low concentrations, the direct alcohol-protein interactions might prevail, giving way to the effect on the lipid membrane at higher concentrations (Lundbæk, 2008). However, it is also worth considering that the incorporation of alcohols into the lipid bilayer of the membrane leads to its increased fluidity and hence increased permeability for ions, possibly leading to dissipation of their gradients (Petrov and Okorokov, 1990).

In general, the efficiency of primary alcohols to cause anaesthetic effects as well as inhibit membrane proteins (or exhibit any of their toxic effects) increases with the length of their carbon chain, which has been attributed to the concomi-

tant increase of their hydrophobicity index (i.e. solubility in lipids; Pringle et al. (1981); Lovinger (1997); Alkire and Gorski (2004)). This correlation between hydrophobicity and toxicity of alcohols has been shown in various bacteria, such as *Escherichia coli*, *Pseudomonas putida* and *Acinetobacter calcoacetidus* (Sikkema et al., 1995; Ramos et al., 2002; Kabelitz et al., 2003), as well as in the yeast *Saccharomyces cerevisiae* (Gray and Sova, 1956; Ingram and Buttke, 1984; Fujita et al., 2004).

While at first becoming more effective with the elongation of the carbon chain, the potency of the homologous alcohol series often suddenly drops to almost non-existent upon reaching a certain carbon chain length (Pringle et al., 1981; Franks and Lieb, 1985). This cut-off effect has been shown to originate in the existence of anaesthetics/alcohol-binding amphiphilic protein pocket of finite dimensions (Franks and Lieb, 1985). Therefore, upon increasing of the carbon chain length above the cut-off point, the substrate is sterically hindered from binding into the pocket and in turn fails to exhibit an effect on the protein. This view is further supported by the fact that the partition of alcohols into membranes is not negatively affected by their increased length (Franks and Lieb, 1986). However, beyond the length at which the cut-off occurs, the alcohols no longer disturb the order of the lipids in the membrane, and may even cause the membrane to become more ordered (Miller et al., 1989).

1.4.1 Effect of alcohols on humans

Due to its perfect hydrophobic-hydrophilic balance, together with small molecular weight, ethanol is transported effectively by all bodily fluids and readily passes through membranes, including the blood-brain barrier, leading to more or less uniform distribution across the body (Zakhari, 2006). Ethanol exposure of humans is therefore a whole-body experience.

Effects of alcohols on the central nervous system

In humans, alcohol (most notably ethanol) is best known for its effects on the central nervous system (CNS). Due to its psychoactive properties, ethanol has been used recreationally for tens of thousands of years. The alcohol-induced feeling of well-being seems to be connected with release of endorphins, elevated serotonin and dopamine transmission (Murphy et al., 1982) and direct effects on the opioid receptors (implicated in addiction development; Zaleski et al. (2004)).

In general, alcohol effects on the CNS include changes in the levels and function of neurotransmitters, enzymes, receptors, and other molecules (such as DNA and microRNA), culminating in the synaptic changes in the brain circuitry regulating compulsive behaviour and inhibition. This is thought to be a form of adaptation to chronic exposure to alcohol/ethanol and can lead to development of alcoholism (Wilke et al., 1994).

In humans, *n*-alcohols are known to produce general anaesthesia (Dundee et al., 1969). Their potency rises with their carbon chain length, but levels off

after undecanol and completely disappears after tridecanol (Pringle et al., 1981). While dodecanol is one of the most potent, tetradecanol is practically inactive, consistent with the "protein mechanism" of general anaesthesia (Franks and Lieb, 1985). Indeed, according to more recent research and reports, proteins seem to be the primary sites of alcohol action (Peoples et al., 1996). The alcohol methylene group interacts directly with specific amino acid residues of the proteins via hydrogen bonds and van der Waals interactions (Harris et al., 2008). It is possible that a single binding site may accommodate multiple ethanol molecules. On the other hand, alcohols have been shown to interact with the lipid bilayer only at concentrations much higher than clinically relevant, again supporting a direct alcohol-protein interaction (Pang et al., 1980; Peoples et al., 1996).

Alcohols are known to directly affect the function of various ion channels, particularly those gated by ligands (Harris et al., 1997; Mihic et al., 1997), but also those gated by voltage. Among those *inhibited* by alcohols are for example rat glutamate receptors (Wong et al., 1998), voltage-gated Ca^{2+} channels (resulting in lower neuron excitability, loss of motor coordination and attention deficits; Zaleski et al. (2004)) and Na^{+} channels of human excitable cells, producing an open-channel block and hence modified action potential profiles. A cut-off is observed at nonanol (Horishita and Harris, 2008).

On the other hand, interaction of inwardly rectifying potassium channels GIRK and Kir3 (Kobayashi et al., 1999; Lewohl et al., 1999), the capsaicin and cannabinoid receptor TRVP1 (important in the perception of heat and pain; Blednov and Harris (2009)) and glycine receptors (important in behaviour regulation; Mascia et al. (2000)) with ethanol *enhances* their activity, which is also true for $GABA_A$ and $GABA_B$ receptors (ligand-gated chloride channels; Lobo and Harris (2008)). Their hyperactivation leads to sedation, relaxation and loss of inhibitions (Charlton et al., 1997) due to elevated γ-aminobutyric acid signalling and partly due to inhibition of dopamine release.

Regulation of some channels, however, directly depends on the length of the alcohol. For example, while the activity of neuronal nicotinic acetylcholine receptors in humans is enhanced by ethanol, propanol and butanol, longer alcohols inhibit them. The cut-off seems to be determined by the molecular volume of the alcohols (Godden et al., 2001).

Effects of alcohols on genetics

Most alcohol-induced genomic changes are caused by chronic exposure. Probably the most striking are the changes of epigenetic traits, i.e. the structure of chromatin (Guerri and Pascual, 2010), brought about by ethanol effect on various enzymes. Excessive drinking leads to reduced histone acetylation (Warnault et al., 2013) and overall changes in the DNA methylation profile, changing expression patterns and levels of certain genes. While histone deacetylation is connected with alcohol withdrawal-induced anxiety and stress (Pandey et al., 2008), a direct link between DNA methylation and alcohol dependence has been proposed (Warnault et al., 2013). Furthermore, epigenetic changes in offspring of parents consuming

alcohol in excess during pregnancy have been reported (Finegersh and Homanics, 2014).

Besides its effects on chromatin, ethanol may also directly affect the expression machinery. Indeed, ethanol activates some transcription factors, such as the heat shock factor protein 1 (HSF1), leading to elevated expression of one of the GABA receptor subunits and hence changing overall activity of the receptor. Long-term treatment of humans with ethanol also activated the CREB (cAMP response element-binding protein) transcription factor, leading to increased NR2B (an NMDA receptor subunit) gene transcription (Rani et al., 2005). This can be dangerous, since NMDA receptors tend to become hyperactive upon alcohol withdrawal, which can lead to agitation and sometimes epileptic seizures.

It has been discovered quite recently that not only transcription, but also translation of genetic information can be affected by alcohols. MicroRNAs (miRNAs) are short, non-coding RNA sequences that specifically regulate translation of some mRNAs. It has been shown that chronic exposure to ethanol causes global changes in miRNA expression in human alcoholic brains (Li and van der Vaart, 2011), though the mechanism is still unclear. Interestingly, manipulation of a single miRNA can produce robust changes on the molecular level and in turn behavioural changes. For example, elevation of miR-9 (suggested to regulate neuronal differentiation) levels leads to downregulation of the large-conductance calcium and voltage-gated potassium channel BK. This in turn contributes to alcohol tolerance (Pietrzykowski et al., 2008).

Effects of alcohols on the cardiovascular system

Dependent on the dose and frequency of administration, alcohol can be both beneficial and harmful to the cardiovascular system. The turning point seems to be between two and three drinks, i.e. beers or glasses of wine, per day (Zakhari, 1997).

The beneficial effects of moderate drinking include elevated concentration of high-density lipoproteins (Linn et al., 1993), enhanced cellular signalling within the endothelium, decreased platelet (Foegh and Virmani, 1993) and clot formation and stimulation of blood clot dissolution (Iso et al., 1993), as well as enhanced blood flow due to elevated fluidity of red blood cell membranes, leading to their higher deformability (Sonmez et al., 2013). Taken together, these effects help protect against coronary artery disease as well as stroke (Palomäki and Kaste, 1993) and heart-attack.

On the other hand, excessive drinking has been linked directly to elevated risk of heart muscle disorders (including depressed contractile function due to affected calcium release from the sarcoplasmic reticulum, actin and myosin function and oxygen supply; Capasso et al. (1991); Zakhari (1997)), arrhythmia (due to thickening and scarring of the connective tissue and lack of oxygen; Zakhari (1997)), high blood pressure (Beilin and Puddey, 1992) and both embolic (Qureshi et al., 2017) and haemorrhagic (Iso et al., 1995) stroke.

1.4.2 Alcohol-induced stress in yeast

Among the primary effects of ethanol on yeast are modification of the plasma membrane fluidity (Thomas et al., 1978; D'Amore et al., 1990; Alexandre et al., 1994), destruction of various membrane structures and stimulation of Pma1p H^+-ATPase activity (probably due to partial dissipation of the trans-membrane proton gradient; Cartwright et al. (1987); Rosa and Sá-Correia (1991, 1992)). Longer primary alcohols (hexanol to dodecanol), however, inhibit the pump. The highest inhibition is achieved by alcohols from octanol to dodecanol. Upon elongation of the carbon chain to 13 carbon atoms, the inhibitory efficiency drops to almost zero (cut-off). This effect has been proposed to originate in the interaction with the plasma membrane lipids surrounding Pma1p, the alcohols acting as surfactants (Kubo et al., 2003).

Ethanol diffuses freely across biological membranes in yeast allowing relatively rapid equalization of concentrations in the intracellular and extracellular pools. Accumulation of ethanol in growing yeast cultures eventually leads to decreased rates of fermentation (under both aerobic and anaerobic conditions), decreased growth rates and loss of viability (Ingram and Buttke, 1984; Carlsen et al., 1991). This might be caused by non-competitive inhibition of the protein-mediated import of a plethora of nutrients, such as ammonium, amino acids, sugars, and organic acids (Thomas and Rose, 1979; Leão and van Uden, 1982, 1984; Iglesias et al., 1991; Casal et al., 1998).

Once inside the cell, ethanol decreases the glycolytic rate by competitively inhibiting phosphoglycerate kinase, phosphoglycerate mutase and pyruvate decarboxylase. The remaining nine enzymes of the glycolytic pathway are also inhibited, however in a non-competitive way (Millar et al., 1982). Besides affecting glucose metabolism, alcohols also reversibly inhibit sporulation (Trujillo and Laible, 1970), but are not sporicidal (McDonnell and Russell, 1999).

On the genomic level, ethanol (over a wide concentration range) causes complete destruction of mitochondrial DNA, giving rise to respiration-deficient ρ^0 mutants (Bandas and Zakharov, 1980; Jiménez and Benítez, 1988; Ibeas and Jimenez, 1997). On the other hand, damage to nuclear DNA was shown to occur only in repair-deficient strains (Jiménez and Benítez, 1988; Ristow et al., 1995).

1.4.3 Cellular response and tolerance to ethanol-stress in yeast

Yeast have developed a wide range of responses enabling them to deal with various types of high ethanol-related damage and stress. These include changes in gene expression, membrane composition and increase in chaperone proteins that help stabilize denatured proteins. These mechanisms allow them to proliferate normally at ethanol concentrations lethal to other microorganisms (3-4 % w/v) and often even higher, up to 18 % in the case of some sake producing strains (Watanabe et al., 2007). *Brettanomyces* and *Zygosaccharomyces* have similar ethanol tolerance to that of *Saccharomyces*.

In contrast to very high toxicity of methanol for humans (Wallace and Green, 2009), yeast tolerate it rather well, generally even better than ethanol (Troyer, 1953, 1955). Nevertheless, alcohols (predominantly longer, e.g. butanol[1]) still represent a form of chemical stress with its primary target being the plasma membrane. The alcohol tolerance is determined predominantly by its lipid composition (Thomas et al., 1978; Beaven et al., 1982; Ingram and Buttke, 1984; Mishra and Prasad, 1988). To be more specific, yeast grown in the presence of ethanol increase the content of mono-unsaturated fatty acids (Beaven et al., 1982; You et al., 2003) and ergosterol (Thomas et al., 1978; Walker-Caprioglio et al., 1990; Castillo Agudo, 1992; Daum et al., 1998; Swan and Watson, 1998; Aguilera et al., 2006) in their membranes, which seems to be aimed at counterbalancing the alcohol-mediated changes in membrane fluidity and stabilizing the membrane. In fact, a correlation between ethanol tolerance and increased degree of fatty acid saturation and ergosterol content in the plasma membrane of *S. cerevisiae* has been reported on multiple occasions (Beaven et al., 1982; Ghareib et al., 1988; Mishra and Prasad, 1989; Mishra and Kaur, 1991; Alexandre et al., 1994; You et al., 2003). Being connected to lipid fluidity of the membrane, it is of no surprise that ethanol tolerance is diminished by rising of the ambient temperature (van Uden, 1983). Change in fatty acid composition is also one of the adaptive processes employed by *E. coli* grown in the presence of alcohols (Ingram, 1976).

However, the changes in lipid composition are not limited to the degree of (un)saturation. After 4-hour exposure of *S. cerevisiae* cells to moderate ethanol concentrations (0-12 %), the total glycolipid content of the plasma membrane was shown to increase. Also increased was the amount of glucose bound in the glycolipids, in contrast to the decreased galactose levels. This effect is probably connected to changes in β-galactosidase activity upon ethanol treatment (Malhotra and Singh, 2006).

On the molecular level, ethanol triggers the activation of stress-related transcription factors Msn2p and Msn4p (general stress response), Asr1p (Betz et al., 2004; Ding et al., 2010) and Hsf1p (heat shock response; Lee et al. (2000)), inducing the transcription of up to 14 heat shock proteins (such as Hsp30p; Piper et al. (1994, 1997); Swan and Watson (1998); Piper et al. (1997); Galeote et al. (2007); Vianna et al. (2008)). The heat shock proteins directly contribute to ethanol tolerance, presumably by acting as chaperones, stabilizing denatured proteins, a function they share with trehalose, whose increased intracellular concentrations confer the yeast more resistant to ethanol (Leão and van Uden, 1984; Ogawa et al., 2000). Furthermore, a group of genes related to the integrity of the cell wall has been identified as required for ethanol tolerance (Takahashi et al., 2001)

The chemical composition of the cultivation media also plays an important role in ethanol tolerance. Cultivation in the presence of Mg^{2+}, inositol, amino acids and high salt concentrations all lead to higher ethanol tolerance. While the

[1]There is a general barrier for growth between 1-2 % (*E. coli*, *Z. mobilis*, non-*Saccharomyces* yeast). Only a few microorganisms are able to tolerate 2 % butanol. Several *S. cerevisiae* strains exhibit limited growth at 2 % butanol. Two *Lactobacillus* strains are able to grow in 3% butanol (Knoshaug and Zhang, 2009).

magnesium effect is connected to the biosynthesis of heat shock proteins (Petrov and Okorokov, 1990; Birch and Walker, 2000), amino acids (proline, isoleucine, methionine and phenylalanine) are incorporated into the plasma membrane and counteract the ethanol-caused fluidization of the membrane (Takagi et al., 2005; Hu et al., 2005). Cultivation at high salt leads to modification in the lipid composition of the membrane (Russell, 1989; Tunblad-Johansson et al., 1987; Hosono, 1992). In general, osmotolerance, thermotolerance and ethanol tolerance seem to correlate (Sharma et al., 1996; Birch and Walker, 2000).

Increased ethanol tolerance is interesting not only scientifically, but also economically, due to the necessity of alternative (and renewable) energy/fuel sources. Ethanol has shown to be of great promise as a potential biofuel due to its renewability and environmental friendliness (Farrell et al., 2006).

1.5 Membrane potential

1.5.1 Definition of membrane potential

The plasma membrane potential ($\Delta\Psi$) is defined as the electric potential difference between the interior and the exterior of the semi-permeable plasma membrane. The difference is the result of various processes connected with the movement of ions across the membrane, giving rise to the electrochemical gradients of various ionic species. In resting state of the membrane, the willingness of an ionic species to flow through the membrane is given by its electrochemical potential $\tilde{\mu}_i$:

$$\tilde{\mu}_i = \tilde{\mu}_i^0 + RT\ln a_i + z_i F\psi, \tag{1.1}$$

where $\tilde{\mu}_i^0$ stands for standard electrochemical potential of the given component of the solution, a_i denotes the activity of said component and z_i the number of its elementary charges. T is the thermodynamic temperature, R the universal gas constant and F the Faraday constant. ψ is the electrical potential of the given phase, independent of the specific components.

As evident from the equation, the electrochemical gradient has two components, the osmotic ($RT\ln a_i$) and the electric ($z_i F\psi$). In the case of alike environments inside and outside of the membrane, and hence no difference in the electrochemical potentials, the resulting gradient is determined by the Gibbs free energy of a particle upon its passage through the membrane.

When considering a membrane potential created due to unequal ion distribution, we can make use of the Goldman-Hodgkin-Katz equation to describe it:

$$\Delta\psi = \frac{RT}{F} ln \frac{\sum P_c[C_{out}] + \sum P_a[A_{in}]}{\sum P_c[C_{in}] + \sum P_a[A_{out}]}, \tag{1.2}$$

where $[C_{in}]$ ($[A_{in}]$) and $[C_{out}]$ ($[A_{out}]$) represent the molar concentrations of the cation (anion) in question inside and outside of the cell, respectively. P_c (P_a) represent permeability coefficients of the respective cations (anions). The summations run over all present ion species, where the major contributors are H^+, K^+, Na^+ and Cl^-. Note that only monovalent ions are taken into account, since only such are present in living cells in significant concentrations.

Just as in other organisms, the charge across the resting yeast plasma membrane is distributed in a way that the interior is negative compared to the exterior. This difference between electric potentials is denoted as the resting membrane potential $\Delta\psi = \psi_{in} - \psi_{out}$, being the sum of resting potentials of all present ions. Its typical value in almost all living cells is ca. -70-100 mV.

In the resting state, the distribution of any ion species across the membrane with a fixed membrane potential can be described by the Nernst equation:

$$\psi = \frac{RT}{zF} ln \frac{[I_{out}]}{[I_{in}]}, \tag{1.3}$$

where z is the number of elementary charges of the ion and $[I_{in}]$ and $[I_{out}]$ represent the molar concentrations of the ion inside and outside the cell, respectively.

1.5.2 Means of measurement of membrane potential

Currently, there is a plethora of methods for measurements of membrane potential. However, not all are appropriate for yeast cells in particular due to their size and presence of the cell wall (such as the use of microelectrodes), or are not appropriate for the monitoring of dynamic processes (e.g. radiolabelled lipophilic cations).

On the other hand, utilization of fluorescent potentiometric probes is not limited in these two ways. Their use is non-invasive and their response to changes in membrane potential in cell suspensions is relatively rapid. Furthermore, their manipulation is simple and safe.

There are two main categories of potentiometric fluorescent probes, electrochromic and ratiometric:

- The response of a **electrochromic probe** is very rapid, in the order of milliseconds. The change in the fluorescence signal is caused by a direct interaction of the probe with the electric field which can either change the space-orientation of the probe or give rise to electrochromism, i.e. change of absorbance spectra due to the application of the electrical field.

- **Redistribution probes**, on the other hand, are lipophilic compounds with a delocalized charge which enables them to pass with ease through the studied membrane. In the case of negative potential on the inside and a cationic character of the probe, the probe passes trough the membrane until the

concentrations inside and outside of the cells respond to the membrane potential according to the Nernst equation (Eq. 1.3). The establishment of the equilibrium across the plasma membrane is slower compared to electrochromic probes, in the order of seconds to minutes.

An example of a potentiometric redistribution fluorescent probe used in yeast is diS-C_3(3) (3,3'-dipropylthiacarbocyanine iodide; Fig. 1.7). It is an iodide salt which in polar environments dissociates into the iodide anion and active probe cation with a delocalized π-electron system. Together with the aliphatic character of its side chains, this facilitates the influx of the probe into cells through the hydrophobic region of the cytoplasmic membrane (Peña et al., 1984).

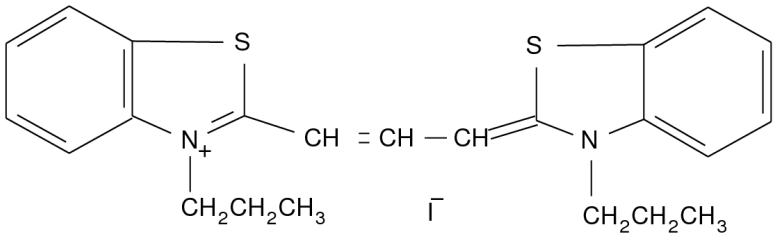

Figure 1.7: The fluorescent probe diS-C_3(3) (3,3'-dipropylthiacarbocyanine iodide). The diS-C_3(3) probe molecule has two aromatic rings and a quaternary ammonium group, giving it its lipophilic and cationic character, respectively.

Since the internal side of the yeast plasma membrane is negative relative to its outer side, the probe influx into the cells is driven not only by its concentration, but also electrical gradient. The final ratio of inner to outer concentration of the probe in equilibrium is given by the Nernst equation for membrane potential (Eq. 1.3). The probe can therefore be readily used to monitor relatively rapid changes in cytoplasmic and/or mitochondrial membrane potential in cells undergoing different types of stress - chemical, metabolic, heat shock etc. (Gášková et al., 2001, 2007).

Furthermore, the diS-C_3(3) probe is also a substrate of major PDR pumps Pdr5p and Snq2p (Gášková et al., 2002). Its use is therefore not limited to monitoring of membrane potential, but it also enables us to study the performance of important plasma membrane-bound proteins under various conditions (Gášková et al., 2002; Hendrych et al., 2009) and their activity and/or expression in cells cultivated in various growth media (Maláč et al., 2005). The use of the diS-C_3(3) probe also provides a means of discovering inhibitors of Pdr5p and Snq2p (Chládková et al., 2004) and possibly other pumps with the capacity to transport the probe.

1.5.3 Maintenance of membrane potential and ion homeostasis

Both intake of nutrients, and efflux of metabolites or xenobiotics across the plasma membrane are invariantly dependent on a source of energy. While some of these

processes are fuelled by the hydrolysis of ATP, other derive the energy necessary for transport from the electrochemical gradients of various ions, such as H^+ or K^+. The adjustment of these gradients also plays an important role in regulation of both cytosolic pH and osmotic pressure. This is partly mediated by voltage-gated channels whose activity directly responds to the membrane potential. Its maintenance is therefore one of the most crucial tasks of any living cell and its complete dissipation leads to death.

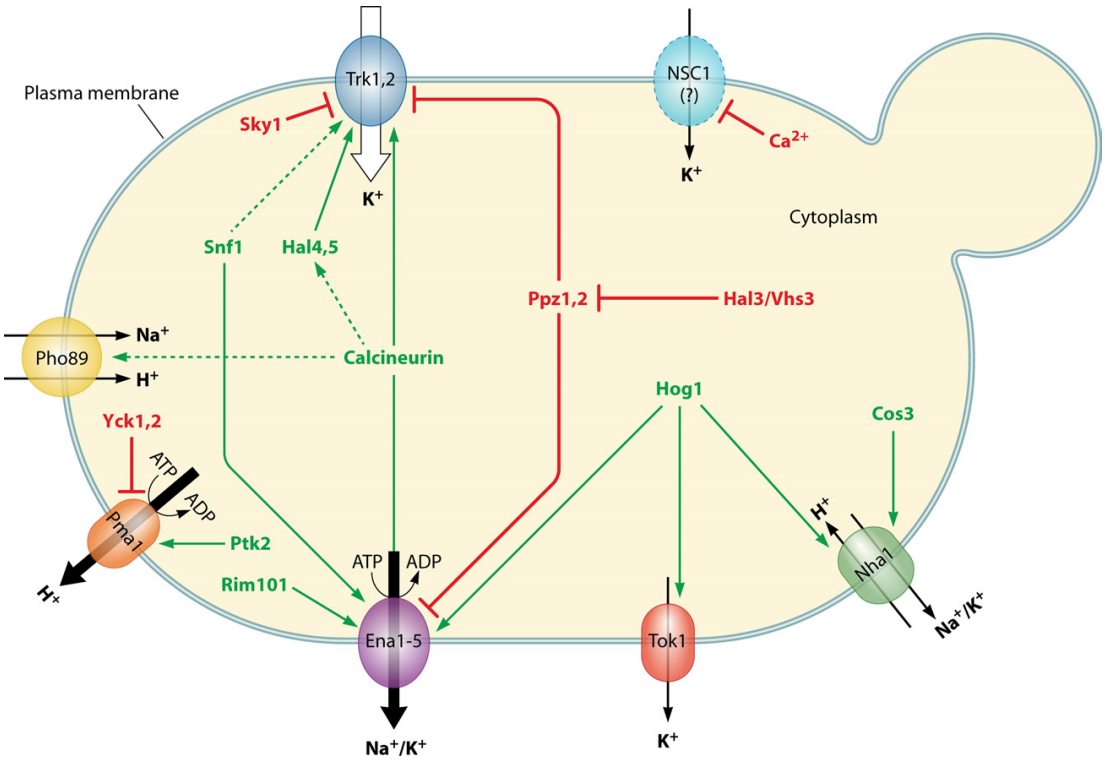

Figure 1.8: Alkali metal cation transporters of the yeast plasma membrane and their regulatory network. Dotted lines indicate interactions that are not fully documented. Reprinted from Ariño et al. (2010).

In the yeast *Saccharomyces cerevisiae*, plasma membrane potential is controlled mainly by the regulation of H^+ and K^+ fluxes. Since the plasma membrane is not readily permeable for ions, the maintenance of their gradients has to be mediated by integral membrane transporters (Fig. 1.8). While the primary active transporters (Pma1p and Ena1-5p) are responsible for the build-up of the gradients, their dissipation is the result of diffusion facilitated by the opening of channels (Tok1p). Secondary active transporters (Nha1p and possibly Trk1p and Trk2p) use the gradient of one ion to create the gradient of another. In this section the most important transporters, both active and passive, involved in the maintenance of ion gradients and membrane potential in yeast *S. cerevisiae* are described.

Maintenance of the proton-motive force

Pma1p H^+-ATPase is a 918 amino acids long (99.6 kDa) integral membrane protein (Malpartida and Serrano, 1980) whose gene has been shown to be highly conserved in various fungi (Wach et al., 1992), Figure 1.9. Pma1p uses hydrolysis of ATP molecules to drive transport of protons outside of the cell (Villalobo et al., 1981; Malpartida and Serrano, 1981; Perlin et al., 1984; Goormaghtigh et al., 1986), at the rate of 20-100 H^+ per second (Serrano, 1988).

Besides playing an important role in the cytosolic pH regulation, enabling the yeast to maintain it roughly constant in a wide range of extracellular pH (Eraso and Gancedo, 1987), the H^+ pumping process leads to the creation of H^+ gradient across the plasma membrane which can be used as fuel for secondary active transport of sugars, amino acids, nucleosides etc. (Serrano, 1988; Portillo, 2000). In addition, the H^+ gradient generated by Pma1p is a major component of the plasma membrane potential.

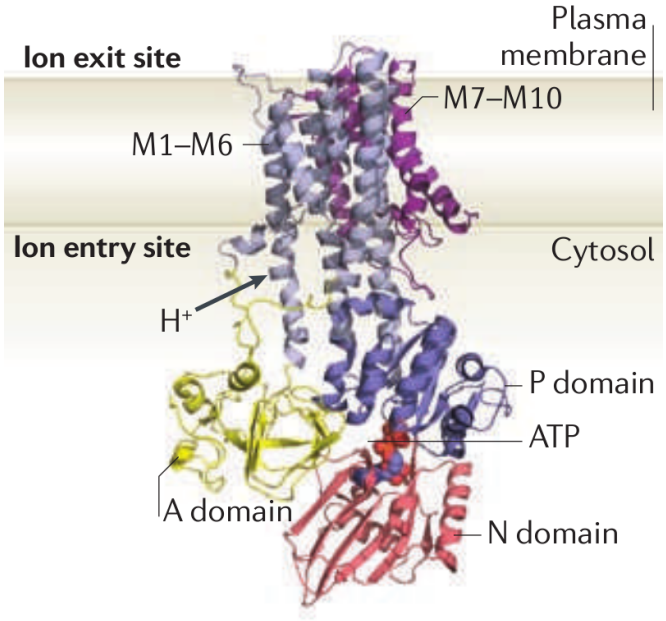

Figure 1.9: Structure and domain organization of Pma1p. The cytoplasmic domains are: A - actuator, N - nucleotide binding and P - phosphorylation domain. Reprinted from Morth et al. (2011).

Pma1p belongs to the P-type cation transporting ATPases, a widely conserved group that includes the mammalian plasma membrane Na^+/K^+-ATPase and Ca^{2+}-ATPase (Kühlbrandt, 2004). Upon interaction of a cytoplasmic H^+ with the enzyme, ATP is bound and hydrolyzed resulting in a high energy phosporylated intermediate, giving this class of ATPases its name. The formation of the phosporylated intermediate leads to a conformational change of the protein resulting in the transfer of the bound proton to the extracellular space, followed by the release of ADP and phosphate. The stoichiometry of this transport in

Neurospora crassa and *Escherichia coli* H^+-ATPases has been reported to be 1 transported H^+ per 1 hydrolysed ATP molecule (Perlin and Slayman, 1986). Because of high homology of membrane H^+-ATPases among fungi and bacteria, it is very probable that this is also true for the H^+-ATPase of yeast *S. cerevisiae*.

The mature Pma1p protein is formed by 10 trans-membrane α-helices, that are the determinant of specificity and that form a H^+ transport pathway (Lecchi et al. (2007); see also Fig. 1.9), and by a cytosolic section, consisting of a small (containing part of the sequence of the A domain; the rest is located on the N-terminal domain) and a large loop (containing the sequence of the N and P domains; Fig. 1.9 and 1.10) exhibiting its catalytic function.

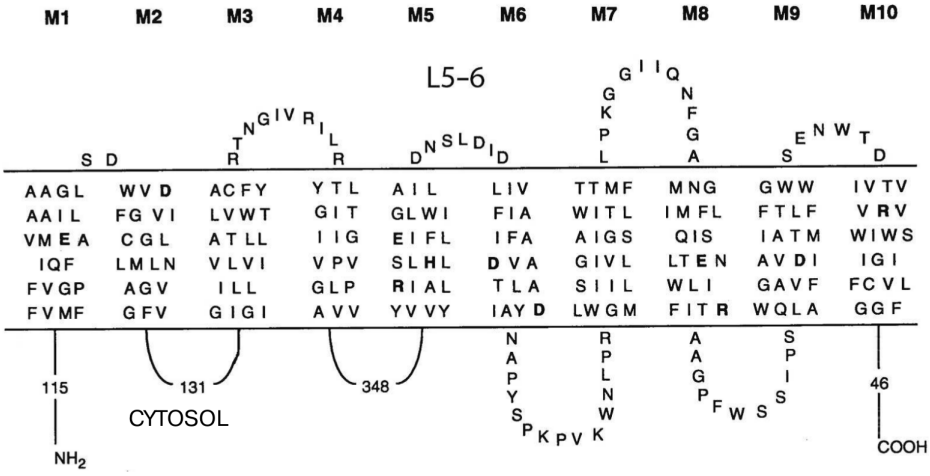

Figure 1.10: Schematic topology of the *S. cerevisiae* Pma1p. M1-M10 denote the transmembrane segments, with the L5-6 loop between M5 and M6 depicted. On the side of the cytosol, the small and large loops are the first and second from the left, respectively. Numbers indicate amino acid residues in the cytosolic parts of the enzyme. Reprinted from Petrov (2015).

Unlike its close homologue Pma2p (89 % amino acid sequence identity; Fernandes and Sá-Correia (2003)), Pma1p is essential for the cell (Serrano et al., 1986; Viegas et al., 1994), with the requirement of at least 20 % of its overall activity for the cells to be able to survive (Cid et al., 1987). In fact, Pma1p accounts for up to 25 % (50 % in exponentially growing cells; Serrano (1991)) of all the plasma membrane proteins, making it the most abundant protein there (Toulmay and Schneiter, 2007). It is therefore not surprising that it is also the biggest consumer of ATP, contributing to ∼20 % of its overall consumption (Portillo, 2000; Lecchi et al., 2007).

The Pma1p activity is modulated on both transcriptional and post-translational level. Namely, the expression of the *PMA1* gene varies with growth phase, being significantly depressed after the post-diauxic transition (DeRisi et al., 1997; Gasch et al., 2000; Segal et al., 2003; Brauer et al., 2005; Hlaváček et al., 2009), consistent with its growth-dependent activity pattern (Eraso and Gancedo, 1987; Nso et al., 2002). The extent of Pma1p expression also depends on the carbon source, being highest when the cells are grown on glucose and lowest when grown

on ethanol (full order: glucose > fructose > galactose ≈ sucrose > raffinose > ethanol; Rao et al. (1993); Gasch et al. (2000)). Re-addition of glucose to starved cells also leads to extensive induction of *PMA1* gene expression within 60 minutes (Rao et al., 1993).

On the post-translational level the activity of Pma1p is modulated mainly by the availability of fermentable sugars (primarily glucose; Serrano (1983)) and acidity (Eraso and Gancedo, 1987; Portillo, 2000). Glucose (re-)addition to cells initially leads to rapid 5- to 10-fold increase in the ATPase catalytic activity, connected with increased V_{max}, decreased K_m and a shift in pH optimum from 5.6-5.7 to 6-7 (Serrano, 1983). This process requires active metabolism of the sugar (Capieaux et al., 1989) and apparently involves disruption of the acetylated tubulin complex that interacts with the enzyme, releasing it from this interaction and resulting in the observed Pma1p activation (Campetelli et al., 2005).

In contrast to the glucose effect on kinetic parameters of the enzyme, cytosolic acidification under growth conditions, caused for example by weak acids (Holyoak et al., 1996), causes a change only in K_m (Eraso and Gancedo, 1987; Carmelo et al., 1997) and does not effect the pH optimum of the enzyme (Eraso and Gancedo, 1987), suggesting a distinct mechanism of activation (Lecchi et al., 2007). In fact, the G-protein Gpa2p involved in the glucose-induced activation of Pma1p, and working in parallel with the glucose sensor Snf3p (Trópia et al., 2006), is not required in the case of activation by weak acids (dos Passos et al., 1992; Pereira et al., 2008). Furthermore, both phospholipase C and protein kinase C activities are essential for the glucose-induced activation process (Souza et al., 2001), as is the action of the Ptk2p protein kinase (Goossens et al., 2000). However, involvement of these in the acid-induced activation has not been reported to date.

On the other hand, activation by glucose and acids share some similarities (Pereira et al., 2008). For example, activation by fermentable substrates is controlled by an auto-inhibitory domain located at the C-terminus (Portillo et al., 1989, 1991), as is the activation by external acidification and nitrogen starvation (Benito et al., 1992). Removal of this C-terminal domain (either proteolytically or on the genomic level) leads to a complete loss of this regulation and a massive (50-fold) increase of Pma1p activity regardless of glucose/acid presence (Portillo et al., 1989).

On the post-translational level, the activity of Pma1p may also be affected by inhibitors, such as omeprazole in acidic environment (Seto-Young et al., 1997), orthovanadate, Dio-9, DCCD and several others (for review see Goffeau and Slayman (1981)), and also by fungicides, such as BM2 that not only inhibits the protein but also blocks the azole antimycotic resistance of the yeast (Monk et al., 2005). Pma1 activity is negatively influenced also by the lysosomotropic compound DM-11 (Witek et al., 1997).

Potassium uptake

Trk1p and **Trk2p** (transport of K^+) are 1235 (141.1 kDa) and 889 (101.1 kDa) amino acids long integral plasma membrane proteins, respectively, with orthologs in a variety of yeasts, fungi and higher plants (Rodríguez-Navarro, 2000). They are localized in the glycolipid-enriched microdomains of the plasma membrane (Yenush et al., 2005). The two K^+ transporter proteins (also able to uptake Rb^+) share a 55 % sequence homology (Ko and Gaber, 1991) and apparently also the structural motif. Both Trk1p and Trk2p contain 12 membrane spanning domains (Gaber et al., 1988; Ko et al., 1990; Ko and Gaber, 1991) which form four identical subunits with a high level of identity with those of the other transporter. Together, these four subunits have been proposed to form the K^+-selective pore (Durell and Guy (1999); Haro and Rodríguez-Navarro (2002); Fig. 1.11) with two binding sites for cations, normally cotransporting two identical (K^+) cations (Haro and Rodríguez-Navarro, 2002).

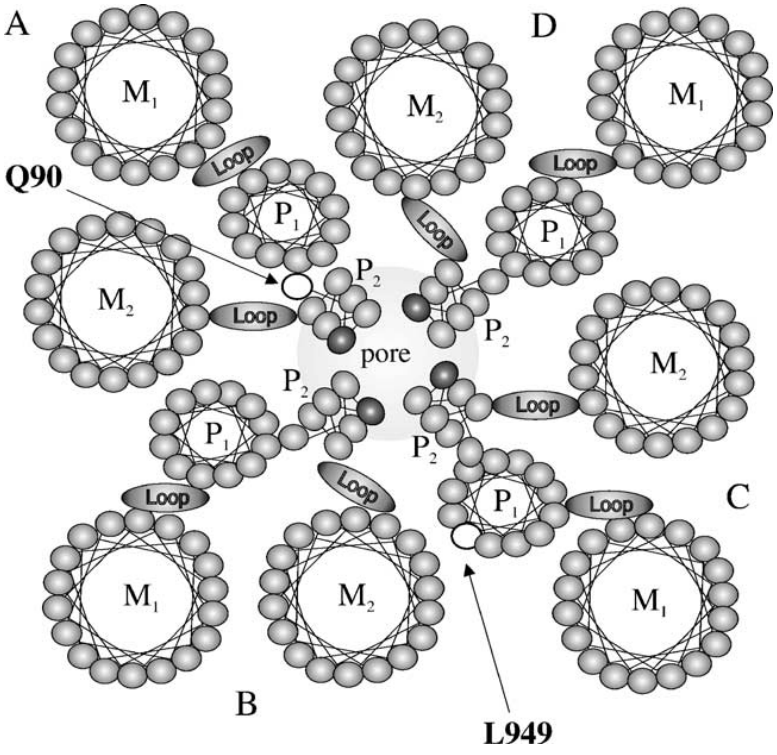

Figure 1.11: A schematic model of the Trk1p transporter tetra-M1PM2 structure. M_i denote the hydrophobic domains connected by α-helical P segments. Residues Q90 and L949 have been identified as important for the transport process. Fragments connecting the four M1PM2 elements have been omitted for clarity. Reprinted from Haro and Rodríguez-Navarro (2002).

Potassium is taken up through this pore against a significant electrochemical gradient, most probably utilizing the energy stored in the proton-motive force of the plasma membrane (i.e. the H^+ electrochemical gradient; Ko and Gaber (1991)). Affinity of the transport via each of the two proteins seems to vary

with growth history of the culture, K^+ abundance and presence of the other transporter (Ariño et al., 2010). After its uptake, K^+ is sequestrated into various organelles (Roomans and Sevéus, 1976; Okorokov et al., 1980; Herrera et al., 2013).

In wild-type cells the potassium uptake is facilitated mainly (if not exclusively) by the Trk1p transporter, enabling the cells to grow already at micromolar K^+ concentrations (Ramos et al., 1985; Gaber et al., 1988). Mutants lacking a functional *TRK1* gene are viable, but need at least millimolar K^+ concentrations to grow properly, for which they depend on the weakly expressed Trk2p transporter (Ko et al., 1990; Ramos et al., 1994; Vidal et al., 1995). Double *trk1 trk2* mutants require at least 10 mM K^+ to grow, relying on non-specific mechanisms for K^+ uptake. Furthermore, their plasma membrane is hyperpolarized (Madrid et al., 1998) and they are hypersensitive to low extracellular pH. At 50 mM K^+ and above, their growth rate is indistinguishable from their *TRK1- TRK2*-competent parent strain (Madrid et al., 1998; Bihler et al., 1998, 2002).

Besides their normal function as K^+ and Rb^+ uptake mechanisms, an additional function of Trk proteins have been reported, namely efflux of halides (I^-, Br^- and Cl^-), but also non-halides (SCN^- and NO_3^-; Bihler et al. (1999); Kuroda et al. (2004); Rivetta et al. (2011). The physiological role of this efflux remains unclear, but it may play a role in charge balancing (Rivetta et al., 2011).

Apart from Trk1p and Trk2p, there seems to be another potassium uptake system in the yeast plasma membrane, the **NSC1** (non-selective cation channel). It displays very low affinity for K^+ and works independently of both Trk1p and Trk2p (Bihler et al., 1998). Apart from potassium, the system also facilitates entry of lithium, sodium and ammonium cations into the cell (Bihler et al., 2002). It may be inhibited by mM concentrations of Ca^{2+} and other divalent cations, low extracellular pH, hygromycin B and, less extensively, tetraethylammonium. It has been demonstrated that NSC1 is the principal low-affinity uptake route for potassium in yeast (Bihler et al., 2002). Unfortunately, the gene(s) coding the protein(s) has yet to be identified (Ariño et al., 2010).

Potassium release

Tok1p (also known as *YPK1*; (Bertl et al., 1993), *YKC1*; Zhou et al. (1995), *YORK*; Lesage et al. (1996) and *DUK1*; Reid et al. (1996)) is a 691 amino acids long (77.4 kDa) voltage-dependent integral plasma membrane channel with strong outward directionality and high selectivity for potassium (Bertl et al., 1993; Ketchum et al., 1995; Fairman et al., 1999). While being the only K^+-specific efflux mechanism in yeast (Gustin et al., 1990; Bertl et al., 1993; Ketchum et al., 1995; Zhou et al., 1995), a small inward potassium current mediated by the channel has also been reported in the absence of Trk1p and Trk2p transporters (Fairman et al., 1999). It has also been reported that the presence of a functional Tok1p channel renders cells sensitive to Cs^+, most probably because it facilitates its influx (Bertl et al., 2003).

As predicted from its nucleotide sequence found on chromosome X (ORF J0911; Miosga et al. (1994)), Tok1p contains 8 transmembrane segments and two pore-forming P domains (Ketchum et al. (1995); Fig. 1.12). While P domains are structural entities common to all known K^+-selective ion channels (Ahmed et al., 1999), Tok1p is the first identified to contain two of them within a single polypeptide (Ketchum et al., 1995; Zhou et al., 1995; Goldstein et al., 2001). Furthermore, each of these domains forms a functional channel permeable to potassium, making the Tok1p channel unique in both its function and structure. It can therefore be considered a "founding member" of a new class of K^+ channels (Ketchum et al., 1995; Bertl et al., 1998). The uniqueness of the channel was also supported by the complete absence of homology of its sequence with any known protein at the time of discovery of its ORF (Miosga et al., 1994).

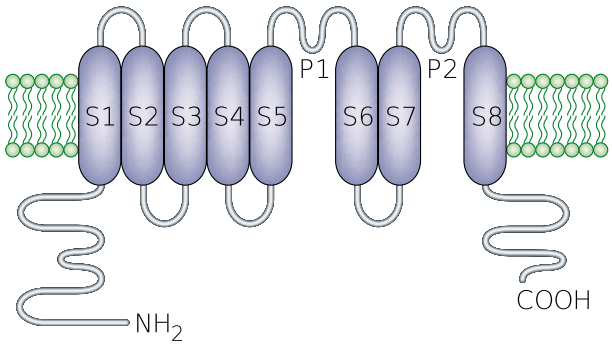

Figure 1.12: Predicted Tok1p channel topology. The channel is predicted to form two P domains (P1 and P2) and 8 transmembrane segments (S1-S8). Both C- and N-terminus are cytosolic. Reprinted from Goldstein et al. (2001).

Consistent with the prediction of Miosga et al. (1994), the Tok1p channel is expressed rather weakly, with only ∼40 protein molecules per cell, an estimate based on current measurements carried out first on isolated-patches (Bertl et al., 1993) and later on whole cells (Bertl et al., 1998). Nevertheless, the Tok1p expression is elevated after the diauxic-shift of a growing culture (DeRisi et al., 1997; Gasch et al., 2000; Brauer et al., 2005). To our best knowledge, there are currently no known expression regulators of the channel.

The Tok1p channel is predominantly closed at negative membrane voltages, but is opened by plasma membrane depolarization in a sigmoid manner (Bertl et al., 1993). The opening is dependent not on the absolute membrane potential value, but is triggered when $\Delta\Psi$ becomes more positive than the Nernst equilibrium potential for K^+ (Bertl et al., 1993; Ketchum et al., 1995; Vergani et al., 1997; Fairman et al., 1999; Loukin and Saimi, 1999). Hence, the Tok1p channel activity is modulated by external K^+ concentration. The activated state of the channel typically displays long flickery openings separated by gaps (Bertl et al., 1993). Once the channel is opened, K^+ accumulated in the cells can be released to regenerate membrane potential (Bertl et al., 1998). The outward potassium currents can be induced indirectly (i.e. the activation involves some, presently unknown, soluble cytoplasmic components) by activation of protein kinase C, but

not protein kinase A (Lesage et al., 1996). The channel is also phosphorylated at its C-terminus by the Hog1p MAP kinase and is proposed to play a minor role in the immediate response of the cell to osmotic stress (Proft and Struhl, 2004).

Opening of Tok1p under steady-state conditions is dependent on ATP in the cytoplasmic solution (Bertl et al., 1998) and is partially regulated by the cytosolic C-terminus that prevents closures of the channel (Loukin and Saimi, 2002). When expressed in *Xenopus* oocytes, the Tok1p channel has also been reported to mediate K^+ currents induced by the action of volatile anaesthetics (Gray et al., 1998). On the other hand, the channel is inhibited by tetraethylammonium ions (TEA^+; Gustin et al. (1990); Ketchum et al. (1995); Bertl et al. (1998), quinine (Lesage et al., 1996), extracellular Cs^+ and Ba^{2+} ions (Ketchum et al., 1995; Vergani et al., 1997) and low intracellular pH (while being insensitive to changes of extracellular pH in the range of 8.0-5.5; Lesage et al. (1996); Bertl et al. (1998)). Furthermore, there have been reports that the Tok1p channel is a target of the yeast viral killer toxin K1 (Ahmed et al., 1999) which is believed to act both from intra- as well as extracellular side of the plasma membrane (Sesti et al., 2001). While the binding of the toxin to the extracellular side of Tok1p is believed to cause, at least under certain conditions, opening of the channel, efflux of potassium and cell death (Ahmed et al., 1999), its binding to the intracellular side has been shown to inhibit the channel opening, therefore rendering the virus-infected cells immune to the extracellular toxin (Sesti et al., 2001). However, the K1 toxin interaction with the Tok1p channel and its physiological consequences are subject to debate (Breinig et al., 2002).

The behaviour of the channel can be described with a kinetic model with a single open state and three independent, parallel, closed states with distinct lifetimes: *gap* (long), *block* (short: 2-3 ms) and *interrupt* (very short: ∼0.3 ms). The channel can change between the open state and any of the closed states, but not directly from one closed state into another (Bertl et al., 1993).

While the Tok1p channel has been known for over two decades (Bertl et al., 1993; Ketchum et al., 1995; Zhou et al., 1995) and its electrophysiology has been well described (Gustin et al., 1990; Bertl et al., 1993), knowledge about its physiological function *in vivo* is still very limited. To this date, despite extensive efforts, no clear phenotype has been observed upon deletion of the *tok1* gene (Miosga et al., 1994; Zhou et al., 1995; Reid et al., 1996; Marešová et al., 2006, 2009). Furthermore, the deletion does not cause a change in intracellular concentration of either K^+ or Rb^+, as measured by atomic spectrophotometry. So far, it has only been shown that the deletion of the *tok1* gene results in plasma membrane depolarization, whereas overexpression of the *TOK1* gene leads to hyperpolarization of the yeast plasma membrane (Marešová et al., 2006).

Sodium efflux

Since sodium ions are toxic for the cell, they are not actively accumulated by yeast. However, their concentration might rise due to saline environment, NSC1-facilitated influx and due to the use of the Na^+ gradient across the plasma mem-

brane as fuel for inorganic phosphate import by Pho89p, the only yeast nutrient transporter known to require sodium for its activity (Martinez and Persson, 1998). Yeast therefore need to rid themselves of Na^+ against its electrochemical gradient, depending on two different systems.

The ***ENA*** (*exitus natru*) gene cluster (particularly *ENA1*) is a major sodium tolerance determinant in yeast *Saccharomyces cerevisiae*. The various *ENA* genes, usually localized in tandem on chromosome IV, encode identical or very similar P-ATPases (Haro et al., 1991; Martinez et al., 1991; Garciadeblas et al., 1993; Wieland et al., 1995). The exact number of these genes varies depending on the particular strain. Loss of the complete gene cluster results in hypersensitivity to sodium and lithium ions (Haro et al., 1991; Posas et al., 1995; Wieland et al., 1995; Gómez et al., 1996) and also impaired growth at alkaline pH (Haro et al., 1991; Platara et al., 2006). While Ena1p is highly effective in Na^+ export, Ena2p is more specific for Li^+ (Wieland et al., 1995) and K^+ which the Ena proteins also extrude (Benito et al., 2002).

Under standard growth conditions the number of Ena1p, Ena2p and Ena5p is estimated to be around 700 molecules per cell (Ghaemmaghami et al., 2003). Their expression is increased in the response to saline stress (e.g. presence of high NaCl) and alkaline pH (Wieland et al., 1995).

Based on their amino acid sequence, they have been predicted to form 9-10 transmembrane domains. This is consistent with the plasma membrane localization of Ena1p and Ena2p (Wieland et al., 1995). However, under conditions of overexpression, Ena1p has been also reported in intracellular membranes (Benito et al., 1997).

Nha1p (Na^+/H^+ antiporter) is a 985 amino acids long (109.3 kDa) Na^+/H^+ antiporter localized predominantly in detergent-resistant, ergosterol-rich fractions of the plasma membrane, requiring presence of sphingolipids for stabilization (Mitsui et al., 2009). Nha1p is indeed very stable with its half-life reaching up to 6 hours (Ariño et al., 2010). Besides sodium, the protein also transports potassium with similar affinity and its further substrates are lithium and rubidium, providing the cell with means of general cation detoxification (Bañuelos et al., 1998; Kinclová et al., 2001b). The functional Nha1p transporter is most probably a homodimer that requires more than one H^+ for transport of a single substrate ion (Ohgaki et al., 2005; Mitsui et al., 2009).

Based on its amino acid sequence, Nha1p has been predicted to form 12 transmembrane segments with a very short N-terminal tail and a relatively large C-terminal domain (both cytosolic), accounting for roughly half of the protein weight. The C-terminus seems to be involved in post-translational regulation of the protein (Kinclová-Zimmermannová and Sychrová, 2006; Simón et al., 2001, 2003; Kinclová et al., 2001b), being phosphorylated upon osmotic shock by the Hog1p kinase. The C-terminal tail phosphorylation leads to a change in Nha1p activity (Proft and Struhl, 2004), transiently inhibiting the Nha1p-mediated potassium efflux (Kinclová-Zimmermannová and Sychrová, 2006).

In contrast to *ENA* genes, expression of the *NHA1* gene, localized at chromosome XII, is constitutive, amounting to ∼1500 molecules per cell (Ghaemmaghami et al., 2003). The transcription does not seem to be induced by salts, changes in pH, nor osmotic shock, which suggests that Nha1p plays a housekeeping role in potassium homeostasis and maintenance of intracellular pH (Bañuelos et al., 1998; Sychrová et al., 1999; Brett et al., 2005). Like the Ena protein cluster, Nha1p plays an important role in tolerance against high extracellular salt concentrations and helps maintain high K^+/Na^+ ratio in the cytoplasm. While the Ena1p is important for proper cell growth at high KCl and NaCl concentrations at high pH when Nha1p is inhibited (Haro et al., 1991), Nha1p is important at acidic pH (Bañuelos et al., 1998). Hence, these two systems are somewhat complementary in their function.

Under certain circumstances, such as rapid alkalinization of the cytosol, Nha1p can act as a kind of a "safety valve", using the K^+ gradient to drive influx of protons into the cytosol (Ortega and Rodríguez-Navarro, 1985; Bañuelos et al., 1998; Kinclová et al., 2001b). Besides this important function in pH homeostasis and cation (Na^+ and Li^+) detoxification, Nha1p has been also shown to be involved in regulation of the cell cycle (Simón et al., 2001, 2003), cell volume and membrane potential (Kinclová-Zimmermannová et al., 2006; Marešová et al., 2006; Zahrádka and Sychrová, 2012), and in the rapid response to osmotic shock (Bañuelos et al., 1998; Kinclová et al., 2001a,b; Proft and Struhl, 2004). In all of these, Nha1p is probably somehow linked to the activity of Trk1p (and/or Trk2p; Kinclová et al. (2001a)).

Chapter 2

Material and Methods

2.1 Material

2.1.1 Yeast strains

The *S. cerevisiae* strains used in this study are listed in Table 2.1. They were stored at -20 °C in glycerol media designed for culture freezing. Pre-cultures on solid media were stored at 4 °C for no longer than a month.

Strain	Genotype
US50-18C	*MATα, PDR1-3, ura3, his1*
AD12	US50-18C *yor1::hisG, snq2::hisG* [1]
AD13	US50-18C *yor1::hisG, snq2::hisG* [1]
AD1-3	US50-18C *yor1::hisG, snq2::hisG, pdr5::hisG* [1]
AD1-3-*tok1*	AD1-3 *tok1::HPH* [2]
AD1-3 p_{TEF1}-pHl	AD1-3 p_{TEF1}-*pHl* [3]

[1] Decottignies et al. (1998)
[2] Constructed for this work by Ing. Otakar Hlaváček PhD., Institute of Microbiology, CR Academy of Sciences
[3] Constructed for this work by RNDr. Tomáš Hendrych PhD., Department of Genetics and Microbiology, Faculty of Science, Charles University

Table 2.1: *Saccharomyces cerevisiae* strains used in this study.

In the context of the study of Tok1p contribution to the plasma membrane potential maintenance, the strains AD1-3, AD1-3-*tok1* and AD1-3 p_{TEF1}-pHl are referred to as parent strain, *tok1* mutant and pHluorin-expressing variant of the parent strain, respectively.

The *tok1* mutant was prepared by deleting the *TOK1* gene from the AD1-3 strain using homologous recombination. The pUG6-32 plasmid (*hph* marker – resistance to hygromycin B) was used as a PCR template for preparing the disruption cassette. The plasmid had been constructed previously from plasmids pUG6 and pAG32 (Euroscarf, Bad Homburg, Germany) to enable the *hph* marker rescue, as the original pAG32 plasmid does not contain *loxP* sites (Goldstein and

McCusker, 1999). A plasmid with the same function is now available from Euroscarf under the name pUG75 (Hegemann and Heick, 2011).

The AD1-3 p_{TEF1}-pHl strain harbouring pHluorin with a strong constitutive pTEF1 promoter instead of the *HIS3* gene was prepared using homologous recombination with two overlapping cassettes. One, containing the pTEF1 promoter, was prepared with pYM-N20 plasmid (*nat* marker - resistance to nourseothricin, Euroscarf, Bad Homburg, Germany) as PCR template, the other with pHluorin was obtained from plasmid pVT100U kindly provided by Dr. Aleš Holoubek. Correct cytosolic localization was verified by confocal fluorescence microscopy.

Both mutant strains retained the growth characteristics of their parent strain (monitored by measuring optical density at 578 nm [OD_{578}] of the growing culture with an Amersham Biosciences Novaspec III spectrophotometer), in agreement with previous research in the case of *tok1* deletion (Marešová et al., 2006).

2.1.2 Overview of used chemicals

Compound	M.W.	Producer
Agar	-	Carl ROTH
Bactopeptone	-	Oxoid
D-glucose	180.16	Sigma-Aldrich
Ethanol	46.07	Lach-Ner
Glycerol	92.10	Lach-Ner
Yeast extract	-	Serva

Table 2.2: Overview of cultivation media components used in this study.

2.1.3 Cultivation media and buffers

Yeast cultivation

Liquid cultivation medium (YPD), per 1000 ml:
yeast extract - 20 g, peptone - 10 g, D-glucose - 20 g

Medium for culture freezing (storing), per 100 ml:
yeast extract - 2 g, peptone - 1 g, D-glucose - 10 g, glycerol - 60 g

YPD agar for cultivation on Petri dishes, per 1000 ml:
agar - 10 g, yeast extract - 10 g, peptone - 10 g, D-glucose - 20 g

Top YPGE agar for drug susceptibility assays, per 1000 ml:
agar - 10 g, yeast extract - 10 g, peptone - 10 g, glycerol - 20 g, ethanol - 20 g

Compound	M.W.	Producer
Ethanol for UV spectroscopy	46.07	Lach-Ner
1-propanol	60.10	Sigma-Aldrich
1-butanol	74.12	Sigma-Aldrich
1-pentanol	88.15	Sigma-Aldrich
1-hexanol	102.18	Sigma-Aldrich
Ammonium acetate	77.08	Sigma-Aldrich
Citric acid	192.13	Lach-Ner
Dimethyl formamide (DMF)	73.10	Fluka
Dimethylsulfoxide (DMSO)	78.13	Fluka
Hydrochloric acid (HCl) 35%	36.46	Lachema
$Na_2HPO_4 \cdot 12H_2O$ (reagent grade)	358.14	Sigma-Aldrich
Potassium chloride (KCl)	74.56	Fluka
Sodium azide (NaN_3)	65.01	Sigma-Aldrich
Sodium chloride (NaCl)	58.44	Sigma-Aldrich
Sodium hydroxide (NaOH), pellets	40.00	Sigma-Aldrich

Table 2.3: Overview of chemicals and stressors used in this study.

Compound	M.W.	Producer	Solvent
2-deoxy-D-glucose	164.16	Sigma	distilled water
BAC	337.00	Fluka	distilled water
CCCP	204.60	Fluka	DMF
diS-C_3(3)	520.49	Fluka	ethanol
DM-11	308.00	*	distilled water
FK506 (fujimycin)	804.32	RC Laboratories	ethanol
Fluconazole	306.27	Sigma-Aldrich	DMSO
Ketoconazole	531.43	Sigma-Aldrich	DMSO
Nigericin	746.90	Sigma-Aldrich	ethanol
NQO	190.17	Supelco	distilled water
ODDC	623.80	Schülke & Mayr	distilled water
TEA^+Cl^-	165.71	Sigma-Aldrich	distilled water

BAC - benzalkonium chloride, CCCP - carbonyl cyanide *m*-chlorophenyl hydrazone, diS-C_3(3) - 3,3'-dipropylthiacarbocyanine iodide, DM-11 - 2-dodecanoyloxyethyldimethylammonium chloride, NQO - 4-nitroquinoline 1-oxide, ODDC - octenidine dichloride, TEA^+Cl^- - tetraethyl ammonium chloride

* - The lysosomotropic compound DM-11 (2-dodecanoyloxyethyldimethylammonium chloride) was synthesized in the laboratory of Prof. S. Witek (Univ. Wroclaw; Witek et al. (1997)) and kindly provided by Dr. A. Krasowska.

Table 2.4: Overview of chemical stressors and PDR inhibitors used in this study.

Bottom YPG agar for drug susceptibility assays, per 1000 ml:
agar - 20 g, yeast extract - 10 g, peptone - 10 g, glycerol - 20 g

Measuring and calibration buffers

Citrate-phosphate (C-P) buffer, per 1000 ml:
$Na_2HPO_4 \cdot 12H_2O$ - 3.60 g (10 mM), titrated with citric acid to pH 6

Citrate-phosphate (C-P) buffer for pH measurement calibration, per 1000 ml:
$Na_2HPO_4 \cdot 12H_2O$ - 3.60 g (10 mM), KCl - 3.73 g (50 mM), NaCl - 2.87 g (50 mM), sodium azide 0.65 g (10 mM), ammonium acetate 15.42 g (200 mM), titrated with either hydrochloric acid od NaOH to desired pH.

2.2 Methods

2.2.1 Yeast cultivation and preparation

Small amount of cells from the glycerol stock was spread on YPD Petri dishes with a sterile inoculation loop and grown in an incubator (*Incucell - BMT medical technologies s.r.o.*) at 30 °C for 48 hours. A small amount of the grown culture was then transferred with a sterile inoculation loop into 10 ml of liquid YPD medium (in a 50 ml Erlenmeyer flask) and grown in a shaking water bath (*GFL 1083*) at 30 °C for 24 hours. These pre-cultures were then stored in a refrigerator at 4 °C for up to a week and used to inoculate the main cultures with 5-10 µl (depending on the experiment and cultivation time). The main cultures were then grown at 30 °C until the desired OD_{578} was reached.

2.2.2 Measurement of PDR pump activity and membrane potential changes with diS-C_3(3) fluorescent probe

Cells were cultivated as described in 2.2.1 and harvested upon reaching the desired OD_{578}. They were washed twice with double-distilled water and resuspended in C-P buffer (see 2.1.3). The concentration of cells was set to OD_{578}=0.13 ($2.5 \cdot 10^6$ cells/ml) and 3 ml aliquots of the cell suspension were taken in PMMA cuvettes (1×1 cm). These were then labelled with the diS-C_3(3) dye to a final concentration of $2 \cdot 10^{-8}$ M 30 seconds before the acquisition of the first emission spectrum.

Fluorescence emission spectra were recorded with spectrofluorimeters *FluoroMax-3*® and *FluoroMax-4*® (Jobin-Yvon Horiba, SPEX) equipped with a xenon lamp (excitation wavelength: 531 nm; acquisition range: 560-590 nm; step: 1 nm; integration time: 0.3 s; slits of used excitation and emission monochromators: 10 nm bandpass) at 2-3 min intervals. Scattered light was eliminated with an orange glass filter (Zeiss 1752 - cut-off at 540 nm / B+W 39 040 4x MRC - cut-off at 550 nm).

The dependence of the diS-C_3(3) fluorescence emission maximum wavelength, λ_{max}, on time is depicted by the so-called staining curve (Denksteinová et al., 1997; Gášková et al., 1998). When appropriate, the tested compound was added to the desired final concentration either 10 minutes before or 10-20 minutes after

the beginning of staining. The samples were kept at room temperature and occasionally gently stirred by turning upside-down. To partially automate the measurements of staining curves, including λ_{max} determination, the program HUGO was used (Hendrych, 2009).

The method enables us to monitor both PDR pump activity and membrane potential. While these two attributes are independent (Gášková et al., 2002) of each other, the resulting staining curves are a combination of the two. Therefore, when monitoring the effect of various substances on membrane potential, it is of great advantage to use PDR pump-deficient strains. However, it should be emphasized here that the equilibrium staining (λ^{eq}_{max}) values cannot be directly converted to underlying membrane potential values in mV (Plášek et al., 2012). Using our calibration-free method, only differences in plasma membrane potentials under two different conditions (e.g. presence of a stressor or absence of a gene) can be acquired using the difference in equilibrium staining values ($\Delta\lambda^{eq}_{max}$). The conversion of this difference to membrane potential changes in mV relies on the fact that λ^{eq}_{max} values are clearly linked to the B/A ratio of the fractions of bound dye spectra and free dye spectra in the final spectrum (Plášek and Gášková, 2014). The difference of their logarithms, $log(B/A)_2 - log(B/A)_1$, assessed through $\Delta\lambda^{eq}_{max}$ can be used to calculate the difference of underlying membrane potentials: $\Delta\Psi_2 - \Delta\Psi_1 = (RT/F)[log(B/A)_2 - log(B/A)_1]$, where R, T and F are the universal gas constant, absolute temperature and Faraday constant, respectively.

2.2.3 Monitoring of cytosolic pH by the means of synchronously scanned pHluorin fluorescence

pHluorin-expressing AD1-3 cells (section 2.1.1) were cultivated (section 2.2.1) and harvested as for the fluorescence measurement (section 2.2.2). They were resuspended in 10 mM C-P buffer (same as for membrane potential measurements; see 2.1.3), to a final cell density three times higher to provide better signal-to-noise ratio. Cytosolic pH (pH_{cyt}) was measured using the method of synchronously scanned fluorescence, as described by Plášek et al. (2015), with the aforementioned modification of the used buffer to bring the experimental conditions closer to those used for membrane potential measurements.

Calibration was carried out in the same buffer as the measurements, with the addition of 50 mM KCl and 50 mM NaCl to stabilize the cells; 10 mM sodium azide to inhibit the Pma1p H^+ATPase through cellular ATP depletion; and 200 mM ammonium acetate to equilibrate the pH across the vacuolar and plasma membranes (Preston et al., 1989; Ali et al., 2004). The buffer was then titrated with either HCl or NaOH to various pH values in the range of 4.6 to 8.2. Synchronously scanned fluorescence spectra of the pHluorin-expressing cells resuspended in this set of buffers were measured over the course of an hour. From the obtained values, only the ones stable in time were used for the calibration curve (Fig. 2.1) which is in very good correspondence with that obtained pre-

viously with digitonin-treated cells in 10 mM citrate-phosphate buffer, therefore validating the use of our calibration buffer (Orij et al., 2009).

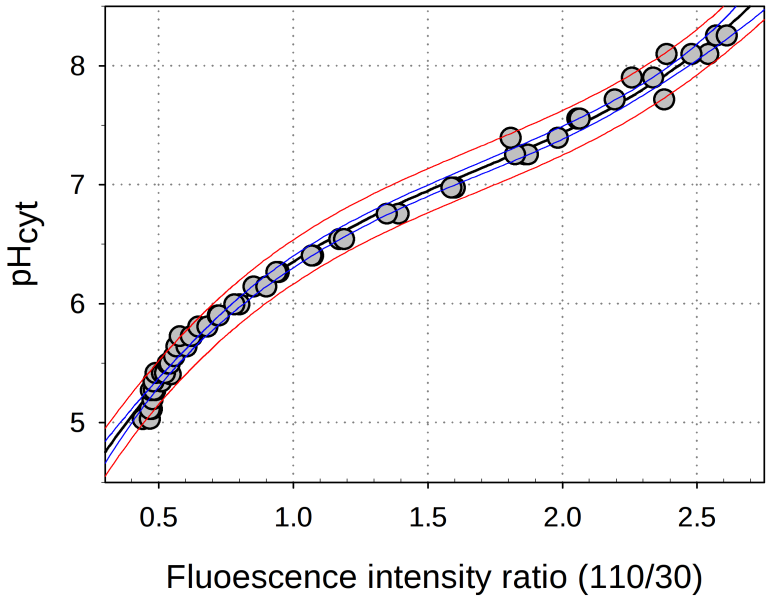

Figure 2.1: Calibration curve used for the pH_{cyt} measurements. The experimental data are depicted by grey circles. Black line is the dependence fitted to the cubic equation: pH_{cyt}=3.609+4.384**IR*-2.044**IR*^{2}+0.405**IR*^{3}; *IR* - intensity ratio. Blue and red lines enclose the areas of 95 % confidence and 95 % prediction bands, respectively.

In the actual measurements, synchronously scanned fluorescence spectra were measured for ca. 120 minutes to follow the time course of pH_{cyt} changes. Where appropriate, the stressors were added either ∼10 minutes before (TEA^+) or ∼12 minutes after the start of the assay. Accumulated spectra were processed as described by Plášek et al. (2015) and the pH_{cyt} values were calculated from the obtained ratios according to the calibration curve. During the experiments, the samples were gently stirred by turning upside-down three times just before each measurement.

Each pH_{cyt} measurement included 3-4 extra samples with the studied cells resuspended in various calibration buffers to verify the coincidence with the calibration curve. These were measured both before and after the measurement of pH_{cyt}.

2.2.4 Monitoring of extracellular pH with a pH meter

Exponential cells were cultivated and harvested as described above (see 2.2.1 and 2.2.2, respectively) and resuspended in double-distilled water to final concentration equivalent to OD_{578}=2.0. Extracellular pH was recorded with one minute intervals using an *Inolab 7310* pH meter using a *Sentix 81* pH electrode. Cell

suspensions were continuously gently stirred with a magnetic stirrer. Glucose and alcohols were manually injected to final concentrations specified in the figure legends, at designated times.

2.2.5 Monitoring of pHluorin localization and cell wall integrity via confocal microscopy

Cells for both cytosolic pHluorin localization (pHluorin-expressing variant of the AD1-3 strain) and cell wall integrity (AD1-3 strain) measurements were cultivated (section 2.2.1) and harvested as for the fluorescence measurements (section 2.2.2). They were resuspended in 10 mM C-P buffer (same as for membrane potential measurements; see 2.1.3), to the same final density.

The cells were then treated with respective chemicals (glucose, CCCP, DM-11, ODDC or BAC) and in the case of cell wall integrity measurements also with calcofluor (2 µl/ml cell suspension). Cells were then fixed with 1 % agarose gel on microscopic slides to prevent their movement and the effect of the stressors on pHluorin localization was monitored using an Olympus IX83/FV1200 laser scanning microscope with a water immersion objective UPLSAPO 60x/1.2. Images obtained with the scanning microscope were cropped and their contrast was digitally enhanced using the open source digiKam (version 4.12.0) software where appropriate.

2.2.6 Monitoring of drug susceptibility via Kirby-Bauer disc diffusion assay

Exponential cells were cultivated and harvested as described above (see 2.2.1 and 2.2.2, respectively) and resuspended in sterile C-P buffer. Consequently, the cells were diluted in YPGE top agar of 45 °C to a final concentration of 2.5×10^6 cells/ml and poured onto YPG plates (for agar and C-P buffer composition, see 2.1.3).

Tested chemicals (2 µl) were spotted onto Whatman paper discs lying on the top of the top agar. After 48 hours at 30 °C, the plates were photographed and the sizes of the growth-inhibition zones were measured.

To find out whether the alcohols under study are substrates of Pdr5p and Snq2p pumps, two types of the disc-diffusion test were performed: the standard version (Kolaczkowski et al., 1998), using AD12, AD13 and AD1-3 cells, and its simplified variation designed to detect Pdr5p substrates only, therefore only using AD12 cells. In the latter, the tested alcohol was spotted on two paper discs, one of which had been pretreated with FK506 (2 µl of 50 mM ethanol solution) 15 minutes before, in effect simulating the AD1-3 cells, since FK506 is a potent Pdr5p inhibitor.

To determine whether a particular alcohol is able to inhibit the extrusion of a known substrate (BAC, ketoconazole or nigericin for Pdr5p; 4-NQO for Snq2p) by the pumps, we used a 'double addition' mode of the standard disc-diffusion

test (Hendrych et al., 2009). The tested alcohols were added 15 minutes before the known substrate.

2.2.7 Monitoring of drug susceptibility via plating tests

Cells were grown to the desired growth-phase as described in section 2.2.1 and harvested as for the fluorescence measurements (section 2.2.2). They were then resuspended in 10 mM C-P buffer (same as for membrane potential measurements; see 2.1.3), to a final cell density two times higher.

The cells were then incubated with various concentrations of alcohols, DM-11, ODDC or BAC at room temperature with continuous gentle stirring. At designated times aliquots of 100 µl were taken from the samples and diluted 10-fold three times (i.e. to the final 1000-fold dilution). Three to five replicate aliquots of 100 µl were then plated on 1 % YPD agar plates (1 % agar, 1 % yeast extract, 1 % peptone, 2 % glucose) and incubated for 2 days at 30 °C. Colonies were counted and the relative survival rates were calculated. For control samples the number of colonies per plate was about 200.

2.2.8 Monitoring of cellular material release via measurements of absorbance at 260 nm

Cells were cultivated (see 2.2.1) and harvested as for the fluorescence measurements (section 2.2.2). They were resuspended in 10 mM C-P buffer (same as for membrane potential measurements; see 2.1.3), to the same final cell density.

Aliquots of the cell suspension were incubated with various concentrations of either the respective alcohol or BAC at room temperature with continuous gentle stirring. Aliquots of 3 ml were taken at designated times, centrifuged once and 2 ml of the supernatant were used for absorption measurements. The absorption spectra were accumulated using 1×1 cm quartz cuvettes using a Varian Cary 50 UV spectrophotometer (acquisition range: 200-400 nm; step: 1 nm; integration time: 0.2 s). The absorbance was determined after baseline correction as the average of values measured in the interval of 260±2 nm.

2.2.9 Monitoring of the extent of permeabilization via propidium iodide staining

Cells were cultivated (see 2.2.1) and harvested as for the fluorescence measurements (section 2.2.2). They were then resuspended in 10 mM C-P buffer (same as for membrane potential measurements; see 2.1.3), to the same final cell density.

Aliquots of 0.5 ml were then incubated in Eppendorf tubes with various BAC concentrations for the desired period of time and occasionally gently stirred. The aliquots were then stained by adding 1 µl of propidium iodide solution and incubated for 10 minutes. 20 µl were then transferred to a SD100 Cell counting chamber and the amount of permeabilized cells was measured in a Nexcelom Bioscience LLC Cellometer® Vision using the VB595-502 emission filter. The data

were analysed using the Cellometer Vision software. Propidium iodide, counting chambers, the emission filter and analysis software were all provided by Nexcelom Bioscience LLC with the instrument.

2.2.10 Preparation of permeabilized cells

Cells were cultivated (see 2.2.1) and harvested as for the fluorescence measurements (section 2.2.2). They were then resuspended in 10 mM C-P buffer (same as for membrane potential measurements; see 2.1.3), to the same final cell density. In order to permeabilize the cells, two methods were used:

(a) **Permeabilization induced by heat shock**: The cell suspension was submerged in a water bath of 60 °C for 10 minutes (Gášková et al., 1999) and then kept on ice for 5 minutes.

(b) **Chemically-induced permeabilization**: The cells in suspension were exposed to 3 µM octenidine dihydrochloride (ODDC) for 15 minutes (this exposure time and ODDC concentration are sufficient to achieve full permeabilization, as shown by Kodedová et al. (2011)). The cells were then washed twice in distilled water to remove the drug and resuspended in C-P buffer to their original concentration before washing.

The cells were then used as a suspension of solely permeabilized cells or mixed with untreated cells to obtain the desired permeabilized:intact cells ratio.

Chapter 3

Results and Discussion

3.1 Motivation and specification of the aims of the thesis

Sometimes I do miss my motivation a bit.
I hope she is well, wherever she is. [1]

As mentioned in the introduction, the effect of chemical stressors may be studied in the context of their action on the plasma membrane and the enzymes embedded in it. The diS-$C_3(3)$ fluorescence assay enables us to study the way the stressors influence the activity of multidrug resistance (MDR) proteins and the effects they have on plasma membrane potential ($\Delta\Psi$), either by affecting the proteins involved in $\Delta\Psi$ maintenance or the lipid bilayer itself. The results of the thesis are divided accordingly into two parts.

The evolutionary need to protect oneself combined with natural selection and overuse of antibiotics and sanitation products over the past decades inevitably gave rise to the phenomenon of **multidrug resistance** (MDR). Mediated in part by proteins (also called pumps) that actively and effectively expel a wide range of unrelated substances out of the cell, MDR is responsible for the inefficiency of sanitation, sterilization of working surfaces and most importantly failure of treatment of diseases ranging from bacterial infections through mycoses all the way to cancer. In order to enhance the treatment efficiency and lessen the side effects, it is of great importance to find ways to inhibit the proteins mediating MDR.

The first part of the doctoral thesis builds on previous work of our Biophysics Group, mainly the development of the diS-$C_3(3)$ fluorescence assay and the findings that it can be conveniently used to monitor the activity of Pdr5p and Snq2p ABC (ATP-binding cassette) transporters, the main culprits of MDR in the yeast *S. cerevisiae*. The assay is based on the fact that the used fluorescence probe,

[1] adapted from mademyday.com

diS-C_3(3) (3,3'-dipropylthiocarbocyanine iodide), is a substrate of both of these transporters that pump it out of the cell. Inhibition of the pumps therefore leads to higher staining of the cell.

Ethanol and other alcohols have been known to the big benefit of mankind for thousands of years. Their effect on humans, especially in the context of cognitive functioning and cardiovascular system, have been well documented. While it had originally been assumed that the effect of alcohols originates within their interaction with the lipids of cell membranes, cases of direct alcohol-protein interactions were later reported as well. Furthermore, it has been shown in the yeast *S. cerevisiae* that ethanol and other alcohols inhibit a range of permeases for various substrates (e.g. sugars, ammonium and amino acids) in a non-competitive way. The degree of inhibition has been shown to be dependent on the solubility of the alcohol in the lipid phase. While the molecular basis of this inhibition is still subject to debate, the end result is always lowering of protein activity.

Since alcohols interact with a wide range of proteins, from receptors and channels to transporters, we were interested in studying the effect of short n-alcohols (from ethanol to hexanol) on the *S. cerevisiae* MDR pumps Pdr5p and Snq2p.

The existence and extent of **plasma membrane potential** ($\Delta\Psi$) is the result of a plethora of electrogenic processes connected with transport of various substances across the plasma membrane. Due to the importance of membrane potential, the processes involved in its creation and maintenance need to be tightly regulated. While the role of the Pma1p H^+-ATPase in these processes has been studied extensively in the last 30-40 years, the role of potassium deserves further and closer attention.

One of the proteins involved in potassium movement across the plasma membrane is the highly specific K^+ channel Tok1p. Displaying strong outward directionality, its opening is induced by membrane depolarization, as has been reported by a range of electrophysiological studies. While identified before ∼30 years and characterized in detail in the context of its biophysics under various conditions, the physiological role and importance of the channel *in vivo* remains unclear.

We have therefore decided to study the response of the channel to depolarization-inducing chemical stress and its contribution to membrane potential under such conditions. Our attention was focused mainly on the answering of the following questions:

1. How effectively can the Tok1p-mediated potassium currents counterbalance chemically induced depolarization?

2. Does the stressor's mode of action affect the activity of the Tok1p channel?

3. If so, which side effects of the stressors exert minimal/maximal influence on its activity?

To answer these questions, we deployed several chemical stressors with known modes of action and known impact on plasma membrane potential and followed their effect on the Tok1p channel activity using the diS-C_3(3) assay. This part of

the thesis is based on the knowledge that in the absence of pumps extruding the fluorescence probe out of the cytosol, the overall staining is governed solely by the plasma membrane potential of the cell.

3.2 Alcohols act as inhibitors of *S. cerevisiae* PDR pumps Pdr5p and Snq2p

3.2.1 Determination of the amount of permeabilized cells

As discussed in section 1.5.2, the diS-C_3(3) fluorescence assay is a very suitable method for the studying of Pdr5p and Snq2p activity and for identification of their inhibitors. Elevated accumulation of the diS-C_3(3) probe in the cells, resulting in a red shift of the overall fluorescence signal, is generally caused either by hyperpolarization of the cells or by inhibition of pump-facilitated probe export. However, the red shift can also be caused by permeabilization of a part of the cells in the suspension (Gášková et al., 2001; Kodedová et al., 2011), which can lead to misinterpretation of the data. It is therefore crucial that we are able to monitor this undesired effect.

The most convenient way to monitor the amount of permeabilized cells in suspensions used in a fluorescence measurement is the application of the so-called CD cocktail (Hendrych et al., 2009; Kodedová et al., 2011) which combines the activity of the protonophore carbonyl cyanide *m*-chlorophenyl hydrazone (CCCP) and a Pma1p inhibitor, the lysosomotropic compound 2-dodecanoyloxyethyldimethylammonium chloride (DM-11; Witek et al. (1997)). Addition of their equimolar mixture to cells results in complete depolarization of intact plasma membranes due to inability of the DM-11-inhibited Pma1p to counteract the CCCP-mediated influx of protons, leading to a shift of staining to λ_{max} ∼570 nm, i.e. very close to the λ_{max} of the unbound probe in aqueous solutions. However, when the CD cocktail is added to permeabilized cells stained with diS-C_3(3), no blue shift (i.e. a shift towards shorter wavelengths) is observed, since the proton gradients (as well as gradients of other ions) have already been dissipated. The CD cocktail can therefore be used to estimate the amount of permeabilized cells in a diS-C_3(3)-stained suspension. This is useful especially after exposure of cells to one or more chemical stressors over an extended period of time.

In order to make use of the cocktail, however, it is first necessary to perform a calibration experiment. Permeabilized Pdr5p-expressing AD12 and pump-deficient AD1-3 cells were prepared as described in section 2.2.10 and mixed with intact cells in defined ways to obtain various permeabilized:intact cells ratios. The suspensions were then stained with the diS-C_3(3) fluorescent probe, followed by the addition of the CD cocktail ∼45 minutes later. Subsequently, $\lambda^{eq}_{max/CD}$ was recorded, Figure 3.1.

It is readily observable from Figure 3.1 that the diS-C_3(3) staining of both strains is dependent on the amount of permeabilized cells in the sample. Fully viable AD1-3 cells (lacking both Pdr5p and Snq2p; Fig. 3.1(a)) are stained gradually according to their membrane potential and an equilibrium is achieved after ∼30-40 minutes, a staining rate typical for pump-deficient strains (Gášková et al., 1998). However, as the percentage of permeabilized cells elevates, so does the staining level and also its rapidity. Suspensions containing exclusively permeabilized cells stain practically immediately.

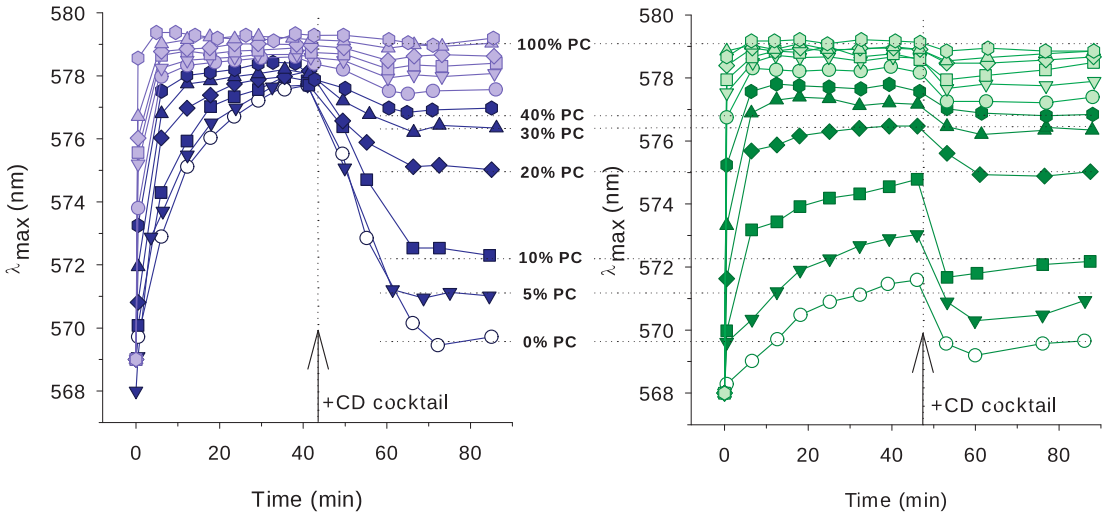

(a) AD1-3 (b) AD12

Figure 3.1: Calibration of the fluorescence response of suspensions to CD cocktail addition, depending on the amount of permeabilized cells. Staining curves of **(a)** AD1-3 and **(b)** AD12 cell suspensions containing various amounts of permeabilized cells (PC): 0 % - empty circles, 5 % - dark inverted triangles, 10 % - dark squares, 20 % - dark diamonds, 30 % - dark triangles, 40 % - dark hexagons, 50 % - light circles, 60 % - light inverted triangles, 70 % - light squares, 80 % light diamonds, 90 % - light triangles and 100 % - light hexagons. The arrows and vertical dotted lines indicate the addition of the CD cocktail (i.e. 10 µM CCCP + 10 µM DM-11). Data are representative of three independent measurements.

Addition of the CD cocktail to intact AD1-3 cells leads to λ_{max} levels almost identical to those characteristic for the unbound probe in aqueous media. When permeabilized cells are present in the suspension, however, the resulting λ_{max} is considerably higher, as permeabilized cells do not respond to the CD cocktail. The final staining level is directly dependent on the amount of permeabilized cells and is hence a good indicator thereof.

The effect of the presence of permeabilized cells on suspension staining is even more striking in the case of the Pdr5p-expressing AD12 strain (Fig. 3.1(b)), since the probe is actively exported by the pump, leading to relatively low staining. Importantly, however, presence of pumps plays no role in the fluorescence response to CD cocktail, as is readily observable from the comparison of Figure 3.1(a) and Figure 3.1(b). Qualitatively equal results as with the AD12 strain were obtained with the Snq2p-expressing AD13 strain (data not shown). Note that the estimate of the amount of permeabilized cells in the suspension is not accurate above 40 % due to non-linear response of the diS-C_3(3) probe above ∼578 nm (Plášek and Gášková, 2014). Even in such a case, the application of the CD cocktail provides invaluable insight into the intactness of the cells in the suspension and therefore validity of obtained results.

The reliability of the permeabilization procedure (and hence the calibration itself) was verified by the means of a plating test (section 2.2.7), where the dependence of cell survival (in terms of the number of colony forming units; relative

to suspensions of fully intact cells) on the fraction of permeabilized cells was monitored, Figure 3.2.

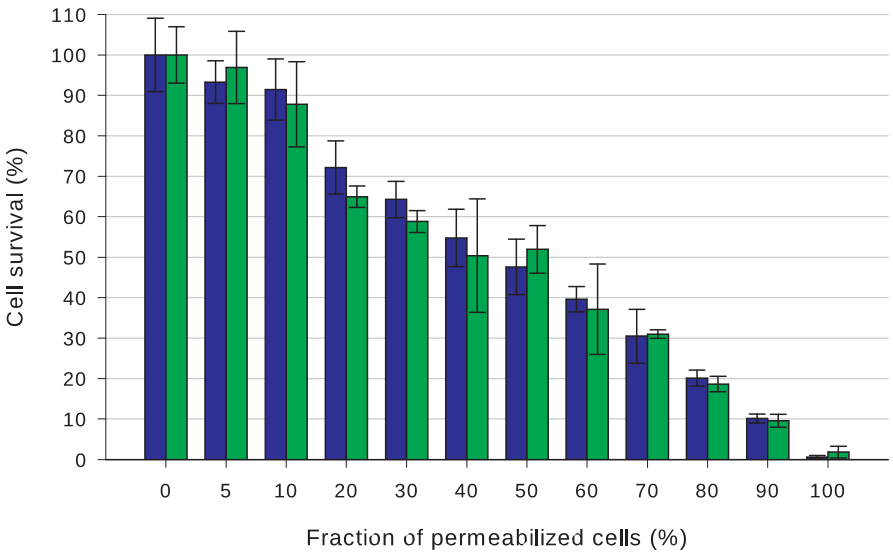

Figure 3.2: Cell survival rate directly mirrors the amount of permeabilized cells in the suspensions of AD1-3 and AD12 cells. As the two different approaches of permeabilized cells preparation (section 2.2.10) yielded the same results within the standard error, only the data for heat-shock permeabilized cells are presented here. Data are calculated from two independent measurements, consisting of three biological replicas each. Error bars indicate SDs.

3.2.2 Effect of alcohols on the activity of the pumps Pdr5p and Snq2p

As mentioned above, staining of pump-expressing strains is relatively low compared to their pump-deficient counterpart(s) due to active efflux of the diS-C_3(3) fluorescent probe. In turn, inhibition of the pump(s) leads to elevated staining, identical to that of the pump-deficient control(s) once full inhibition is achieved. Any possible effect of an inhibitor on membrane potential will be of the same degree in all treated strains, since pleiotropic drug resistance (PDR) pump activity and membrane potential are independent (Gášková et al., 2001).

The possible inhibition of PDR pumps by alcohols was studied in exponential Pdr5p- (AD12) and Snq2p-expressing (AD13) cells by the means of the diS-C_3(3) fluorescence assay (section 2.2.2). Their staining was compared with the pump-deficient AD1-3 isogenic strain, Figure 3.3. Exponential cells were chosen due to significantly elevated expression of PDR pumps in this growth phase compared to older cells (Mamnun et al., 2004; Čadek et al., 2004; Maláč et al., 2005). Alco-

hols (ethanol to hexanol[2]) were added to the cell suspensions ∼10 minutes after the probe to various, relatively low (max 3 %), final concentrations. While many studies in the past were concerned with finding the optimal inhibitory concentration for various alcohols (Leão and van Uden, 1982, 1984; Casal et al., 1998), we focused on the comparison of the alcohol effects at low concentrations. Since ethanol is tolerated very well by yeast (as discussed in detail in section 1.4.3), it served as the reference compound.

Keeping the high tolerance in mind, it is hardly surprising that ethanol (up to the tested 3 %) produces only a negligible effect on the activity of both Pdr5p and Snq2p. Starting from propanol, however, the alcohol-treatment of cell suspensions leads to a red shift (i.e. a shift to longer wavelengths) of staining of both AD12 and AD13 cells. As described in section 3.2.1, apart from pump inhibition, the observed red shift might also be connected to permeabilization of cells due to the action of the used alcohols. Indeed, addition of the CD cocktail reveals that higher alcohol concentrations lead to a certain degree of permeabilization, especially in the case of longer alcohols, most notably hexanol, Figure 3.3. Nevertheless, even in the concentration range where the permeabilization is negligible (i.e. staining of CD cocktail-treated cells is close to 570 nm), there is still a significant effect of alcohols on the pump activity. Application of the CD cocktail clearly reveals that yeast cells can be permeabilized by the action of alcohols if their concentration is sufficiently high. This means that the alcohols may exhibit a dual action on the cells, i.e. inhibit MDR pumps as well as cause permeabilization.

As is readily observable from Figure 3.3, the effect of alcohols on PDR pumps depends both on their concentration and on the length of their carbon chain. Specifically, gradually elevating the concentration to 3 % leads to more extensive inhibition in the case of all studied alcohols with the exception of ethanol. Elongation of the carbon chain of the alcohol also leads to higher inhibition efficiency, just as it was reported for both general anaesthesia (effect on lipids; Pringle et al. (1981)) and direct alcohol-protein interactions (Peoples et al., 1996; Kubo et al., 2003). As a direct comparison, consider the corresponding staining of AD12 (or AD13) cells treated with 2 % propanol, 0.2 % pentanol and 0.07 % hexanol.

The fact that concentrations of ethanol up to 3 % produce negligible effects on the PDR pump activity and plasma membrane integrity is not very surprising, since ethanol is a natural product of *S. cerevisiae* metabolism and the yeast are able to tolerate it well. We were therefore interested if further elevation of ethanol concentration might produce any effect, Figure 3.4. While the membrane potential is unaffected by up to 9 % ethanol (leading to depolarization when elevated further), there is a clear inhibitory effect observable already after exposure of cells to 6 % ethanol, reaching its full potential at 15 %. Importantly, while causing deep depolarization, even exposure to such a high ethanol concentration for ∼60 minutes does not cause permeabilization of the plasma membrane, as verified by the use of the CD cocktail.

[2]Methanol is generally even less toxic for yeast than ethanol (Troyer, 1953, 1955). Alcohols with longer carbon chain lengths than hexanol were not used due to their very limited (almost non-existent) solubility in distilled water.

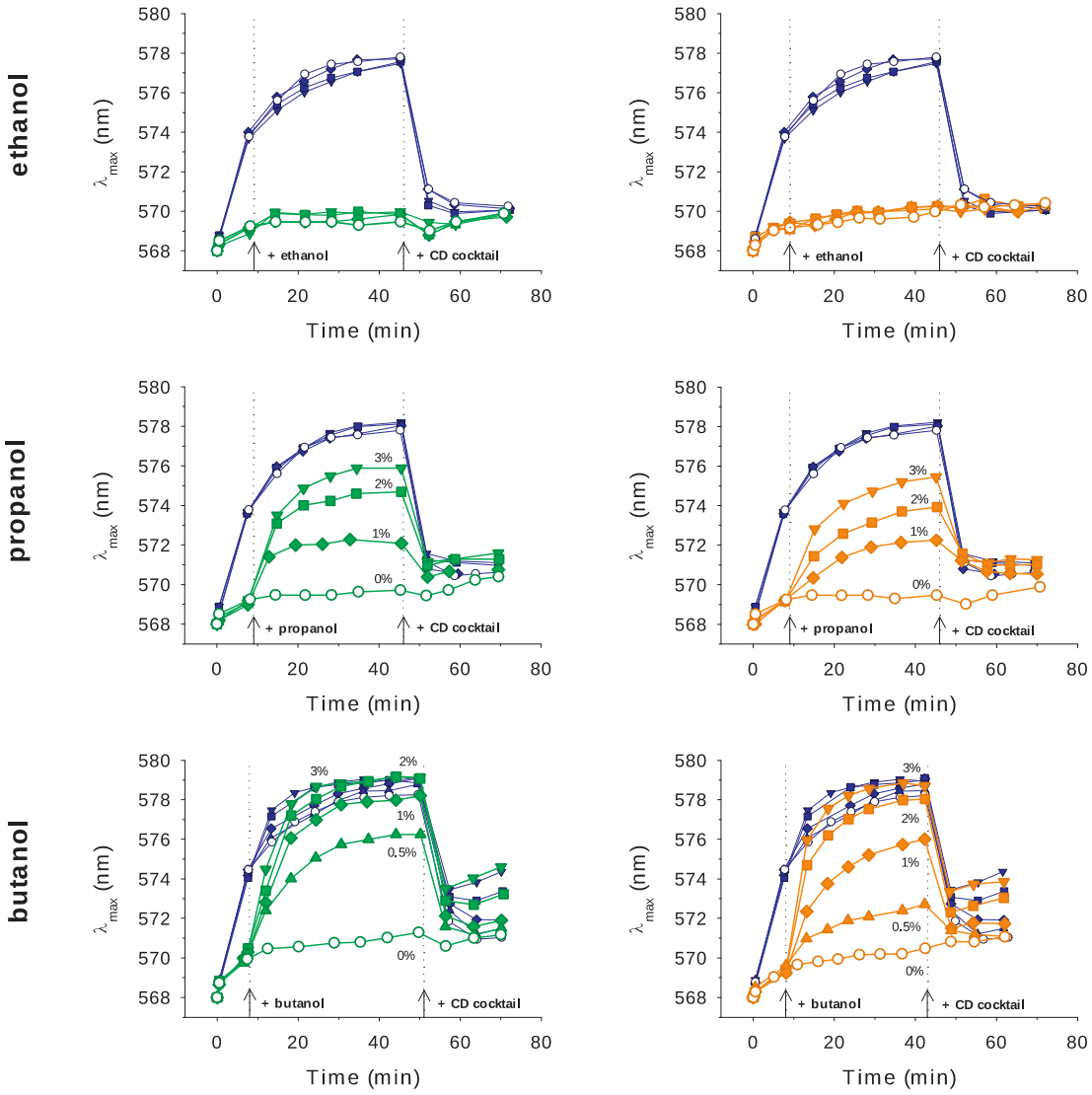

(a) AD12 (b) AD13

Figure 3.3: Elongation of the alcohol carbon chain length leads to rise in both Pdr5p and Snq2p inhibition activity. Staining of exponentially growing **(a)** Pdr5p-expressing AD12 and **(b)** Snq2p-expressing AD13 cells exposed to various concentrations of the respective alcohol: 0 % - empty circles, 3 % - full inverted triangles, 2 % - full squares, 1 % - full diamonds, 0.5 % - full triangles; compared with the staining of equally treated pump-deficient AD1-3 strain. Alcohols were added ∼10 minutes after the probe (left-hand arrow, first vertical dotted line) and consequently CD cocktail (10 µM CCCP + 10 µM DM-11) was added ∼40 minutes after the respective alcohol (right-hand arrow, second vertical dotted line). Data are representative of three independent measurements.

The results point to the fact that the ability of alcohols to inhibit the Pdr5p and Snq2p pumping activity is directly dependent on their chain length. Whether this effect is caused by the changing polarity or size of the molecule cannot be said with certainty at this point.

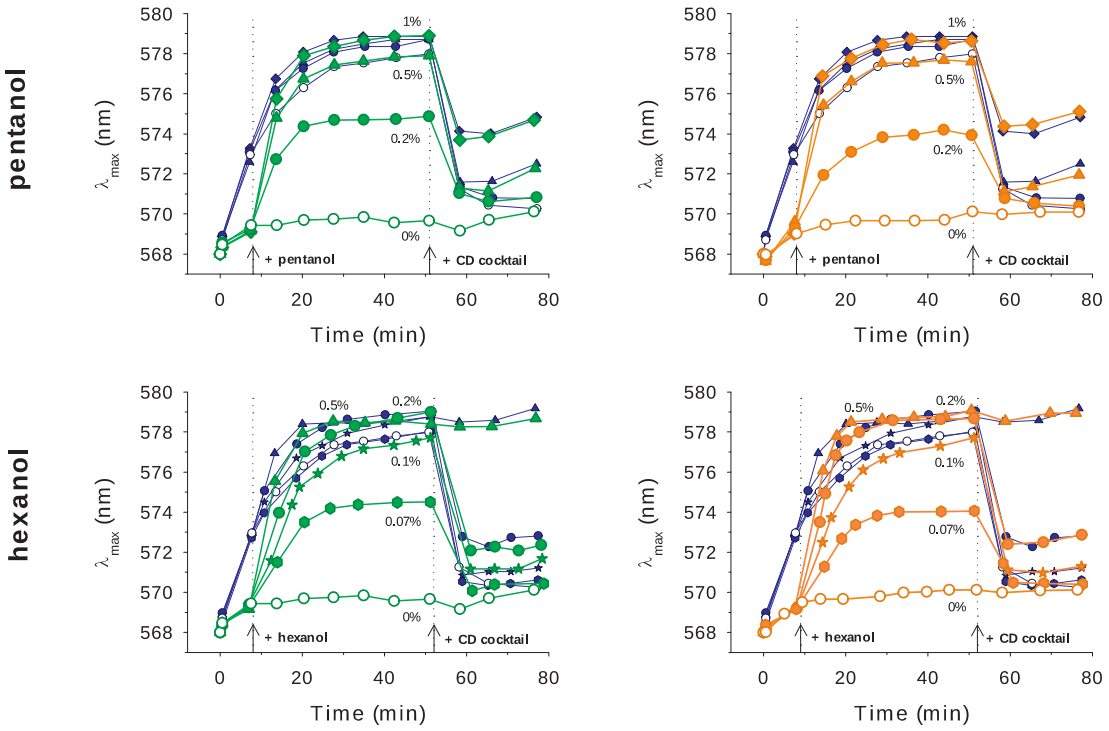

(a) AD12 (b) AD13

Figure 3.3: (continued) Elongation of the alcohol carbon chain length leads to rise in both Pdr5p and Snq2p inhibition activity. Staining of exponentially growing **(a)** Pdr5p-expressing AD12 and **(b)** Snq2p-expressing AD13 cells exposed to various concentrations of the respective alcohol: 0 % - empty circles, 1 % - full diamonds, 0.5 % - full triangles, 0.2 % - full circles, 0.1 % - full stars, 0.07 % - full hexagons; compared with the staining of equally treated pump-deficient AD1-3 strain. Alcohols were added ∼10 minutes after the probe (left-hand arrow, first vertical dotted line) and consequently CD cocktail (10 µM CCCP + 10 µM DM-11) was added ∼40 minutes after the respective alcohol (right-hand arrow, second vertical dotted line). Data are representative of three independent measurements.

The inhibition effect of alcohols may have several underlying causes which need to be properly addressed before a conclusion about the character of the alcohol-pump interaction can be drawn. Particularly, the alcohols may:

(a) cause depletion of ATP in the intracellular space leading to down-regulation of Pdr5p and Snq2p pumping activity due to insufficient energy sources for active transport.

(b) be substrates of Pdr5p and/or Snq2p, competing for transport with the diS-C_3(3) probe.

(c) affect the fluidity of the plasma membrane resulting in modified membrane-protein interactions, hence affecting the activity of the pumps.

(d) act as allosteric modulators of Pdr5p and/or Snq2p by changing either the conformation of the protein or free energy of its conformational changes.

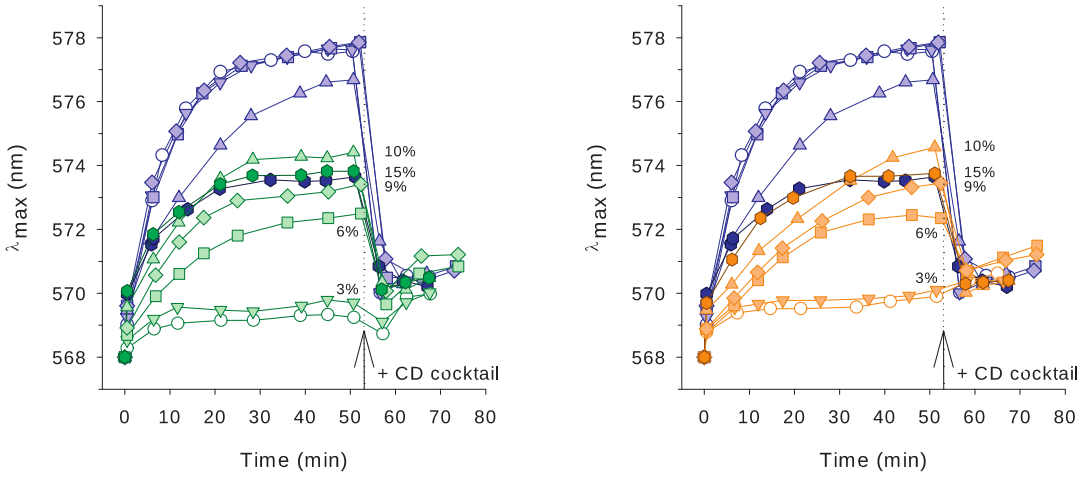

(a) AD12 (b) AD13

Figure 3.4: Higher concentrations of ethanol inhibit Pdr5p and Snq2p, while exhibiting no effect on plasma membrane integrity. Staining of exponentially growing **(a)** Pdr5p-expressing AD12 and **(b)** Snq2p-expressing AD13 cells exposed to various concentrations of ethanol: 0 % - empty circles, 3 % - inverted triangles, 6 % - squares, 10 % - triangles, 15 % - hexagons; compared with the staining of equally treated pump-deficient AD1-3 strain. Ethanol was added ∼10 minutes before the probe and consequently CD cocktail (10 µM CCCP + 10 µM DM-11) was added ∼50 minutes after the probe (vertical dotted line with an arrow). Data are representative of three independent measurements.

It is quite possible that, at least under certain circumstances, several of these effects work together to produce the resulting pump inhibition.

3.2.3 Effect of alcohols on plasma membrane integrity and permeability for ions and small molecules

As demonstrated by the addition of the CD cocktail, alcohols can cause permeabilization of the plasma membrane (Fig. 3.3), which might lead to efflux of ions and small molecules. We therefore monitored the concentration-dependent effect of alcohols on the ability of cells to acidify the surrounding medium and on the efflux of UV-absorbing molecular species, e.g. ATP. Both of these methods are routinely used to study the lethality of chemical stressors (Bennis et al., 2004; Marešová et al., 2009).

In order to monitor their glucose-induced ability to acidify the environment, exponential AD1-3 cells were prepared as described in section 2.2.4. The premise of the experiment is that an elevation of the plasma membrane permeability leads to lower extent of acidification due to the steady influx of protons into the cells (Leão and van Uden, 1984). Indeed, as can be seen in Figure 3.5, addition of alcohols to exponential glucose-treated AD1-3 cells (i.e. with activated Pma1p H^+-ATPase and hence under conditions of greatest attainable transmembrane pH gradient) leads to concentration-dependent alkalinization of the media. While ethanol causes practically no change in acidification within the monitored con-

centration range, elongation of the alcohol carbon chain clearly leads to more extensive impact on the plasma membrane permeability, as reflected in more extensive alkalinization.

The increase in medium alkalinization with the carbon chain length is in good correspondence with the fluorescence determination of the amount of permeabilized cells after exposure to alcohols. Specifically, the concentrations of various alcohols that lead to the same increase of staining after CD cocktail application (Fig. 3.3) also give rise to the same level of alkalinization (compare for instance 3 % butanol with 1 % pentanol).

Leakage of UV-absorbing molecular species was monitored in exponential AD1-3 cells (prepared as described in section 2.2.8) treated with alcohols in a range of concentrations and exposure times. As readily seen from Figure 3.6, the studied concentrations of alcohols (except for 0.5 % and 1 % hexanol) do not cause a significant leakage of substances absorbing at 260 nm even after 60-minute exposure. Hence, the damage to the plasma membrane integrity is not extensive.

Comparing Figures 3.3, 3.5 and 3.6 clearly shows that low concentrations of ethanol do not produce any effect on PDR pump activity, permeabilization nor acidification of the medium. For all the other studied alcohols, however, it is possible to find a relatively low concentration that does not affect the medium acidification and does not cause permeabilization, while producing a clear inhibitory effect on both Pdr5p and Snq2p.

3.2.4 Inhibition of Pdr5p and Snq2p by alcohols is not caused by ATP depletion

It is a well known fact that acidification of the yeast cytosol leads to activation of the Pma1p H^+-ATPase (dos Passos et al., 1992; Hendrych et al., 2009). Since we show in section 3.2.3 that alcohols facilitate influx of protons into the cell, we have to consider activation of Pma1p as a possible consequence. Indeed, this has been previously reported for ethanol (Cartwright et al., 1987; Rosa and Sá-Correia, 1991, 1992). In turn, since Pma1p is the greatest ATP consumer in the cell (Portillo, 2000; Lecchi et al., 2007), its activation could lead to significant lowering of cytosolic ATP, to a level insufficient to fuel the Pdr5p and Snq2p probe pumping activity. This would then lead to elevated staining of the pump-expressing strains, closer to that of the pump-free control.

We examined this possibility by comparing the staining of exponential AD12 and AD13 cells upon their exposure to alcohols in both de-energized cells and cells energized by the addition of glucose. Since hexanol induces the most extensive pump inhibition among the studied alcohols (as well as exhibiting the most extensive effect on the plasma membrane), data obtained with hexanol-treated cells were selected to demonstrate the effect, Figure 3.7.

Addition of 0.07 % hexanol to pump-expressing glucose-free AD12 or AD13 cells produces a response typical for inhibition of the pumps, i.e. a red shift in staining. This effect is not caused by permeabilization, as verified by the CD cock-

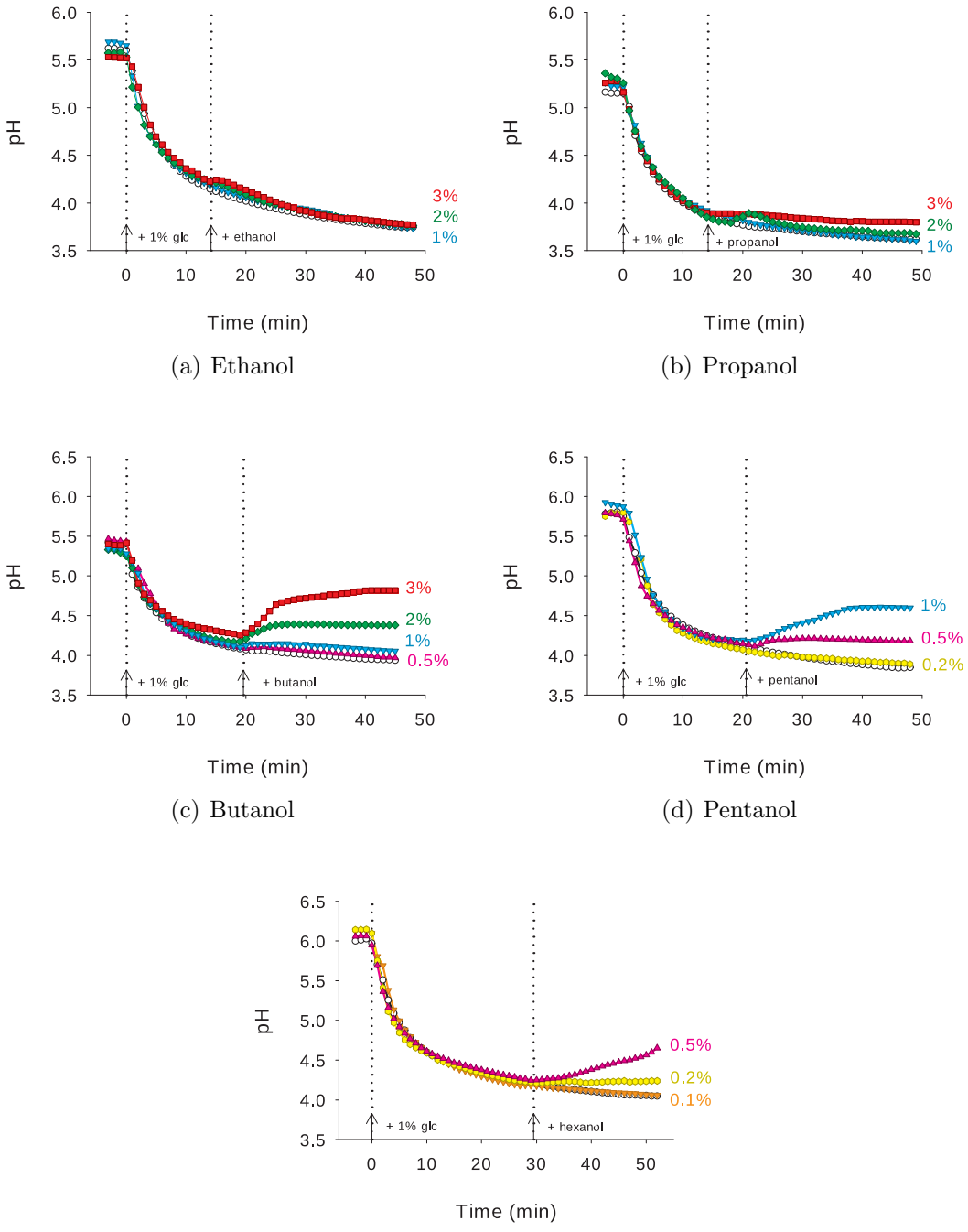

Figure 3.5: The effect of alcohols on glucose-induced medium acidification is concentration- and chain length-dependent. The changes in extracellular pH of exponential AD1-3 cells following the addition of 1 % glucose (left-hand arrows at time zero) were measured. Alcohols were added 15-20 minutes after glucose (right-hand arrows) to the final concentrations of: 3 %, 2 %, 1 %, 0.5 %, 0.2 %, 0.1 %, 0 % (the actual concentration range depends on the particular alcohol used). Data are representative of two independent measurements.

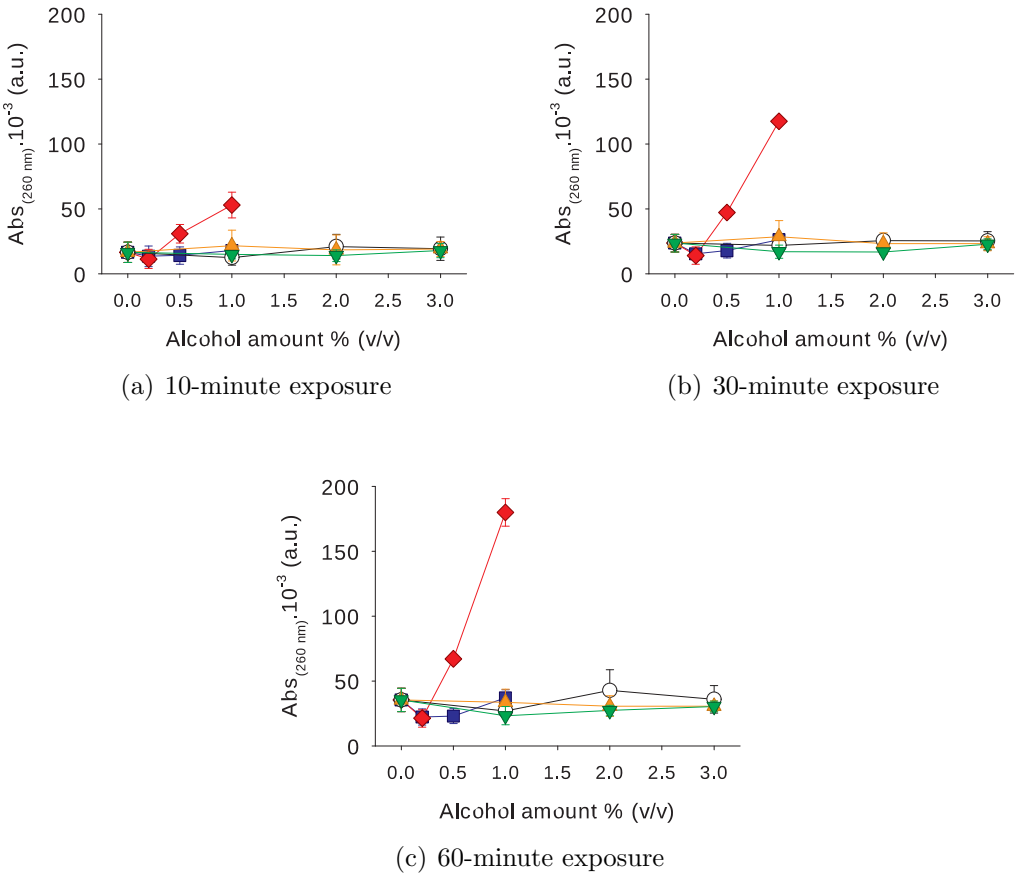

(a) 10-minute exposure

(b) 30-minute exposure

(c) 60-minute exposure

Figure 3.6: Alcohols, with the exception of hexanol, do not cause extensive damage to the plasma membrane on the time scale of 60 minutes. Absorbance of cell suspensions was measured at 260 nm in supernatants of exponential AD1-3 cells treated for **(a)** 10, **(b)** 30, and **(c)** 60 minutes with different alcohols: ethanol, propanol, butanol, pentanol, hexanol. Data represent means ± SD from three independent measurements.

tail addition (Fig. 3.7). Pretreatment of cells with glucose leads to Pma1p activation and hyperpolarization of the plasma membrane. The resulting staining level of AD12 and AD13 cells is given by the end equilibrium between the active pump-mediated probe export and the hyperpolarization-driven probe influx. Further treatment of the cells with 0.07 % hexanol results in elevation of staining, indicating pump inhibition, to a level higher than in the absence of glucose. Nevertheless, the difference between the hexanol-treated cells and the controls remains the same, indicating that the hexanol-induced inhibition of either pump is not affected by the presence of glucose, i.e. source of energy. Hence, we can conclude that depletion of ATP is not the effect underlying the alcohol-mediated inhibition of Pdr5p and Snq2p.

It should be noted that, contrary to the action of FK506 on Pdr5p (Kodedová et al., 2011), the inhibitory effect of alcohols can be reversed simply by washing with buffer, as indicated by the low staining of washed cells, Figure 3.8. The

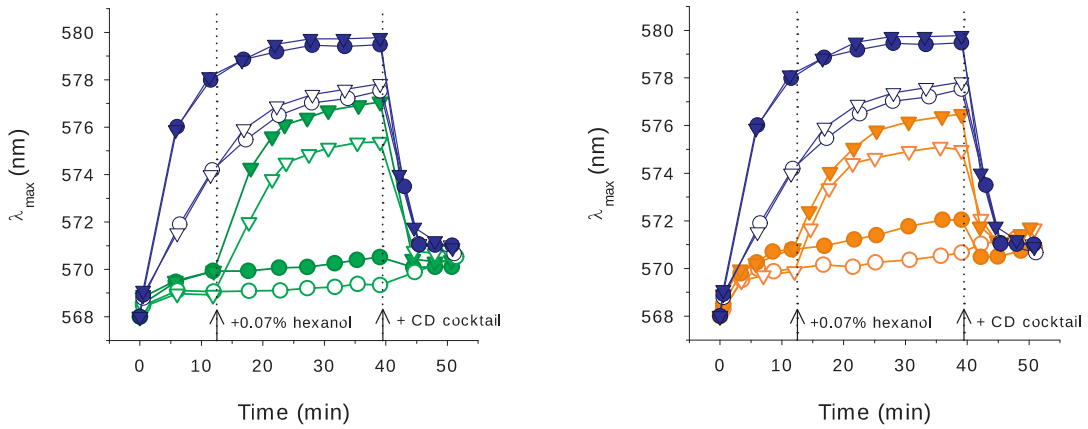

(a) AD12 (b) AD13

Figure 3.7: The inhibitory effect of alcohols on Pdr5p and Snq2p is not caused by depletion of ATP. Effect of the studied alcohols on the pumps in question was compared in glucose-energized (full symbols) and non-energized (empty symbols) exponential **(a)** AD12 and **(b)** AD13 cells; compared with equally treated AD1-3 cells. Glucose was added in all cases 5 minutes before the probe to the final concentration of 10 mM. Hexanol was added ∼12 minutes after the probe (inverted triangles; left-hand arrows and vertical dotted lines) to the final concentration of 0.07 %. Hexanol-free controls are depicted by circles. CD cocktail (10 µM CCCP plus 10 µM DM-11) was added ∼30 minutes after hexanol (right-hand arrows and vertical lines). Data are representative of three independent measurements.

degree of reversal is directly proportional to the number of washing procedures. The reversibility of the inhibition supports our conclusion that it is not mediated by ATP depletion, but rather by a direct interaction of alcohols either with the membrane lipids or the proteins themselves, either as substrates or as allosteric modulators. Furthermore, it also shows that the change in physical properties of the plasma membrane caused by the action of alcohols is not extensive and seems to be reversible as well.

3.2.5 Alcohol-induced inhibition of Pdr5p and Snq2p is not caused by competition with diS-C_3(3) probe for transport

The ability of some plasma membrane proteins to export foreign substances out of the cytosol provides the cell with a great advantage against other species, and their environment in general. Substrate specificities of such transporters can be resolved for example by:

(a) locally exposing a plate culture of pump-deficient cells to the substance of interest and monitoring how well it is able to grow in its presence, relative to its pump-expressing counterpart - the *Kirby-Bauer disc diffusion test* (section 2.2.6).

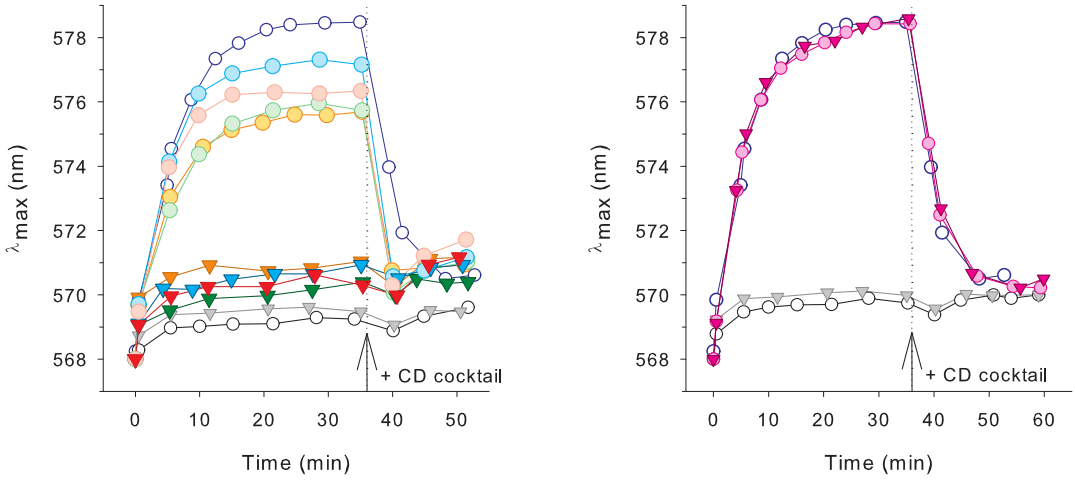

(a) AD12 cells treated with alcohols

(b) AD12 cells treated with FK506

Figure 3.8: The inhibitory effect of alcohols, but not FK506, on Pdr5p can be reversed by simple washing of the cells. Staining of exponentially growing Pdr5p-expressing AD12 cells (empty black circles; inverted grey triangles after washing) treated with **(a)** alcohols (circles) and treated with alcohols and then washed (inverted triangles). The concentration of alcohols was set to produce approximately the same inhibition effect without causing permeabilization: 3 % propanol, 1 % butanol, 0.5 % pentanol, 0.1 % hexanol; compared with the staining of untreated AD1-3 strain. **(b)** Staining of exponentially growing Pdr5p-expressing AD12 cells treated with FK506 (circles) and treated with FK506 and then washed (inverted triangles); compared with the staining of untreated pump-deficient AD1-3 strain. In both **(a)** and **(b)**, CD cocktail (10 µM CCCP + 10 µM DM-11) was added in both cases ∼35 minutes after the probe. For simplicity, only Pdr5p-expressing AD12 cells are shown. Staining of Snq2p-expressing AD13 cells is comparable, including the effect of alcohols and their washing away. The Pdr5p-specific inhibitor FK506 produces no effect on AD13 cells. Data are representative of three independent measurements.

(b) exposing the pump-deficient cells (in a suspension) to the substance in question for a defined period of time and then comparing their survival rate (ability to form colonies) with that of their pump-expressing counterparts treated in the same way - the *plating test* (section 2.2.7).

For the disc diffusion test, exponential cells were prepared as described in section 2.2.6. As the first step, the regular set-up was employed, i.e. the pump-expressing strains AD12 and AD13 were treated with alcohols and the inhibition zones were compared with the pump-free strain AD1-3, Figure 3.9(a). It is clear at first sight that, despite the reported alcohol-induced growth inhibition (Ingram and Buttke, 1984), there are no visible growth-inhibition zones in the case of any strain or alcohol, with the exception of hexanol. In this case, however, the inhibition zones are of the same size in all strains and hence suggest that hexanol is not a substrate of either pump.

The regular disc diffusion tests were supplemented by their simplified version, where we used the Pdr5p-expressing AD12 cells exclusively and simulated the pump-free AD1-3 strain by adding FK506, a potent Pdr5p inhibitor (Kralli and Yamamoto, 1996; Egner et al., 1998), to the cells alongside with the monitored

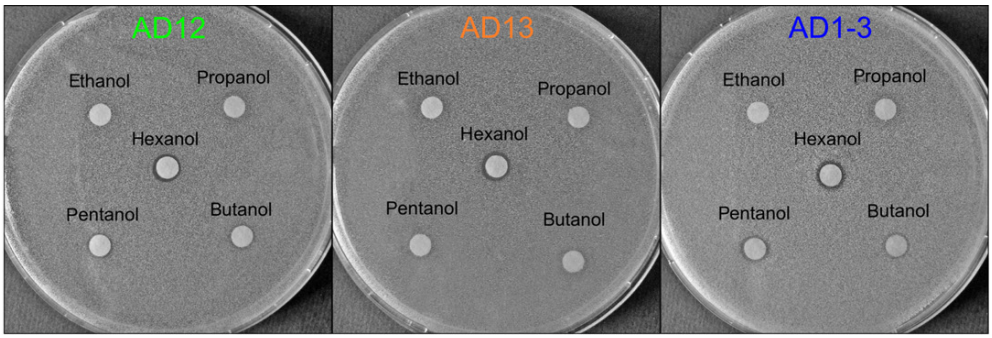

(a) Regular Kirby-Bauer disc diffusion test

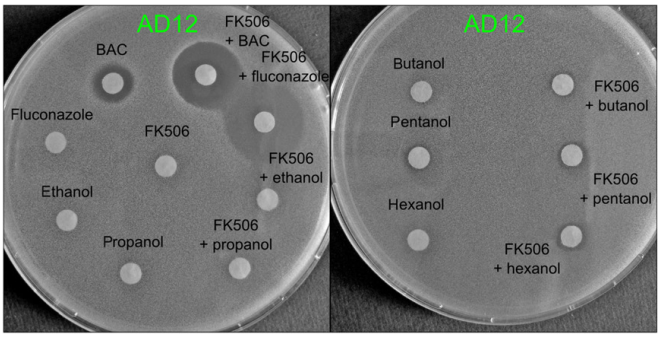

(b) Simplified Kirby-Bauer disc diffusion test

Figure 3.9: Exposure of cells to alcohols in a Kirby-Bauer disc diffusion test does not create growth inhibition zones and provides no indication that alcohols are substrates of either Pdr5p or Snq2p. (a) Exponential cells of the Pdr5p-expressing AD12, Snq2p-expressing AD13 and pump-deficient AD1-3 strain were exposed to various alcohols by spotting 2 µl of each on a Whatman paper disc. Photographs are representative of three independent measurements. **(b)** Exponential AD12 cells were exposed to alcohols and Pdr5p substrates fluconazole (15 mM) and benzalkonium chloride (BAC; 15 mM) either alone or in combination with FK506, a potent Pdr5p inhibitor (to simulate pump-deficient AD1-3 cells). Photographs are representative of three independent measurements.

compound, either an alcohol or a known Pdr5p inhibitor (fluconazole or benzalkonium chloride; BAC). As clearly visible in Figure 3.9(b), addition of FK506 (either alone or in a combination with an alcohol or even fluconazole) to the cells does not give rise to any growth inhibition zone. In fact, the only visible growth inhibition zone is that formed after the addition of BAC and is enlarged by co-addition with FK506.

The simplest explanation for the inconsistency between the reported and observed effect of alcohols on yeast growth seems to be that alcohols diffuse rather rapidly in agar (the diffusion coefficient of ethanol in 4 % agarose beads at 25°C is 8.0-9.5·10^{-6} $cm^2.s^{-1}$; Westrin (1990)) and their local concentration is therefore very low and insufficient to cause inhibition of growth. Hexanol, due to its much lower solubility in aqueous environments does not diffuse as rapidly and stays concentrated enough in the immediate proximity of the disc to cause growth inhibition.

We have verified this possibility by modifying the disc-diffusion assay in a way that we placed multiple Whatman paper discs in close vicinity and spotted 2 µl of respective alcohols on each, Figure 3.10, effectively raising the local alcohol concentration. In the case of propanol (as well as ethanol; not shown), there is no inhibition visible regardless of the number of paper discs, consistent with regular disc-diffusion assays. However, the longer alcohols clearly show inhibition of growth in the areas of multiple discs placed in close vicinity. It is therefore clear that the rapid diffusion is indeed the cause of the absence of growth-inhibition zones in the regular disc-diffusion assay (Fig. 3.9(a)).

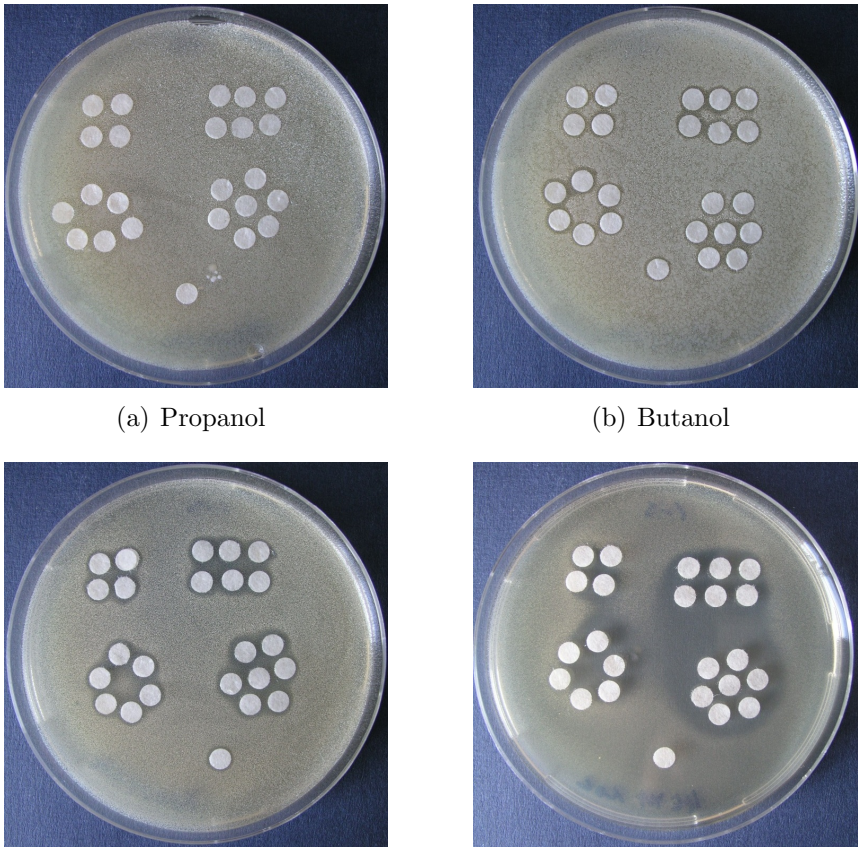

(a) Propanol (b) Butanol

(c) Pentanol (d) Hexanol

Figure 3.10: The absence of inhibition zones in regular disc-diffusion assays is caused by rapid diffusion of alcohols in the agar plates. Exponential cells of the pump-deficient AD1-3 were exposed to various alcohols by spotting 2 µl of each on either a single Whatman paper disc, or multiple discs placed in close vicinity of each other. Photographs are representative of three independent measurements.

For the plating tests, exponential cells were prepared as described in section 2.2.7. Figure 3.11 shows that all three strains exhibit the same ability to withstand the stress posed by 30-minute exposure to various concentrations of alcohols. This, together with the disc diffusion tests, clearly indicates that the alcohols are not actively transported from the cells by either Pdr5p or Snq2p.

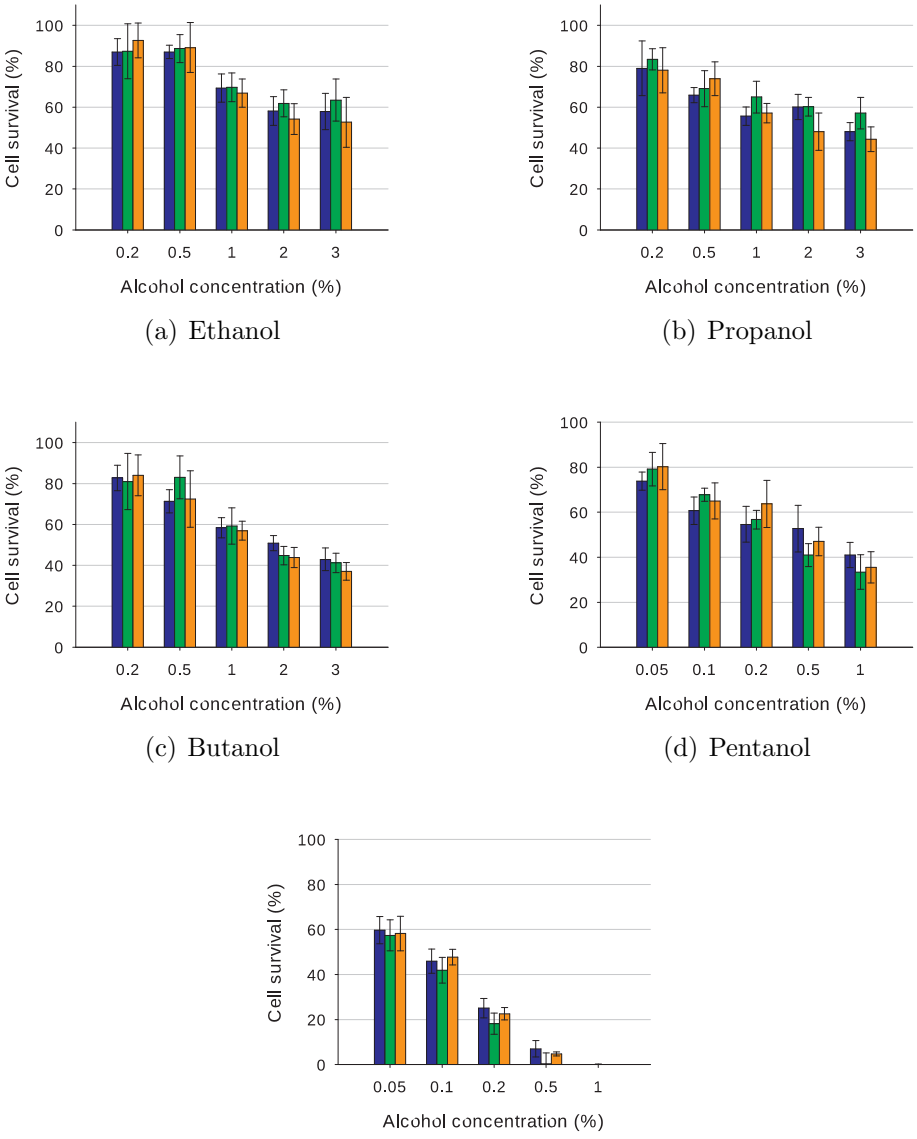

Figure 3.11: Alcohols are not substrates of Pdr5p nor Snq2p. Exponential cells of the Pdr5p-expressing AD12, Snq2p-expressing AD13 and pump-deficient AD1-3 strain were exposed to various concentrations of alcohols for 30 minutes and plated. Their colony forming units were counted and compared with non-treated cells. Data represent means ± SDs obtained from two independent measurements containing three biological replicates each.

3.2.6 Alcohols are true inhibitors of Pdr5p and Snq2p

By unambiguously showing that the inhibition of Pdr5p and Snq2p is not caused by either depletion of ATP or competition with the probe for transport, the only remaining option is that alcohols interact directly either with the lipids of the plasma membrane or with the proteins themselves, which results in their lower activity.

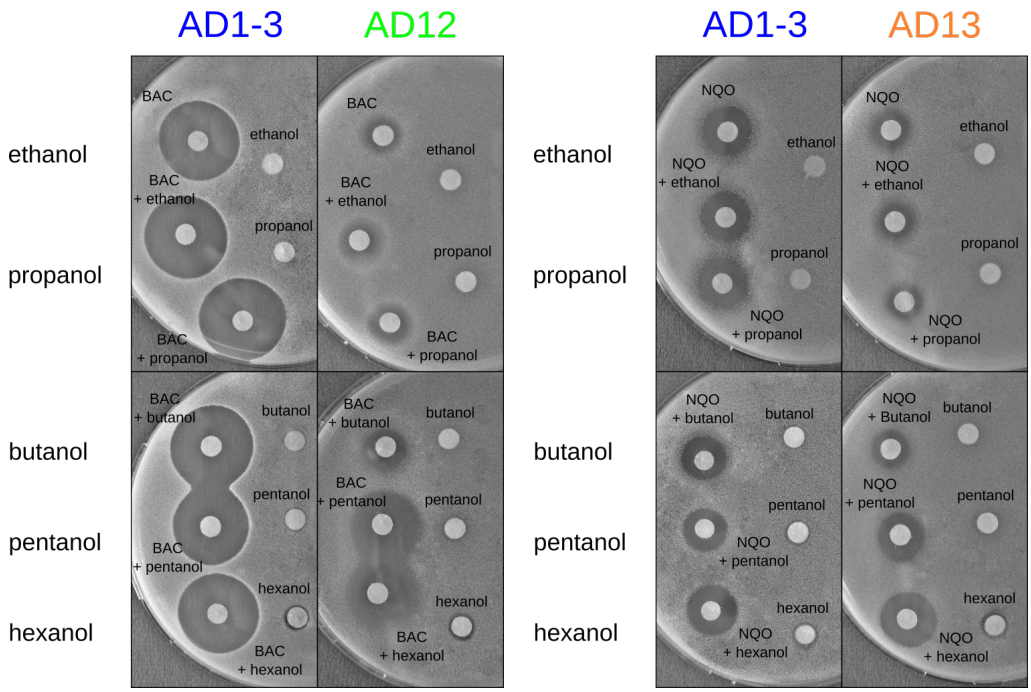

(a) benzalkonium chloride (b) NQO

Figure 3.12: Alcohols inhibit transport of known Pdr5p and Snq2p substrates. Exponential cells of the Pdr5p-expressing AD12, Snq2p-expressing AD13 and pump-deficient AD1-3 strain were exposed to various alcohols and known substrates of their respective pumps, either alone or in a combination, by spotting 2 µl of each on a Whatman paper disc. **(a)** benzalkonium chloride (15 mM; Pdr5p substrate); **(b)** NQO - 4-nitroquinoline 1-oxide (1.6 mM; Snq2p substrate). Photographs are representative of three independent measurements.

In order to verify this proposition, we examined the ability of Pdr5p and Snq2p to transport their benchmark substrates (Pdr5p: nigericin, ketoconazole and benzalkonium chloride; Snq2p: 4-nitroquinoline 1-oxide [NQO]) in the absence and presence of alcohols by the means of a disc diffusion test (section 2.2.6; double-addition mode), Figure 3.12. As is evident in the case of the AD12 strain, combined addition of benzalkonium chloride (BAC) and alcohols from ethanol to butanol leads only to a slight enlargement of the growth inhibition zone compared to treatment with BAC alone. Combined addition with pentanol and hexanol, however, gives rise to growth inhibition zones almost identical to those formed on the pump-deficient AD1-3 strain background. This points to extensive inhibition of Pdr5p-mediated BAC transport by both pentanol and hexanol. The small effect of shorter alcohols is possibly caused by their fast diffusion in the agar plate, as discussed in section 3.2.5, and hence a concentration that is insufficient to cause inhibition of transport (note also the concentrations shown to inhibit the pump-mediated probe transport in the fluorescence assay, Fig. 3.3). The same character of alcohol-induced effects on the growth inhibition zones is observed in the case of NQO, supporting the explanation. In the case of nigericin and ketoconazole,

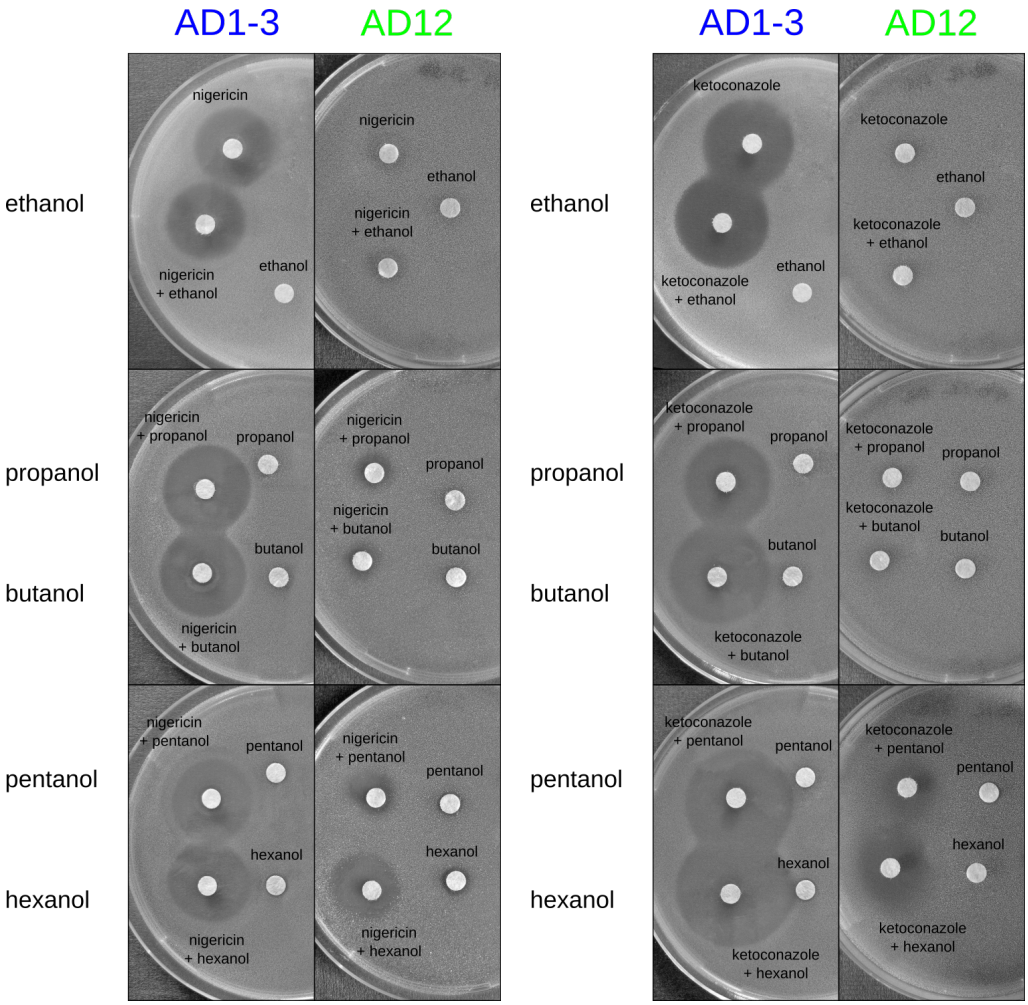

(a) Nigericin (b) Ketoconazole

Figure 3.12: (continued) Alcohols inhibit transport of known Pdr5p and Snq2p substrates. Exponential cells of the Pdr5p-expressing AD12, Snq2p-expressing AD13 and pump-deficient AD1-3 strain were exposed to various alcohols and known substrates of their respective pumps, either alone or in a combination, by spotting 2 µl of each on a Whatman paper disc. **(c)** nigericin (20 mM; Pdr5p and Yor1p substrate); **(d)** ketoconazole (1.5 mM; Pdr5p substrate). Photographs are representative of three independent measurements.

the situation is again, very similar. However, hexanol seems to be a more effective inhibitor than pentanol in these two cases.

In order to confirm that the absence of inhibitory effect is indeed connected to the fast diffusion of short alcohols, we compared the survival of exponential Pdr5p-expressing AD12 and pump-deficient AD1-3 strains exposed to 1.5 µM BAC and alcohols, either separately or combined, for 30 minutes, in a plating test (section 2.2.7). The AD12 strain is able to proliferate significantly better in the presence of BAC than the pump-deficient AD1-3 strain, consistent with our previous research (Kodedová et al., 2011). As evident from Figure 3.13, this difference disappears when the cells are exposed to BAC in the combination with

butanol, pentanol or hexanol. It is, however, only partially reduced by the use of 3 % propanol, while ethanol produces no tangible effect on Pdr5p, consistent with the results of the fluorescence assay (Fig. 3.3).

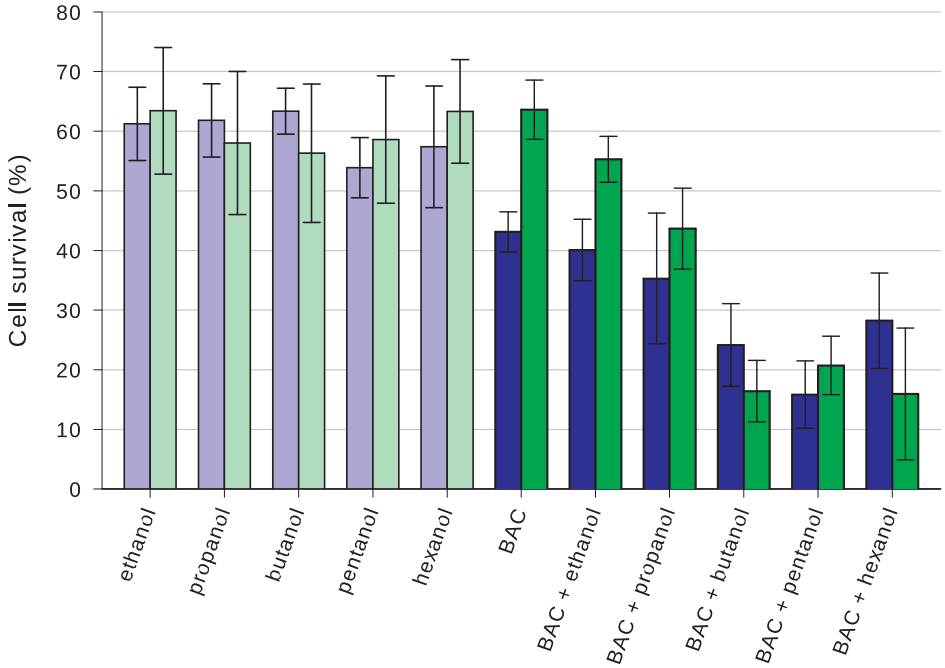

Figure 3.13: Propanol and higher alcohols inhibit benzalkonium chloride transport mediated by Pdr5p. Exponential cells of the pump-deficient AD1-3 and Pdr5p-expressing AD12 strain were exposed to various alcohols (ethanol - 3 %; propanol - 3 %; butanol - 1 %; pentanol - 0.5 %, and hexanol - 0.1 %) and 1.5 µM benzalkonium chloride, either alone or in their combination, for 30 minutes and then assayed for survival. Data represent means ± SD from three independent measurements.

The role of alcohols in Pdr5p and Snq2p inhibition seems to be inarguably proven in the previous experiments. However, the antifungal mechanism of action of various substances, including BAC, includes mechanical damage to the plasma membrane (Kodedová et al., 2011). We therefore need to consider the possibility that the lower survival of cells could be caused by permeabilization of the plasma membrane due to the combined addition of an alcohol with a substrate.

As discussed above, the amount of permeabilized cells in a suspension is easily determined by the addition of the CD cocktail in a fluorescence assay. In order to exclude permeabilization, we therefore exposed AD12 and AD1-3 cells to the combination of hexanol (most potent inhibitor as well as most aggressive towards the plasma membrane) with Pdr5p substrates BAC and ketoconazole and monitored the staining after the addition of the CD cocktail, Figure 3.14. As is evident from the same staining after CD cocktail addition, the treatment of AD12 and AD1-3 cells with either BAC or ketoconazole alone does not lead to permeabilization of the plasma membrane, Fig. 3.14(a). The only visible effect

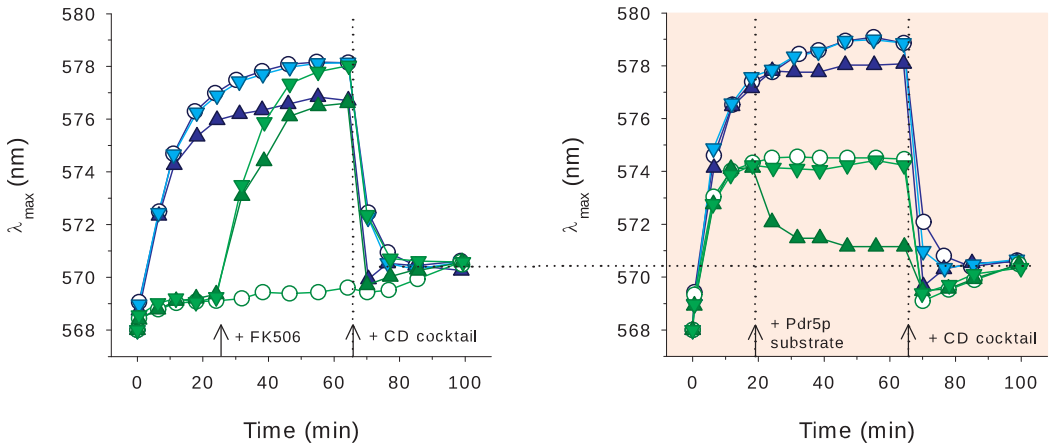

(a) In the absence of hexanol (b) In the presence of 0.07 % hexanol

Figure 3.14: Combined effect of Pdr5p substrates and hexanol does not lead to permeabilization of the plasma membrane. Exponential cells of the Pdr5p-expressing AD12 and pump-deficient AD1-3 strain were treated with: **(a)** nothing (empty circles), 1.5 µM BAC (triangles) and 15 µM ketoconazole (inverted triangles) 5 minutes before the addition of the probe. 10 µM FK506 was added to AD12 cells ∼25 minutes after the probe (left-hand arrow and vertical dotted line) to detect any residual Pdr5p activity. **(b)** 0.07 % hexanol 5 minutes before the addition of the probe. Pdr5p substrates were added ∼20 minutes after the probe (left-hand arrow and vertical dotted line): empty circles - nothing, triangles - 1.5 µM BAC, inverted triangles - 15 µM ketoconazole. In both cases the CD cocktail was added ∼65 minutes after the probe (right-hand arrow and vertical dotted line.) Data are representative of three independent measurements.

is the slight depolarization caused by the action of BAC, while ketoconazole has no immediate effect on the membrane potential. Furthermore, when cells are pre-treated with 0.07 % hexanol and then subjected to either BAC or ketoconazole, there is, again, no detectable permeabilization, Figure 3.14(b). We can therefore safely conclude that the inhibition of Pdr5p and Snq2p by the action of alcohols is not connected to damage of the plasma membrane, but is indeed caused by their direct interaction(s) with the proteins and/or their lipid microenvironment. This is further supported by the fact that the inhibition is reversible, decreasing after the removal of alcohols by simple washing (Fig. 3.8).

3.3 Yeast Tok1p channel is a major contributor to membrane potential maintenance under chemical stress

When monitoring membrane potential and its changes, it is of great convenience to use strains deficient in PDR pumps (as described in more detail in section 2.2.2). We therefore used the Pdr5p and Snq2p-deficient strain (AD1-3) and its isogenic *tok1* mutant (AD1-3 *tok*1Δ). In these strains the probe response is defined solely by the membrane potential and is not distorted by the action of Pdr5p and Snq2p multidrug resistance pumps (Čadek et al., 2004; Maláč et al., 2005). Furthermore, we monitored the performance of Tok1p in suspensions of washed cells devoid of glucose, as the role of Tok1p channel is masked by Pma1p activity in the presence of the sugar (Marešová et al., 2009).

3.3.1 Effect of growth phase and glucose presence on the contribution of Tok1p channel to membrane potential

The depolarization of the plasma membrane in the suspension of washed cells devoid of glucose represents a practical benchmark for the contribution of Tok1p channel to $\Delta\Psi$ maintenance under chemical stress. Exponential and post-diauxic cells of the two strains were prepared as described in section 2.2.2 and their staining in both absence and presence of glucose was monitored, Figures 3.15(a) and 3.15(b).

Washed exponential cells exhibit significantly lower staining compared to cells with added glucose, which indicates their relative depolarization. Furthermore, as revealed by lower equilibrium staining values (λ^{eq}_{max}), the cells of the *tok1* mutant are significantly depolarized relative to the parental strain, consistent with previous research (Marešová et al., 2006, 2009).

The difference between the staining of the parental strain and the *tok1* mutant (light blue area in Fig. 3.15(a)) displays the time-dependent Tok1p channel contribution to $\Delta\Psi$ maintenance. The difference in equilibrium staining of the two strains ($\Delta\lambda^{eq}_{max}$) is 1.6 ± 0.2 nm corresponding to $\Delta\Psi$ difference of 14.6 ± 2.8 mV, cf. (Plášek and Gášková, 2014). This is quite a significant difference, as it corresponds to 48 ± 6 % of $\Delta\Psi$ change caused by glucose addition to *tok1* mutant cells. Furthermore, relatively low concentrations of glucose (in comparison to those routinely used in growth media, i.e. 2 % equal to 128 mM) lead to merging of the staining curves of the strains. This indicates that the Tok1p channel is inactivated by high membrane potential, consistent with previous studies (Marešová et al., 2009). In the post-diauxic phase, on the other hand, there is practically no difference in the membrane potential of the two strains regardless of the presence of glucose (and hence hyperpolarization), Figure 3.15(b).

To explain the depolarization of the exponential cells of the *tok1* mutant relative to the parental strain, it is necessary to consider that the preparation of ex-

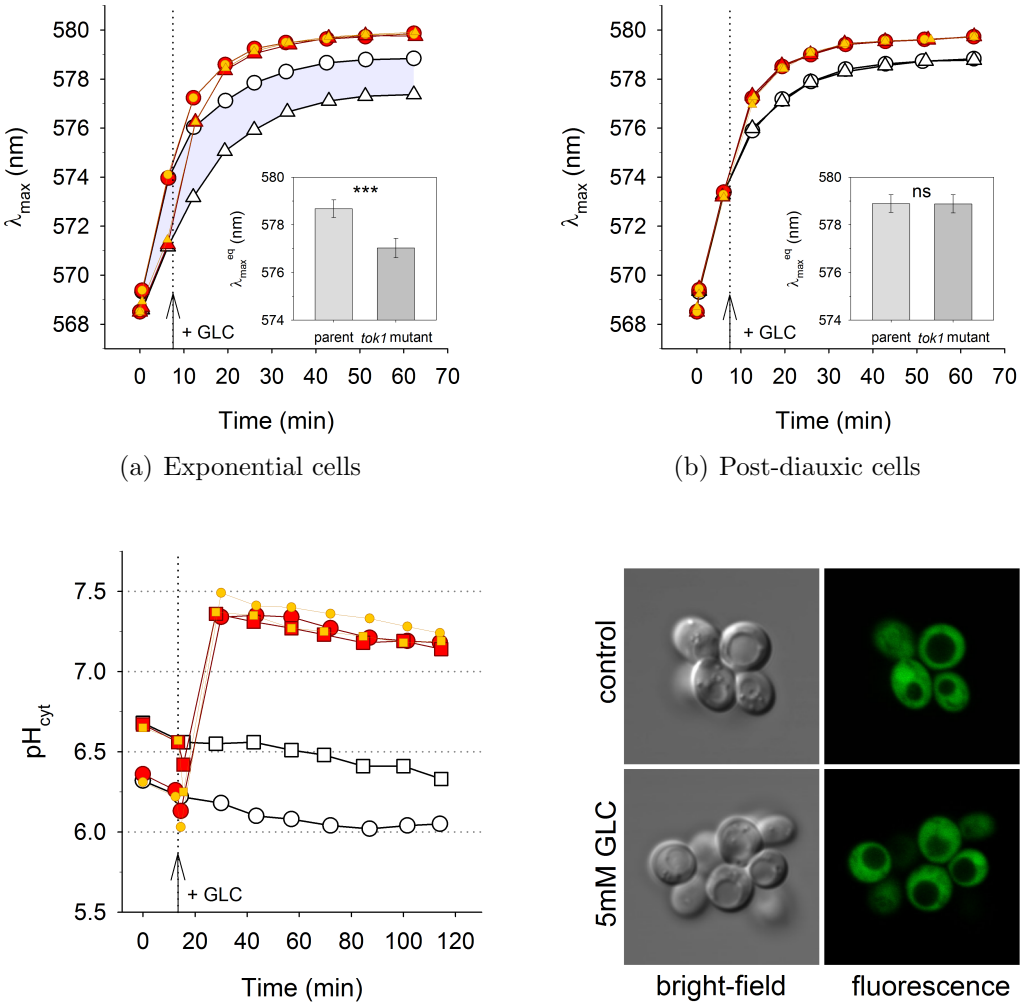

(a) Exponential cells

(b) Post-diauxic cells

(c) Cytosolic pH

(d) pHluorin localization

Figure 3.15: Contribution of Tok1p channel to $\Delta\Psi$ maintenance depends on cell age and presence of glucose. (a, b) Staining curves of the parental strain (circles) and *tok1* mutant (triangles) grown to (a) exponential and (b) post-diauxic phase and exposed to 5 (red) or 50 mM (orange) glucose added ∼8 minutes after the probe (vertical dotted line with arrow). Empty black symbols - controls. Data are representative of ten independent measurements. Inserts represent means ± SDs calculated from twelve independent $\lambda_{max/60}$ assessments. "ns" and the asterisks indicate P-values obtained from a t-test: ns (not significant) - t-test P value ≥ 0.05; *** - t-test P value < 0.001. **(c)** Effect of 5 (red) and 50 mM (orange) glucose on cytosolic pH (pH_{cyt}) of exponential (circles) and post-diauxic (squares) cells of the pHluorin-expressing variant of the parental strain. Empty black symbols - controls. Glucose was added ∼15 minutes after the beginning of the measurement (vertical dotted line with arrow). Data are representative of five independent measurements. **(d)** Exclusively cytosolic localization of pHluorin in post-diauxic cells in both absence and presence of 5 mM glucose. Micrographs are representative of three independent measurements of five biological replicas each. Exponential cells exhibit the same pHluorin localization (data not shown).

ponential cells for the fluorescence measurement involves removal of glucose from the cells' surroundings. This leads to down-regulation of Pma1p activity (Serrano, 1983) and consequently depolarization of the plasma membrane. In the parental strain the depolarization is compensated by Tok1p channel opening and K^+ release, resulting in partial restoration of membrane potential (Bertl et al., 1998). The *tok1* mutant is unable to release potassium and therefore stays depolarized relative to the parental strain. On the other hand, the post-diauxic culture is adapted to an environment completely devoid of glucose. The transfer of such cells to the glucose-free $\Delta\Psi$ measurement buffer therefore does not affect their Pma1p activity. Thus, even in the situation of higher channel expression relative to exponential cells (DeRisi et al., 1997; Gasch et al., 2000; Brauer et al., 2005), there is practically no difference in the membrane potential of the two strains (Fig. 3.15(b)). This clearly demonstrates that the level of $\Delta\Psi$ corresponding to $\lambda_{max} \sim 579$ nm under our experimental conditions is high enough to keep the channel in one of the two inactive states.

Cytosolic pH (pH_{cyt}) is known to affect the opening capacity of the Tok1p channel (Lesage et al., 1996; Bertl et al., 1998). It should therefore be noted that under our experimental conditions, the pH_{cyt} of untreated exponential cells is almost constantly lower than pH_{cyt} of post-diauxic cells, by 0.30 ± 0.15 pH units (Fig. 3.15(c)). Nevertheless, addition of glucose leads to extensive and quite rapid alkalization which reaches the same final value in both growth phases. The rise in pH_{cyt} is in both cases preceded by a small transient acidification, which is consistent with previous research (Thevelein et al., 1987). This drop in pH_{cyt} originates in the initial steps of glycolysis. Correct cytosolic localization of the pH reporter, pHluorin, is documented in Figure 3.15(d) for post-diauxic cells, both untreated and treated with glucose. Exponential cells exhibit the same localization patterns (data not shown).

The relatively lower pH_{cyt} of exponential cells most likely originates in Pma1p down-regulation (Serrano, 1983) and V-ATPase disassembly (Kane, 1995; Seol et al., 2001) upon glucose removal from exponential cells. Glucose (re)addition leads to hyperpolarization and extensive alkalinization in both phases, indicating the possibility of Pma1p and V-ATPase activation by glucose not only in exponential (Kane, 1995; Seol et al., 2001), but also in post-diauxic cells.

Taken together, we can clearly see that, even in the absence of chemical stress, our experimental set-up reveals a clear difference in Tok1p contribution to membrane potential in exponential and post-diauxic cells. Thus, the results indicate considerable contribution of the Tok1p channel to $\Delta\Psi$ maintenance when Pma1p activity is reduced in the absence of glucose, either by its removal or by the completion of the diauxic transition.

3.3.2 Characterisation of Tok1p channel activity under chemical stress induced by a model depolarizing agent CCCP

In order to understand the functioning of the Tok1p channel under conditions of chemical stress leading to plasma membrane depolarization, we selected the protonophore carbonyl cyanide *m*-chlorophenyl hydrazone (CCCP) as the model depolarizing agent due to its well-described effect on yeast cells. CCCP is a weak lipophilic acid that mediates passive proton transport across cellular membranes according to the respective electrochemical gradients (Heytler and Prichard, 1962; Kasianowicz et al., 1984; Purwin et al., 1986; Gášková et al., 1998). This proton flow results not only in plasma membrane depolarization (Preston et al., 1989) but also cytosolic acidification (Purwin et al., 1986; Plášek et al., 2017).

We expected the CCCP-induced plasma membrane depolarization to trigger Tok1p channel opening (once the Nernst equilibrium potential for K^+ was surpassed) leading to potassium release. On the other hand, the cytosolic acidification is known to trigger activation of Pma1p, leading to extensive export of protons out of the cytosol. This process is aimed at both keeping the pH_{cyt} constant and at re-polarization of the plasma membrane (Brandão et al., 1992; dos Passos et al., 1992; Pereira et al., 2008; Hendrych et al., 2009).

In order to set the experimental conditions in a way that there is a clearly detectable contribution of the Tok1p channel to the maintenance of plasma membrane potential, we considered following factors:

- cell culture growth phase
- activation of Pma1p by glucose
- time of stressor addition relative to the beginning of cell staining with diS-C_3(3)
- extent of stressor-induced cytosolic acidification
- effect of known inhibitors of Tok1p (tetraethylammonium ion, TEA^+) and Pma1p (2-dodecanoyloxyethyldimethylammonium chloride, DM-11)

Exponential (Fig. 3.16(a)) and post-diauxic (Fig. 3.16(b)) cells of the parental strain and the *tok1* mutant were subjected to a sublethal concentration of CCCP at two different times relative to the time of probe addition (12 and 50 minutes). Staining of exponential cells of the parental strain is not significantly affected by CCCP, consistent with previous research of our group (Hendrych et al., 2009), indicating a practically negligible effect on membrane potential. However, addition of CCCP to *tok1* mutant cells and post-diauxic cells of the parental strain leads to quite rapid and transient drop in staining, indicating depolarization. This is followed by relatively slow redistribution of the probe between the cytosol and external buffer, indicating membrane potential restoration.

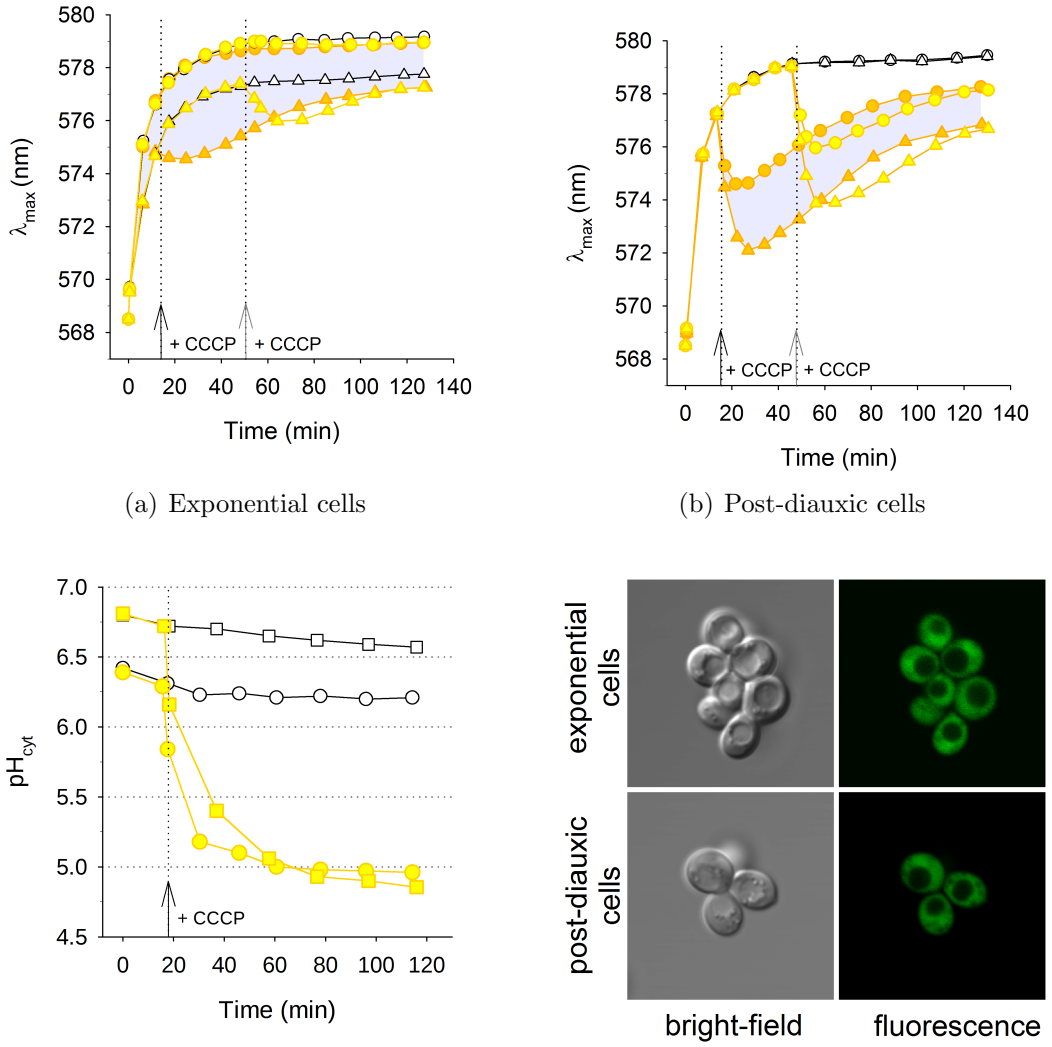

(a) Exponential cells

(b) Post-diauxic cells

(c) Cytosolic pH

(d) pHluorin localization

Figure 3.16: Contribution of Tok1p to post-CCCP ΔΨ re-building in equilibrium is independent of addition time. (a, b) Staining curves of the parental strain (circles) and *tok1* mutant (triangles) grown to (a) exponential and (b) post-diauxic phase and exposed to 10 µM CCCP added at times t = 12 (orange) or 50 minutes (yellow) relative to the probe (vertical dotted lines with arrows). Empty black symbols - controls. Data are representative of ten independent measurements. **(c)** Effect of 10 µM CCCP (yellow) on pH_{cyt} of exponential (circles) and post-diauxic (squares) cells of the pHluorin-expressing variant of the parental strain. Empty black symbols - controls. CCCP was added ~18 minutes after the beginning of the measurement (vertical dotted line with arrow). Data are representative of ten independent measurements. **(d)** Exclusively cytosolic localization of pHluorin in exponential and post-diauxic cells exposed to 10 µM CCCP. Micrographs are representative of three independent measurements of five biological replicas each.

The marked differences in the staining curve profiles corresponding to various times of CCCP addition can be attributed to unequal amounts of diS-C_3(3) fluorescent probe accumulated in the cells before depolarization is induced. Re-

gardless of this difference, however, the staining level in equilibrium (λ^{eq}_{max}) of CCCP-treated cells is independent of the time of its addition for each given strain and growth phase (Figs. 3.16(a) and 3.16(b)). The λ^{eq}_{max} therefore represent an unambiguous measure of plasma membrane depolarization induced by CCCP. It should be noted that not the membrane potential transients, but rather the steady-state $\Delta\Psi$ values represent the physiologically relevant parameter by which to characterize the response of cells and the Tok1p channel to chemical stress.

Despite the inability of the staining curves to precisely follow fast changes of $\Delta\Psi$ (due to relatively slow redistribution of the probe), they still report the existence of a pronounced transient depolarization caused by the addition of CCCP to *tok1* mutant cells and to post-diauxic cells of the parental strain. The staining curves also reveal that about 10 minutes after the initial depolarization, $\Delta\Psi$ begins to rise again towards a new equilibrium value due to Pma1p activation. The initial depolarizing effect of CCCP in post-diauxic cells of both strains is considerably more pronounced than in the exponential cells. Note also that the CCCP-induced drop of pH_{cyt} is greater in post-diauxic (from 6.7 ± 0.2 to 5.0 ± 0.2 in about 60 min after CCCP addition) than in exponential cells (from 6.3 ± 0.2 to 5.0 ± 0.3), Figure 3.16(c)[3]. It should be emphasized that the response of pHluorin to immediate pH_{cyt} changes is faster than about 3 sec (Plášek et al., 2017). Therefore, the slow changes in pH following the initially rapid drop after CCCP addition (Fig. 3.16(c)) are not due to methodological limitations, but represent actual slow changes of pH_{cyt} occurring in washed cells devoid of glucose. While undoubtedly of interest, the elucidation of this pH_{cyt} decline was beyond the scope of our study.

Observed λ^{eq}_{max} data report following relationships between steady-state $\Delta\Psi$ values in CCCP-treated cells and untreated controls:

- *Exponential phase:* In the cells of the parental strain, there is only a slight temporary CCCP-induced $\Delta\Psi$ drop that is rapidly and completely restored. The *tok1* mutant glucose-free controls have lower $\Delta\Psi$ relative to the parental strain. The CCCP-induced temporary $\Delta\Psi$ drop is more pronounced than in the parental strain. Nevertheless, it is still almost completely recovered (Fig. 3.16(a)).

- *Post-diauxic phase:* For both strains, the CCCP-induced transient $\Delta\Psi$ drop is more pronounced than in the exponential phase. The final steady state depolarization induced by CCCP addition is therefore also deeper than in the exponential cells (Fig. 3.16(b)).

To clearly demonstrate that the difference between the staining of the parental strain and the *tok1* mutant ($\Delta\lambda_{max}$) corresponds to Tok1p channel activity, we used TEA^+ (tetraethylammonium ion), an established inhibitor of the channel (Gustin et al., 1990; Bertl et al., 1998). In suspensions treated solely with

[3]Fig. 3.16(d) clearly shows correct cytosolic localization of the pH_{cyt} reporter, and intact vacuolar membrane after exposure of cells to CCCP.

TEA^+ (of 100 mM concentration) the cells exhibited some depolarization relative to the control, regardless of strain and growth phase, as reported by λ_{max}^{eq} (Figs. 3.17(a) and 3.17(b)). This depolarization is accompanied by slight cytosolic alkalization (≤0.1 pH units) in both growth phases (Figs. 3.18(a) and 3.18(b)), as found in the parallel experiment performed with the pHluorin-expressing strain.

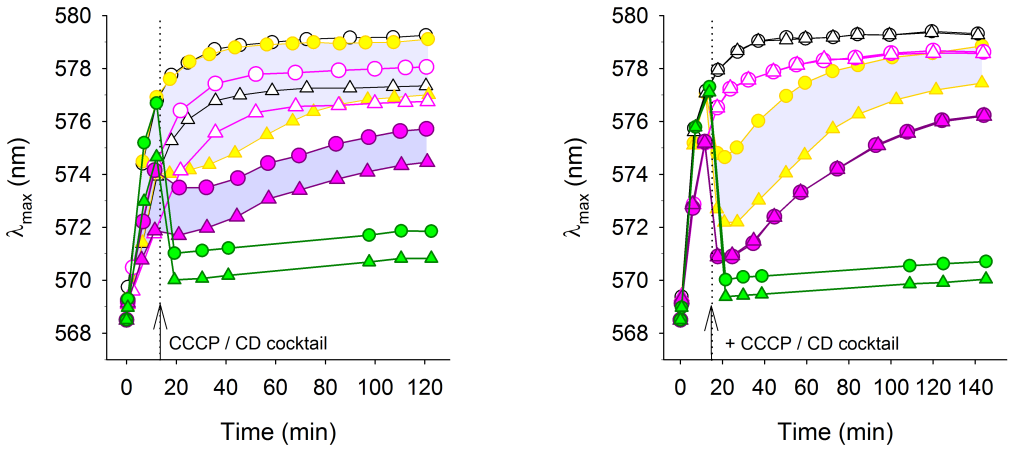

(a) Exponential cells (b) Post-diauxic cells

Figure 3.17: Tok1p response to CCCP-induced depolarization in the presence of known inhibitors of Tok1p (TEA^+) and Pma1p (DM-11) Staining curves of the parental strain (circles) and *tok1* mutant (triangles) grown to **(a)** exponential and **(b)** post-diauxic phase and exposed to 10 µM CCCP (yellow), 10 µM CD cocktail (10 µM CCCP + 10 µM DM-11; green), 100 mM TEA^+ (empty pink symbols) or the combination of TEA^+ and CCCP (filled pink symbols). Empty black symbols - controls. TEA^+ was added ∼10 minutes before and CCCP / CD cocktail ∼15 minutes after the beginning of the respective measurement (vertical dotted line with arrow). Data are representative of ten independent measurements.

In the exponential phase, the extent of TEA^+-induced depolarization (measured by the difference between corresponding λ_{max}^{eq} of controls and TEA^+-treated cells) of the parental strain is roughly twice as extensive as that of equally treated *tok1* mutant. This results in smaller $\Delta\lambda_{max}^{eq}$ between the two strains. Conversion of $\Delta\lambda_{max}^{eq}$ to changes of $\Delta\Psi$, cf. (Plášek and Gášková, 2014), indicates that the contribution of Tok1p channel to $\Delta\Psi$ maintenance after TEA^+ addition (amounting to 8.0 ± 0.9 mV) is significantly smaller than in the absence of the inhibitor (19.8 ± 0.3 mV). In the post-diauxic phase the change of λ_{max} in response to TEA^+ addition is the same in the two strains and the staining curves of the two strains overlap almost perfectly both in the presence and in the absence of the inhibitor. Furthermore, pretreatment of the cells with TEA^+ completely abolishes the Tok1p contribution to $\Delta\Psi$ in response to CCCP-mediated depolarization only in post-diauxic cells, as indicated by the coincidence of the staining curves (compare Figs. 3.17(a) and 3.17(b)).

When using an established Tok1p channel inhibitor, one expects the difference between the staining of the two strains (corresponding to the Tok1p channel

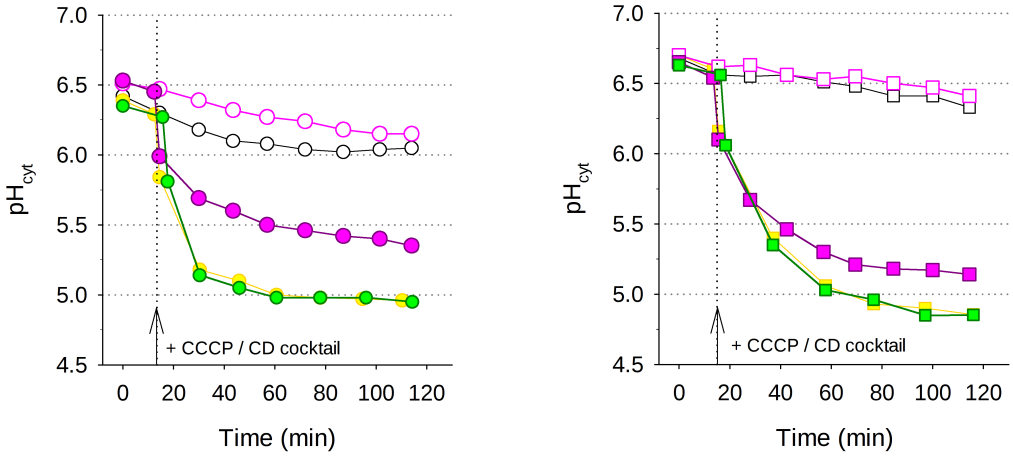

(a) pH$_{cyt}$ - exponential cells

(b) pH$_{cyt}$ - post-diauxic cells

Figure 3.18: Response of pH$_{cyt}$ to known inhibitors of Tok1p (TEA$^+$) and Pma1p (DM-11) in combination with CCCP Effect of 10 µM CCCP (yellow), 100 mM TEA$^+$ (empty pink symbols) or their combination (filled pink symbols), and 10 µM CD cocktail (green) on pH$_{cyt}$ of **(a)** exponential and **(b)** post-diauxic cells of the pHluorin-expressing variant of the parental strain. Empty black symbols - controls. TEA$^+$ was added ∼10 minutes before and CCCP / CD cocktail ∼15 minutes after the beginning of the respective measurement (vertical dotted line with arrow). Data are representative of five independent measurements.

activity) to disappear completely. Indeed, in post-diauxic cells the extent of depolarization caused by the addition of TEA$^+$ is small and of the same extent in both strains, demonstrating the absence of any Tok1p channel contribution to $\Delta\Psi$ (Fig. 3.17(b)). In exponential cells (Fig. 3.17(a)) the use of the inhibitor does make the difference between the staining of the two strains less extensive. However, it does not result in complete merging of the staining curves. To understand the origin of this difference, we need to consider that the Tok1p channel is induced to open by the washing procedure and glucose removal (resulting in Pma1p down-regulation) preceding the addition of the inhibitor. Nevertheless, conversion of the respective $\Delta\lambda^{eq}_{max}$ to changes of $\Delta\Psi$ in millivolts (Plášek and Gášková, 2014) clearly shows that the Tok1p channel contribution to $\Delta\Psi$ maintenance after TEA$^+$ addition (amounting to ∼8 mV) is considerably smaller than in the absence of the inhibitor (∼20 mV). Since the difference between $\Delta\Psi$ of the strains originates in K$^+$ redistribution, the fact that the inhibition of the efflux-oriented Tok1p channel leads to decrease of this difference points to the existence of a simultaneous influx and efflux of potassium across the plasma membrane, consistent with general belief (Ortega and Rodríguez-Navarro, 1985; Lapathitis and Kotyk, 1998; Ariño et al., 2010; Volkov, 2015). The influx (i.e. reuptake) is most probably mediated by the action of Trk1p and Trk2p transporters.

We suggested above that the observed $\Delta\Psi$ restoration following the initial depolarization after CCCP addition is most likely the result of Pma1p activation,

which is a known effect of the protonophore (dos Passos et al., 1992; Brandão et al., 1992; Pereira et al., 2008; Hendrych et al., 2009). To prove this unambiguously, we used the lysosomotropic compound DM-11 (2-dodecanoyloxyethyldimethylammonium chloride), a known Pma1p inhibitor, that not only blocks its H^+-ATPase activity but also prevents its further activation (Witek et al., 1997). Addition of an equimolar solution of DM-11 and CCCP (the so-called CD cocktail) to both exponential (Fig. 3.16(a)) and post-diauxic (Fig. 3.16(b)) cells leads to complete depolarization of the plasma membrane due to rapid dissipation of the proton gradient that the inhibited Pma1p is unable to compensate (Hendrych et al., 2009). The depolarization is not followed by a significant restoration of λ_{max} (and hence $\Delta\Psi$), clearly indicating that the rise in staining in the absence of DM-11 is indeed the result of CCCP-induced Pma1p activation.

Curiously, however, the Tok1p channel activity after CD cocktail addition is somewhat lower than after the treatment with CCCP alone, by 6 mV in exponential and 2 mV in post-diauxic cells (see Table 3.1, cf. Plášek and Gášková (2014)). In contrast, cytosolic acidification following CD cocktail addition is practically identical to that caused by the addition of CCCP alone (Figs. 3.18(a) and 3.18(b)). It is therefore possible that the action of DM-11 causes slight inactivation of the channel.

	Tok1p contribution to $\Delta\Psi$ / CCCP-treated cells	Tok1p contribution to $\Delta\Psi$ / CD cocktail-treated cells
Exponential cells	17.3 ± 1.6 mV	11.3 ± 2.0 mV
Post-diauxic cells	10.3 ± 2.5 mV	8.6 ± 1.3 mV

Table 3.1: Contribution of Tok1p channel to $\Delta\Psi$ under chemically induced depolarization caused by protonophore CCCP (10 µM) alone and CD cocktail (10 µM CCCP + 10 µM DM-11), respectively. Means and SDs were calculated from ten independent repeats.

The results obtained with CCCP and TEA^+-treated cells show that it is more convenient to use post-diauxic cells for monitoring of Tok1p contribution to $\Delta\Psi$ maintenance under the conditions of chemical stress. Their chemically-induced depolarization is, in contrast to exponential cells, not preceded by depolarization caused by down-regulation of Pma1p upon glucose removal. Furthermore, the channel expression is higher in this growth-phase (DeRisi et al., 1997; Gasch et al., 2000; Brauer et al., 2005), making post-diauxic cells even more favourable for assays to be carried out with further chemical stressors.

3.3.3 Tok1p channel activity increases in cells treated with Pma1p inhibitor DM-11

The Pma1p inhibitor DM-11 (2-dodecanoyloxyethyldimethylammonium chloride) is known to cause depolarization of not only the parental strain used in this study (Hendrych et al., 2009), but also of other strains Palková et al. (2009). We therefore decided to study the contribution of Tok1p to the plasma membrane

maintenance in cells exposed to the compound. DM-11 is a weak base with lysosomotropic properties. Deprotonated form of such compounds readily penetrates cellular membranes, and their protonated form accumulates in acidic compartments such as vacuoles, lysosomes or endosomes. Upon exceeding the critical micellar concentration, lysosomotropic compounds can cause disruption of membranes of these subcellular compartments (Miller et al., 1983; Dubowchik et al., 1994; Obłak and Krasowska, 2010). In the case of vacuoles and lysosomes, such disruption results in the release of hydrolytic enzymes into the cytosol leading to autolysis of the cell. As mentioned above, DM-11 also inhibits the plasma membrane H^+-ATPase Pma1p and prevents its further activation (Witek et al., 1997), leading to depolarization (Hendrych et al., 2009). This depolarization most likely reflects the extent of H^+ consumption from the extracellular environment (Palková et al., 2009).

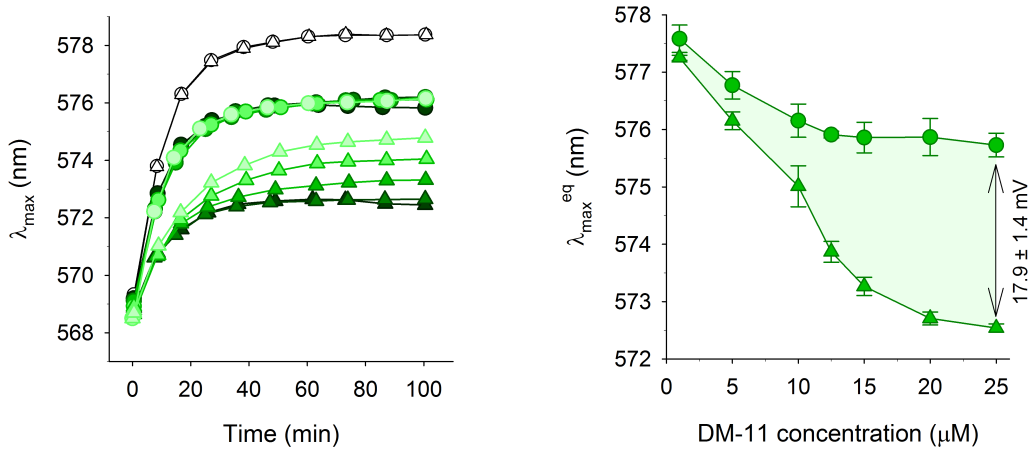

(a) Staining curves (b) Equilibrium staining

Figure 3.19: Tok1p contribution to ΔΨ restoration following exposure to DM-11. **(a)** Staining curves of the parental strain (circles) and *tok1* mutant (triangles) grown to post-diauxic phase and exposed to various concentration of DM-11 (light to dark green: 10, 12.5, 15, 20 and 25 μM) added ∼10 minutes before the probe. Lower concentrations omitted for clarity. Empty black symbols - controls. Data are representative of ten independent measurements. **(b)** Dependence of λ_{max}^{eq} of the parental strain (circles) and *tok1* mutant (triangles) on the used concentration of DM-11. Data represent means ± SDs calculated from ten independent measurements of staining curves.

Increasing the concentration of DM-11 leads to lower staining, indicating depolarization, in the cells of both strains, Figures 3.19(a) and 3.19(b)). For concentrations above 10 μM, the depolarization of the *tok1* mutant becomes gradually deeper than that of the parental strain. In contrast, the staining of the parental strain is constant in the concentration range of 10 to 25 μM. The difference between the staining of the two strains, indicating Tok1p channel activity, becomes gradually more extensive with deeper depolarization, in a manner consistent with the studies of the channel's electrophysiology (Bertl et al., 1993; Ketchum et al.,

1995; Lesage et al., 1996; Bertl et al., 1998). The highest Tok1p channel activity after treatment of cells with DM-11 corresponds to 17.9 ± 1.4 mV, as indicated by the arrow in Figure 3.19(b). While it seems that elevation of the DM-11 concentration might lead to more extensive Tok1p channel activation, exposure of cells to concentrations above 25 µM leads to compromised viability of the cells (Fig. 3.20(b)), making them unsuitable for membrane potential measurements.

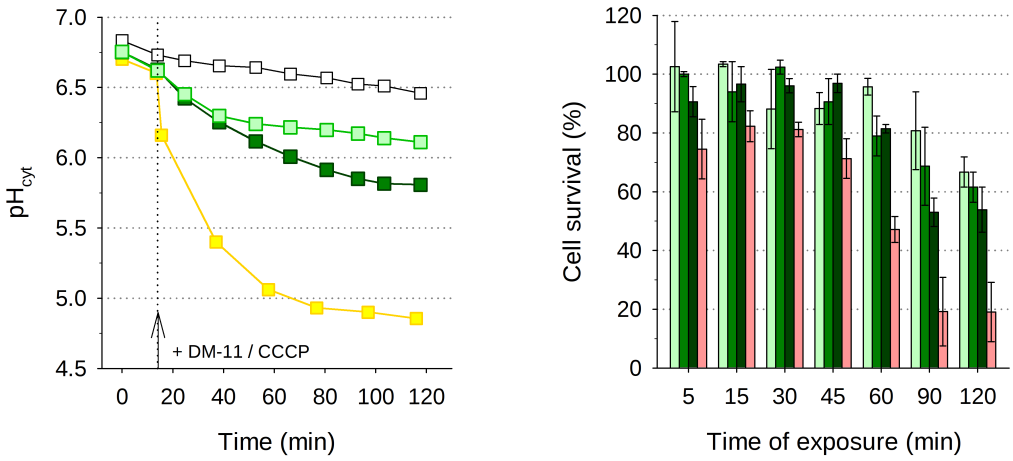

(a) Cytosolic pH

(b) Cell survival

Figure 3.20: Effect of DM-11 on pH$_{cyt}$ and cell viability. (a) Effect of 10 (light green) and 20 µM (dark green) DM-11 on pH$_{cyt}$. Empty black symbols - controls. DM-11 was added ∼18 minutes after the beginning of the measurement (vertical dotted line with arrow). 10 µM CCCP (yellow) shown for comparison. Data are representative of five independent measurements. **(b)** Viability of the parental strain after exposure to various concentrations of DM-11 (light to dark green: 10, 20, 25 µM; coral: 30 µM). Data represent means ± SDs calculated from three independent measurements of three biological replicates each.

When the cells are treated with DM-11 alone, the cytosolic acidification is much less extensive than that caused either by CCCP alone, Fig. 3.20(a), or by the combination of DM-11 with CCCP in the CD cocktail, Figures 3.18(a) and 3.18(b).

3.3.4 Tok1p channel activity increases in cells treated with the surface active compound ODDC

Another compound with a known depolarizing effect is octenidine dihydrochloride (ODDC; Kodedová et al. (2011)). As a cationic surface-active compound, ODDC binds readily to negatively charged microbial envelopes leading to their disruption. The combined effect of leaking cytoplasmic and mitochondrial (Ellabib et al., 1990) membrane results in a broad antimicrobial spectrum (Kramer and Müller, 2008) already at very low concentrations (Harke, 1989; Ghannoum et al., 1990; Hübner et al., 2010; Koburger et al., 2010) and short exposure times (Kodedová et al., 2011). A very important feature of the action of ODDC is that it is not

absorbed by human epithelial cells, including wound tissue (Hübner et al., 2010). It can therefore be used as an efficient antiseptic to treat or prevent infections of skin, mucous membranes and wounds with no adverse effects (Harke and Goroncy-Barnes, 1991). It is especially effective against biofilm-forming organisms (Hübner et al., 2010).

Figures 3.21(a) and 3.21(b) demonstrate that raising the concentration of ODDC leads to gradual depolarization of the *tok1* mutant plasma membrane, similar in character to that following exposure of cells to DM-11. Membrane potential of ODDC-treated parental strain is only slightly lower than that of controls and remains constant from 12.5 to 175 nM. The difference in staining of the two strains therefore becomes gradually more extensive with deeper depolarization. This indicates elevated Tok1p channel activity, in a manner consistent with electrophysiological studies (Gustin et al., 1990; Bertl et al., 1993). Furthermore, the Tok1p channel seems to be able to almost completely compensate the depolarization induced by ODDC of up to 175 nM. The highest Tok1p channel activity after treatment of cells with ODDC corresponds to 29.9 ± 3.4 mV (in response to 175 nM ODDC), as indicated by the arrow in Figure 3.21(b).

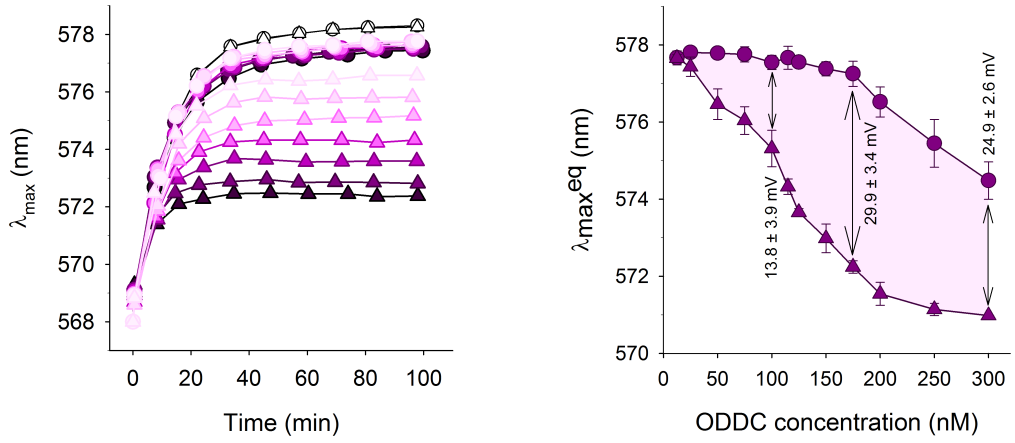

(a) Staining curves (b) Equilibrium staining

Figure 3.21: Tok1p contribution to ΔΨ restoration following exposure to ODDC. (a) Staining curves of the parental strain (circles) and *tok1* mutant (triangles) grown to post-diauxic phase and exposed to various concentrations of ODDC (light to dark: 50, 75, 100, 115, 125, 150 and 175 nM) added ∼10 minutes before the probe. Higher concentrations omitted for clarity. Empty black symbols - controls. Data are representative of ten independent measurements. **(b)** Dependence of λ_{max}^{eq} of the parental strain (circles) and *tok1* mutant (triangles) on the used concentration of ODDC. Data represent means ± SDs calculated from ten independent measurements of staining curves.

Raising the ODDC concentrations to 200 nM and above results in lower equilibrium staining of the parental strain. λ_{max}^{eq} of the *tok1* mutant also decreases with increasing ODDC concentration, but not as rapidly as in the case of the parental strain. This indicates concentration-dependent lowering of Tok1p chan-

nel contribution to $\Delta\Psi$ at concentrations above 200 nM (Fig. 3.21(b)). This might be caused by various effects of ODDC on cell surface structures, e.g. weakening of the cell envelope, as was shown to be the result of one-hour incubation of cells with 240 nM ODDC (Ghannoum et al., 1990). However, while the cell envelope might be affected, we have shown using the plating test that even 90-minute exposure of cells to a concentration as high as 300 nM does not lead to a statistically significant loss of cell survival (Fig. 3.22(b)).

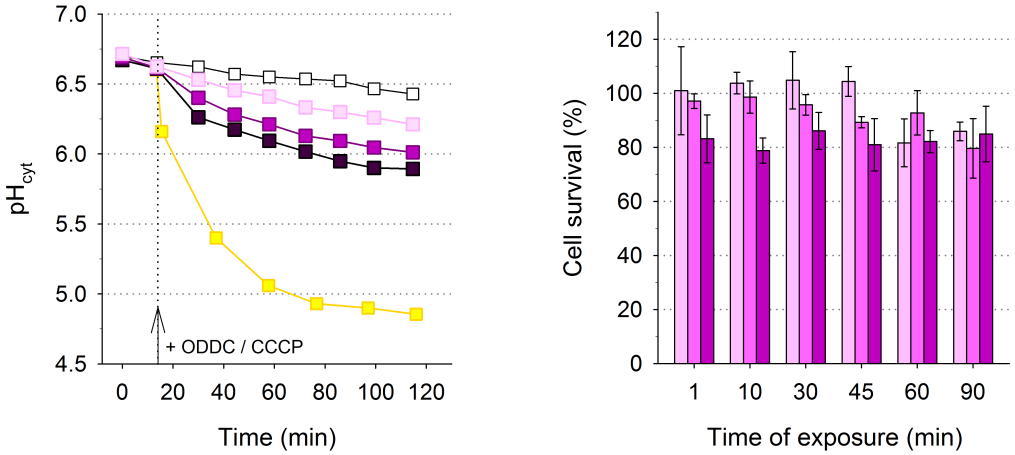

(a) Cytosolic pH (b) Cell survival

Figure 3.22: Effect of ODDC on pH$_{cyt}$ and cell viability. (a) Effect of various concentrations of ODDC on pH$_{cyt}$ (light to dark: 100, 200, 300 nM). Empty black symbols - controls. ODDC was added ∼18 minutes after the beginning of the measurement (vertical dotted line with arrow). 10 µM CCCP (yellow) for comparison. Data are representative of five independent measurements. **(b)** Viability of the parental strain after exposure to various concentrations of ODDC (light to dark: 100, 200, 300 nM). Data represent means ± SDs calculated from three independent measurements of three biological replicas each.

Simultaneously with the plasma membrane depolarization, ODDC causes relatively low, concentration-dependent, cytosolic acidification (0.6 ± 0.3 pH units after almost 2-hour exposure to 300 nM ODDC) compared to the effect of CCCP (1.7 ± 0.4 pH units), Figure 3.22(a).

Comparing the contribution of Tok1p channel to $\Delta\Psi$ at the corresponding level of depolarization of the *tok1* mutant (572.3 nm) following the addition of ODDC (∼30 mV, Fig. 3.21(a) or 3.21(b)) and CCCP (∼16.5 mV, Fig. 3.16(b)) clearly demonstrates that the effect of cytosolic acidification on the channel activity is considerable. In this case, deepening the acidification by 1 pH unit causes a loss of about 45 % of the channel's activity. Curiously, however, even at pH$_{cyt}$ ∼6.0, when the Tok1p opening probability is believed to be only about 15 % (Lesage et al., 1996), the channel is still able to almost completely counterbalance the loss of $\Delta\Psi$ caused by the action of up to 175 nM ODDC.

When compared to DM-11, exposure of the parental strain to ODDC leads to less extensive depolarization, indicating higher contribution of the channel to

$\Delta\Psi$ relative to that after the exposure of DM-11 (by ∼11 mV). To bring an insight into the lower Tok1p channel activity after exposure to DM-11 compared to ODDC, one needs to consider the cytosolic acidification at concentrations leading to the same depolarization (Fig. 3.19(a), 3.20(a) and 3.21(a), 3.22(a)). However, since the compounds cause comparable extent of cytosolic acidification, the effect of pH_{cyt} on Tok1p channel activity after exposure to the compounds is also comparable.

Since DM-11 is known to interact with Pma1p (Witek et al., 1997), it is possible that it also interacts with the Tok1p channel, causing slight inactivation. This interaction can be either direct or mediated by affecting the immediate lipid environment of the channel after incorporation in the plasma membrane, a known action of the compound (Kane, 1995). While the elucidation of the actual inactivation mechanism is beyond the scope of the present study, it is clear that not only cytosolic acidification (as was the case under CCCP-induced depolarization), but also other effects of the stressor may influence the Tok1p channel activity.

3.3.5 Tok1p channel is inhibited by BAC in a concentration-dependent manner

In order to gain deeper understanding of the various stressor-mediated effects that may lead to lowering of the Tok1p channel opening capacity, we deployed BAC (benzalkonium chloride), a synthetic quaternary ammonium compound with a broad antimicrobial spectrum (Fazlara and Ekhtelat, 2012). BAC has found a wide range of use from sanitation of surfaces and production lines in the food industry (Kuda et al., 2008), through clinical sanitation and topical treatment in health care facilities as well as first-aid kits, to antimicrobial preservation at low concentrations (Pernak, 1999; Mangalappalli-Illathu and Korber, 2006). Very common is also the use of BAC in rinse-free hand sanitizers (Moadab et al., 2001) and intranasal treatments, where it serves a preservative function and appears to be well-tolerated by human cells even after tong-term use (Marple et al., 2004).

Being a cationic surface active compound, BAC induces plasma membrane disorganization which affects its general permeability. While causing depolarization at low concentrations, the use of higher concentrations inevitably leads to leakage of low molecular weight materials (Salton, 1968) and damage to the plasma membrane, promoting further uptake of the compound. Once inside the cell, BAC affects cell metabolism. In fact, it has been clearly shown that BAC toxicity lies predominantly within metabolic inhibition rather than plasma membrane damage (Kodedová et al., 2011).

As evident from Figures 3.23(a) and 3.23(b), the response of the Tok1p channel to BAC is considerably distinct from all CCCP, DM-11 and ODDC. While the exposure of cells to low concentrations (1 and 1.5 µM) leads to a response comparable in character to that produced by ODDC and DM-11, indicating stable extent of depolarization (Fig. 3.23(a)), exposure to higher concentrations exhibits a "two-phase" character. In this case, the initial quasi-equilibrium depolarization

is followed by another slow decrease of $\Delta\Psi$ and establishing of a new equilibrium (Fig. 3.23(a)). Furthermore, the difference between respective λ_{max}^{eq} values found for the parental strain and the *tok1* mutant decreases for BAC concentrations over 2.5 µM (Fig. 3.23(b)). On the other hand, the equilibrium difference gradually increased with increasing concentration of DM-11 (Fig. 3.19(b)) and ODDC (Fig. 3.21(b)).

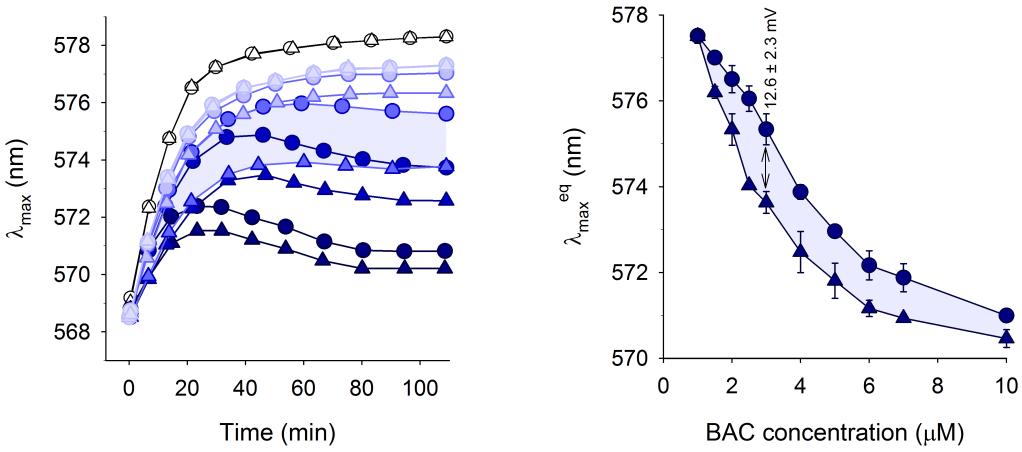

(a) Staining curves (b) Equilibrium staining

Figure 3.23: Tok1p is inhibited by BAC in a concentration-dependent manner. (a) Staining curves of the parental strain (circles) and *tok1* mutant (triangles) grown to post-diauxic phase and exposed to various concentration of BAC (light to dark blue: 1, 1.5, 2.5, 4 and 10 µM) added ∼10 minutes before the probe. Empty black symbols - controls. Data are representative of ten independent measurements. **(b)** Dependence of λ_{max}^{eq} of the parental strain (circles) and *tok1* mutant (triangles) on the used concentration of BAC. Data represent means ± SDs calculated from ten independent measurements of staining curves.

Besides extensive depolarization, addition of BAC causes slight, concentration-dependent, acidification. The effect of BAC on pH_{cyt} is almost equal to that caused by DM-11 and ODDC at concentrations causing the same extent of depolarization (Fig. 3.24).

In the case of the the lysosomotropic compound DM-11, membrane depolarization reflects the extent of H^+ entering the cytosol that is not counterbalanced by Pma1p due to its inhibition by the compound (Palková et al., 2009). On the other hand, the $\Delta\Psi$ decrease caused by BAC is associated with a leakage of intracellular molecules, including those absorbing light at 260 nm, such as ATP (Fig. 3.25(a); Salton (1968)). Within the range of BAC concentrations used for $\Delta\Psi$ measurements (Fig. 3.23(b)) the leakage of intracellular material increases very slowly compared to the sharp rise following the increase of BAC concentration to 50 µM. Furthermore, as monitored by propidium iodide staining, BAC concentrations ≤10 µM cause only a very limited fraction of the suspension to become permeabilized (Fig. 3.25(b)). Taken together, these results indicate that BAC-induced depolarization is not a trivial consequence of membrane permeabilization.

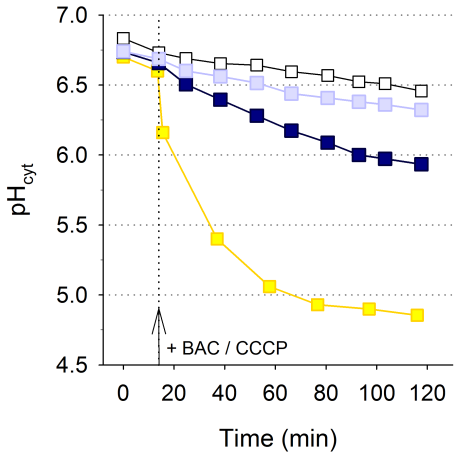

Figure 3.24: Effect of BAC on pH$_{cyt}$. Effect of 1 (light blue) and 10 µM (dark blue) BAC on pH$_{cyt}$. Empty black symbols - controls. BAC was added ∼18 minutes after the beginning of the measurement (vertical dotted line with arrow). 10 µM CCCP (yellow) shown for comparison. Data are representative of five independent measurements.

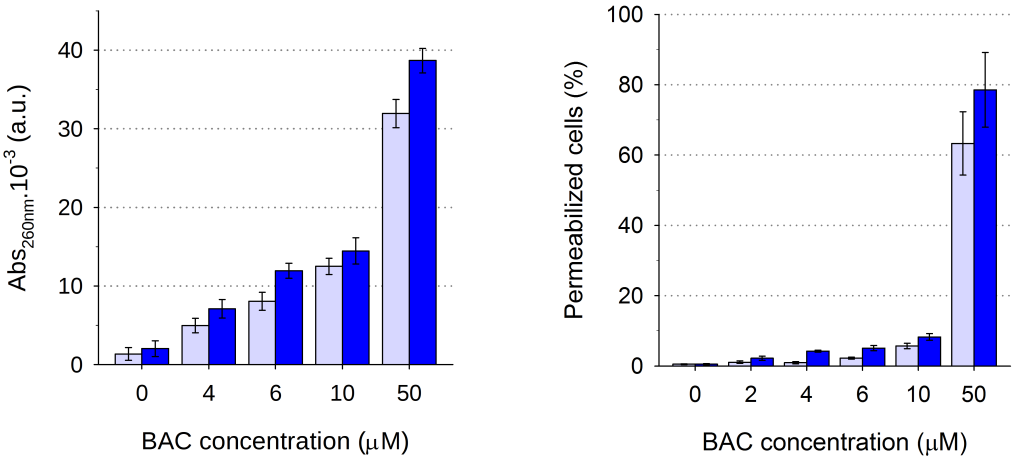

(a) Intracellular material release (b) Permeabilization of cells

Figure 3.25: Used concentrations of BAC do not have detrimental effect on the plasma membrane. (a) Dependence of release of low molecular-weight intracellular material absorbing light at 260 nm on the used concentration of BAC. **(b)** Dependence of the amount of permeabilized cells on the used concentration of BAC. In both cases, data were obtained from measurements in suspensions of the parental strain cells, exposed to BAC for 60 (light) or 120 (dark) minutes. Data represent means ± SDs calculated from three independent measurements of three biological replicates each.

Many processes within living cells, many of which are connected to activity of membrane transporters, are directly dependent on the presence of ATP in the cytoplasm. In fact, an electrophysiological study has shown that the opening of the Tok1p channel is one such case (Bertl et al., 1998). We were therefore interested

in monitoring the effect of ATP depletion on Tok1p channel activity. For this purpose, washed post-diauxic cells were incubated for 2 hours in C-P buffer with 5 mM 2-deoxy-D-glucose (2DG; Fig. 3.26). As above, the difference between λ_{max}^{eq} values of the parental strain and that of the *tok1* mutant is a good measure of Tok1p activity. Addition of 2.5 µM BAC to cells pretreated with 2DG seems to result in slight depolarization. However, it is rather small (within the standard error) and of the same extent in both strains. Moreover, higher concentrations of BAC do not provide any indication of 2DG-mediated effect either. We therefore conclude that neither the depletion of ATP by incubating the cells with 2DG, nor the starvation of washed cells without glucose has any significantly detrimental effect on the Tok1p channel activity *in vivo*, at least under our experimental conditions.

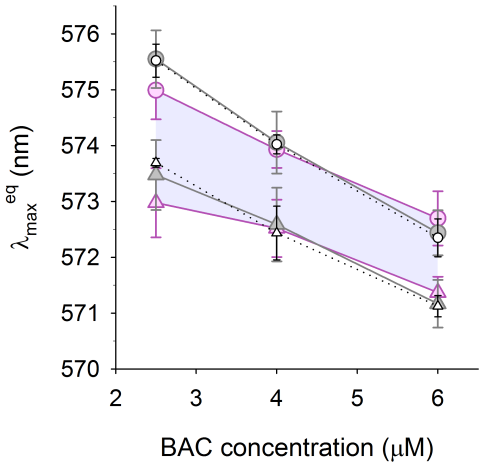

Figure 3.26: Depletion of intracellular ATP by 2-hour incubation with 2-deoxy-D-glucose (2DG) does not affect Tok1p channel opening capacity. The concentration-dependent equilibrium staining levels (λ_{max}^{eq}) of BAC-treated post-diauxic cells of the parental strain (circles) and *tok1* mutant (triangles) incubated with 5 mM 2-deoxy-D-glucose (2DG) for 2 hours to deplete intracellular ATP (pink); effect of 0-hour (empty black) and 2-hour (grey) starvation in absence of 2DG shown for comparison. Data represent means ± SDs calculated from three independent measurements.

Our results indicate that in contrast to DM-11 and ODDC, increasing the concentration of BAC leads to lowering of Tok1p channel activity (as revealed by the difference between probe accumulation in the parental strain and the *tok1* mutant). The underlying cause of this effect could be extensive cytosolic acidification. However, as demonstrated by Figure 3.24, the effect of BAC on pH_{cyt} is not significantly different (if possibly slightly less extensive) from the effect of DM-11 and ODDC at concentrations causing the same extent of depolarization. It is therefore clear that the subpar contribution of Tok1p to $\Delta\Psi$ after exposure of cells to BAC is not the result of low pH_{cyt}, and that not only the ultimate effect of a stressor, but also its mode of action is an important determinant of Tok1p opening capacity.

Despite our extensive efforts to pinpoint a simple cause of the observed decrease of Tok1p channel activity, we have not been able to find one related to the cell metabolism. We therefore conclude that BAC most probably exerts is influence on the Tok1p channel by a direct interaction, which is supported by the known binding of BAC molecules not only to phospholipids but also proteins in the plasma membrane of bacteria (Maris, 1995). Furthermore, the relatively slow decrease of membrane potential and, concomitantly, Tok1p activity following the treatment of cells with BAC (Fig. 3.23(a)) suggests that the possible interaction of BAC with the channel takes place predominantly from the intracellular side. Since BAC is known to modify the properties of the plasma membrane, it is also possible that the inhibitory effect is caused by the interaction of BAC with the immediate lipid microenvironment of the Tok1p channel, as we have shown to be the case of the inhibitory action of alcohols on Pdr5p and Snq2p activity (section 3.2.6).

3.3.6 Comparison of Tok1p channel activity in response to depolarization caused by ODDC, BAC and DM-11

In this work we made use of a small set of chemical stressors known to cause plasma membrane depolarization, each by a distinct mechanism of action. These substances were used to search for a hypothetical relationship between the extent of yeast plasma membrane depolarization and Tok1p channel activity, as assessed from the difference in staining of the parental strain and the *tok1* mutant.

To directly and conveniently compare the effect of the stressors on Tok1p channel opening, we plotted the dependence of the channel's activity in equilibrium on the respective depolarization of treated *tok1* mutant cells, expressed either in nm (Fig. 3.27(a)) or directly in mV (Fig. 3.27(b)). The latter approach provides us with an additional advantage of the possibility to directly compare the absolute values of Tok1p-mediated membrane potential repolarization in response to exposure of the cells to various stressors.

As evident from Figure 3.27, there is almost no difference between the stressors at concentrations leading to low depolarizations (up to ∼10 mV). As the depolarization becomes deeper, however (above ∼15 mV), the differences in the Tok1p channel activity are revealed as a direct consequence of the distinct modes of action of the compounds. The most striking difference between the stressors can be observed when the depolarization lies within the range of 30–40 mV (Fig. 3.27(b)). While the channel is able to counterbalance astounding ∼75 % of the depolarization caused by ODDC within said range, inducing equivalent depolarization by BAC enables the Tok1p channel to counterbalance only about 25 % of the lost membrane potential. This clearly points to the adverse and possibly direct effects of the latter on the channel, as discussed above. Repolarization efficiency in the response to exposure to DM-11 lies somewhere in the middle between ODDC and BAC, just below 50 %.

As discussed above, the selected stressors elicit similar degree of cytosolic acidification in the treated cells, making their direct comparison quite straightforward.

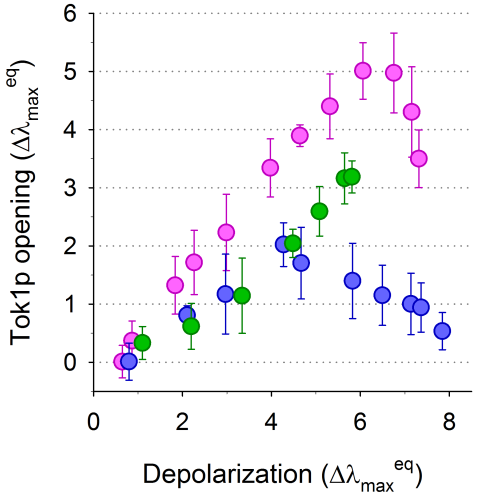

(a) Expressed in $\Delta\lambda_{max}^{eq}$

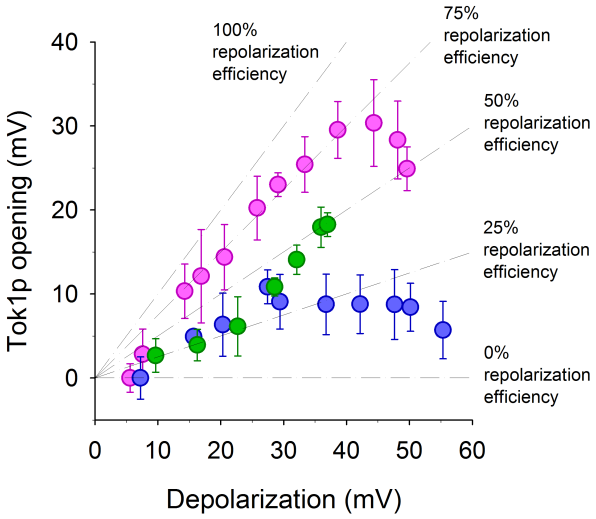

(b) Expressed in mV

Figure 3.27: Mode of action of a stressor influences the Tok1p channel activity in response to depolarization in a concentration-dependent manner. Extent of Tok1p channel opening in response to depolarization caused by various concentrations of DM-11 (green), ODDC (pink) and BAC (blue) expressed in **(a)** $\Delta\lambda_{max}^{eq}$ and **(b)** mV. Data represent means ± SDs calculated from λ_{max}^{eq} from five independent measurements. The DM-11 dependence is cut short compared to BAC and ODDC, since higher concentrations lead to loss of membrane integrity.

CCCP was not included into this analysis as it induces much greater pH_{cyt} change than the other stressors. Despite the comparable effect of DM-11, ODDC and BAC on pH_{cyt}, Figure 3.27 clearly displays differences in Tok1p channel activity in response to each of these compounds.

Our results clearly show that when assessing the contribution of the Tok1p channel to membrane potential maintenance under chemical stress, it is not sufficient to consider the extent of depolarization as the sole determinant. More specifically, the used stressor might cause further effects that can negatively influence the opening capacity of the channel (Fig. 3.28). These include transfer of hydrogen ions into the cell and acidification of the cytosol, direct interaction with the plasma membrane and possibly influx of the compound into the cell. The influx may in turn lead to further effects either on metabolism or membrane structures within the cytoplasm, or interaction with the plasma membrane or the Tok1p channel itself from the intracellular side. While the application of a stressor does not have to necessarily lead to all of them, we see that the effects are somewhat intertwined and not completely independent. Our results indicate that the most adverse effects of a stressor on the Tok1p channel activity are produced by its direct interaction with the Tok1p channel and/or by affecting its immediate lipid environment.

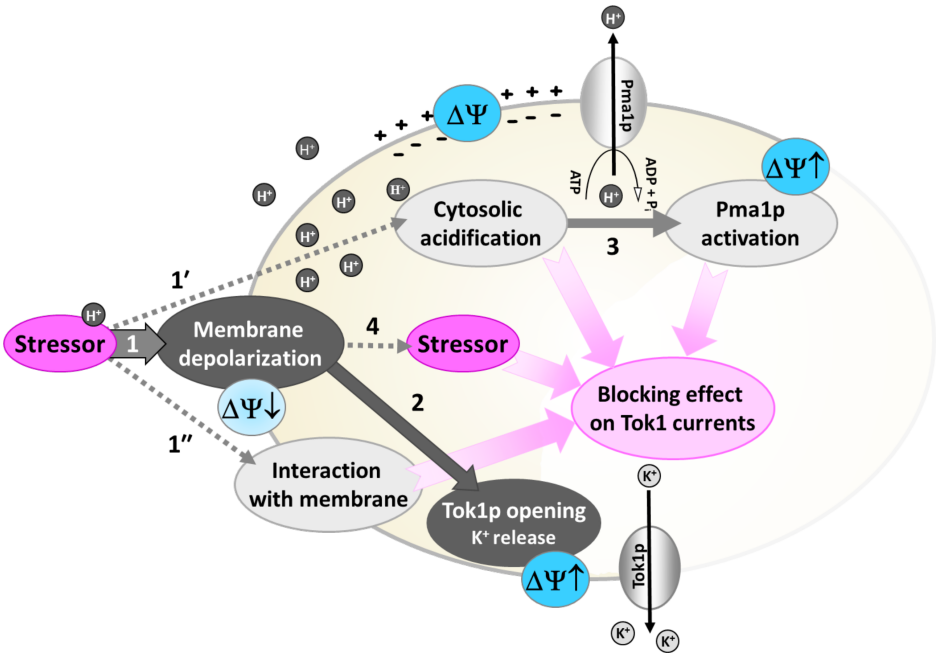

Figure 3.28: Overview of different possible actions of chemical stressors, not limited to influence on membrane potential Besides causing **(1)** plasma membrane depolarization, leading to **(2)** Tok1p channel opening, the chemical stressor may also: **(1')** cause cytosolic acidification, leading to **(3)** Pma1p activation and rise in $\Delta\Psi$; **(1")** interact with the plasma membrane, and **(4)** pass through the plasma membrane into the cytosol and affect cellular metabolism or interact with the channel directly. All of the above may cause lowering of the Tok1p channel activity.

Chapter 4

Conclusions

The main aim of the doctoral thesis has been the monitoring of the effect of various compounds on both multidrug resistance proteins Pdr5p and Snq2p, and on membrane potential, focusing on the activity of the potassium channel Tok1p. As the dominant approach, the diS-$C_3(3)$ fluorescence assay was used, supported by other methods, such as disc-diffusion assays, plating tests, monitoring of both intracellular and extracellular pH, confocal microscopy and other.

The results have already been published in peer-reviewed scientific journals (Attachments I and II) and presented either orally or in the form of a poster at international conferences (Attachments III to VII).

The first part of the thesis focuses on the effect of short linear alcohols on the function of multidrug resistance pumps Pdr5p and Snq2p. Alcohols have been known for some time to exhibit an inhibitory effect on various receptors, channels and transporters. We therefore decided to verify the possibility that alcohols could also inhibit the action of Pdr5p and Snq2p and hence contribute to the fight against multidrug resistance. In the case of a positive result, we also aimed to explain the origin of the inhibition.

Focusing on low concentrations of short n-alcohols (ethanol to hexanol), we found that all of these compounds variously affect the activity of both Pdr5p and Snq2p. The inhibitory efficiency proved to increase with both concentration and length of the alcohols. While very high concentrations of ethanol are necessary to produce a full inhibitory effect (15 %; simultaneously causing deep depolarization), a concentration of hexanol as low as 0.1 % produces a comparable effect, while affecting neither membrane potential nor integrity of the plasma membrane. What is especially fascinating is the low concentration at which alcohols exhibit their effective inhibitory action. We have shown that the inhibition is not caused by the loss of plasma membrane integrity, nor depletion of ATP. Rather, it originates in direct interaction with the Pdr5p and Snq2p protein molecules. Alternatively, the inhibition may stem from affected mechanical properties of the plasma membrane, such as fluidity. Our conclusion is further supported by the full reversibility of the inhibitory action of alcohols by simple washing of the cells with the measurement buffer.

The alcohols can be used therapeutically in a combination with currently available antifungals and possibly antibiotics or chemotherapy drugs (if their effect proves to be of a wide enough specificity) in order to make the available means of treatment more effective.

The second part of the thesis focuses on the activity of the potassium channel Tok1p and its contribution to membrane potential. While we have also examined the Tok1p channel behaviour in non-stress conditions, our main interest was monitoring of the channel's activity and contribution to plasma membrane potential maintenance under chemically-induced stress. We were further interested in effects of the stressors beside the actual depolarization and how these may affect the activity of the Tok1p channel.

Our analysis has shown that the capacity of the channel to counterbalance chemically-induced depolarization is amazing, amounting up to 75 % in some cases. In absolute values, the maximum contribution of the Tok1p channel to membrane potential is around 35-40 mV. Considering that the absolute value of membrane potential is believed to be ∼100 mV, it is plain that the channel is much more important in maintenance of this critical cellular parameter than has been previously believed. The astonishing capacity of the channel is further underlined by the fact than based on electrophysiological reports, there are only around 50 Tok1p channel molecules in the plasma membrane.

We have further shown that when assessing the Tok1p channel contribution to membrane potential maintenance, it is essential to consider not only the extent of depolarization, but also the mode of action of the used stressor and its possible side effects. The most extensive negative effects are caused by direct interaction of the stressor either with the channel or its immediate lipid microenvironment.

Bibliography

Adey, G., Wardley-Smith, B. and White, D. (1975). Mechanism of inhibition of bacterial luciferase by anaesthetics. *Life Sci.*, **17**, 1849–1854.

Aguilar-Uscanga, B. and François, J. M. (2003). A study of the yeast cell wall composition and structure in response to growth conditions and mode of cultivation. *Lett. Appl. Microbiol.*, **37**(3), 268–274.

Aguilera, F., Peinado, R. A., Millán, C., Ortega, J. M. and Mauricio, J. C. (2006). Relationship between ethanol tolerance, H^+-ATPase activity and the lipid composition of the plasma membrane in different wine yeast strains. *Int. J. Food Microbiol.*, **110**(1), 34–42.

Ahmed, A., Sesti, F., Ilan, N., Shih, T., Sturley, S. L. and Goldstein, S. A. N. (1999). A molecular target for viral killer toxin: TOK1 potassium channels. *Cell*, **99**, 291–293.

Akache, B. and Turcotte, B. (2002). New regulators of drug sensitivity in the family of yeast zinc cluster proteins. *J. Biol. Chem.*, **277**(24), 21254–21260.

Alexandre, H., Berlot, J. P. and Charpentier, C. (1994). Effect of ethanol on membrane fluidity of protoplasts from *Saccharomyces cerevisiae* and *Kloeckera apiculata* grown with or without ethanol, measured by fluorescence anisotropy. *Biotechnol. Tech.*, **8**(5), 295–300.

Ali, R., Brett, C. L., Mukherjee, S. and Rao, R. (2004). Inhibition of sodium/proton exchange by a Rab-GTPase-activating protein regulates endosomal traffic in yeast. *J. Biol. Chem.*, **279**(6), 4498–4506.

Alkire, M. T. and Gorski, L. A. (2004). Relative amnesic potency of five inhalational anesthetics follows the Meyer-Overton rule. *Anesthesiology*, **101** (2), 417–429.

Ames, G. F.-L. (1986). Bacterial periplasmic transport systems: structure, mechanism, and evolution. *Annu. Rev. Biochem.*, **55**, 397–425.

Ariño, J., Ramos, J. and Sychrová, H. (2010). Alkali metal cation transport and homeostasis in yeasts. *Microbiol. Mol. Biol. Rev.*, **74**(1), 95–120.

Balzi, E., Chen, W., Ulaszewski, S., Capieaux, E. and Goffeau, A. (1987). The multidrug resistance gene *PDR1* from *Saccharomyces cerevisiae*. *J. Biol. Chem.*, **262**(35), 16871–16879.

Balzi, E., Wang, M., Leterme, S., Vandyck, L. and Goffeau, A. (1994). PDR5, a novel yeast multidrug resistance conferring transporter controlled by the transcription regulator PDR1. *J. Biol. Chem.*, **269**(3), 2206–2214.

Balzi, E. and Goffeau, A. (1994). Genetics and biochemistry of yeast multidrug resistance. *Biochim. Biophys. Acta - Bioenerg.*, **1187**(2), 152–162.

Bandas, E. L. and Zakharov, I. A. (1980). Induction of rho$^-$ mutations in yeast *Saccharomyces cerevisiae* by ethanol. *Mutat. Res. - Fundam. Mol. Mech. Mutagen.*, **71**(2), 193–199.

Bañuelos, M. A., Sychrová, H., Bleykasten-Grosshans, C., Souciet, J.-L. and Potier, S. (1998). The Nha1 antiporter of *Saccharomyces cerevisiae* mediates sodium and potassium efflux. *Microbiology*, **144**, 2749–2758.

Barnes, G., Drubin, D. G. and Stearns, T. (1990). The cytoskeleton of *Saccharomyces cerevisiae*. *Curr. Opin. Cell Biol.*, **2**(1), 109–115.

Bauer, B. E., Wolfger, H. and Kuchler, K. (1999). Inventory and function of yeast ABC proteins: About sex, stress, pleiotropic drug and heavy metal resistance. *Biochim. Biophys. Acta - Biomembr.*, **1461**(2), 217–236.

Beaven, M. J., Charpentier, C. and Rose, A. H. (1982). Production and tolerance of ethanol in relation to phospholipid fatty-acyl composition in *Saccharomyces cerevisiae* NCYC 431. *Microbiology*, **128**(7), 1447–1455.

Beilin, L. J. and Puddey, I. B. (1992). Alcohol and hypertension. *Clin. Exp. Hypertens. Part A Theory Pract.*, **14**(1-2), 119–138.

Benito, B., Portillo, F. and Lagunas, R. (1992). *In vivo* activation of the yeast plasma membrane ATPase during nitrogen starvation. Identification of the regulatory domain that controls activation. *FEBS Lett.*, **300**(3), 271–274.

Benito, B., Quintero, F. J. and Rodríguez-Navarro, A. (1997). Overexpression of the sodium ATPase of *Saccharomyces cerevisiae*: Conditions for phosphorylation from ATP and P_i. *Biochim. Biophys. Acta - Biomembr.*, **1328** (2), 214–226.

Benito, B., Garciadeblás, B. and Rodríguez-Navarro, A. (2002). Potassium- or sodium-efflux ATPase, a key enzyme in the evolution of fungi. *Microbiology*, **148**, 933–941.

Bennis, S., Chami, F., Chami, N., Bouchikhi, T. and Remmal, A. (2004). Surface alteration of *Saccharomyces cerevisiae* induced by thymol and eugenol. *Lett. Appl. Microbiol.*, **38**(6), 454–458.

Bertl, A., Bihler, H., Reid, J. D., Kettner, C. and L, S. C. (1998). Physiological characterization of the yeast plasma membrane outward rectifying K^+ channel, DUK1 (TOK1), *in situ*. *J. Membr. Biol.*, **162**, 67–80.

Bertl, A., Ramos, J., Ludwig, J., Lichtenberg-Frate, H., Reid, J., Bihler, H., Calero, F., Martinez, P. and Ljungdah, P. O. (2003). Characterization of potassium transport in wild-type and isogenic yeast strains carrying all combinations of *trk1*, *trk2* and *tok1* null mutations. *Mol. Microbiol.*, **47**(3), 767–780.

Bertl, A., Slayman, C. L. and Gradmann, D. (1993). Gating and conductance in an outward-rectifying K^+ channel from the plasma membrane of *Saccharomyces cerevisiae*. *J. Membr. Biol.*, **132**, 183–199.

Betz, C., Schlenstedt, G. and Bailer, S. M. (2004). Asr1p, a novel yeast Ring/PHD finger protein, signals alcohol stress to the nucleus. *J. Biol. Chem.*, **279**(27), 28174–28181.

Bihler, H., Slayman, C. L. and Bertl, A. (1998). NSC1: A novel high-current inward rectifier for cations in the plasma membrane of *Saccharomyces cerevisiae*. *FEBS Lett.*, **432**(1-2), 59–64.

Bihler, H., Gaber, R. F., Slayman, C. L. and Bertl, A. (1999). The presumed potassium carrier Trk2p in *Saccharomyces cerevisiae* determines an H^+-dependent, K^+-independent current. *FEBS Lett.*, **447**(1), 115–120.

Bihler, H., Slayman, C. L. and Bertl, A. (2002). Low-affinity potassium uptake by *Saccharomyces cerevisiae* is mediated by NSC1, a calcium-blocked non-specific cation channel. *Biochim. Biophys. Acta - Biomembr.*, **1558**(2), 109–118.

Birch, R. M. and Walker, G. M. (2000). Influence of magnesium ions on heat shock and ethanol stress responses of *Saccharomyces cerevisiae*. *Enzyme Microb. Technol.*, **26**(9-10), 678–687.

Bissinger, P. H. and Kuchler, K. (1994). Molecular cloning and expression of the *Saccharomyces cerevisiae STS1* gene product: A yeast ABC transporter conferring mycotoxin resistance. *J. Biol. Chem.*, **269**(6), 4180–4186.

Blednov, Y. A. and Harris, R. A. (2009). Deletion of vanilloid receptor (TRPV1) in mice alters behavioral effects of ethanol. *Neuropharmacology*, **56** (4), 814–820.

Boles, E. and Hollenberg, C. P. (1997). The molecular genetics of hexose transport in yeasts. *FEMS Microbiol. Rev.*, **21**(1), 85–111.

Bose, I., Reese, A. J., Ory, J. J., Janbon, G. and Doering, T. L. (2003). A yeast under cover: the capsule of *Cryptococcus neoformans*. *Eukaryot. Cell*, **2**(4), 655–663.

Brandão, R. L., Castro, I. M., Passos, J. B., Nicoli, J. R. and Thevelein, J. M. (1992). Glucose-induced activation of the plasma membrane H^+-ATPase in *Fusarium oxysporum*. *J. Gen. Microbiol.*, **138**, 1579–1586.

Brauer, M. J., Saldanha, A. J., Dolinski, K. and Botstein, D. (2005). Homeostatic adjustment and metabolic remodeling in glucose-limited yeast cultures. *Mol. Biol. Cell*, **16**, 2503–2517.

Breinig, F., Tipper, D. J. and Schmitt, M. J. (2002). Kre1p, the plasma membrane receptor for the yeast K1 viral toxin. *Cell*, **108**(3), 395–405.

Brett, C. L., Tukaye, D. N., Mukherjee, S. and Rao, R. (2005). The yeast endosomal $Na^+(K^+)/H^+$ exchanger Nhx1 regulates cellular pH to control vesicle trafficking. *Mol. Biol. Cell*, **16**, 1396–1405.

Browne, B. L., Clendon, V. M. C. and Bedwell, D. M. (1996). Mutations within the first LSGGQ motif of Ste6p cause defects in a -factor transport and mating in *Saccharomyces cerevisiae*. *J. Bacteriol.*, **178**(6), 1712–1719.

Cabib, E., Bowers, B. and Roberts, R. L. (1983). Vectorial synthesis of a polysaccharide by isolated plasma membranes. *Proc. Natl. Acad. Sci. USA*, **80**(11), 3318–3321.

Cabib, E. and Arroyo, J. (2013). How carbohydrates sculpt cells: chemical control of morphogenesis in the yeast cell wall. *Nat. Rev. Microbiol.*, **11**(9), 648–655.

Čadek, R., Chládková, K., Sigler, K. and Gášková, D. (2004). Impact of the growth phase on the activity of multidrug resistance pumps and membrane potential of *S. cerevisiae*: Effect of pump overproduction and carbon source. *Biochim. Biophys. Acta - Biomembr.*, **1665**(1-2), 111–117.

Campetelli, A. N., Previtali, G., Arce, C. A., Barra, H. S. and Casale, C. H. (2005). Activation of the plasma membrane H^+-ATPase of *Saccharomyces cerevisiae* by glucose is mediated by dissociation of the H^+-ATPase-acetylated tubulin complex. *FEBS J.*, **272**(22), 5742–5752.

Capasso, J. M., Li, P., Guideri, G. and Anversa, P. (1991). Left ventricular dysfunction induced by chronic alcohol ingestion in rats. *Am. J. Physiol.*, **261**(1 Pt 2), H212–H219.

Capieaux, E., Vignais, M. L., Sentenac, A. and Goffeau, A. (1989). The yeast H^+-ATPase gene is controlled by the promoter binding factor TUF. *J. Biol. Chem.*, **264**(13), 7437–7446.

Carlsen, H. N., Degn, H. and Lloyd, D. (1991). Effects of alcohols on the respiration and fermentation of aerated suspensions of baker's yeast. *J. Gen. Microbiol.*, **137**(12), 2879–2883.

Carmelo, V., Santos, H. and Sá-Correia, I. (1997). Effect of extracellular acidification on the activity of plasma membrane ATPase and on the cytosolic and vacuolar pH of *Saccharomyces cerevisiae*. *Biochim. Biophys. Acta - Biomembr.*, **1325**(1), 63–70.

Cartwright, C. P., Veazey, F. J. and Rose, A. H. (1987). Effect of ethanol on activity of the plasma-membrane ATPase in, and accumulation of glycine by, *Saccharomyces cerevisiae*. *J. Gen. Microbiol.*, **133**(4), 857–865.

Casal, M., Cardoso, H. and Leão, C. (1998). Effects of ethanol and other alkanols on transport of acetic acid in *Saccharomyces cerevisiae*. *Appl. Environ. Microbiol.*, **64**(2), 665–668.

Castillo Agudo, L. (1992). Lipid content of *Saccharomyces cerevisiae* strains with different degrees of ethanol tolerance. *Appl. Microbiol. Biotechnol.*, **37**, 647–651.

Chanson, M., Bruzzone, R., Bosco, D. and Meda, P. (1989). Effects of *n*-alcohols on junctional coupling and amylase secretion of pancreatic acinar cells. *J. Cell. Physiol.*, **139**(1), 147–156.

Charlton, M. E., Sweetnam, P. M., Fitzgerald, L. W., Terwilliger, R. Z., Nestler, E. J. and Duman, R. S. (1997). Chronic ethanol administration regulates the expression of $GABA_A$ receptor α_1 and α_5 subunits in the ventral tegmental area and hippocampus. *J. Neurochem.*, **68**(1), 121–127.

Cheng, Q. and Michels, C. A. (1991). *MAL11* and *MAL61* encode the inducible high-affinity maltose transporter of *Saccharomyces cerevisiae*. *J. Bacteriol.*, **173**(5), 1817–1820.

Cherry, J. M., Ball, C., Weng, S., Juvik, G., Schmidt, R., Adler, C., Dunn, B., Dwight, S., Riles, L., Mortimer, R. K. and Botstein, D. (1997). Genetic and physical maps of *Saccharomyces cerevisiae*. *Nature*, **387** (6632 Suppl), 67–73.

Chládková, K., Hendrych, T., Gášková, D., Goroncy-Bermes, P. and Sigler, K. (2004). Effect of biocides on *S. cerevisiae*: relationship between short-term membrane affliction and long-term cell killing. *Folia Microbiol.*, **49** (6), 718–724.

Cid, A., Perona, R. and Serrano, R. (1987). Replacement of the promoter of the yeast plasma membrane ATPase gene by a galactose-dependent promoter and its physiological consequences. *Curr. Genet.*, **12**(2), 105–110.

Cosgrove, D. J. (1997). Creeping walls, softening fruit, and penetrating pollen tubes: The growing roles of expansins. *Proc. Natl. Acad. Sci. USA*, **94**(11), 5504–5505.

Cowart, L. A. and Obeid, L. M. (2007). Yeast sphingolipids: Recent developments in understanding biosynthesis, regulation, and function. *Biochim. Biophys. Acta - Mol. Cell Biol. Lipids*, **1771**(3), 421–431.

Cui, Z., Hirata, D., Tsuchiya, E., Osada, H. and Miyakawa, T. (1996). The multidrug resistance-associated protein (MRP) subfamily (Yrs1/Yor1) of *Saccharomyces cerevisiae* is important for the tolerance to a broad range of organic anions. *J. Biol. Chem.*, **271**(25), 14712–14716.

Cui, Z., Shiraki, T., Hirata, D. and Miyakawa, T. (1998). Yeast gene *YRR1*, which is required for resistance to 4-nitroquinoline *N*-oxide, mediates transcriptional activation of the multidrug resistance transporter gene *SNQ2*. *Mol. Microbiol.*, **29**(5), 1307–1315.

Cui, Z., Hirata, D. and Miyakawa, T. (1999). Functional analysis of the promoter of the yeast *SNQ2* gene encoding a multidrug resistance transporter that confers the resistance to 4-nitroquinoline *N*-oxide. *Biosci. Biotechnol. Biochem.*, **63**(1), 162–167.

D'Amore, T., Panchal, C. J., Russell, I. and Stewart, G. G. (1990). A study of ethanol tolerance in yeast. *Crit. Rev. Biotechnol.*, **9**(4), 287–304.

Daum, G., Lees, N. D., Bard, M. and Dickson, R. (1998). Biochemistry, cell biology and molecular biology of lipids of *Saccharomyces cerevisiae*. *Yeast*, **14**(16), 1471–1510.

de Groot, P. W., Ruiz, C., Vázquez de Aldana, C. R., Duenas, E., Cid, V. J., Del Rey, F., Rodríquez-Peña, J. M., Pérez, P., Andel, A., Caubín, J., Arroyo, J., García, J. C., Gil, C., Molina, M., García, L. J., Nombela, C. and Klis, F. M. (2001). A genomic approach for the identification and classification of genes involved in cell wall formation and its regulation in *Saccharomyces cerevisiae*. *Comp. Funct. Genomics*, **2**(3), 124–142.

de Nobel, J. G. and Barnett, J. A. (1991). Passage of molecules through yeast cell walls: a brief essay-review. *Yeast*, **7**(4), 313–323.

de Nobel, J. G., Klis, F. M., Priem, J., Munnik, T. and van den Ende, H. (1990). The glucanase-soluble mannoproteins limit cell wall porosity in *Saccharomyces cerevisiae*. *Yeast*, **6**(6), 491–499.

Dean, M., Hamon, Y. and Chimini, G. (2001). The human ATP-binding cassette transporter superfamily. *J. Lipid Res.*, **42**, 1007–1017.

Decottignies, A. and Goffeau, A. (1997). Complete inventory of the yeast ABC proteins. *Nat. Genet.*, **15**(2), 137–145.

Decottignies, A., Lambert, L., Catty, P., Degand, H., Epping, E. A., Moye-Rowley, W. S., Balzi, E. and Goffeau, A. (1995). Identification and characterization of SNQ2, a new multidrug ATP binding cassette transporter of the yeast plasma membrane. *J. Biol. Chem.*, **270**(30), 18150–18157.

Decottignies, A., Grant, A. M., Nichols, J. W., de Wet, H., McIntosh, D. B. and Goffeau, A. (1998). ATPase and multidrug transport activities of the overexpressed yeast ABC protein Yor1p. *J. Biol. Chem.*, **273** (20), 12612–12622.

Delaveau, T., Delahodde, A., Carvajal, E., Šubík, J. and Jacq, C. (1994). *PDR3*, a new yeast regulatory gene, is homologous to *PDR1* and controls the multidrug resistance phenomenon. *Mol. Gen. Genet.*, **244**(5), 501–11.

Denksteinová, B., Gášková, D., Heřman, P., Večeř, J., Malínský, J., Plášek, J. and Sigler, K. (1997). Monitoring of membrane potential changes in *Saccharomyces cerevisiae* by diS-C_3(3) fluorescence. *Folia Microbiol.*, **42**(3), 221–224.

DeRisi, J. L., Iyer, V. R. and Brown, P. O. (1997). Exploring the metabolic and genetic control of gene expression on a genomic scale. *Science*, **278**(5338), 680–686.

Dick, D. M. and Foroud, T. (2002). Genetic strategies to detect genes involved in alcoholism and alcohol-related traits. *Alcohol Res. Health*, **26**(3), 172–180.

Ding, J., Huang, X., Zhao, N., Gao, F., Lu, Q. and Zhang, K. Q. (2010). Response of *Saccharomyces cerevisiae* to ethanol stress involves actions of protein Asr1p. *J. Microbiol. Biotechnol.*, **20**(12), 1630–1636.

dos Passos, J. B., Vanhalewyn, M., Brandão, R. L., Castro, I. M., Nicoli, J. R. and Thevelein, J. M. (1992). Glucose-induced activation of plasma membrane H^+-ATPase in mutants of the yeast *Saccharomyces cerevisiae* affected in cAMP metabolism, cAMP-dependent protein phosphorylation and the initiation of glycolysis. *Biochim. Biophys. Acta*, **1136**(1), 57–67.

Dubowchik, G. M., Padilla, L., Edinger, K. and Firestone, R. A. (1994). Reversal of doxorubicin resistance and catalytic neutralization of lysosomes by a lipophilic imidazole. *Biochim. Biophys. Acta - Biomembr.*, **1191** (1), 103–108.

Dundee, J. W., Isaac, M. and Clarke, R. S. J. (1969). Use of alcohol in anesthesia. *Anesth. Analg.*, **48**(4), 665–669.

Dupres, V., Dufrêne, Y. F. and Heinisch, J. J. (2010). Measuring cell wall thickness in living yeast cells using single molecular rulers. *ACS Nano*, **4** (9), 5498–5504.

Durán, A., Bowerst, B. and Cabib, E. (1975). Chitin synthetase zymogen is attached to the yeast plasma membrane. *Proc. Natl. Acad. Sci. USA*, **72** (10), 3952–3955.

Durell, S. R. and Guy, H. R. (1999). Structural models of the KtrB, TrkH, and Trk1,2 symporters based on the structure of the KcsA K^+ channel. *Biophys. J.*, **77**(2), 789–807.

Egner, R., Mahé, Y., Pandjaitan, R. and Kuchler, K. (1995). Endocytosis and vacuolar degradation of the plasma membrane-localized Pdr5 ATP-binding cassette multidrug transporter in *Saccharomyces cerevisiae*. *Mol. Cell. Biol.*, **15**(11), 5879–5887.

Egner, R., Rosenthal, F. E., Kralli, A., Sanglard, D. and Kuchler, K. (1998). Genetic separation of FK506 susceptibility and drug transport in the yeast Pdr5 ATP-binding cassette multidrug resistance transporter. *Mol. Biol. Cell*, **9**(2), 523–543.

Ellabib, M., Ghannoum, M. A. and Whittaker, P. A. (1990). Effects of the pyridinamines octenidine and pirtenidine on yeast mitochondrial function. *Biochem. Soc. Trans.*, **18**(2), 342–343.

Eraso, P. and Gancedo, C. (1987). Activation of yeast plasma membrane ATPase by acid pH during growth. *FEBS Lett.*, **224**(1), 187–192.

Ernst, R., Kueppers, P., Klein, C. M., Schwarzmueller, T., Kuchler, K. and Schmitt, L. (2008). A mutation of the H-loop selectively affects rhodamine transport by the yeast multidrug ABC transporter Pdr5. *Proc. Natl. Acad. Sci. USA*, **105**(13), 5069–5074.

Ernst, R., Klemm, R., Schmitt, L. and Kuchler, K. (2005). Yeast ATP-binding cassette transporters: Cellular cleaning pumps. *Methods Enzymol.*, **400** (05), 460–484.

Fairman, C., Zhou, X. L. and Kung, C. (1999). Potassium uptake through the TOK1 K^+ channel in the budding yeast. *J. Membr. Biol.*, **168**(2), 149–157.

Farge, E. (1995). Increased vesicle endocytosis due to an increase in the plasma membrane phosphatidylserine concentration. *Biophys. J.*, **69**, 2501–2506.

Farrell, A. E., Plevin, R. J., Turner, B. T., Jones, A. D., O'Hare, M. and Kammen, D. M. (2006). Ethanol can contribute to energy and environmental goals. *Science*, **311**(5760), 506–508.

Fazlara, A. and Ekhtelat, M. (2012). The disinfectant effects of benzalkonium chloride on some important foodborne pathogens. *Am. J. Agric. Environ. Sci.*, **12**(1), 23–29.

Fernandes, A. R. and Sá-Correia, I. (2003). Transcription patterns of *PMA1* and *PMA2* genes and activity of plasma membrane H^+-ATPase in *Saccharomyces cerevisiae* during diauxic growth and stationary phase. *Yeast*, **20** (3), 207–219.

Ferreira-Pereira, A., Marco, S., Decottignies, A., Nader, J., Goffeau, A. and Rigaud, J.-L. (2003). Three-dimensional reconstruction of the *Saccharomyces cerevisiae* multidrug resistance protein Pdr5p. *J. Biol. Chem.*, **278**(14), 11995–11999.

Finegersh, A. and Homanics, G. E. (2014). Paternal alcohol exposure reduces alcohol drinking and increases behavioral sensitivity to alcohol selectively in male offspring. *PLoS One*, **9**(6), e99078.

Foegh, M. L. and Virmani, R. (1993). Molecular biology of intimal proliferation. *Curr. Opin. Cardiol.*, **8**, 938–950.

Franks, N. P. and Lieb, W. R. (1978). Where do general anaesthetics act? *Nature*, **274**(5669), 339–342.

Franks, N. P. and Lieb, W. R. (1984). Do general anaesthetics act by competitive binding to specific receptors? *Nature*, **310**(5978), 599–601.

Franks, N. P. and Lieb, W. R. (1985). Mapping of general anaesthetic target sites provides a molecular basis for cutoff effects. *Nature*, **316**, 349–351.

Franks, N. P. and Lieb, W. R. (1986). Partitioning of long-chain alcohols into lipid bilayers: Implications for mechanisms of general anesthesia. *Proc. Natl. Acad. Sci. USA*, **83**(83), 5116–5120.

Fry, S. C. (1986). Cross-linking of matrix polymers in the growing cell walls of angiosperms. *Annu. Rev. Plant Physiol.*, **37**(1), 165–186.

Fujita, K., Matsuyama, A., Kobayashi, Y. and Iwahashi, H. (2004). Comprehensive gene expression analysis of the response to straight-chain alcohols in *Saccharomyces cerevisiae* using cDNA microarray. *J. Appl. Microbiol.*, **97**(1), 57–67.

Gaber, R. F., Styles, C. A. and Fink, G. R. (1988). *TRK1* encodes a plasma membrane protein required for high-affinity potassium transport in *Saccharomyces cerevisiae*. *Mol. Cell. Biol.*, **8**(7), 2848–2859.

Gaigg, B., Timischl, B., Corbino, L. and Schneiter, R. (2005). Synthesis of sphingolipids with very long chain fatty acids but not ergosterol is required for routing of newly synthesized plasma membrane ATPase to the cell surface of yeast. *J. Biol. Chem.*, **280**(23), 22515–22522.

Galeote, V. A., Alexandre, H., Bach, B., Delobel, P., Dequin, S. and Blondin, B. (2007). Sfl1p acts as an activator of the *HSP30* gene in *Saccharomyces cerevisiae*. *Curr. Genet.*, **52**(2), 55–63.

Garciadeblas, B., Rubio, F., Quintero, F. J., Bañuelos, M. A., Haro, R. and Rodríguez-Navarro, A. (1993). Differential expression of two genes encoding isoforms of the ATPase involved in sodium efflux in *Saccharomyces cerevisiae*. *MGG Mol. Gen. Genet.*, **236**(2-3), 363–368.

Gasch, A. P., Spellman, P. T., Kao, C. M., Carmel-Harel, O., Eisen, M. B., Storz, G., Botstein, D. and Brown, P. O. (2000). Genomic expression programs in the response of yeast cells to environmental changes. *Mol. Biol. Cell*, **11**(12), 4241–4257.

Gášková, D., Brodská, B., Holoubek, A. and Sigler, K. (1999). Factors and processes involved in membrane potential build-up in yeast: diS-C_3(3) assay. *Int. J. Biochem. Cell Biol.*, **31**(5), 575–584.

Gášková, D., Čadek, R., Chaloupka, R., Plášek, J. and Sigler, K. (2001). Factors underlying membrane potential-dependent and -independent fluorescence responses of potentiometric dyes in stressed cells: diS-C_3(3) in yeast. *Biochim. Biophys. Acta - Biomembr.*, **1511**(1), 74–79.

Gášková, D., Čadek, R., Chaloupka, R., Vacata, V., Gebel, J. and Sigler, K. (2002). Monitoring the kinetics and performance of yeast membrane ABC transporters by diS-C_3(3) fluorescence. *Int. J. Biochem. Cell Biol.*, **34**(8), 931–937.

Gášková, D., DeCorby, A. and Lemire, B. D. (2007). DiS-C_3(3) monitoring of *in vivo* mitochondrial membrane potential in *C. elegans*. *Biochem. Biophys. Res. Commun.*, **354**(3), 814–819.

Gášková, D., Brodská, B., Heřman, P., Večeř, J., Sigler, K., Benada, O. and Plášek, J. (1998). Fluorescent probing of membrane potential in walled cells: diS-C_3(3) assay in *Saccharomyces cerevisiae*. *Yeast*, **1197**(14), 1189–1197.

Ghaemmaghami, S., Huh, W.-K., Bower, K., Howson, R. W., Belle, A., Dephoure, N., O'Shea, E. K. and Weissman, J. S. (2003). Global analysis of protein expression in yeast. *Nature*, **425**(6959), 737–741.

Ghannoum, M. A., Elteen, K. A., Ellabib, M. and Whittaker, P. A. (1990). Antimycotic effects of octenidine and pirtenidine. *J. Antimicrob. Chemother.*, **25**(2), 237–245.

Ghareib, M., Youssef, K. A. and Khalil, A. A. (1988). Ethanol tolerance of *Saccharomyces cerevisiae* and its relationship to lipid content and composition. *Folia Microbiol.*, **33**(6), 447–452.

Godden, E. L., Harris, R. A. and Dunwiddie, T. V. (2001). Correlation between molecular volume and effects of *n*-alcohols on human neuronal nicotinic acetylcholine receptors expressed in *Xenopus* oocytes. *J. Pharmacol. Exp. Ther.*, **296**(3), 716–722.

Goffeau, A. and Slayman, C. W. (1981). The proton-translocating ATPase of the fungal plasma membrane. *Biochim. Biophys. Acta Rev. Bioenerg.*, **639** (3-4), 197–223.

Goldstein, A. L. and McCusker, J. H. (1999). Three new dominant drug resistance cassettes for gene disruption in *Saccharomyces cerevisiae*. *Yeast*, **15** (14), 1541–1553.

Goldstein, D. B. (1984). The effects of drugs on membrane fluidity. *Annu. Rev. Pharmacol. Toxicol.*, **24**, 43–64.

Goldstein, S. A., Bockenhauer, D., O'Kelly, I. and Zilberberg, N. (2001). Potassium leak channels and the KCNK family of two-P-domain subunits. *Nat. Rev. Neurosci.*, **2**(3), 175–184.

Golin, J., Ambudkar, S. V. and May, L. (2007). The yeast Pdr5p multidrug transporter: How does it recognize so many substrates? *Biochem. Biophys. Res. Commun.*, **356**(1), 1–5.

Gómez, M. J., Luyten, K. and Ramos, J. (1996). The capacity to transport potassium influences sodium tolerance in *Saccharomyces cerevisiae*. *FEMS Microbiol. Lett.*, **135**(2-3), 157–160.

Goormaghtigh, E., Chadwick, C. and Scarborough, G. A. (1986). Monomers of the *Neurospora* plasma membrane H^+-ATPase catalyze efficient proton translocation. *J. Biol. Chem.*, **261**(16), 7466–7471.

Goossens, A., de La Fuente, N., Forment, J., Serrano, R. and Portillo, F. (2000). Regulation of yeast H^+-ATPase by protein kinases belonging to a family dedicated to activation of plasma membrane transporters. *Mol. Cell. Biol.*, **20**(20), 7654–7661.

Gottesman, M. M. and Pastan, I. (1993). Biochemistry of multidrug resistance mediated by the multidrug transporter. *Annu. Rev. Biochem.*, **62**, 385–427.

Gray, A. T., Winegar, B. D., Leonoudakis, D. J., Forsayeth, J. R. and Yost, C. S. (1998). TOK1 is a volatile anesthetic stimulated K^+ channel. *Anesthesiology*, **88**(4), 1076–1084.

Gray, W. D. and Sova, C. (1956). Relation of molecule size and structure to alcohol inhibition of glucose utilization by yeast. *J. Bacteriol.*, **72**(3), 349–356.

Greenberg, M. L. and Axelrod, D. (1993). Anomalously slow mobility of fluorescent lipid probes in the plasma membrane of the yeast *Saccharomyces cerevisiae*. *J. Membr. Biol.*, **131**(2), 115–127.

Guerri, C. and Pascual, M. (2010). Mechanisms involved in the neurotoxic, cognitive, and neurobehavioral effects of alcohol consumption during adolescence. *Alcohol*, **44**(1), 15–26.

Gustin, M. C. (1988). A mechanosensitive ion channel in the yeast plasma membrane. *Science*, **242**, 762–765.

Gustin, M. C., Martinac, B., Saimi, Y., Culbertson, M. R. and Kung, C. (1990). Ion channels in yeast. *Science*, **233**(394), 1195–1197.

Haase, E., Servos, J. and Brendel, M. (1992). Isolation and characterization of additional genes influencing resistance to various mutagens in the yeast *Saccharomyces cerevisiae*. *Curr. Genet.*, **21**(4-5), 319–324.

Hakomori, S.-I. (1990). Bifunctional role of glycosphingolipids. Modulators for transmembrane signaling and mediators for cellular interactions. *J. Biol. Chem.*, **265**(31), 18713–18716.

Hamada, H., Ishiguro, H., Yamamoto, A., Shimano-Futakuchi, S., Ko, S. B. H., Yoshikawa, T., Goto, H., Kitagawa, M., Hayakawa, T., Seo, Y. and Naruse, S. (2005). Dual effects of *n*-alcohols on fluid secretion from guinea pig pancreatic ducts. *Am. J. Physiol. Cell Physiol.*, **288**, C1431–C1439.

Hampsey, M. (1997). A review of phenotypes in *Saccharomyces cerevisiae*. *Yeast*, **13**(12), 1099–1133.

Harke, H. P. (1989). Octenidine dihydrochloride, properties of a new antimicrobial agent. *Zentralbl. Hyg. Umweltmed.*, **188**(1-2), 188–193.

Harke, H. P. and Goroncy-Barnes, P. (1991). Mucous membrane antisepsis: octenidine dihydrochloride as a new active agent. *Hyg. Med.*, **16**, 46–50.

Haro, R. and Rodríguez-Navarro, A. (2002). Molecular analysis of the mechanism of potassium uptake through the TRK1 transporter of *Saccharomyces cerevisiae*. *Biochim. Biophys. Acta - Biomembr.*, **1564**(1), 114–122.

Haro, R., Garciadeblas, B. and Rodríguez-Navarro, A. (1991). A novel P-type ATPase from yeast involved in sodium transport. *FEBS Lett.*, **291**(2), 189–191.

Harris, R. A., Mihic, S. J., Brozowski, S., Hadingham, K. and Whiting, P. J. (1997). Ethanol, flunitrazepam, and pentobarbital modulation of $GABA_A$ receptors expressed in mammalian cells and *Xenopus* oocytes. *Alcohol. Clin. Exp. Res.*, **21**(3), 444–451.

Harris, R. A., Trudell, J. R. and Mihic, S. J. (2008). Ethanol's molecular targets. *Sci. Signal.*, **1**(28), re7.

Hartland, R. P., Vermeulen, C. A., Klis, F. M., Sietsma, J. H. and Wessels, J. G. (1994). The linkage of (1-3)-β-glucan to chitin during cell wall assembly in *Saccharomyces cerevisiae*. *Yeast*, **10**, 1591–1599.

Hegemann, J. H. and Heick, S. B. (2011). Delete and repeat: A comprehensive toolkit for sequential gene knockout in the budding yeast *Saccharomyces cerevisiae*. *Methods Mol. Biol.*, **765**, 189–206.

Hellauer, K., Akache, B., MacPherson, S., Sirard, E. and Turcotte, B. (2002). Zinc cluster protein Rdr1p is a transcriptional repressor of the *PDR5* gene encoding a multidrug transporter. *J. Biol. Chem.*, **277**(20), 17671–17676.

Hendrych, T. (2009). *Ovlivnění činnosti membránových transportních systémů kvasinek stresovými faktory*. Doctoral thesis, Charles University, Prague.

Hendrych, T., Kodedová, M., Sigler, K. and Gášková, D. (2009). Characterization of the kinetics and mechanisms of inhibition of drugs interacting with the *S. cerevisiae* multidrug resistance pumps Pdr5p and Snq2p. *Biochim. Biophys. Acta - Biomembr.*, **1788**(3), 717–723.

Herrera, R., Álvarez, M. C., Gelis, S. and Ramos, J. (2013). Subcellular potassium and sodium distribution in *Saccharomyces cerevisiae* wild-type and vacuolar mutants. *Biochem. J.*, **454**(3), 525–532.

Heytler, P. and Prichard, W. (1962). A new class of uncoupling agents - carbonyl cyanide phenylhydrazones. *Biochem. Biophys. Res. Commun.*, **7**(4), 272–275.

Higgins, C. F. (1995). The ABC of channel regulation. *Cell*, **82**(5), 693–696.

Higgins, C. F. and Linton, K. J. Introduction. In Holland, I. B., Cole, S. P. C., Kuchler, K. and Higgins, C. F., editors, *ABC Proteins from Bacteria to Man*, page xvii. Academic Press, London, 2003. ISBN 0-12-352551-9.

Hikkel, I., Lucau-Danila, A., Delaveau, T., Marc, P., Devaux, F. and Jacq, C. (2003). A general strategy to uncover transcription factor properties identifies a new regulator of drug resistance in yeast. *J. Biol. Chem.*, **278**(13), 11427–11432.

Hiraga, K., Yamamoto, S., Fukuda, H., Hamanaka, N. and Oda, K. (2005). Enniatin has a new function as an inhibitor of Pdr5p, one of the ABC transporters in *Saccharomyces cerevisiae*. *Biochem. Biophys. Res. Commun.*, **328**(4), 1119–1125.

Hirata, D., Yano, K., Miyahara, K. and Miyakawa, T. (1994). *Saccharomyces cerevisiae YDR1*, which encodes a member of the ATP-binding cassette (ABC) superfamily, is required for multidrug resistance. *Curr. Genet.*, **26**(4), 285–294.

Hlaváček, O., Kučerová, H., Harant, K., Palková, Z. and Váchová, L. (2009). Putative role for ABC multidrug exporters in yeast quorum sensing. *FEBS Lett.*, **583**(7), 1107–1113.

Holyoak, C. D., Stratford, M., McMullin, Z., Cole, M. B., Crimmins, K., Brown, A. J. P. and Coote, P. J. (1996). Activity of the plasma membrane H^+-ATPase and optimal glycolytic flux are required for rapid adaptation and growth of *Saccharomyces cerevisiae* in the presence of the weak-acid preservative sorbic acid. *Appl. Environ. Microbiol.*, **62**(9), 3158–3164.

Horishita, T. and Harris, R. A. (2008). *n*-Alcohols inhibit voltage-gated Na^+ channels expressed in *Xenopus* oocytes. *J. Pharmacol. Exp. Ther.*, **326** (1), 270–277.

Hosono, K. (1992). Effect of salt stress on lipid composition and membrane fluidity of the salt-tolerant yeast *Zygosaccharomyces rouxii*. *J. Gen. Microbiol.*, **138**, 91–96.

Hu, C., Bai, F. and An, L. (2005). Protein amino acid composition of plasma membranes affects membrane fluidity and thereby ethanol tolerance in a self-flocculating fusant of *Schizosaccharomyces pombe* and *Saccharomyces cerevisiae*. *Chin. J. Biotechnol.*, **21**(5), 809–813.

Hübner, N. O., Siebert, J. and Kramer, A. (2010). Octenidine dihydrochloride, a modern antiseptic for skin, mucous membranes and wounds. *Skin Pharmacol. Physiol.*, **23**(5), 244–258.

Ibeas, J. I. and Jimenez, J. (1997). Mitochondrial DNA loss caused by ethanol in *Saccharomyces* flor yeasts. *Appl. Environ. Microbiol.*, **63**(1), 7–12.

Iglesias, R., Ferreras, J. M., Arias, F. J., Muñoz, R. and Girbés, T. (1991). Effect of continued exposition to ethanol on activity of the ammonium and fructose transport systems in *Saccharomyces cerevisiae* var. *ellipsoideus*. *Biotechnol. Bioeng.*, **37**(4), 389–391.

Ingram, L. O. (1976). Adaption of membrane lipids to alcohols. *J. Bacteriol.*, **125**(2), 670–678.

Ingram, L. O. and Buttke, T. M. (1984). Effects of alcohols on microorganisms. *Adv. Microb. Physiol.*, **25**, 253–300.

Iso, H., Folsom, A. R., Koike, K. A., Sato, S., Wu, K. K., Shimamoto, T., Iida, M. and Komachi, Y. (1993). Antigens of tissue plasminogen activator and plasminogen activator inhibitor 1: Correlates in nonsmoking Japanese and Caucasian men and women. *Thromb. Haemost.*, **70**(3), 475–480.

Iso, H., Kitamura, A., Shimamoto, T., Sankai, T., Naito, Y., Sato, S., Kiyama, M., Iida, M. and Komachi, Y. (1995). Alcohol intake and the risk of cardiovascular disease in middle-aged Japanese men. *Stroke*, **26**(5), 767–773.

Janderová, B. and Bendová, O. *Úvod do biologie kvasinek*. Nakladatelství Karolinum, Praha, 1999. ISBN 80-7184-990-1.

Jiménez, J. and Benítez, T. (1988). Yeast cell viability under conditions of high temperature and ethanol concentrations depends on the mitochondrial genome. *Curr. Genet.*, **13**(6), 461–469.

Kaback, H. R., Sahin-Tóth, M. and Weinglass, A. B. (2001). The kamikaze approach to membrane transport. *Nat. Rev. Mol. Cell. Biol.*, **2**(8), 610–620.

Kabelitz, N., Santos, P. M. and Heipieper, H. J. (2003). Effect of aliphatic alcohols on growth and degree of saturation of membrane lipids in *Acinetobacter calcoaceticus*. *FEMS Microbiol. Lett.*, **220**(2), 223–227.

Kane, P. M. (1995). Disassembly and reassembly of the yeast vacoular H^+-ATPase *in vivo*. *J. Biol. Chem.*, **270**(14), 17025–17032.

Kang, M. S., Elango, N., Mattia, E., Au-Young, J., Robbins, P. W. and Cabib, E. (1984). Isolation of chitin synthetase from *Saccharomyces cerevisiae*. Purification of an enzyme by entrapment in the reaction product. *J. Biol. Chem.*, **259**(23), 14966–14972.

Kapteyn, J. C., Montijn, R. C., Vink, E., de la Cruz, J., Llobell, A., Douwes, J. E., Shimof, H., Lipke, P. N. and Klis, F. M. (1996). Retention of *Saccharomyces cerevisiae* cell wall proteins through a phosphodiester-Iinked β-1,3-/β-1,6-glucan heteropolymer. *Glycobiology*, **6**(3), 337–345.

Kasianowicz, J., Benz, R. and McLaughlin, S. (1984). The kinetic mechanism by which CCCP (carbonyl cyanide *m*-chlorophenylhydrazone) transports protons across membranes. *J. Membr. Biol.*, **82**(2), 179–190.

Katzmann, D. J., Burnett, P. E., Golin, J., Mahé, Y. and Moye-Rowley, W. S. (1994). Transcriptional control of the yeast *PDR5* gene by the *PDR3* gene product. *Mol. Cell. Biol.*, **14**(7), 4653–4661.

Katzmann, D. J., Hallstrom, T. C., Voet, M., Wysock, W., Golin, J., Volckaert, G. and Moye-Rowley, W. S. (1995). Expression of an ATP-binding cassette transporter-encoding gene (*YOR1*) is required for oligomycin resistance in *Saccharomyces cerevisiae*. *Mol. Cell. Biol.*, **15**(12), 6875–6883.

Ketchum, K. A., Joiner, W. J., Sellers, A. J., Kaczmarek, L. K. and Goldstein, S. A. (1995). A new family of outwardly rectifying potassium channel proteins with two pore domains in tandem. *Nature*, **376**(6542), 690–695.

Kihara, A. and Igarashi, Y. (2004). Cross talk between sphingolipids and glycerophospholipids in the establishment of plasma membrane asymmetry. *Mol. Biol. Cell*, **15**, 494–4959.

Kinclová, O., Potier, S. and Sychrová, H. (2001a). The *Zygosaccharomyces rouxii* strain CBS732 contains only one copy of the *HOG1* and the *SOD2* genes. *J. Biotechnol.*, **88**(2), 151–158.

Kinclová, O., Ramos, J., Potier, S. and Sychrová, H. (2001b). Functional study of the *Saccharomyces cerevisiae* Nha1p C-terminus. *Mol. Microbiol.*, **40**(3), 656–668.

Kinclová-Zimmermannová, O. and Sychrová, H. (2006). Functional study of the Nha1p C-terminus: Involvement in cell response to changes in external osmolarity. *Curr. Genet.*, **49**(4), 229–236.

Kinclová-Zimmermannová, O., Gášková, D. and Sychrová, H. (2006). The Na^+,K^+/H^+-antiporter Nha1 influences the plasma membrane potential of *Saccharomyces cerevisiae*. *FEMS Yeast Res.*, **6**(5), 792–800.

Knoshaug, E. P. and Zhang, M. (2009). Butanol tolerance in a selection of microorganisms. *Appl. Biochem. Biotechnol.*, **153**(1-3), 13–20.

Ko, C. H. and Gaber, R. F. (1991). *TRK1* and *TRK2* encode structurally related K^+ transporters in *Saccharomyces cerevisiae*. *Mol. Cell. Biol.*, **11**(8), 4266–4273.

Ko, C. H., Buckley, A. M. and Gaber, R. F. (1990). *TRK2* is required for low affinity K^+ transport in *Saccharomyces cerevisiae*. *Genetics*, **125**(2), 305–312.

Kobayashi, T., Ikeda, K., Kojima, H., Niki, H., Yano, R., Yoshioka, T. and Kumanishi, T. (1999). Ethanol opens G-protein-activated inwardly rectifying K^+ channels. *Nat. Neurosci.*, **2**, 1091–1097.

Koburger, T., Hübner, N. O., Braun, M., Siebert, J. and Kramer, A. (2010). Standardized comparison of antiseptic efficacy of triclosan, PVP-iodine, octenidine dihydrochloride, polyhexanide and chlorhexidine digluconate. *J. Antimicrob. Chemother.*, **65**(8), 1712–1719.

Kodedová, M., Sigler, K., Lemire, B. D. and Gášková, D. (2011). Fluorescence method for determining the mechanism and speed of action of surface-active drugs on yeast cells. *Biotechniques*, **50**(1), 58–63.

Kolaczkowski, M., Kolaczowska, A., Łuczyński, J. and Goffeau, A. (1998). *In vivo* characterization of the drug resistence profile of the major ABC transporters and other components of the yeast pleiotrophic drug resistance network. *Microb. Drug Resist.*, **4**(3), 143–158.

Kolaczkowski, M., van der Rest, M., Cybularz-Kolaczkowska, A., Soumillion, J. P., Konings, W. N. and Goffeau, A. (1996). Anticancer drugs, ionophoric peptides, and steroids as substrates of the yeast multidrug transporter Pdr5p. *J. Biol. Chem.*, **271**(49), 31543–31548.

Kollár, R., Reinhold, B. B., Petráková, E., Yeh, H. J. C., Ashwell, G., Drgonová, J., Kapteyn, J. C., Klis, F. M. and Cabib, E. (1997). Architecture of the yeast cell wall. *J. Biol. Chem.*, **272**(28), 17762–17775.

Korpi, E. R., Mäkelä, R. and Uusi-Oukari, M. (1998). Ethanol: Novel actions on nerve cell physiology explain impaired functions. *News Physiol. Sci.*, **13**, 164–170.

Kralli, a. and Yamamoto, K. R. (1996). An FK506-sensitive transporter selectively decreases intracellular levels and potency of steroid hormones. *J. Biol. Chem.*, **271**(29), 17152–17156.

Kramer, A. and Müller, G. Octenidindihydrochlorid. In Kramer, A. and Assadian, O., editors, *Wallhäußers Praxis der Sterilisation, Antiseptik und Konservierung*, pages 799–805. Georg Thieme Verlag KG, Stuttgart, 1^{st} edition, 2008. ISBN 9783131411211.

Kubo, I., Fujita, T., Kubo, A. and Fujita, K.-i. (2003). Modes of antifungal action of alkanols against *Saccharomyces cerevisiae*. *Bioorg. Med. Chem.*, **11**(6), 1117–1122.

Kuda, T., Yano, T. and Kuda, M. T. (2008). Resistances to benzalkonium chloride of bacteria dried with food elements on stainless steel surface. *LWT - Food Sci. Technol.*, **41**(6), 988–993.

Kühlbrandt, W. (2004). Biology, structure and mechanism of P-type ATPases. *Nat. Rev. Mol. Cell Biol.*, **5**(4), 282–295.

Kuroda, T., Bihler, H., Bashi, E., Slayman, C. L. and Rivetta, A. (2004). Chloride channel function in the yeast TRK-potassium transporters. *J. Membr. Biol.*, **198**(3), 177–92.

Lage, H. (2003). ABC-transporters: Implications on drug resistance from microorganisms to human cancers. *Int. J. Antimicrob. Agents*, **22**(3), 188–199.

Lamping, E., Monk, B. C., Niimi, K., Holmes, A. R., Tsao, S., Tanabe, K., Niimi, M., Uehara, Y. and Cannon, R. D. (2007). Characterization of three classes of membrane proteins involved in fungal azole resistance by functional hyperexpression in *Saccharomyces cerevisiae*. *Eukaryot. Cell*, **6**(7), 1150–1165.

Lapathitis, G. and Kotyk, A. (1998). Univalent cation fluxes in yeast. *Biochem. Mol. Biol. Int.*, **44**(2), 371–380.

Le Crom, S., Devaux, F., Marc, P., Zhang, X., Moye-Rowley, W. S. and Jacq, C. (2002). New insights into the pleiotropic drug resistance network from genome-wide characterization of the *YRR1* transcription factor regulation system. *Mol. Cell. Biol.*, **22**(8), 2642–2649.

Leão, C. and van Uden, N. (1982). Effects of ethanol and other alkanols on the glucose transport system of *Saccharomyces cerevisiae*. *Biotechnol. Bioeng.*, **24**(11), 2601–2604.

Leão, C. and van Uden, N. (1984). Effects of ethanol and other alkanols on passive proton influx in the yeast *Saccharomyces cerevisiae*. *Biochim. Biophys. Acta*, **774**, 43–48.

Lecchi, S., Nelson, C. J., Allen, K. E., Swaney, D. L., Thompson, K. L., Coon, J. J., Sussman, M. R. and Slayman, C. W. (2007). Tandem phosphorylation of Ser-911 and Thr-912 at the C terminus of yeast plasma membrane H^+-ATPase leads to glucose-dependent activation. *J. Biol. Chem.*, **282**(49), 35471–35481.

Lee, S., Carlson, T., Christian, N., Lea, K., Kedzie, J., Reilly, J. P. and Bonner, J. J. (2000). The yeast heat shock transcription factor changes conformation in response to superoxide and temperature. *Mol. Biol. Cell*, **11** (5), 1753–1764.

Leonard, J. P., Rathod, P. K. and Golin, J. (1994). Loss of function mutation in the yeast multiple drug resistance gene *PDR5* causes a reduction in chloramphenicol efflux. *Antimicrob. Agents Chemother.*, **38**(10), 2492–2494.

Leppert, G., McDevitt, R., Falco, S. C., Van Dyk, T. K., Ficke, M. B. and Golin, J. (1990). Cloning by gene amplification of two loci conferring multiple drug resistance in *Saccharomyces*. *Genetics*, **125**(1), 13–20.

Lesage, F., Guillemare, E., Fink, M., Duprat, F., Lazdunski, M., Romey, G. and Barhanin, J. (1996). A pH-sensitive yeast outward rectifier K^+ channel with two pore domains and novel gating properties. *J. Biol. Chem.*, **271**(8), 4183–4187.

Lesage, G. and Bussey, H. (2006). Cell wall assembly in *Saccharomyces cerevisiae*. *Microbiol. Mol. Biol. Rev.*, **70**(2), 317–43.

Levin, D. E. (2011). Regulation of cell wall biogenesis in *Saccharomyces cerevisiae*: The cell wall integrity signaling pathway. *Genetics*, **189**(4), 1145–1175.

Lewohl, J. M., Wilson, W. R., Mayfield, R. D., Brozowski, S. J., Morrisett, R. A. and Harris, R. A. (1999). G-protein-coupled inwardly rectifying potassium channels are targets of alcohol action. *Nat. Neurosci.*, **2** (12), 1084–1090.

Lewohl, J. M., Nunez, Y. O., Dodd, P. R., Tiwari, G. R., Harris, R. A. and Mayfield, R. D. (2011). Up-regulation of microRNAs in brain of human alcoholics. *Alcohol. Clin. Exp. Res.*, **35**(11), 1928–1937.

Li, C., Peoples, R. W. and Weight, F. F. (1994). Alcohol action on a neuronal membrane receptor: evidence for a direct interaction with the receptor protein. *Proc. Natl. Acad. Sci.*, **91**(17), 8200–8204.

Li, M. D. and van der Vaart, A. D. (2011). MicroRNAs in addiction: Adaptation's middlemen? *Mol. Psychiatry*, **16**(12), 1159–1168.

Linn, S., Carroll, M., Johnson, C., Fulwood, R., Kalsbeek, W. and Briefel, R. (1993). High-density lipoprotein cholesterol and alcohol consumption in US White and Black adults: Data from NHANES II. *Am. J. Public Health*, **83**(6), 811–816.

Linton, K. J. and Higgins, C. F. (1998). The *Escherichia coli* ATP-binding cassette (ABC) proteins. *Mol. Microbiol.*, **28**(1), 5–13.

Lobo, I. A. and Harris, R. A. (2008). $GABA_A$ receptors and alcohol. *Pharmacol. Biochem. Behav.*, **90**(1), 90–94.

Loukin, S. H. and Saimi, Y. (1999). K^+-dependent composite gating of the yeast K^+ channel, Tok1. *Biophys. J.*, **77**(6), 3060–3070.

Loukin, S. H. and Saimi, Y. (2002). Carboxyl tail prevents yeast K^+ channel closure: proposal of an integrated model of TOK1 gating. *Biophys. J.*, **82**(2), 781–792.

Lovinger, D. M. (1997). Alcohols and neurotransmitter gated ion channels: past, present and future. *Naunyn. Schmiedebergs. Arch. Pharmacol.*, **356**(3), 267–282.

Lucau-Danila, A., Delaveau, T., Lelandais, G., Devaux, F. and Jacq, C. (2003). Competitive promoter occupancy by two yeast paralogous transcription factors controlling the multidrug resistance phenomenon. *J. Biol. Chem.*, **278**(52), 52641–52650.

Lundbæk, J. A. (2008). Lipid bilayer-mediated regulation of ion channel function by amphiphilic drugs. *J. Gen. Physiol.*, **131**(5), 421–429.

Lussier, M., White, A. M., Sheraton, J., di Paolo, T., Treadwell, J., Southard, S. B., Horenstein, C. I., Chen-Weiner, J., Ram, A. F., Kapteyn, J. C., Roemer, T. W., Vo, D. H., Bondoc, D. C., Hall, J., Zhong, W. W., Sdicu, A. M., Davies, J., Klis, F. M., Robbins, P. W. and Bussey, H. (1997). Large scale identification of genes involved in cell surface biosynthesis and architecture in *Saccharomyces cerevisiae*. *Genetics*, **147**(2), 435–50.

Madrid, R., Gómez, M. J., Ramos, J. and Rodríguez-Navarro, A. (1998). Ectopic potassium uptake in *trk1 trk2* mutants of *Saccharomyces cerevisiae* correlates with a highly hyperpolarized membrane potential. *J. Biol. Chem.*, **273**(24), 14838–14844.

Mahé, Y., Parle-McDermott, A., Nourani, A., Delahodde, A., Lamprecht, A. and Kuchler, K. (1996). The ATP-binding cassette multidrug transporter Snq2 of *Saccharomyces cerevisiae*: A novel target for the transcription factors Pdrl and Pdr3. *Mol. Microbiol.*, **20**(1), 109–117.

Maláč, J., Urbánková, E., Sigler, K. and Gášková, D. (2005). Activity of yeast multidrug resistance pumps during growth is controlled by carbon source and the composition of growth-depleted medium: diS-C_3(3) fluorescence assay. *Int. J. Biochem. Cell Biol.*, **37**(12), 2536–2543.

Malhotra, R. and Singh, B. (2006). Ethanol-induced changes in glycolipids of *Saccharomyces cerevisiae*. *Appl. Biochem. Biotechnol.*, **128**(3), 205–213.

Malpartida, F. and Serrano, R. (1981). Proton translocation catalysed by the purified yeast plasma membrane ATPase reconstituted in liposomes. *FEBS Lett.*, **131**(2), 351–354.

Malpartida, F. and Serrano, R. (1980). Purification of the yeast plasma membrane ATPase solubilized with a novel zwitterionic detergent. *FEBS Lett.*, **111**(1), 69–72.

Malínská, K., Malínský, J., Opekarová, M. and Tanner, W. (2003). Visualization of protein compartmentation within the plasma membrane of living yeast cells. *Mol. Biol. Cell*, **14**, 4427–4436.

Malínský, J., Opekarová, M., Grossmann, G. and Tanner, W. (2013). Membrane microdomains, rafts, and detergent-resistant membranes in plants and fungi. *Annu. Rev. Plant Biol.*, **64**(1), 501–529.

Mamnun, Y. M., Schüller, C. and Kuchler, K. (2004). Expression regulation of the yeast PDR5 ATP-binding cassette (ABC) transporter suggests a role in cellular detoxification during the exponential growth phase. *FEBS Lett.*, **559**(1-3), 111–117.

Mangalappalli-Illathu, A. K. and Korber, D. R. (2006). Adaptive resistance and differential protein expression of *Salmonella enterica* serovar enteritidis biofilms exposed to benzalkonium chloride. *Antimicrob. Agents Chemother.*, **50**(11), 3588–3596.

Marešová, L., Urbánková, E., Gášková, D. and Sychrová, H. (2006). Measurements of plasma membrane potential changes in *Saccharomyces cerevisiae* cells reveal the importance of the Tok1 channel in membrane potential maintenance. *FEMS Yeast Res.*, **6**(7), 1039–1046.

Marešová, L., Muend, S., Zhang, Y. Q., Sychrová, H. and Rao, R. (2009). Membrane hyperpolarization drives cation influx and fungicidal activity of amiodarone. *J. Biol. Chem.*, **284**(5), 2795–2802.

Marger, M. D. and Saier, M. H. (1993). A major superfamily of transmembrane facilitators that catalyse uniport, symport and antiport. *Trends Biochem. Sci.*, **18**(1), 13–20.

Maris, P. (1995). Modes of action of disinfectants. *Rev. Sci. Tech.*, **14**(1), 47–55.

Marple, B., Roland, P. and Benninger, M. (2004). Safety review of benzalkonium chloride used as a preservative in intranasal solutions: An overview of conflicting data and opinions. *Otolaryngol. - Head Neck Surg.*, **130**(1), 131–141.

Martinez, P. and Persson, B. L. (1998). Identification, cloning and characterization of a derepressible Na^+-coupled phosphate transporter in *Saccharomyces cerevisiae*. *Mol. Gen. Genet.*, **258**(6), 628–638.

Martinez, R., Latreille, M. T. and Mirande, M. (1991). A *PMR2* tandem repeat with a modified C-terminus is located downstream from the *KRS1* gene encoding lysyl-tRNA synthetase in *Saccharomyces cerevisiae*. *Mol. Genet. Genomics*, **227**(1), 149–154.

Mascia, M. P., Trudell, J. R. and Harris, R. A. (2000). Specific binding sites for alcohols and anesthetics on ligand-gated ion channels. *Proc. Natl. Acad. Sci. USA*, **97**(16), 9305–9310.

McDonnell, G. and Russell, A. D. (1999). Antiseptics and disinfectants: Activity, action, and resistance. *Clin. Microbiol. Rev.*, **12**(1), 147–179.

Mihic, S. J., Ye, Q., Wick, M. J., Koltchine, V. V., Krasowski, M. D., Finn, S. E., Mascia, M. P., Valenzuela, C. F., Hanson, K. K., Greenblatt, E. P., Harris, R. A. and Harrison, N. L. (1997). Sites of alcohol and volatile anaesthetic action on $GABA_A$ and glycine receptors. *Nature*, **389**(6649), 385–389.

Millar, D. G., Griffiths-Smith, K., Algar, E. and Scopes, R. K. (1982). Activity and stability of glycolitic enzymes in the presence of ethanol. *Biotechnol. Lett.*, **4**(9), 601–606.

Miller, D. K., Griffiths, E., Lenard, J. and Firestone, R. A. (1983). Cell killing by lysosomotropic detergents. *J. Cell Biol.*, **97**(6), 1841–1851.

Miller, K. W., Firestone, L. L., Alifimoff, J. K. and Streicher, P. (1989). Nonanesthetic alcohols dissolve in synaptic membranes without perturbing their lipids. *Proc. Natl. Acad. Sci. USA*, **86**(3), 1084–1087.

Miosga, T., Witzel, A. and Zimmermann, F. K. (1994). Sequence and function analysis of a 9.46 kb fragment of *Saccharomyces cerevisiae* chromosome X. *Yeast*, **10**(7), 965–973.

Mishra, P. and Kaur, S. (1991). Lipids as modulators of ethanol tolerance in yeast. *Appl. Microbiol. Biotechnol.*, **34**(6), 697–702.

Mishra, P. and Prasad, R. (1988). Role of phospholipid head groups in ethanol tolerance of *Saccharomyces cerevisiae*. *J. Gen. Microbiol.*, **134**, 3205–3211.

Mishra, P. and Prasad, R. (1989). Relationship between ethanol tolerance and fatty acyl composition of *Saccharomyces cerevisiae*. *Appl. Microbiol. Biotechnol.*, **30**(3), 294–298.

Mitsui, K., Hatakeyama, K., Matsushita, M. and Kanazawa, H. (2009). *Saccharomyces cerevisiae* Na^+/H^+ antiporter Nha1p associates with lipid rafts and requires sphingolipid for stable localization to the plasma membrane. *J. Biochem.*, **145**(6), 709–720.

Miyahara, K., Mizunuma, M., Hirata, D., Tsuchiya, E. and Miyakawa, T. (1996). The involvement of the *Saccharomyces cerevisiae* multidrug resistance transporters Pdr5p and Snq2p in cation resistance. *FEBS Lett.*, **399**(3), 317–320.

Moadab, A., Rupley, K. F. and Wadhams, P. (2001). Effectiveness of a nonrinse, alcohol-free antiseptic hand wash. *J. Am. Podiatr. Med. Assoc.*, **91** (6), 288–293.

Monk, B. C., Niimi, K., Lin, S., Knight, A., Kardos, T. B., Cannon, R. D., Parshot, R., King, A., Lun, D. and Harding, D. R. K. (2005). Surface-active fungicidal D-peptide inhibitors of the plasma membrane proton pump that block azole resistance. *Antimicrob. Agents Chemother.*, **49**(1), 57–70.

Morth, J. P., Pedersen, B. P., Buch-Pedersen, M. J., Andersen, J. P., Vilsen, B., Palmgren, M. G. and Nissen, P. (2011). A structural overview of the plasma membrane Na^+,K^+-ATPase and H^+-ATPase ion pumps. *Nat. Rev. Mol. Cell Biol.*, **12**(1), 60–70.

Möykkynen, T. and Korpi, E. R. (2012). Acute effects of ethanol on glutamate receptors. *Basic Clin. Pharmacol. Toxicol.*, **111**(1), 4–13.

Mueckler, M., Caruso, C., Baldwin, S. A., Panico, M., Blench, I., Morris, H. R., Allard, W. J., Lienhard, G. E. and Lodish, H. F. (1985). Sequence and structure of a human glucose transporter. *Science*, **229** (4717), 941–945.

Murphy, J. M., McBride, W. J., Lumeng, L. and Li, T. K. (1982). Regional brain levels of monoamines in alcohol-preferring and -nonpreferring lines of rats. *Pharmacol. Biochem. Behav.*, **16**(1), 145–149.

Nagy, Z., Montigny, C., Leverrier, P., Yeh, S., Goffeau, A., Garrigos, M. and Falson, P. (2006). Role of the yeast ABC transporter Yor1p in cadmium detoxification. *Biochimie*, **88**(11), 1665–1671.

Nelson, D. L. and Cox, M. M. *Lehninger Principles of Biochemistry*. W. H. Freeman and Company, New York, 5^{th} edition, 2008. ISBN 978-0-7167-7108-1.

Nes, W. D., Janssen, G. G., Crumley, F. G., Kalinowska, M. and Akihisa, T. (1993). The structural requirements of sterols for membrane function in *Saccharomyces cerevisiae*. *Arch. Biochem. Biophys.*, **300**(2), 724–33.

Nguyen, T. H., Fleet, G. H. and Rogers, P. L. (1998). Composition of the cell walls of several yeast species. *Appl. Microbiol. Biotechnol.*, **50**(2), 206–212.

Nso, E., Goffeau, A. and Dufour, J. P. (2002). Fluctuations during growth of the plasma membrane H^+-ATPase activity of *Saccharomyces cerevisiae* and *Schizosaccharomyces pombe*. *Folia Microbiol.*, **47**(4), 401–406.

Obłak, E. and Krasowska, A. (2010). Biologiczna aktywność zwiazków lizosomotropowych (The biological activity of lysosomotropic agents). *Postep. Hig. Med. Dosw.*, **64**(64), 459–465.

Oehlen, B. and Cross, F. R. (1994). Signal transduction in the budding yeast *Saccharomyces cerevisiae*. *Curr. Opin. Cell Biol.*, **6**(6), 836–841.

Ogawa, Y., Nitta, A., Uchiyama, H., Imamura, T., Shimoi, H. and Ito, K. (2000). Tolerance mechanism of the ethanol-tolerant mutant of sake yeast. *J. Biosci. Bioeng.*, **90**(3), 313–320.

Ohgaki, R., Nakamura, N., Mitsui, K. and Kanazawa, H. (2005). Characterization of the ion transport activity of the budding yeast Na^+/H^+ antiporter, Nha1p, using isolated secretory vesicles. *Biochim. Biophys. Acta - Biomembr.*, **1712**(2), 185–196.

Okorokov, L. A., Lichko, L. P. and Kulaev, I. S. (1980). Vacuoles: Main compartments of potassium, magnesium, and phosphate ions in *Saccharomyces carlsbergensis* cells. *J. Bacteriol.*, **144**(2), 661–665.

Op den Kamp, J. A. F. (1979). Lipid asymmetry in membranes. *Annu. Rev. Biochem.*, **48**, 47–71.

Orij, R., Postmus, J., Beek, A. T., Brul, S. and Smits, G. J. (2009). *In vivo* measurement of cytosolic and mitochondrial pH using a pH-sensitive GFP derivative in *Saccharomyces cerevisiae* reveals a relation between intracellular pH and growth. *Microbiology*, **155**(1), 268–278.

Orlean, P. (2012). Architecture and biosynthesis of the *Saccharomyces cerevisiae* cell wall. *Genetics*, **192**(3), 775–818.

Orlean, P., Arnold, E. and Tanner, W. (1985). Apparent inhibition of glycoprotein synthesis by *S. cerevisiae* mating pheromones. *FEBS*, **184**(2), 313–317.

Ortega, M. D. and Rodríguez-Navarro, A. (1985). Potassium and rubidium effluxes in *Saccharomyces cerevisiae*. *Z. Naturforsch.*, **40c**(9-10), 721–725.

Palková, Z., Váchová, L., Gášková, D. and Kučerová, H. (2009). Synchronous plasma membrane electrochemical potential oscillations during yeast colony development and aging. *Mol. Membr. Biol.*, **26**(4), 228–235.

Palomäki, H. and Kaste, M. (1993). Regular light-to-moderate intake of alcohol and the risk of ischemic stroke. Is there a beneficial effect? *Stroke*, **24** (12), 1828–1832.

Pandey, S. C., Ugale, R., Zhang, H., Tang, L. and Prakash, A. (2008). Brain chromatin remodeling: A novel mechanism of alcoholism. *J. Neurosci.*, **28**(14), 3729–3737.

Pang, K. Y., Braswell, L. M., Chang, L., Sommer, T. J. and Miller, K. W. (1980). The perturbation of lipid bilayers by general anesthetic: A quantitative test of the disordered lipid hypothesis. *Mol. Pharmacol.*, **18**(1), 84–90.

Patton, J. L. and Lester, R. L. (1991). The phosphoinositol sphingolipids of *Saccharomyces cerevisiae* are highly localized in the plasma membrane. *Microbiology*, **173**(10), 3101–3108.

Patton, J. L., Srinivasan, B., Dickson, R. C. and Lester, R. L. (1992). Phenotypes of sphingolipid-dependent strains of *Saccharomyces cerevisiae*. *J. Bacteriol.*, **174**(22), 7180–7184.

Peña, A., Uribe, S., Pardo, J. P. and Borbolla, M. (1984). The use of a cyanine dye in measuring membrane potential in yeast. *Arch. Biochem. Biophys.*, **231**(1), 217–225.

Peoples, R. W., Chaoying, L. and Weight, F. F. (1996). Lipid vs protein theories of alcohol action in the nervous system. *Annu. Rev. Pharmacol. Toxicol.*, **36**(1), 185–201.

Pereira, M. B. P., Tisi, R., Fietto, L. G., Cardoso, A. S., França, M. M., Carvalho, F. M., Trópia, M. J. M., Martegani, E., Castro, I. M. and Brandão, R. L. (2008). Carbonyl cyanide *m*-chlorophenylhydrazone induced calcium signaling and activation of plasma membrane H^+-ATPase in the yeast *Saccharomyces cerevisiae*. *FEMS Yeast Res.*, **8**(4), 622–630.

Perlin, D. S., Kasamo, K., Brooker, R. J. and Slayman, C. W. (1984). Electrogenic H^+ translocation by the plasma membrane ATPase of *Neurospora*. Studies on plasma membrane vesicles and reconstituted enzyme. *J. Biol. Chem.*, **259**(12), 7884–7892.

Perlin, D. S. and Slayman, C. W. (1986). H^+/ATP stoichiometty of proton pumps from *Neurospora crassa* and *Escherichia coli*. *Arch. Biochem. Biophys.*, **248**(1), 53–61.

Pernak, J. (1999). Antimicrobial activities of new analogues of benzalkonium chloride. *Eur. J. Med. Chem.*, **34**(9), 765–771.

Petrov, V. V. (2015). Role of loop L5-6 connecting transmembrane segments M5 and M6 in biogenesis and functioning of yeast Pma1 H^+-ATPase. *Biochem.*, **80**(1), 31–44.

Petrov, V. V. and Okorokov, L. A. (1990). Increase of the anion and proton permeability of *Saccharomyces carlsbergensis* plasmalemma by *n*-alcohols as a possible cause of its de-energization. *Yeast*, **6**(4), 311–318.

Pietrzykowski, A. Z., Friesen, R. M., Martin, G. E., Puig, S. I., Nowak, C. L., Wynne, P. M., Siegelmann, H. T. and Treistman, S. N. (2008). Posttranscriptional regulation of BK channel splice variant stability by miR-9 underlies neuroadaptation to alcohol. *Neuron*, **59**(2), 274–287.

Piper, P. W., Talreja, K., Panaretou, B., Moradas-Ferreira, P., Byrne, K., Praekelt, U. M., Meacock, P., Recnacq, M. and Boucherie, H. (1994). Induction of major heat-shock proteins of *Saccharomyces cerevisiae*, including plasma membrane Hsp30, by ethanol levels above a critical threshold. *Microbiology*, **140**(11), 3031–3038.

Piper, P. W., Ortiz-Calderon, C., Holyoak, C., Coote, P. and Cole, M. (1997). Hsp30, the integral plasma membrane heat shock protein of *Saccharomyces cerevisiae*, is a stress-inducible regulator of plasma membrane H^+-ATPase. *Cell Stress Chaperones*, **2**, 12–24.

Plášek, J. and Gášková, D. (2014). Complementary methods of processing diS-$C_3(3)$ fluorescence spectra used for monitoring the plasma membrane potential of yeast: Their pros and cons. *J. Fluoresc.*, **24**(2), 541–547.

Plášek, J., Gášková, D., Lichtenberg-Fraté, H., Ludwig, J. and Höfer, M. (2012). Monitoring of real changes of plasma membrane potential by diS-$C_3(3)$ fluorescence in yeast cell suspensions. *J. Bioenerg. Biomembr.*, **44**(5), 559–569.

Plášek, J., Melcrová, A. and Gášková, D. (2015). Enhanced sensitivity of pHluorin-based monitoring of intracellular pH changes achieved through synchronously scanned fluorescence spectra. *Anal. Chem.*, **87**(19), 9600–9604.

Plášek, J., Babuka, D., Gášková, D., Jančíková I, Zahumenský, J. and Hoefer, M. (2017). A novel method for assessment of local ph in periplasmic space and of cell surface potential in yeast. *J Bioenerg Biomembr*, **49**(3), 273–279.

Platara, M., Ruiz, A., Serrano, R., Palomino, A., Moreno, F. and Ariño, J. (2006). The transcriptional response of the yeast Na^+-ATPase *ENA1* gene to alkaline stress involves three main signaling pathways. *J. Biol. Chem.*, **281**(48), 36632–36642.

Plemper, R. K., Egner, R., Kuchler, K. and Wolf, D. H. (1998). Endoplasmic reticulum degradation of a mutated ATP-binding cassette transporter Pdr5 proceeds in a concerted action of Sec61 and the proteasome. *J. Biol. Chem.*, **273**(49), 32848–32856.

Pomorski, T., Lombardi, R., Riezman, H., Devaux, P. F., van Meer, G. and Holthuis, J. C. (2003). Drs2p-related P-type ATPases Dnf1p and Dnf2p are required for phospholipid translocation across the yeast plasma membrane and serve a role in endocytosis. *Mol. Biol. Cell*, **14**(3), 1240–1254.

Portillo, F. (2000). Regulation of plasma membrane H^+-ATPase in fungi and plants. *Biochim. Biophys. Acta*, **1469**(1), 31–42.

Portillo, F., de Larrinoa, I. F. and Serrano, R. (1989). Deletion analysis of yeast plasma membrane H^+-ATPase and identification of a regulatory domain at the carboxyl-terminus. *FEBS Lett.*, **247**(2), 381–385.

Portillo, F., Eraso, P. and Serrano, R. (1991). Analysis of the regulatory domain of yeast plasma membrane H^+-ATPase by directed mutagenesis and intragenic suppression. *FEBS Lett.*, **287**(1-2), 71–74.

Posas, F., Camps, M. and Ariño, J. (1995). The PPZ protein phosphatases are important determinants of salt tolerance in yeast cells. *J. Biol. Chem.*, **270** (22), 13036–13041.

Prasad, R. and Panwar, S. (2004). Physiological functions of multidrug transporters in yeast. *Curr. Sci.*, **86**(1), 62–73.

Prasad, R., Panwar, S. L. and Smriti (2002). Drug resistance in yeasts - An emerging scenario. *Adv. Microb. Physiol.*, **46**, 155–201.

Preston, R. A., Murphy, R. F. and Jones, E. W. (1989). Assay of vacuolar pH in yeast and identification of acidification-defective mutants. *Proc. Natl. Acad. Sci. USA*, **86**(18), 7027–7031.

Pringle, M. J., Brown, K. B. and Miller, K. W. (1981). Can the lipid theories of anesthesia account for the cutoff in anesthetic potency in homologous series of alcohols? *Mol. Pharmacol.*, **19**, 49–55.

Proft, M. and Struhl, K. (2004). MAP kinase-mediated stress relief that precedes and regulates the timing of transcriptional induction. *Cell*, **118**(3), 351–361.

Purwin, C., Nicolay, K., Scheffers, W. A. and Holzer, H. (1986). Mechanism of control of adenylate cyclase activity in yeast. *J. Biol. Chem.*, **261**(19), 8744–8749.

Qureshi, A. I., Safdar, K., Patel, M., Janssen, R. S. and Frankel, M. R. (2017). Stroke in young Black patients. Risk factors, subtypes, and prognosis. *Stroke*, **26**, 1995–1998.

Ram, A. F. J., Wolters, A., Ten Hoopen, R. and Klis, F. M. (1994). A new approach for isolating cell wall mutants in *Saccharomyces cerevisiae* by screening for hypersensitivity to calcofluor white. *Yeast*, **10**(8), 1019–1030.

Ramos, J., Contreras, P. and Rodríguez-Navarro, A. (1985). A potassium transport mutant of *Saccharomyces cerevisiae*. *Arch. Microbiol.*, **143**, 88–93.

Ramos, J., Alijo, R., Haro, R. and Rodriguez-Navarro, A. (1994). TRK2 is not a low-affinity potassium transporter in *Saccharomyces cerevisiae*. *J. Bacteriol.*, **176**(1), 249–252.

Ramos, J. L., Duque, E., Gallegos, M.-T., Godoy, P., Ramos-González, M. I., Rojas, A., Terán, W. and Segura, A. (2002). Mechanisms of solvent tolerance in gram-negative bacteria. *Annu. Rev. Microbiol.*, **56**(1), 743–768.

Rani, C. S. S., Qiang, M. and Ticku, M. K. (2005). Potential role of cAMP response element-binding protein in ethanol-induced *N*-methyl-D-aspartate receptor 2B subunit gene transcription in fetal mouse cortical cells. *Mol. Pharmacol.*, **67**(6), 2126–2136.

Rao, R., Drummond-Barbosa, D. and Slayman, C. W. (1993). Transcriptional regulation by glucose of the yeast *PMA1* gene encoding the plasma membrane H^+-ATPase. *Yeast*, **9**(10), 1075–1084.

Reid, J. D., Lukas, W., Shafaatian, R., Bertl, A., Scheurmann-Kettner, C., Guy, H. R. and North, R. A. (1996). The *S. cerevisiae* outwardly-rectifying potassium channel (DUK1) identifies a new family of channels with duplicated pore domains. *Receptors Channels*, **4**(1), 51–62.

Ristow, H., Seyfarth, A. and Lochmann, E. R. (1995). Chromosomal damages by ethanol and acetaldehyde in *Saccharomyces cerevisiae* as studied by pulsed field gel electrophoresis. *Mutat. Res. - Fundam. Mol. Mech. Mutagen.*, **326**(2), 165–170.

Rivera, J., Feldmesser, M., Cammer, M. and Casadevall, A. (1998). Organ-dependent variation of capsule thickness in *Cryptococcus neoformans* during experimental murine infection. *Infect. Immun.*, **66**(10), 5027–5030.

Rivetta, A., Kuroda, T. and Slayman, C. (2011). Anion currents in yeast K^+ transporters (TRK) characterize a structural homologue of ligand-gated ion channels. *Pflugers Arch.*, **462**(2), 315–330.

Rodriguez, R. J., Low, C., Bottema, C. D. K. and Parks, L. W. (1985). Multiple functions for sterols in *Saccharomyces cerevisiae*. *Biochim. Biophys. Acta*, **837**(3), 336–343.

Rodríguez-Navarro, A. (2000). Potassium transport in fungi and plants. *Biochim. Biophys. Acta*, **1469**(1), 1–30.

Rogers, B., Decottignies, A., Kolaczkowski, M., Carvajal, E., Balzi, E. and Goffeau, A. (2001). The pleitropic drug ABC transporters from *Saccharomyces cerevisiae*. *J. Mol. Microbiol. Biotechnol.*, **3**, 207–214.

Roomans, G. M. and Sevéus, L. A. (1976). Subcellular localization of diffusible ions in the yeast *Saccharomyces cerevisiae*: Quantitative microprobe analysis of thin freeze-dried sections. *J. Cell Sci.*, **21**, 119–127.

Rosa, M. F. and Sá-Correia, I. (1991). *In vivo* activation by ethanol of plasma membrane ATPase of *Saccharomyces cerevisiae*. *J. Gen. Microbiol.*, **57** (3), 830–835.

Rosa, M. F. and Sá-Correia, I. (1992). Ethanol tolerance and activity of plasma membrane ATPase in *Kluyveromyces marxianus* and *Saccharomyces cerevisiae*. *Enzyme Microb. Technol.*, **14**(1), 23–27.

Russell, N. J. (1989). Adaptive modifications in membranes of halotolerant and halophilic microorganisms. *J. Bioenerg. Biomembr.*, **21**(1), 93–113.

Salton, M. R. J. (1968). Lytic agents, cell permeability, and monolayer penetrability. *J. Gen. Physiol.*, **52**(1), 227–252.

Schekman, R. and Brawley, V. (1979). Localized deposition of chitin on the yeast cell surface in response to mating pheromone. *Proc. Natl. Acad. Sci. USA*, **76**(2), 645–649.

Scherrer, R., Louden, L. and Gerhardt, P. (1974). Porosity of the yeast cell wall and membrane. *J. Bacteriol.*, **118**(2), 534–540.

Seeman, P. (1972). The membrane actions of anesthetics and tranquilizers. *Biochem. Pharmacol.*, **24**(4), 583–655.

Segal, E., Shapira, M., Regev, A., Pe'er, D., Botstein, D., Koller, D. and Friedman, N. (2003). Module networks: identifying regulatory modules and their condition-specific regulators from gene expression data. *Nat. Genet.*, **34**(2), 166–176.

Seol, J. H., Shevchenko, A., Shevchenko, A. and Deshaies, R. J. (2001). Skp1 forms multiple protein complexes, including RAVE, a regulator of V-ATPase assembly. *Nat. Cell Biol.*, **3**(4), 384–391.

Serrano, R., Kiellandbrandt, M. C. and Fink, G. R. (1986). Yeast plasma membrane ATPase is essential for growth and has homology with (Na^+ + K^+), K^+- and Ca^{2+}-ATPases. *Nature*, **319**(6055), 689–693.

Serrano, R. (1980). Effect of ATPase inhibitors on the proton pump of respiratory-deficient yeast. *Eur. J. Biochem.*, **105**(2), 419–424.

Serrano, R. (1983). *In vivo* glucose activation of the yeast plasma membrane ATPase. *FEBS Lett.*, **156**(1), 11–14.

Serrano, R. (1988). Structure and function of proton translocafing ATPase in plasma membranes of plants and fungi. *Biochim. Biophys. Acta - Rev. Biomembr.*, **947**, 1–28.

Serrano, R. Transport across yeast vacuolar and plasma membrane. In Jones, E. W. and Broach, J. R., editors, *The Molecular and Cellular Biology of the Yeast* Saccharomyces*: Genome Dynamics, Protein Synthesis, and Energetics*, pages 523–583. Cold Spring Harbor Laboratory Press, New York, 1^{st} edition, 1991. ISBN 978-0879693633.

Servos, J., Haase, E. and Brendel, M. (1993). Gene *SNQ2* of *Saccharomyces cerevisiae*, which confers resistance to 4-nitroguinoline-*N*-oxide and other chemicals, encode a 169 kDa protein homologous to ATP-dependent permeases. *Mol. Gen. Genet.*, **238**(2-3), 214–218.

Sesti, F., Shih, T. M., Nikolaeva, N. and Goldstein, S. A. N. (2001). Immunity to K1 killer toxin: Internal TOK1 blockade. *Cell*, **105**(5), 637–644.

Seto-Young, D., Monk, B., Mason, A. B. and Perlin, D. S. (1997). Exploring an antifungal target in the plasma membrane H^+-ATPase of fungi. *Biochim. Biophys. Acta - Biomembr.*, **1326**(2), 249–256.

Sharma, S. C., Raj, D., Forouzandeh, M. and Bansal, M. P. (1996). Salt-induced changes in lipid composition and ethanol tolerance in *Saccharomyces cerevisiae*. *Appl. Biochem. Biotechnol.*, **56**(2), 189–195.

Shematek, E. M., Braatz, J. A. and Cabibg, E. (1980). Biosynthesis of the yeast cell wall. *J. Biol. Chem.*, **255**(3), 888–894.

Sikkema, J., de Bont, J. A. and Poolman, B. (1995). Mechanisms of membrane toxicity of hydrocarbons. *Microbiol. Rev.*, **59**(2), 201–222.

Simón, E., Clotet, J., Calero, F., Ramos, J. and Ariño, J. (2001). A screening for high copy suppressors of the *sit4 hal3* synthetically lethal phenotype reveals a role for the yeast Nha1 antiporter in cell cycle regulation. *J. Biol. Chem.*, **276**(32), 29740–29747.

Simón, E., Barceló, A. and Ariño, J. (2003). Mutagenesis analysis of the yeast Nha1 Na^+/H^+ antiporter carboxy-terminal tail reveals residues required for function in cell cycle. *FEBS Lett.*, **545**(2-3), 239–245.

Singer, S. J. and Nicolson, G. L. (1972). The fluid mosaic model of the structure of cell membranes. *Science*, **175**(4023), 720–731.

Sipos, G. and Kuchler, K. (2006). Fungal ATP-binding cassette (ABC) transporters in drug resistance & detoxification. *Curr. Drug Targets*, **7**(4), 471–481.

Skrzypek, M., Lester, R. L. and Dickson, R. C. (1997). Suppressor gene analysis reveals an essential role for sphingolipids in transport of glycosylphosphatidylinositol-anchored proteins in *Saccharomyces cerevisiae*. *J. Bacteriol.*, **179**(5), 1513–20.

Sonmez, M., Ince, H. Y., Yalcin, O., Ajdžanović, V., Spasojević, I., Meiselman, H. J. and Baskurt, O. K. (2013). The effect of alcohols on red blood cell mechanical properties and membrane fluidity depends on their molecular size. *PLoS One*, **8**(9), 1–12.

Souza, M. A. A., Trópia, M. J. and Brandão, R. L. (2001). New aspects of the glucose activation of the H^+-ATPase in the yeast *Saccharomyces cerevisiae*. *Microbiology*, **147**(10), 2849–2855.

Swan, T. M. and Watson, K. (1998). Stress tolerance in a yeast sterol auxotroph: Role of ergosterol, heat shock proteins and trehalose. *FEMS Microbiol. Lett.*, **169**(1), 191–197.

Sychrová, H., Ramírez, J. and Peña, A. (1999). Involvement of Nha1 antiporter in regulation of intracellular pH in *Saccharomyces cerevisiae*. *FEMS Microbiol. Lett.*, **171**(2), 167–172.

Taglicht, D. and Michaelis, S. (1998). *Saccharomyces cerevisiae* ABC proteins and their relevance to human health and disease. *Methods Enzymol.*, **292**, 130–162.

Takagi, H., Takaoka, M., Kawaguchi, A. and Kubo, Y. (2005). Effect of L-proline on sake brewing and ethanol stress in *Saccharomyces cerevisiae*. *Appl. Environ. Microbiol.*, **71**(12), 8656–8662.

Takahashi, T., Shimoi, H. and Ito, K. (2001). Identification of genes required for growth under ethanol stress using transposon mutagenesis in *Saccharomyces cerevisiae*. *Mol. Genet. Genomics*, **265**(6), 1112–1119.

Thevelein, J., Beullens, M., Honshoven, F., Hoebeeck, G., Detremerie, K., Griewel, B., den Hollander, J. and Jans, A. (1987). Regulation of the camp level in the yeast saccharomyces cerevisiae: the glucose-induced camp signal is not mediated by a transient drop in the intracellular ph. *J Gen Microbiol*, **133**(8), 2197–2205.

Thomas, D. S. and Rose, A. H. (1979). Inhibitory effect of ethanol on growth and solute accumulation by *Saccharomyces cerevisiae* as affected by plasma-membrane lipid composition. *Arch. Microbiol.*, **55**, 49–55.

Thomas, D. S., Hossack, J. A. and Rose, A. H. (1978). Plasma-membrane lipid composition and etehanol tolerance in *Saccharomyces cerevisiae*. *Arch. Microbiol.*, **117**, 239–245.

Toulmay, A. and Schneiter, R. (2007). Lipid-dependent surface transport of the proton pumping ATPase: A model to study plasma membrane biogenesis in yeast. *Biochimie*, **89**(2), 249–254.

Trópia, M. J. M., Cardoso, A. S., Tisi, R., Fietto, L. G., Fietto, J. L. R., Martegani, E., Castro, I. M. and Brandão, R. L. (2006). Calcium signaling and sugar-induced activation of plasma membrane H^+-ATPase in *Saccharomyces cerevisiae* cells. *Biochem. Biophys. Res. Commun.*, **343**(4), 1234–1243.

Troyer, J. R. (1953). A relation between cell multiplication and alcohol tolerance in yeasts. *Mycologia*, **45**, 20–39.

Troyer, J. R. (1955). Methanol tolerance of three strains of *Saccharomyces cerevisiae* hansen. *Ohio J. Sci.*, **55**(3), 185–187.

Trujillo, R. and Laible, N. (1970). Reversible inhibition of spore germination by alcohols. *Appl. Microbiol.*, **20**(4), 620–623.

Tunblad-Johansson, I., Andre, L. and Adler, L. (1987). The sterol and phospholipid composition of the salt-tolerant yeast *Debaryomyces hansenii* grown at various concentrations of NaCl. *Biochim. Biophys. Acta - Lipids Lipid Metab.*, **921**(1), 116–123.

van der Rest, M. E., Kamminga, A. H., Nakano, A., Anraku, Y., Poolman, B. and Konings, W. N. (1995). The plasma membrane of *Saccharomyces cerevisiae*: Structure, function, and biogenesis. *Microbiol. Rev.*, **59** (2), 304–322.

van Uden, N. (1983). Effects of ethanol on the temperature relations of viability and growth in yeast. *Crit. Rev. Biotechnol.*, **1**(3), 263–272.

Vergani, P., Miosga, T., Jarvis, S. M. and Blatt, M. R. (1997). Extracellular K^+ and Ba^{2+} mediate voltage-dependent inactivation of the outward-rectifying K^+ channel encoded by the yeast gene *TOK1*. *FEBS Lett.*, **405**(3), 337–344.

Ververidis, P., Davrazou, F., Diallinas, G., Georgakopoulos, D., Kanellis, A. K. and Panopoulos, N. (2001). A novel putative reductase (Cpd1p) and the multidrug exporter Snq2p are involved in resistance to cercosporin and other singlet oxygen-generating photosensitizers in *Saccharomyces cerevisiae*. *Curr. Genet.*, **39**(3), 127–136.

Vianna, C. R., Silva, C. L. C., Neves, M. J. and Rosa, C. A. (2008). *Saccharomyces cerevisiae* strains from traditional fermentations of Brazilian cachaça: Trehalose metabolism, heat and ethanol resistance. *Antonie Van Leeuwenhoek*, **93**, 205–217.

Vidal, M., Buckley, A. M., Yohn, C., Hoeppner, D. J. and Gaber, R. F. (1995). Identification of essential nucleotides in an upstream repressing sequence of *Saccharomyces cerevisiae* by selection for increased expression of *TRK2*. *Proc. Natl. Acad. Sci. USA*, **92**(6), 2370–2374.

Viegas, C. A., Supply, P., Capieaux, E., Vandyck, L., Goffeau, A. and Sacorreia, I. (1994). Regulation of the expression of the H^+-ATPase genes *PMA1* and *PMA2* during growth and effects of octanoic-acid in *Saccharomyces cerevisiae*. *Biochim. Biophys. Acta - Gene Struct. Expr.*, **1217**(1), 74–80.

Villalobo, A., Boutry, M. and Goffeau, A. (1981). Electrogenic proton translocation coupled to ATP hydrolysis by the plasma membrane Mg^{2+}-dependent ATPase of yeast in reconstituted proteoliposomes. *J. Biol. Chem.*, **256**(23), 12081–12087.

Volkov, V. (2015). Quantitative description of ion transport via plasma membrane of yeast and small cells. *Front. Plant Sci.*, **6**(11), 425.

Wach, A., Schlesser, A. and Goffeau, A. (1992). An alignment of 17 deduced protein sequences from plant, fungi, and ciliate H^+-ATPase genes. *J. Bioenerg. Biomembr.*, **24**(3), 309–317.

Walker, J. E., Saraste, M., Runswick, M. and Gay, N. J. (1982). Distantly related sequences in the α- and β-subunits of ATP synthase, myosin, kinases and other ATP-requiring enzymes and a common nucleotide binding fold. *EMBO J.*, **1**(8), 945–951.

Walker-Caprioglio, H. M., Casey, W. M. and Parks, L. W. (1990). *Saccharomyces cerevisiae* membrane sterol modifications in response to growth in the presence of ethanol. *Appl. Environ. Microbiol.*, **56**(9), 2853–2857.

Wallace, E. A. and Green, A. S. (2009). Methanol toxicity secondary to inhalant abuse in adult men. *Clin. Toxicol.*, **47**(3), 239–242.

Warnault, V., Darcq, E., Levine, A., Barak, S. and Ron, D. (2013). Chromatin remodeling - a novel strategy to control excessive alcohol drinking. *Transl. Psychiatry*, **3**(2), e231.

Watanabe, M., Tamura, K., Magbanua, J. P., Takano, K., Kitamoto, K., Kitagaki, H., Akao, T. and Shimoi, H. (2007). Elevated expression of genes under the control of stress response element (STRE) and Msn2p in an ethanol-tolerance sake yeast Kyokai no. 11. *J. Biosci. Bioeng.*, **104**(3), 163–170.

Westrin, B. A. (1990). Measurement of the diffusion coefficient of ethanol in agarose gel beads: A reproducibility study. *Biotechnol. Tech.*, **4**(6), 409–414.

Wieland, J., Nitsche, A. M., Strayle, J., Steiner, H. and Rudolph, H. K. (1995). The *PMR2* gene cluster encodes functionally distinct isoforms of a putative Na^+ pump in the yeast plasma membrane. *EMBO J.*, **14**(16), 3870–3882.

Wilke, N., Sganga, M., Barhite, S. and Miles, M. F. Effects of alcohol on gene expression in neural cells. In Jansson, B., Jörnvall, H., Rydberg, U., Terenius, L. and Vallee, B. L., editors, *Toward a Molecular Basis of Alcohol Use and Abuse*, volume 71, pages 49–59. Birkhäuser Verlag, Basel, 1994. ISBN 3-7643-2940-8.

Witek, S., Goffeau, A., Nader, J., Łuczyński, J., Lachowicz, T. M., Kuta, B. and Obłak, E. (1997). Lysosomotropic aminoesters act as H^+-ATPase inhibitors in yeast. *Folia Microbiol.*, **42**(3), 252–254.

Wong, S. M., Tauck, D. L., Fong, E. G. and Kendig, J. J. (1998). Glutamate receptor-mediated hyperexcitability after ethanol exposure in isolated neonatal rat spinal cord. *J. Pharmacol. Exp. Ther.*, **285**(1), 201–207.

Yeagle, P. L. (1989). Lipid regulation of cell membrane structure and function. *FASEB J.*, **3**(7), 1833–1842.

Yenush, L., Merchan, S., Holmes, J. and Serrano, R. (2005). pH-responsive, posttranslational regulation of the Trk1 potassium transporter by the type 1-related Ppz1 phosphatase. *Mol. Cell. Biol.*, **25**(19), 8683–8692.

You, K. M., Rosenfield, C.-L. and Knipple, D. C. (2003). Ethanol tolerance in the yeast *Saccharomyces cerevisiae* is dependent on cellular oleic acid content. *Appl. Environ. Microbiol.*, **69**(3), 1499–1503.

Zahrádka, J. and Sychrová, H. (2012). Plasma-membrane hyperpolarization diminishes the cation efflux via Nha1 antiporter and Ena ATPase under potassium-limiting conditions. *FEMS Yeast Res.*, **12**(4), 439–446.

Zakhari, S. (1997). Alcohol and the cardiovascular system: Molecular mechanisms for beneficial and harmful action. *Alcohol Health Res. World*, **21**(1), 21–29.

Zakhari, S. (2006). Overview: How is alcohol metabolized by the body? *Alcohol Res. & Heal.*, **29**(4), 245–254.

Zaleski, M., Morato, G. S., Silva, V. A. D. and Lemos, T. (2004). Neuropharmacological aspects of chronic alcohol use and withdrawal syndrome. *Rev. Bras. Psiquiatr.*, **26**(Supl I), 40–42.

Zhang, X., Cui, Z., Miyakawa, T. and Moye-Rowley, W. S. (2001). Cross-talk between transcriptional regulators of multidrug resistance in *Saccharomyces cerevisiae*. *J. Biol. Chem.*, **276**(12), 8812–8819.

Zhou, X.-L., Vaillant, B., Loukin, S. H., King, C. and Saimi, Y. (1995). *YKC1* encodes the depolarization-activated K^+ channel in the plasma membrane of yeast. *FEBS Lett.*, **373**, 170–176.

Zinser, E., Sperka-Gottlieb, C. D. M., Fasch, E. V., Kohlwein, S. D., Paltauf, F. and Daum, G. (1991). Phospholipid synthesis and lipid composition of subcellular membranes in the unicellular eukaryote *Saccharomyces cerevisiae*. *J. Bacteriol.*, **173**(6), 2026–2034.

Zlotnik, H., Fernandez, M. P., Bowers, B. and Cabib, E. (1984). *Saccharomyces cerevisiae* mannoproteins form an external cell wall layer that determines wall porosity. *J. Bacteriol.*, **159**(3), 1018–1026.

Zurzolo, C., van Meer, G. and Mayor, S. (2003). The order of rafts. *EMBO Rep.*, **4**(12), 1117–1121.

List of Figures

List of Tables

List of Abbreviations

2DG - 2-deoxy-D-glucose
ABC - ATP-binding cassette
ATP - adenosine triphosphate
BAC - benzalkonium chloride
C-P buffer - citric acid + phosphate buffer
CCCP - carbonyl cyanide *m*-chlorophenyl hydrazone
CD cocktail - CCCP + DM-11 cocktail
CFTR - cystic fibrosis transmembrane conductance regulator
CNS - central nervous system
CREB - cAMP response element-binding protein
DCCD - *N*,*N*'-dicyclohexylcarbodiimide
diS-C_3(3) - 3,3'-dipropylthiacarbocyanine iodide
DM-11 - 2-dodecanoyloxyethyldimethylammonium chloride
DNA - deoxyribonucleic acid
GPI - glycosilphosphatidylinositol
HSF1 - heat shock factor protein 1
MCC - membrane compartment of Can1
MDR - multidrug resistance
MFS - major facilitator superfamily
miRNA - micro ribonucleic acid
NBD - nucleotide binding domain
NMDA - N-methyl-D-aspartate
NQO - 4-nitroquinoline 1-oxide
NR2B - NMDA receptor 2B subunit
ODDC - octenidine dichloride
PDR - pleiotropic drug resistance
RNA - ribonucleic acid
SDS - sodium dodecyl sulfate
TEA^+ - tetraethylammonium cation
TMD - transmembrane domain
YPD - yeast extract + peptone + dextrose
YPG - yeast extract + peptone + glycerol
YPGE - yeast extract + peptone + glycerol + ethanol

Attachments

Attachment I
Scientific article
Gášková, D., Plášek, J., Zahumenský, J., Benešová, I., Buriánková, Ľ., Sigler., K. (2013). Alcohols are inhibitors of *Saccharomyces cerevisiae* multidrug-resistance pumps Pdr5p and Snq2p. *FEMS Yeast Res.*, **13**(8), 782-795.

Attachment II
Scientific article, accepted manuscript
Zahumenský, J., Jančíková, I., Drietomská, A., Švenkrtová, A., Hlaváček, O., Hendrych, T., Plášek, J., Sigler., K., Gášková, D. (2017). Yeast Tok1p channel is a major contributor to membrane potential maintenance under chemical stress. *BBA Biomembr.*, DOI: 10.1016/j.bbamem.2017.06.019.

Attachment III
Conference presentation
Zahumenský, J., Drietomská, A., Sigler., K., Hlaváček, O., Plášek, J., Gášková, D. (2013). Complex regulation of the yeast membrane potential in response to CCCP-induced depolarization and cell acidification. *31st Small Meeting on Yeast Transport and Energetics*, Antalya, Turkey.

Attachment IV
Conference presentation
Gášková, D., Plášek, J., Zahumenský, J., Benešová, I., Buriánková, Ľ., Sigler., K. (2013). Alcohols are inhibitors of *S. cerevisiae* multidrug resistance pumps Pdr5p and Snq2p. *31st Small Meeting on Yeast Transport and Energetics*, Antalya, Turkey.

Attachment V
Conference presentation
Zahumenský, J., Drietomská, A., Švenkrtová, A., Hlaváček, O., Plášek, J., Sigler., K., Gášková, D. (2014). *In vivo* monitoring of membrane potential changes in yeast under CCCP-induced stress: the respective roles of Tok1p and H^+-ATPase. *32nd Small Meeting on Yeast Transport and Energetics*, Montréal, Canada.

Attachment VI

Conference presentation

Zahumenský, J., Drietomská, A., Švenkrtová, A., Hlaváček, O., Hendrych, T., Plášek, J., Sigler., K., Gášková, D. (2015). Comparison of Tok1p and Pma1p roles in membrane potential maintenance of fermenting and respiring *S. cerevisiae* cells challenged with chemically induced acidification and depolarization. *33rd Small Meeting on Yeast Transport and Energetics*, Lisabon, Portugal.

Attachment VII

Conference presentation

Zahumenský, J., Jančíková, I., Švenkrtová, A., Gášková, D. (2016). Tok1p channel plays an important role in membrane potential maintenance under chemical stress. *34th Small Meeting on Yeast Transport and Energetics*, Chania, Crete, Greece.

Attachment I

RESEARCH ARTICLE

Alcohols are inhibitors of *Saccharomyces cerevisiae* multidrug-resistance pumps Pdr5p and Snq2p

Dana Gášková[1], Jaromír Plášek[1], Jakub Zahumenský[1], Ivana Benešová[1], Ľuboslava Buriánková[1] & Karel Sigler[2]

[1]Faculty of Mathematics and Physics, Institute of Physics, Charles University, Prague 2, Czech Republic; and [2]Institute of Microbiology, CR Academy of Sciences, Prague 4, Czech Republic

Correspondence: Dana Gášková, Faculty of Mathematics and Physics, Institute of Physics, Charles University, Ke Karlovu 5, 121 16 Prague 2, Czech Republic. Tel.: +420 221911348; fax: +420 224922797; e-mail: gaskova@karlov.mff.cuni.cz

Received 1 August 2013; revised 20 August 2013; accepted 1 September 2013.

DOI: 10.1111/1567-1364.12088

Editor: Jens Nielsen

Keywords
alcohols; yeast MDR pump; pump inhibitor; fluorescent probe diS-C_3(3); membrane potential.

Abstract

The effect of alcohols on cell membrane proteins has originally been assumed to be mediated by their primary action on membrane lipid matrix. Many studies carried out later on both animal and yeast cells have revealed that ethanol and other alcohols inhibit the functions of various membrane channels, receptors and solute transport proteins, and a direct interaction of alcohols with these membrane proteins has been proposed. Using our fluorescence diS-C_3(3) diagnostic assay for multidrug-resistance pump inhibitors in a set of isogenic yeast Pdr5p and Snq2p mutants, we found that n-alcohols (from ethanol to hexanol) variously affect the activity of both pumps. Beginning with propanol, these alcohols have an inhibitory effect that increases with increasing length of the alcohol acyl chain. While ethanol does not exert any inhibitory effect at any of the concentration used (up to 3%), hexanol exerts a strong inhibition at 0.1%. The alcohol-induced inhibition of MDR pumps was detected even in cells whose membrane functional and structural integrity were not compromised. This supports a notion that the inhibitory action does not necessarily involve only changes in the lipid matrix of the membrane but may entail a direct interaction of the alcohols with the pump proteins.

Introduction

Alcohols, especially ethanol, have long been known to affect living cells and organisms (Korpi *et al.*, 1998; Moykkynen & Korpi, 2012). This effect was often attributed to the interaction of alcohols with membrane lipids (Seeman, 1972; Franks & Lieb, 1978; Goldstein, 1984), but several studies have supported the idea that there exists possibly also a direct interaction of alcohols with certain membrane proteins (Peoples *et al.*, 1996). The lipid theory (Seeman, 1972; Franks & Lieb, 1978; Goldstein, 1984) postulates that alcohols affect primarily membrane fluidity and thereby modify the function of membrane ion channels, receptors, and other proteins. This hypothesis was challenged by the observation that firefly luciferase (a nonmembrane water soluble enzyme) is inhibited by anesthetics, including a homologous series of alcohols (Adey *et al.*, 1975; Franks & Lieb, 1984, 1985). These experiments indicated that alcohols may influence the activity of luciferase through a direct alcohol–protein interaction without the interference of lipids. Furthermore, several studies concerning ligand- or voltage-gated ion channels in neurons (Li *et al.*, 1994, 1998; Lovinger, 1997; Godden *et al.*, 2001; Horishita & Harris, 2008) and ion channels in nonexcitable cells (Chanson *et al.*, 1989; Hamada *et al.*, 2005) have provided evidence that these membrane proteins are also the primary sites of alcohol action.

Both the above-mentioned ability to cause anesthesia and potency to inhibit protein activity are directly correlated with the hydrophobicity of alcohols and anesthetics, usually quantified by their solubility in lipids (Pringle *et al.*, 1981; Lovinger, 1997; Alkire & Gorski, 2004). However, such a correlation exists only up to a certain 'cutoff' limit; in a homologous series of various drugs their potencies increase progressively with the size of the drug but then rather abruptly disappear, for example, above a certain carbon chain length of aliphatic alcohols (Pringle *et al.*, 1981; Franks & Lieb, 1985). To explain the

FEMS YEAST RESEARCH

drug-size-related cutoff effect, it was proposed that amphiphilic receptor proteins contain a hydrophobic pocket of circumscribed dimensions where the alcohols and other drug molecules bind and exert their effects on the receptor (Franks & Lieb, 1985; Li *et al.*, 1994; Korpi *et al.*, 1998). In particular, when the alcohol chain length is increased above the cutoff point, the alcohol molecule is sterically hindered to bind in the pocket and as a result fails to modulate the receptor function.

Taken together, although the primary sites of action in the two theories differ, both theories attribute the ultimate effects of alcohols to alterations in protein function. It is not possible to exclude that both action sites, that is, lipids and proteins, may be involved simultaneously in producing the final effect and that depending on the concentration of alcohols, protein function can be modulated in a different way. At very low concentration, drugs (alcohols) can regulate protein function by a specific interaction with the hydrophobic pocket. At higher concentrations that alter the physical properties of the lipid bilayer, a related nonspecific alcohol effect may considerably modulate the specific effect of drug binding to proteins and thus the observed changes in protein function (Lundbaek, 2008).

In the yeast *Saccharomyces cerevisiae*, it was found that ethanol and other alcohols inhibit activities of permeases for sugars (Leao & van Uden, 1982), ammonium (Leao & van Uden, 1983), amino acids (GAP; Leao & van Uden, 1984a), and organic acids such as acetic acid (Casal *et al.*, 1998) in a noncompetitive way, and the degree of inhibition increases with the lipid solubility of the alcohols. It is important to note that, with the exception of glucose which is transported by facilitated diffusion, all of these solutes are transported by solute–proton symport and therefore require a proton-motive force (Serrano, 1977; Borst-Pauwels, 1981). Therefore, the inhibitory effects induced by alcohols can be caused not only by altering the conformation of permeases and/or their lipid environment (lipid vs. protein theories), but also by dissipation of electrochemical gradient of protons across the plasma membrane (Cartwright *et al.*, 1986; Casal *et al.*, 1998), as alcohols increase the proton permeability of the yeast plasma membrane, that is, they act as uncouplers (Leao & van Uden, 1984b; Petrov & Okorokov, 1990).

Among the variety of membrane transporters in *S. cerevisiae*, whose activity could be affected by alcohols, serious attention is being paid to membrane proteins belonging to the group of multidrug-resistance (MDR) transporters, (Balzi & Goffeau, 1994; Decottignies & Goffeau, 1997; Ernst *et al.*, 2005), which are responsible for the resistance of the cells against a broad spectrum of structurally different xenobiotics (Kolaczkowski *et al.*, 1996, 1998). The major multidrug exporters of *S. cerevisiae* are the ABC transporters Pdr5p, Snq2p, and Yor1p, which show different, but overlapping, substrate specificities (Rogers *et al.*, 2001). It is well established that the *PDR1–3* mutation at the yeast PDR1 transcription regulator locus is responsible for overexpression of the three ABC transporter genes PDR5, SNQ2, and YOR1 (Carvajal *et al.*, 1997; Kolaczkowska & Goffeau, 1999; Nawrocki *et al.*, 2001).

In this study, we examined the inhibitory effect of alcohols (ranging from ethanol to hexanol) on Pdr5p and Snq2p using the diS-C_3(3) diagnostic assay (Hendrych *et al.*, 2009). As shown previously, the fluorescent probe diS-C_3(3) is a substrate of these two pumps, but not of Yor1p and other MDR pumps deleted in AD1-8, that is, Pdr10p, Pdr11p, Pdr15p, and Ycf1p (Gaskova *et al.*, 2002; Cadek *et al.*, 2004). The assay is based on measuring the accumulation of diS-C_3(3) in Pdr5p- or Snq2p-overexpressing cells (strains AD12 and AD13, respectively) in the absence of an inhibitory drug and after its addition (Hendrych *et al.*, 2009). This accumulation was compared with probe accumulation in Pdr5p- and Snq2p-deficient cells of strain AD1-3, which was used as a negative control showing a negligible effect of other MDR pumps on diS-C_3(3) transport. This assay permits not only the detection of pump inhibition by a drug, but also reveals the effect of the drug on plasma membrane potential as a marker of the membrane function and integrity. In this context, it should be noted that unlike the aforementioned transport systems, the activity of these MDR pumps is independent of the membrane potential (Gaskova *et al.*, 2002).

Materials and methods

Yeast strains

The *S. cerevisiae* strains AD1-3 (*MATα, PDR1-3, ura3, his1, yor1Δ::hisG, snq2Δ::hisG, pdr5Δ::hisG*), AD12 (*MATα, PDR1-3, ura3, his1, yor1Δ::hisG, snq2Δ::hisG*) and AD13 (*MATα, PDR1-3, ura3, his1, yor1Δ::hisG, pdr5Δ::hisG*) are derived from the parent strain US 50-18C (*MATα, PDR1-3, ura3, his1*; Decottignies *et al.*, 1998).

Media and cell growth conditions

Yeast was precultured in YPD medium (1% yeast extract, 1% bactopeptone, 2% glucose) at 30 °C for 24 h. A small volume (1–10 μL) of inoculum was added to 10 mL fresh YPD medium, and the main culture was grown until it had reached the early exponential phase.

Spectrofluorometric monitoring of diS-C_3(3) accumulation in cells

Yeast cells from the early exponential growth phase were harvested, washed twice with double-distilled water, and

resuspended in citrate-phosphate (CP) buffer of pH 6.0 to $OD_{578\ (nm)} = 0.1$. The potentiometric fluorescent probe 3,3′-dipropylthiacarbocyanine iodide, diS-$C_3(3)$, was added to 3 mL of yeast cell suspension in 1 × 1 cm cuvette as 10^{-5} M stock solution in ethanol to a final concentration of 2×10^{-8} M. Fluorescence emission spectra of the diS-$C_3(3)$ stained cell suspensions were measured using a FluoroMax-4 spectrofluorometer (Horiba JobinYvon) in intervals of 2–5 min (full emission scan duration 20 s). Excitation wavelength was 531 nm, fluorescence emission range 560–590 nm, and scattered light was eliminated by orange glass filter with a cutoff wavelength of 540 nm.

A membrane potential driven redistribution of diS-$C_3(3)$ from the medium to the cell cytosol is revealed by a so-called staining curve (Denksteinova *et al.*, 1997; Gaskova *et al.*, 1998), that is, the time course of a change in the wavelength of fluorescence emission maximum, λ_{max}, observed during the time elapsed after adding diS-$C_3(3)$ to the cell suspension (λ_{max} shifts from 568 nm observed in pure aqueous solutions to about 581 nm upon diS-$C_3(3)$ binding to cytosolic proteins).

Test alcohols were usually added to the cells suspensions after 10 min of staining with diS-$C_3(3)$, to a desired concentration. When appropriate, another stressor (inhibitor or substrate) was also added to the cell suspension, usually after 30-min exposure to the alcohol. The samples were kept at room temperature and occasionally gently stirred.

Drug susceptibility assay

To find out whether the alcohols under study are substrates of Pdr5p and Snq2p pumps, two types of disk-diffusion test were performed: a standard test (Kolaczkowski *et al.*, 1998), and its simplified version designed to detect Pdr5p substrates only. To perform the standard test, yeast cells (AD1-3, AD12 and AD13) grown to the exponential phase in liquid YPD medium were washed twice with double-distilled water and resuspended in CP buffer (pH 6.0). Then, they were diluted into top agar (seeded with 2.5×10^6 cells per mL) and poured onto YPG plates (2% agar, 1% yeast extract, 1% peptone, 2% glycerol); 1% YPGE top agar (1% agar, 1% yeast extract, 1% peptone, 2% glycerol, 2% ethanol) was used in this study. Alcohols (2 μL) were spotted onto Whatman paper disks lying on the top of the agar.

AD12 cells only were used in the simplified test. Moreover, each of the test alcohols was spotted on two different Whatman disks in this case. Before spotting the test alcohol, FK506 was dropped onto one of these disks (2 μL of 50 mM solution in ethanol) 15 min before the test alcohol. FK506 inhibits Pdr5p and thus simulates the behavior of the pump-deficient strain AD1-3. Known Pdr5p substrates, BAC and fluconazole, were used as positive controls. After 2 days at 30 °C, the plates were photographed and the size of the growth inhibition zones was measured.

To determine whether a particular alcohol is able to inhibit the extrusion of a known substrate (BAC, ketoconazole or nigericin for Pdr5p, 4-NQO for Snq2p) by the pumps, we used a 'double addition' mode of the standard disk-diffusion test (Hendrych *et al.*, 2009). The tested alcohols were added 15 min before the known substrate.

Plating tests

To determine cell viability, washed exponential cells were incubated with alcohol, BAC, and their combination at room temperature with occasional gentle stirring. After 30 min, 10 μL cells were diluted 1000-fold to stop the action of the compound(s) under study, and 3–5 replicate aliquots were plated on 1% YPD agar (1% agar, 1% yeast extract, 1% peptone, 2% glucose) and incubated for 2 days at 30 °C. For control samples, the number of colonies per plate was about 200.

Measurement of extracellular pH

Exponential cells were harvested, washed three times, and resuspended in double-distilled water to an $OD_{578\ (nm)}$ of 2.0. Extracellular pH was recorded every minute with an Inolab 7310 pH meter using a Sentix 81 pH electrode. Cell suspensions were stirred during the pH measurements. Glucose and alcohols were manually injected to final concentrations specified in the figure legends.

Measurement of release of cellular material

The release of cellular material from cells treated with alcohols (which absorbs light at 260 nm) was performed as follows. Exponential cells were harvested, washed twice, and resuspended in double-distilled water to $OD_{578\ (nm)}$ of 0.1. The cell suspension was divided into several equal parts. One was an alcohol-free control, which underwent the same procedure as cells exposed to alcohols. Cells were treated with various concentrations of alcohols (ranging from 0.1% to 3%) for different periods of time: 10, 30, and 60 min. After this treatment, aliquots (3 mL) were centrifuged, and absorption spectra of supernatants (2 mL) were measured using Varian Cary 50 UV spectrophotometer in the range of 190–400 nm. The absorbance at 260 nm was determined and compared with an alcohol-free control.

Preparation of permeabilized cells

Two methods of preparation of permeabilized cells were used: (1) Permeabilization by heat shock. Twice-washed

exponential cells were resuspended in CP buffer (pH 6.0) to $OD_{582\ (nm)}$ of 0.1. The heat shock was carried out by immersing the cell suspension in a water bath at 60 °C for 10 min (Gaskova *et al.*, 1999). After the heat-shock treatment, the cells were kept on ice for 5 min. (2) Permeabilization by an antimicrobial agent ODDC that binds to negatively charged microbial surfaces (Hübner *et al.*, 2010). Twice-washed exponential cells were resuspended in CP buffer (pH 6.0) to $OD_{582\ (nm)}$ of 0.1 and ODDC was added to a final 3 μM concentration. After 15-min exposure to ODDC [this exposure time and ODDC concentration are sufficient to achieve full permeabilization (Kodedova *et al.*, 2011)], the cells were washed twice in double-distilled water to remove the drug and resuspended in CP buffer to an $OD_{582\ (nm)}$ of 0.1.

Chemicals

The following materials were purchased: diS-C_3(3) (3,3′-dipropylthiacarboxycyanine), DMSO, and dimethyl formamide (DMF; Fluka, Prague, Czech Republic), yeast extract (Serva, Heidelberg, Germany), bactopeptone (Oxoid, Brno, Czech Republic), glucose (Penta, Prague, Czech Republic), ethanol for UV spectroscopy, glycerol, citric acid, and $Na_2HPO_4.12H_2O$ (reagent grade; Lach-Ner, Neratovice, Czech Republic), agar (Dr. Kulich, Pharma, Hradec Kralove, Czech Republic), and octenidine dihydrochloride (ODDC; Schülke & Mayr GmbH, Norderstedt, Germany). MDR pump substrates or inhibitors, alcohols, lysosomotropic compound, and protonophore used in this study were obtained from the following sources: benzalkonium chloride (BAC; Fluka), FK506, fluconazole, ketoconazole, nigericin from *Streptomyces hygroscopicus*, 1-propanol, 1-butanol, 1-pentanol, 1-hexanol and CCCP (carbonyl cyanide 3-chlorophenylhydrazone; Sigma, Prague, Czech Republic), 4-NQO (4-nitroquinoline 1- oxide; Supelco). The lysosomotropic compound DM-11 (2-dodecanoyloxyethyldimethylammonium chloride) was synthesized in the laboratory of Prof. S. Witek (Univ. Wroclaw; Witek *et al.*, 1997) and kindly provided by Dr. A. Krasowska.

Results and discussion

Fluorescence calibration of the fraction of permeabilized cells in suspension by a diagnostic CD cocktail

Recently, we have shown that the diS-C_3(3) diagnostic assay is suitable for identifying inhibitors of Pdr5 and Snq2 pumps. This method is based on comparing the accumulation of the benchmark pump substrate diS-C_3(3) in Pdr5p- and/or Snq2p-expressing cells (strains AD12, AD13, and US50-18C) vs. a negative control represented by Pdr5p- and Snq2p-deficient cells (strains AD1-3 and AD23) in the absence of an inhibitor and after its addition (Hendrych *et al.*, 2009). Blocking the active probe efflux from cells by adding pump(s) inhibitor leads to increased intracellular probe concentration, which is followed by a shift of λ_{max} toward longer wavelengths (hereafter called 'red shift'). In other words, when the pump(s) are inhibited, the difference in diS-C_3(3) staining level of pump(s)-deficient and pump(s)-expressing cells disappears, because then the staining levels are given mainly by actual membrane potentials ($\Delta\Psi$).

However, one should be aware that a considerable red shift can also occur due to permeabilization of the cells (Gaskova *et al.*, 2001; Kodedova *et al.*, 2011). It should be therefore verified first that substances tested for their potency to inhibit MDR pumps do not affect cell membrane integrity. As shown previously, the best indicator of membrane permeation is the use of diagnostic CD cocktail (Hendrych *et al.*, 2009; Kodedova *et al.*, 2011). This cocktail is composed of CCCP as protonophore plus the lysosomotropic compound DM-11 acting as an H^+-ATPase inhibitor (Witek *et al.*, 1997). Its addition to stained intact cells leads to the drop of λ_{max} to a level close to the fluorescence of free dye in aqueous medium, thus indicating a marked membrane depolarization. In contrast to intact cells, there is no response of probe fluorescence if the CD cocktail is added to the suspension of permeabilized cells stained with diS-C_3(3) (Hendrych *et al.*, 2009; Kodedova *et al.*, 2011).

To correlate spectral shifts observed after application of CD cocktail with the percent fraction of permeabilized cells, a calibration experiment must be done. We performed this calibration by mixing intact and permeabilized cells of both pump-deficient AD1-3 and pump-expressing AD12 strains in different proportions and measuring $\lambda_{max/CD}$ after CD cocktail addition, Fig. 1a and b. The quality of cell permeabilization, which is crucial for reliable calibration protocol, was checked by measuring the dependence of cell survival on the fraction of permeabilized cells in the suspension, Fig. 1c. We did not observe any significant difference between the results obtained with cells permeabilized by two different methods described in Section 'Chemicals'. Therefore, we present below only data measured with heat-permeabilized cells.

Staining curves of both strains depend significantly on the percentage of permeabilized cells in the sample. The staining curves of intact AD1-3 cells (0% permeabilized cells) lacking the major MDR pumps Pdr5p and Snq2p reflect the probe accumulation in cells that is controlled solely by membrane potential, Fig. 1a. For these curves, a gradual increase in λ_{max} is characteristic; it takes *c.* 30 min to reach equilibrium level of probe accumulation in cells

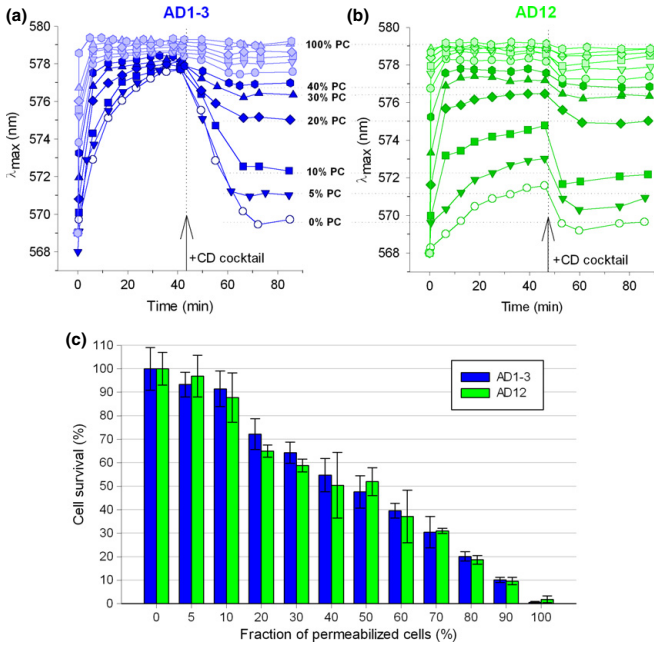

Fig. 1. Fluorescence calibration of the fraction of permeabilized cells in suspension by a diagnostic CD cocktail. Staining curves of suspensions containing different proportions of intact and permeabilized exponential AD1-3 (a) or AD12 (b) cells. All experiments were done by mixing suspensions of intact and heat-permeabilized exponential cells (stock cell suspensions in CP buffer: $OD_{578\ (nm)} = 0.1$). The fraction of permeabilized cells (PC) in suspension: 0% – open circles, 5% – dark (blue for AD1-3 cells, green for AD12 cells) inverted triangles, 10% – dark squares, 20% – dark diamonds, 30% – dark triangles, 40% – dark hexagons, 50% – light (blue for AD1-3 cells, green for AD12 cells) circles, 60% – light inverted triangles, 70% – light squares, 80% – light diamonds, 90% – light triangles, and 100% – light hexagons. The arrows and dotted lines indicate the addition of 10 μM CCCP plus 10 μM DM-11 (CD cocktail). The data in a and b are representative of three independent experiments. (c) Dependence of survival of AD1-3 (blue bars) and AD12 (green bars) cells on the fraction of permeabilized cells in suspension. Error bars indicate SDs derived from two independent experiments consisting of three replicas each.

(Gaskova *et al.*, 1998). Increasing amounts of permeabilized cells markedly affects cell staining. The corresponding staining curves reveal clearly higher initial rates of staining compared to the untreated cells, which is caused by the increasing fraction of fast and highly stained permeabilized cells in cell suspensions (compare λ_{max} values measured at time zero). The addition of CD cocktail to intact cells leads to the drop of λ_{max} to a level near that of free dye in aqueous medium. An increase in the fraction of permeabilized cells leads to a smaller drop in λ_{max} because the permeabilized cells do not respond to CD cocktail.

Contribution of permeabilized cells to an apparent λ_{max} value is much more striking in AD12 cells that stain much less than AD1-3 cells due to active efflux of diS-C_3(3) by the pumps, Fig. 1b. Horizontal dotted lines connecting the final $\lambda_{max/CD}$ values in Fig. 1a and b clearly show that these values are not dependent on the strain; they are determined only by the fraction of permeabilized cells in the sample. This was confirmed also with AD13 cells having only Snq2p (data not shown). The variations in $\lambda_{max/CD}$ values were used in the following experiments as the measure of cell permeabilization caused by alcohols. However, it is fair to note that the determination of the fraction of permeabilized cells higher than 40% is inaccurate. For this reason, the staining curves in Fig. 1a and b are shown in light colours.

The effect of alcohols on activity of Pdr5p and Snq2p

Staining curves revealing the time course of diS-C_3(3) accumulation in exponentially growing cells were measured with both pump-expressing strains (AD12 or AD13) and pump-deficient mutants (AD1-3). Various

alcohols (from ethanol to hexanol) were added to the suspensions of these cells at about 10 min of staining, Fig. 2. Relatively low alcohol concentrations (up to 3%) were used. Rather than finding an optimum inhibitory concentration of each alcohol (Leao & van Uden, 1982, 1983, 1984a; Casal *et al.*, 1998), we aimed at comparing

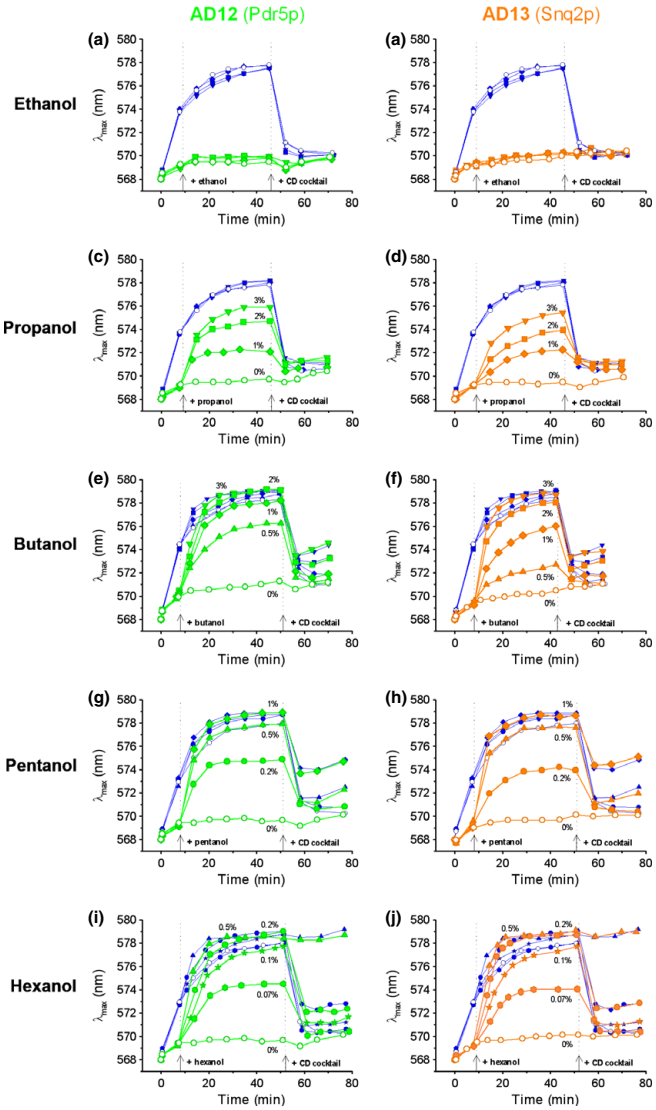

Fig. 2. Alcohols (from ethanol to hexanol) variously affect the *Saccharomyces cerevisiae* multidrug-resistance pumps Pdr5p and Snq2p. Blue symbols – exponential AD1-3 cells (pump-free negative control); green and orange symbols – exponential AD12 (a, c, e, g, i) and AD13 (b, d, f, h, j) cells, respectively. The amounts of alcohol added to cell suspensions: empty circles – 0%, full inverted triangles – 3%, full squares – 2%; full diamonds – 1%; full triangles – 0.5%; full circles – 0.2%; full stars – 0.1%, full hexagons – 0.07%. For greater clarity, if appropriate, the concentrations of alcohols are also listed in the panel. Left-hand arrows with dotted lines indicate alcohol addition. Right-hand arrows with dotted lines indicate the addition of diagnostic CD cocktail (10 μM CCCP plus 10 μM DM-11). Data are representative of three independent experiments.

their effects at low concentrations, with ethanol serving as a reference compound.

As assumed, ethanol exerts a negligible effect on the staining curves in any type of cells at any of the concentrations used (from 1% to 3%), Fig. 2a and b, but the addition of other alcohols beginning with propanol to AD12 and AD13 cells caused an increase in λ_{max} toward the values found with the cells of negative control (AD1-3), Fig. 2c–j. This indicates that the latter alcohols affect seriously both Pdr5p and Snq2p, causing an inhibitory effect.

It can be concluded from the first chapter of 'Results and discussion' that an alcohol-induced cell permeabilization may also contribute to an apparent red shift of λ_{max}. To exclude the possibility that the observed effect of alcohols is merely due to such permeabilization, the actual degree of cell permeabilization was assessed using CD cocktail and measuring the ratio of respective $\lambda_{max/CD}$ values in cells without and with alcohol. As shown in Fig. 2, for each alcohol, the fraction of permeabilized cells is practically negligible for a certain range of low concentrations, while the pump inhibition is still considerable. However, the CD cocktail test revealed that with increasing alcohol concentration, the number of permeabilized cells is no longer negligible. This means that at high concentrations, harmful effects of alcohol on yeast cells can combine MDR pump inhibition with cell permeabilization. It is also clear from Fig. 2 that the pump inhibition is markedly concentration- and alcohol-dependent. In particular, the concentration of alcohol that is sufficient to cause a significant red shift of λ_{max} decreases with increasing acyl chain length, from about 1% for propanol to 0.07% for hexanol. This implies that the potency of various alcohols to reduce the performance of Pdr5p and Snq2p pumps is directly correlated with the chain length.

However, this effect can in general have multiple causes that need to be critically assessed in order to draw conclusions on the mechanism by which alcohol affects the operation of these MDR pumps. Possible causes are the following: (1) depletion of ATP for active probe export from the cells by Pdr5p and Snq2p, (2) alcohols can be pump substrates efficiently competing with the probe for transport, (3) alcohol acts on membrane lipids, resulting in modulation of MDR pump activity ('lipid theory'), and (4) alcohol directly interacts with pump proteins, leading to inhibition of their function ('protein theory'). Very likely, under certain circumstances, several factors can be simultaneously involved in the inhibitory effect of alcohols.

It should be noted that, in contrast to, for example, the Pdr5p inhibitor FK506, the subsequent removal of the alcohols by washing (Kodedova *et al.*, 2011) after the 30-min exposure used in our experiments results in a decrease in the inhibitory action of the alcohols depending on the number of the washing-out steps (data not shown). This means that the observed inhibition of diS-C_3(3) transport is reversible, that is, it decreases after removal of the inhibitory agent. This drop in inhibition can in this case be due to the removal of an alcohol (1) as a pump substrate from the surrounding medium, or (2) from the membrane (both lipid matrix and proteins) as determined by its partition coefficient.

The effect of alcohols on the permeability of *S. cerevisiae* membranes for ions and small metabolites

To evaluate how much alcohols influence the permeability of *S. cerevisiae* membranes for ions and small metabolites, we assessed the concentration-dependent effect of the alcohols on glucose-induced medium acidification (which should be partially reduced by passive transmembrane proton fluxes due the alcohol-induced cell permeability), Fig. 3a, and on release of metabolites absorbing at 260 nm (indicator of membrane integrity), Fig. 3b. Both methods are commonly used to assess the lethal effect of chemical stressors on cell membranes, see for example (Bennis *et al.*, 2004; Maresova *et al.*, 2009).

As shown in Fig. 3a, the addition of alcohols to exponential AD1-3 cells with glucose-activated H^+-ATPase, that is, under conditions of a maximum attainable pH gradient, leads to a concentration-dependent alkalinization of pH_{out}, as a consequence of increased proton permeability of the plasma membrane [a generally accepted fact (Leao & van Uden, 1984b)]. With increasing acyl chain length, the extent of medium alkalinization increases. The increase in alkalinization after addition of alcohols is in a very good correlation with the fluorescence determination of the percentage of permeabilized cells. In particular, the same value of $\lambda_{max/CD}$ of various alcohols coincides with the same extent of alkalinization, compare Figs 2 and 3. A comparison of Figs 2 and 3 also shows an extremely important fact: ethanol causes neither medium alkalinization nor a decrease in pump activity. On the other hand, for alcohols beginning with propanol, a concentration can be found which does not lead to alkalinization, but which still exhibits an inhibitory effect on both pumps.

As demonstrated in Fig. 3b, alcohols at the concentrations used (except 0.5% and 1% hexanol) do not cause any extensive damage to plasma membrane even after 60 min of action (no change in the value of $Abs_{(260\ nm)}$).

Inhibitory effect of alcohols is not caused by depletion of ATP

Acidification of the cytosol results in an activation of the H^+-ATPase (dos Passos *et al.*, 1992; Hendrych *et al.*,

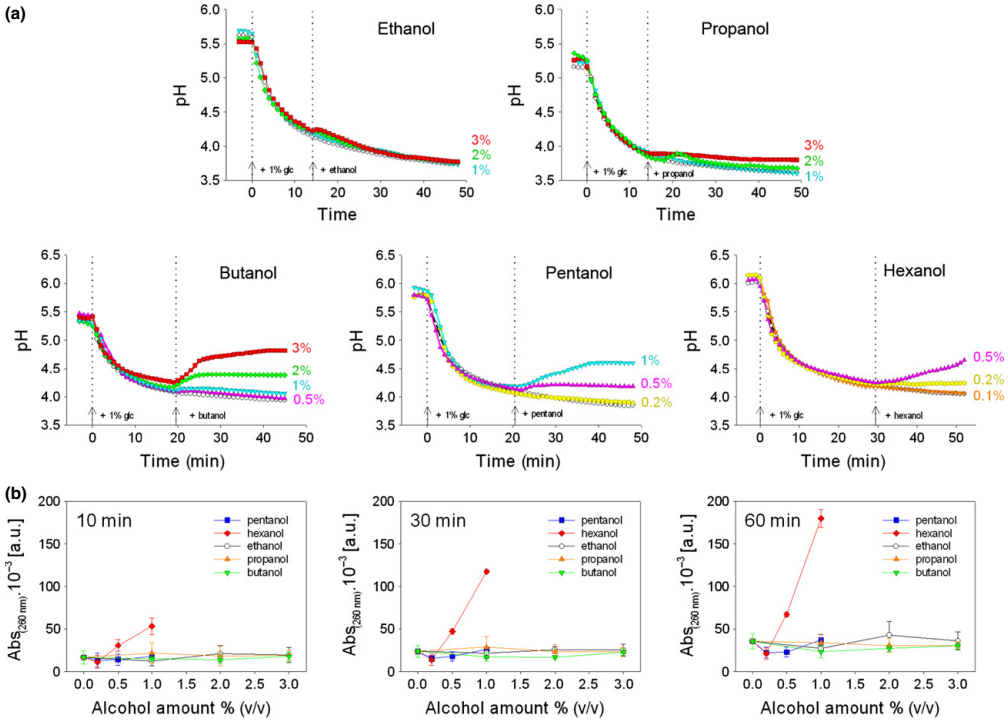

Fig. 3. Concentration-dependent effects of alcohols on glucose-induced medium acidification and cell lysis: *Saccharomyces cerevisiae* AD1-3 exponential cells. (a) The changes in extracellular pH following the addition of 1% glucose (left-hand arrows at time zero). The right-hand arrows indicate addition of alcohols: 1%, 2% and 3% ethanol and propanol, 0.5%, 1%, 2% and 3% butanol, 0.2%, 0.5% and 1% pentanol, 0.1%, 0.2% and 0.5% hexanol. Open circles – no alcohol added. Data are representative of two independent experiments. (b) The absorbance of cell suspensions measured at 260 nm in supernatants of AD1-3 cells treated for 10, 30, and 60 min with different alcohol concentrations. Circles – ethanol, triangles – propanol, inverted triangles – butanol, squares – pentanol, diamonds – hexanol. Data are means from three independent experiments ±SD.

2009). We must therefore take into account the possibility that an alcohol-induced influx of protons into the cells may also activate the H^+-ATPase. Then, the increased consumption of ATP by the enzyme can possibly cause a depletion or at least reduction of ATP concentration needed for active probe export from the cells by the pumps Pdr5p and Snq2p. Lack of energy for the probe export would result in increased cell staining after addition of alcohols relative to the control. To confirm or rule out this type of pump inhibition, we compared the fluorescence response of AD12 and AD13 cells to the addition of alcohols in the presence and absence of 10 mM glucose added 5 min before the probe. We show here the data for hexanol only, because this alcohol exhibits the highest pump inhibition effect, cf. Fig. 2. AD1-3 cells were again used as a negative control.

Figure 4 shows the effect of 0.07% hexanol, which illustrates the typical response to all tested alcohols, that is, the red shift of λ_{max} due to the pump inhibition. The presence of glucose in AD1-3 cell suspension causes a fast H^+-ATPase activation, followed by the hyperpolarization of the cells, which is accompanied by a faster and higher cell staining relative to glucose-free control, while the addition of alcohol had a negligible effect. The hyperpolarization of AD12 and AD13 cells by glucose leads to a small increase in staining as a result of the changed equilibrium between passive probe uptake according to $\Delta\Psi$ and the active probe efflux by the pumps. However, the response to hexanol has the same character both in the absence and presence of glucose. We can therefore rule out the possibility of ATP depletion as a reason of the observed inhibitory effects of alcohols. This conclusion is also supported by the recovery of the pump activity after alcohol removal.

The results of CD cocktail test proved that the degree of cell permeabilization was negligible in this set of experiments.

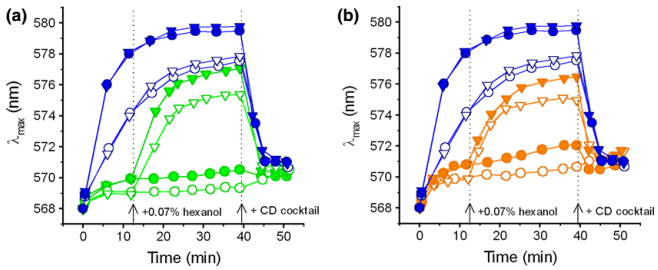

Fig. 4. Inhibitory effect of alcohols is not caused by depletion of ATP. Comparison of the effects of alcohols under study on energized and nonenergized cells is illustrated by the action of 0.07% hexanol. Exponential AD12 (a) and AD13 (b) – green and orange symbols, respectively, and AD1-3 (a and b) – blue symbols were not treated (open symbols) or treated (full symbols) with 10 mM glucose for 5 min before the addition of diS-C_3(3) at time zero. The alcohol (0.07% hexanol) was added to the cells at 12 min of staining (triangles). Circles – controls (hexanol-free). Left-hand arrows indicate hexanol addition; right-hand arrows indicate the addition of diagnostic CD cocktail (10 μM CCCP plus 10 μM DM-11). Data are representative of three independent experiments.

Inhibitory effect of alcohols is not caused by their competition with the probe for transport (i.e. alcohols are not substrates of Pdr5p and Snq2p)

To determine whether alcohols are substrates of Pdr5p and Snq2p, we performed two tests: (1) drug susceptibility assay in both the classical and our simplified version (see Materials and methods) and (2) plating test. As is evident from Fig. 5a (classical disk-diffusion test using a set of mutants isogenic to AD1-3, but deleted in only one MDR pump, i.e. AD12 and AD13) and Fig. 5b (simplified version using only AD12; pump-deficient strain is simulated by the action of FK506 on AD12 cells), alcohols do not form any inhibition zones (except for very small zones in the case of hexanol that are identical for all strains). This finding is surprising because it is known that alcohols inhibit cell growth (Ingram & Buttke, 1984). The most logical explanation seems to be that the alcohols (with the exception of hexanol) diffuse too quickly through the agar and their concentration near the disks is therefore insufficient for growth inhibition.

All the strains showed comparable survival after 30 min exposure to alcohols, Fig. 5c, indicating that the activity of pumps is not involved in the effects of alcohols on the cells. In other words, the alcohols are not substrates of the pumps.

Alcohols act as true inhibitors of Pdr5p and Snq2p

To prove that alcohols act as true inhibitors of both pumps (i.e. their effect on cell membrane results in modulation of pump activity), we used a 'double addition' mode of the classical disk-diffusion test (see Plating tests). BAC (Fig. 6a), nigericin (Fig. 6c), and ketoconazole (Fig. 6d) were used as known substrates for Pdr5p, 4-NQO (Fig. 6b) as a substrate for Snq2p. As evident from the disk-diffusion tests on Pdr5p- or Snq2p-expressing strains, AD12 or AD13, the zones of inhibition formed in the presence of substrates plus pentanol or hexanol reach up to the size that is observed in the Pdr5p- and Snq2p-deficient strain AD1-3. The absence of enlargement of the zones with propanol and butanol plus substrates is most likely due to an insufficient alcohol concentration near the disks for inhibition (given by their too fast diffusion through the agar; compare sufficient concentrations of each alcohol to inhibit the probe efflux by the pumps, see Fig. 2). To confirm this, we performed an analogous assay based on the survival of AD12 and AD1-3 cells exposed to 1.5 μM BAC and alcohols at a suitable inhibitory concentration, and their combinations with BAC for 30 min. AD12 strain shows higher survival when exposed to BAC compared to Pdr5p-deficient AD1-3 strain (Kodedova *et al.*, 2011). This difference (1) disappears after the simultaneous action of BAC and alcohols beginning with butanol (2) is partially reduced with 3% propanol and (3) remains with ethanol which does not inhibit Pdr5p (see Fig. 2; data not shown).

Reduced ability of cells to survive the effect of substrates in the presence of alcohols is not the result of cell permeabilization caused by a combined alcohol-substrate effect

Although it may seem that the role of alcohols as pump inhibitors was clearly proved by preceding experiments, there is still the possibility that their effects in combination with other 'stressors-substrates' can lead to significant damage to the cell membrane and its permeabilization.

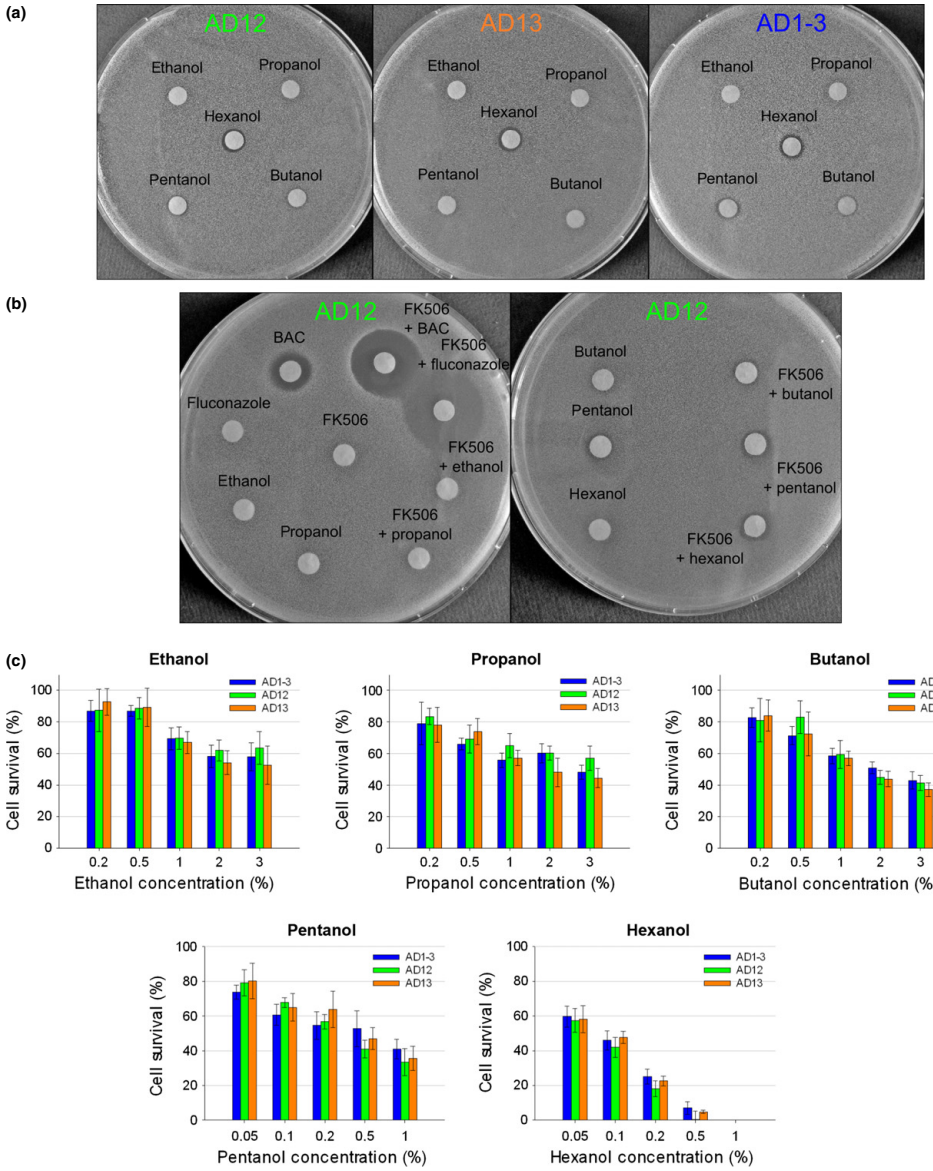

Fig. 5. No evidence that alcohols are substrates for Pdr5p or Snq2p. (a) Growth inhibition zones measured in a classical disk-diffusion test using YPGE top agar in variously pump-expressing strains (AD12, AD13) and the negative control AD1–3 exposed to alcohols (2 μL of alcohols were spotted onto Whatman paper disks). (b) Growth inhibition zones measured in a simplified disk-diffusion test using YPGE top agar in Pdr5p-expressing strain AD12 exposed to Pdr5p substrates BAC (15 mM) and fluconazole (FLU, 15 mM), alcohols, and combinations of all tested compounds with FK506 (50 mM; an inhibitor of Pdr5p) as described in Section 'Materials and methods/Plating tests'. The data in panels a and b are representative of three independent experiments. (c) Cell viability after a 30-min exposure to alcohols (AD1-3, blue bars; Pdr5p-containing AD12, green bars; Snq2p-containing AD13, orange bars). Error bars indicate SDs derived from three independent experiments consisting of three replicas each.

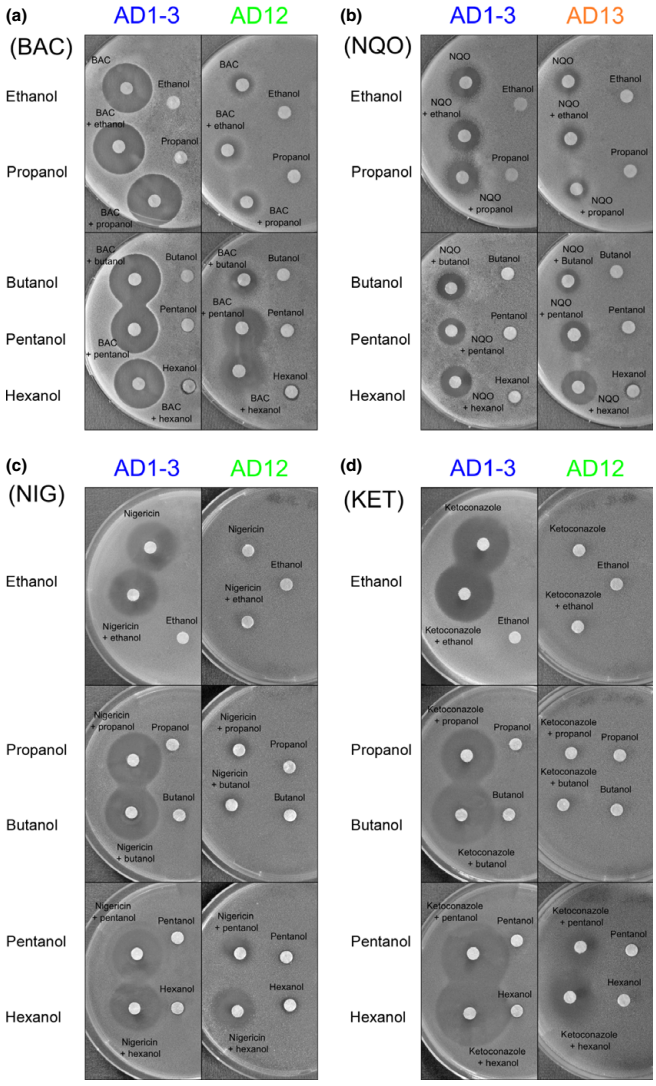

Fig. 6. Alcohols (from ethanol to hexanol) variously inhibit substrate transport mediated by Pdr5p and Snq2p. Comparison of growth inhibition zones of AD12 or AD13 with AD1-3 cells exposed to a substrate of Pdr5p or Snq2p, respectively, to alcohols, and their combinations with the substrate: (a) BAC (15 mM; a substrate of Pdr5p), (b) 4-NQO (NQO, 1.6 mM; a substrate of Snq2p), (c) nigericin (NIG, 20 mM; a substrate of Pdr5p and Yor1p) and (d) ketoconazole (KET, 1.5 mM; a substrate of Pdr5p). The data are representative of three independent experiments. Note that in all cases, addition of an agent that is not a substrate of the given pump, along with alcohol, gives an inhibition zone that is equal to the zone found in the pump-deficient strain AD1-3 (data not shown).

Indeed, the toxic effect of many pump substrates on the cell has a multitarget character including disturbance of the cell membrane, as is the case of BAC (Kodedova *et al.*, 2011).

To prove that the observed pump inhibition by alcohols is not the result of such action, we tested the combined effect of Pdr5p substrates, BAC or ketoconazole, with

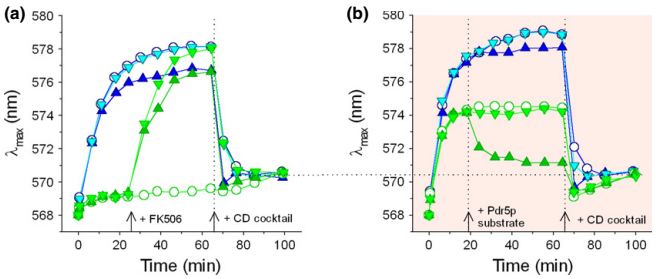

Fig. 7. Combined effect of a Pdr5p substrate and alcohol (hexanol) does not lead to permeabilization of the cells. (a) Exponential AD12 (green symbols) and AD1-3 (blue and cyan symbols) cells were untreated (open circles) or treated with 1.5 μM BAC (triangles) or 15 μM ketoconazole (inverted triangles) for 5 min before the addition of diS-C_3(3) at time zero. 10 μM FK506 was added to AD12 cells after 30-min exposure to the substrate (left-hand arrow) to detect the residual Pdr5p activity. The right-hand arrow indicates the addition of diagnostic CD cocktail. (b) Exponential AD12 (green symbols) and AD1-3 (blue and cyan symbols) cells were treated with 0.05% hexanol for 5 min before the addition of diS-C_3(3) at time zero. Pdr5p substrates were added to the cells at 20 min of staining (left-hand arrow): circles – no substrate; triangles – 1.5 μM BAC; inverted triangles – 15 μM ketoconazole. Right-hand arrow indicates the addition of diagnostic CD cocktail. The horizontal dotted line demonstrates that the addition of diagnostic CD cocktail leads to the same low level of staining (indicating the absence of permeabilized cells in suspension), irrespective of whether the cells were exposed to nothing, single or two stressors. The data are representative of three independent experiments.

hexanol using a diS-C_3(3) diagnostic assay that is very suitable for the determination of the percentage of permeabilized cells in a suspension, Fig. 7. As shown in Fig. 7a, there is no increase in the fraction of permeabilized cells in the suspension during the action of BAC or ketoconazole. BAC only weakly depolarizes the membrane, whereas ketoconazole has no effect on $\Delta\Psi$ (compare the difference in staining of AD1-3 cells pretreated with a substrate). The addition of these substrates to hexanol-treated cells also does not lead to their increased permeabilization, Fig. 7b. We can therefore conclude that alcohols indeed inhibit the ability of Pdr5p and Snq2p to transport the substrate by affecting the pump protein and/or its lipid environment. Moreover, the observed inhibition is reversible, decreasing after removal of the inhibitory agent from the membrane (both lipid matrix and proteins).

Conclusions

In this paper, we present alcohols, especially pentanol and hexanol, as effective inhibitors of two major *S. cerevisiae* MDR pumps – Pdr5p and Snq2p. It seems astonishing that very low concentrations of these relatively simple molecules can be such powerful tools in the fight against MDR resistance. Furthermore, alcohols target, in part, the plasma membrane (it does not matter whether lipid matrix or protein pocket), that is, they do not need to enter the cells to achieve the inhibitory effect and thus avoid the resistance mechanism presented by the pump. They could be useful therapeutically in conjunction with current antifungals – Pdr5p and/or Snq2p substrates – to combat yeast infections.

Acknowledgements

We acknowledge Andre Goffeau (Universite Catholique de Louvain, Louvain-la-Neuve, Belgium) for the isogenic mutant strains. This work was supported by the grant from the Czech Science Foundation (grant no. 205/10/1121).

References

Adey G, Wardleysmith B & White D (1975) Mechanism of inhibition of bacterial luciferase by anaesthetics. *Life Sci* **17**: 1849–1854.

Alkire MT & Gorski LA (2004) Relative amnesic potency of five inhalational anesthetics follows the Meyer–Overton rule. *Anesthesiology* **101**: 417–429.

Balzi E & Goffeau A (1994) Genetics and biochemistry of yeast multidrug resistance. *Biochim Biophys Acta* **1187**: 152–162.

Bennis S, Chami F, Chami N, Bouchikhi T & Remmal A (2004) Surface alteration of *Saccharomyces cerevisiae* induced by thymol and eugenol. *Lett Appl Microbiol* **38**: 454–458.

Borst-Pauwels GWFH (1981) Ion transport in yeast. *Biochim Biophys Acta* **650**: 88–127.

Cadek R, Chladkova K, Sigler K & Gaskova D (2004) Impact of the growth phase on the activity of multidrug-resistance pumps and membrane potential of *S. cerevisiae*: effect of pump overproduction and carbon source. *Biochim Biophys Acta* **1665**: 111–117.

Cartwright CP, Juroszek JR, Beavan MJ, Ruby FMS, Demorais SMF & Rose AH (1986) Ethanol dissipates the protonmotive force across the plasma membrane of *Saccharomyces cerevisiae*. *J Gen Microbiol* **132**: 369–377.

Carvajal E, van den Hazel HB, Cybularz-Kolaczkowska A, Balzi E & Goffeau A (1997) Molecular and phenotypic

characterization of yeast PDR1 mutants that show hyperactive transcription of various ABC multidrug transporter genes. *Mol Gen Genet* **256**: 406–415.

Casal M, Cardoso H & Leao C (1998) Effects of ethanol and other alkanols on transport of acetic acid in *Saccharomyces cerevisiae*. *Appl Environ Microbiol* **64**: 665–668.

Chanson M, Bruzzone R, Bosco D & Meda P (1989) Effects of n-alcohols on junctional coupling and amylase secretion of pancreatic acinar cells. *J Cell Physiol* **139**: 147–156.

Decottignies A & Goffeau A (1997) Complete inventory of the yeast ABC proteins. *Nat Genet* **15**: 137–145.

Decottignies A, Grant AM, Nichols JW, de Wet H, McIntosh DB & Goffeau A (1998) ATPase and multidrug transport activities of the overexpressed yeast ABC protein Yor1p. *J Biol Chem* **273**: 12612–12622.

Denksteinova B, Gaskova D, Herman P, Vecer J, Malinsky J, Plasek J & Sigler K (1997) Monitoring of membrane potential changes in *Saccharomyces cerevisiae* by diS-C_3(3) fluorescence. *Folia Microbiol* **42**: 221–224.

dos Passos JB, Vanhalewyn M, Brandao RL, Castro IM, Nicoli JR & Thevelein JM (1992) Glucose-induced activation of plasma membrane H^+-ATPase in mutants of the yeast *Saccharomyces cerevisiae* affected in cAMP metabolism, cAMP-dependent protein phosphorylation and the initiation of glycolysis. *Biochim Biophys Acta* **1136**: 57–67.

Ernst R, Klemm R, Schmitt L & Kuchler K (2005) Yeast ATP-binding cassette transporters: cellular cleaning pumps. *Methods Enzymol* **400**: 460–484.

Franks NP & Lieb WR (1978) Where do general anaesthetics act? *Nature* **274**: 339–342.

Franks NP & Lieb WR (1984) Do general anaesthetics act by competitive binding to specific receptors? *Nature* **310**: 599–601.

Franks NP & Lieb WR (1985) Mapping of general anaesthetic target sites provides a molecular basis for cutoff effects. *Nature* **316**: 349–351.

Gaskova D, Brodska B, Herman P, Vecer J, Malinsky J, Sigler K, Benada O & Plasek J (1998) Fluorescent probing of membrane potential in walled cells: diS-C_3(3) assay in *Saccharomyces cerevisiae*. *Yeast* **14**: 1189–1197.

Gaskova D, Brodska B, Holoubek A & Sigler K (1999) Factors and processes involved in membrane potential build-up in yeast: diS-C_3(3) assay. *Int J Biochem Cell Biol* **31**: 575–584.

Gaskova D, Cadek R, Chaloupka R, Plasek J & Sigler K (2001) Factors underlying membrane potential-dependent and -independent fluorescence responses of potentiometric dyes in stressed cells: diS-C_3(3) in yeast. *BBA-Biomembranes* **1511**: 74–79.

Gaskova D, Cadek R, Chaloupka R, Vacata V, Gebel J & Sigler K (2002) Monitoring the kinetics and performance of yeast membrane ABC transporters by diS-C_3(3) fluorescence. *Int J Biochem Cell Biol* **34**: 931–937.

Godden EL, Harris RA & Dunwiddie TV (2001) Correlation between molecular volume and effects of n-alcohols on human neuronal nicotinic acetylcholine receptors expressed in *Xenopus oocytes*. *J Pharmacol Exp Ther* **296**: 716–722.

Goldstein DB (1984) The effects of drugs on membrane fluidity. *Annu Rev Pharmacol* **24**: 43–64.

Hamada H, Ishiguro H, Yamamoto A *et al.* (2005) Dual effects of n-alcohols on fluid secretion from guinea pig pancreatic ducts. *Am J Physiol-Cell Physiol* **288**: C1431–C1439.

Hendrych T, Kodedová M, Sigler K & Gášková D (2009) Characterization of the kinetics and mechanisms of inhibition of drugs interacting with the *S. cerevisiae* multidrug resistance pumps Pdr5p and Snq2p. *BBA-Biomembranes* **1788**: 717–723.

Horishita T & Harris RA (2008) n-alcohols inhibit voltage-gated Na+ channels expressed in *Xenopus oocytes*. *J Pharmacol Exp Ther* **326**: 270–277.

Hübner NO, Siebert J & Kramer A (2010) Octenidine dihydrochloride, a modern antiseptic for skin, mucous membranes and wounds. *Skin Pharmacol Physiol* **23**: 244–258.

Ingram LO & Buttke TM (1984) Effects of alcohols on microorganisms. *Adv Microb Physiol* **25**: 253–300.

Kodedova M, Sigler K, Lemire BD & Gaskova D (2011) Fluorescence method for determining the mechanism and speed of action of surface-active drugs on yeast cells. *Biotechniques* **50**: 58–63.

Kolaczkowska A & Goffeau A (1999) Regulation of pleiotropic drug resistance in yeast. *Drug Resist Updat* **6**: 403–414.

Kolaczkowski M, van den Rest M, Cybular-Kolaczkowska A, Soumillion JP, Konings WN & Goffeau A (1996) Anticancer drugs, ionophoric peptides and steroids as substrates of the yeast multidrug transporter Pdr5p. *J Biol Chem* **271**: 31543–31548.

Kolaczkowski M, Kolaczkowska A, Luczynski J, Witek S & Goffeau A (1998) *In vivo* characterization of the drug resistance profile of the major ABC transporters and other components of the yeast pleiotropic drug resistance network. *Microb Drug Resist* **4**: 143–158.

Korpi ER, Makela R & Uusi-Oukari M (1998) Ethanol: novel actions on nerve cell physiology explain impaired functions. *News Physiol Sci* **13**: 164–170.

Leao C & van Uden N (1982) Effects of ethanol and other alkanols on the glucose transport system of *Saccharomyces cerevisiae*. *Biotechnol Bioeng* **24**: 2601–2604.

Leao C & van Uden N (1983) Effects of ethanol and other alkanols on the ammonium transport system of *Saccharomyces cerevisiae*. *Biotechnol Bioeng* **25**: 2085–2090.

Leao C & van Uden N (1984a) Effects of ethanol and other alkanols on the general amino acid permease of *Saccharomyces cerevisiae*. *Biotechnol Bioeng* **26**: 403–405.

Leao C & van Uden N (1984b) Effects of ethanol and other alkanols on passive proton influx in the yeast *Saccharomyces cerevisiae*. *Biochim Biophys Acta* **774**: 43–48.

Li CY, Peoples RW & Weight FF (1994) Alcohol action on a neuronal membrane receptor: evidence for a direct interaction with the receptor protein. *P Natl Acad Sci USA* **91**: 8200–8204.

Li CY, Peoples RW & Weight FF (1998) Ethanol-induced inhibition of a neuronal P2X purinoceptor by an allosteric mechanism. *Br J Pharmacol* **123**: 1–3.

Lovinger DM (1997) Alcohols and neurotransmitter gated ion channels: past, present and future. *Naunyn Schmiedebergs Arch Pharmacol* **356**: 267–282.

Lundbaek JA (2008) Lipid bilayer-mediated regulation of ion channel function by amphiphilic drugs. *J Gen Physiol* **131**: 421–429.

Maresova L, Muend S, Zhang YQ, Sychrova H & Rao R (2009) Membrane hyperpolarization drives cation influx and fungicidal activity of amiodarone. *J Biol Chem* **284**: 2795–2802.

Moykkynen T & Korpi ER (2012) Acute effects of ethanol on glutamate receptors. *Basic Clin Pharmacol* **111**: 4–13.

Nawrocki A, Fey SJ, Goffeau A, Roepstorff P & Larsen PM (2001) The effects of transcription regulating genes PDR1, pdr1-3 and PDR3 in pleiotropic drug resistance. *Proteomics* **1**: 1022–1032. Erratum in: Proteomics 1:1340–1341.

Peoples RW, Li CY & Weight FF (1996) Lipid vs protein theories of alcohol action in the nervous system. *Annu Rev Pharmacol* **36**: 185–201.

Petrov VV & Okorokov LA (1990) Increase in the anion and proton permeability of *Saccharomyces carlsbergensis* plasmalemma by normal alcohols as a possible cause of its deenergization. *Yeast* **6**: 311–318.

Pringle MJ, Brown KB & Miller KW (1981) Can the lipid theories of anesthesia account for the cutoff in anesthetic potency in homologous series of alcohols? *Mol Pharmacol* **19**: 49–55.

Rogers B, Decottignies A, Kolaczkowski M, Carvajal E, Balzi E & Goffeau A (2001) The pleiotropic drug ABC transporters from *Saccharomyces cerevisiae*. *J Mol Microbiol Biotechnol* **3**: 207–214.

Seeman P (1972) The membrane actions of anesthetics and tranquilizers. *Pharmacol Rev* **24**: 583–655.

Serrano R (1977) Energy requirements for maltose transport in yeast. *Eur J Biochem* **80**: 97–102.

Witek S, Goffeau A, Nader J, Luczynski J, Lachowicz TM, Kuta B & Oblak E (1997) Lysosomotropic aminoesters act as H+-ATPase inhibitors in yeast. *Folia Microbiol* **42**: 252–254.

Attachment II

Accepted Manuscript

Yeast Tok1p channel is a major contributor to membrane potential maintenance under chemical stress

Jakub Zahumenský, Iva Jančíková, Andrea Drietomská, Andrea Švenkrtová, Otakar Hlaváček, Tomáš Hendrych, Jaromír Plášek, Karel Sigler, Dana Gášková

PII: S0005-2736(17)30224-9
DOI: doi:10.1016/j.bbamem.2017.06.019
Reference: BBAMEM 82532

To appear in: *BBA - Biomembranes*

Received date: 23 February 2017
Revised date: 2 June 2017
Accepted date: 27 June 2017

Please cite this article as: Jakub Zahumenský, Iva Jančíková, Andrea Drietomská, Andrea Švenkrtová, Otakar Hlaváček, Tomáš Hendrych, Jaromír Plášek, Karel Sigler, Dana Gášková, Yeast Tok1p channel is a major contributor to membrane potential maintenance under chemical stress, ***BBA - Biomembranes*** (2017), doi:10.1016/j.bbamem.2017.06.019

Yeast Tok1p channel is a major contributor to membrane potential maintenance under chemical stress

Jakub Zahumenský[1], Iva Jančíková[1], Andrea Drietomská[1], Andrea Švenkrtová[2,3], Otakar Hlaváček[2], Tomáš Hendrych[4], Jaromír Plášek[1], Karel Sigler[2] and Dana Gášková[1,*]

[1] Charles University, Faculty of Mathematics and Physics, Institute of Physics, Prague, 121 16, Czech Republic

[2] Institute of Microbiology, CR Academy of Sciences, Prague, 142 20, Czech Republic

[3] Institute of Chemical Technology, Faculty of Food and Biochemical Technology, Prague, 166 28, Czech Republic

[4] Department of Genetics and Microbiology, Faculty of Science, Charles University, Prague, 128 44, Czech Republic

*** Correspondence**

Dana Gášková, Charles University, Faculty of Mathematics and Physics, Institute of Physics, Ke Karlovu 5, 121 16, Prague 2, Czech Republic

Tel.: +420 221911348; Fax.: +420 224922797; e-mail: gaskova@karlov.mff.cuni.cz

departmental website: http://biophysics.mff.cuni.cz

Keywords: chemical stress; depolarization; fluorescent probe diS-C_3(3); membrane potential; Tok1p channel

Abbreviations: BAC, benzalkonium chloride; CCCP, carbonyl cyanide *m*-chlorophenylhydrazone; diS-C_3(3), 3,3'-dipropylthiacarbocyanine iodide; DM-11, 2-dodecanoyloxyethyldimethylammonium chloride; ODDC, octenidine dihydrochloride; TEA^+, tetraethylammonium ion

Abstract

Tok1p is a highly specific yeast plasma membrane potassium channel with strong outward directionality. Its opening is induced by membrane depolarization. Although the biophysical properties of Tok1p are well-described, its potentially important physiological role is currently largely unexplored. To address this issue, we examined the Tok1p activity following chemically-induced depolarization by measuring changes of plasma membrane potential (ΔΨ) using the diS-$C_3(3)$ fluorescence assay in a Tok1p-expressing and a Tok1p-deficient strain. We report that Tok1p channel activity in response to chemical stress does not depend solely on the extent of depolarization, as might have been expected, but may also be negatively influenced by accompanying effects of the used compound. The stressors may interact with the plasma membrane or the channel itself, or cause cytosolic acidification. All of these effects may negatively influence the Tok1p channel opening. While ODDC-induced depolarization exhibits the cleanest Tok1p activation, restoring astonishing 75% of lost ΔΨ, higher BAC concentrations reduce Tok1p activity, probably because of direct interactions with the channel and/or its lipid microenvironment. This is not only the first study of the physiological role of Tok1p in ΔΨ maintenance under chemical stress, but also the first estimate of the extent of depolarization the channel is able to counterbalance.

1. Introduction

The plasma membrane potential (ΔΨ) is defined as the electric potential difference between the interior and exterior of a cell. It is the result of various processes connected with the movement of ions across the cell plasma membrane. The highly regulated processes involved in its generation and maintenance are crucial for any living cell to survive and proliferate. In the yeast *Saccharomyces cerevisiae,* ΔΨ is controlled mainly by the regulation of H^+ and K^+ fluxes [1]. In the yeast the main ΔΨ regulator is the extensively studied and well-characterised Pma1p H^+-ATPase. The protein pumps protons out of the cytosol to regulate intracellular pH and create a proton electrochemical gradient across the plasma membrane [2, 3]. Besides Pma1p, several types of active and passive K^+ transporters contribute considerably to ΔΨ maintenance. One such potassium channel is the largely unexplored Tok1p. For review see [4].

Numerous *in vitro* electrophysiological studies have shown that Tok1p is a potassium-specific voltage-gated plasma membrane channel [5] with strong outward directionality [5-7]. It is activated not according to the absolute ΔΨ value, but rather when ΔΨ becomes more positive than the Nernst equilibrium potential for K^+ [5, 7-9]. Under steady-state conditions, this activation is influenced by the cytoplasmic ATP concentration [10]. On the other hand, the activity of Tok1p is

inhibited by external K^+, Cs^+ and Ba^{2+} ions [8], tetraethylammonium ions (TEA^+) [10, 11] and also by intracellular acidosis [10, 12]. Once the channel is opened, the K^+ accumulated in the cells can be released to regenerate membrane potential [10]. Although the biophysical properties of the Tok1p channel are well described by *in vitro* electrophysiology studies using mostly patch-clamp methods [6, 11, 13], knowledge about its actual physiological function *in vivo* is very limited. To date, it has only been shown that the deletion of the *TOK1* gene results in significant plasma membrane depolarization. On the other hand, its overexpression leads to hyperpolarization of the yeast plasma membrane [14, 15].

The *in vitro* electrophysiological studies of transmembrane potassium transport imply that the Tok1p channel is likely to be a significant contributor to the regulation of membrane potential under depolarizing conditions induced by chemical stressors. However, this has not been studied *in vivo* to date. While the membrane potential is set directly by the voltage on the electrodes used in the electrophysiological experiments, the depolarization *in vivo* is the result of the interaction of the cell with a chemical species. This interaction may result in elevated permeability of the plasma membrane and in a change of cytosolic concentration of various ions. This in turn affects membrane potential and cytosolic pH. The compound may even interact and/or interfere with intracellular structures and processes. All of the mentioned effects may affect Tok1p channel activity.

This study is mainly aimed at monitoring the contribution of the Tok1p channel to the maintenance of plasma membrane potential under chemically-induced depolarization. We concentrate on answering the following questions: **(1)** How effectively can the Tok1p-mediated potassium currents counterbalance chemically induced depolarization? **(2)** Does the stressor's mode of action affect the activity of the Tok1p channel? **(3)** If so, which effects of the stressors influence the Tok1p activity most significantly? In order to answer these questions, we investigated the Tok1p channel activity in response to several stressors that are known to depolarize the plasma membrane while exhibiting distinct modes of action [16, 17]. This was performed by monitoring the changes of membrane potential via following the accumulation of the diS-C_3(3) fluorescent probe in the parental strain and mutant strain lacking Tok1p (*tok1*). The use of the known protonophore CCCP (collapsing both the $\Delta\Psi$ and ΔpH across the plasma membrane) enabled us to establish the "experimental window" for determining the contribution of Tok1p to membrane potential regulation under chemical stress.

We present evidence that higher concentrations of surface-active stressors such as BAC significantly reduce the Tok1p channel activity. However, if the side effects of a stressor are negligible (as is the case of low ODDC concentrations), the ability of the channel to compensate depolarization is enormous, reaching up to 75%. This suggests that the physiological importance of

Tok1p in yeast cell membranes lies in particular in maintaining high membrane potential during its fluctuations.

We have previously shown that the diS-C_3(3) fluorescence assay is an appropriate and sensitive tool for monitoring plasma membrane potential ($\Delta\Psi$) changes *in vivo* after the application of various chemical substances [see e.g. 16-18]. The method is based on the use of the potentiometric fluorescent probe 3,3′-dipropylthiacarboxycyanine, diS-C_3(3), that in the absence of multidrug resistance pumps accumulates in the cytosol according to the plasma membrane potential (negative inside). Higher plasma membrane potential is reflected in higher equilibrium intracellular probe concentration and vice versa.

The progressive cytosolic accumulation of the probe is reported by time-dependent increase of the fluorescence emission maximum wavelength (λ_{max}) and takes ~30 min to reach equilibrium due to the presence of the cell wall which acts as a barrier [19, 20]. For the same reason the changes of λ_{max} values following any change of plasma membrane potential are not immediate, but follow a similar time course as the initial staining.

A slight drawback of the diS-C_3(3) fluorescence assay is that it does not enable us to measure absolute values of membrane potential. However, neither do other currently available *in vivo* methods employing some kind of probe response calibration whose reliability is usually difficult, if not impossible to verify. Nevertheless, under conditions of equilibrium staining, changes of $\Delta\Psi$ can be expressed directly in mV [21], which is of great advantage. It should be emphasized here that not the $\Delta\Psi$ transients, but steady-state $\Delta\Psi$ represent the physiologically relevant parameter to characterize the adaptive response of cells to chemical stress.

2. Materials and Methods

2.1. Yeast strains and plasmids

Yeast strains used in this study are AD1-3 (*MATα, PDR1-3, ura3, his1, yor1::hisG, snq2::hisG, pdr5::hisG*) [22], hereafter referred to as "parental strain", its isogenic *tok1* deletion mutant and AD1-3 p_{TEF1}-YpHl (the latter referred to as "pHluorin-expressing strain"; both prepared in the context of this work). The AD1-3 strain is deficient in multidrug resistance pumps [16, 17]. Therefore, the potentiometric fluorescent probe diS-C_3(3) accumulates in the cytosol solely according to the plasma membrane potential.

The *tok1* mutant was prepared by deleting the *TOK1* gene from the AD1-3 strain using homologous recombination. The pUG6-32 plasmid (*hph* marker – resistance to hygromycin B) was used as a PCR template for preparing the disruption cassette. The plasmid had been constructed

previously from plasmids pUG6 and pAG32 (Euroscarf, Bad Homburg, Germany) to enable the *hph* marker rescue, as the original pAG32 plasmid does not contain *loxP* sites [23]. A plasmid with the same function is now available from Euroscarf under the name pUG75 [24].

The AD1-3 p_{TEF1}-YpHl strain harbouring pHluorin with a strong constitutive pTEF1 promoter instead of the *HIS3* gene was prepared using homologous recombination with two overlapping cassettes. One, containing the pTEF1 promoter, was prepared with pYM-N20 plasmid (*nat* marker – resistance to nourseothricin, Euroscarf, Bad Homburg, Germany) as PCR template, the other with pHluorin was obtained from plasmid pVT100U kindly provided by Dr. Aleš Holoubek. Correct cytosolic localization in both absence and presence of chemical stress was verified by the means of confocal fluorescence microscopy.

Both mutant strains retained the growth characteristics of their parental strain (monitored by measuring optical density at 578 nm (OD_{578}) of the growing culture with an Amersham Biosciences Novaspec III spectrophotometer; data not shown), in agreement with previous research in the case of *tok1* deletion [14].

2.2. Media and cell growth conditions

Yeast precultures were grown at 30°C for 24 h in YPD medium: 1% yeast extract (Serva, Heidelberg, Germany), 1% bactopeptone (Oxoid, Brno, Czech Republic) and 2% glucose (Sigma). An inoculum of 5–10 µl was added to 10 ml fresh YPD medium and the culture was grown until it reached the desired growth phase.

2.3. Chemicals

The following materials were purchased: 3,3′-dipropylthiacarbocyanine iodide, diS-C_3(3), and dimethyl formamide (Fluka); yeast extract (Serva); agar (Carl ROTH); bactopeptone (Oxoid); glucose, ethanol for UV spectroscopy, glycerol, citric acid and $Na_2HPO_4 \cdot 12H_2O$ (Sigma). The chemical stressors were obtained from the following sources: CCCP (Sigma); BAC (Fluka); ODDC (Schülke & Mayr GmbH); DM-11 was synthesized in the laboratory of Prof. Stanislaw Witek [25] (Wroclaw University, Wroclaw, Poland) and kindly provided by Dr. Anna Krasowska.

2.4. Fluorescence measurements of diS-C3(3) accumulation in cells

Yeast cells from either exponential or post-diauxic growth phase were harvested, washed twice with double-distilled water, and resuspended in glucose-free 10 mM citrate-phosphate (CP) buffer of pH 6.0 to $OD_{578} = 0.1$ (equal to 2.5×10^6 cells/ml). The potentiometric fluorescent probe diS-C_3(3) was added to 3 ml of yeast cell suspension in a 1×1 cm UV-grade fluorometric cuvette (Kartell, Italy) as

10^{-5} M stock solution in ethanol to the final concentration of 2×10^{-8} M. Fluorescence emission spectra of the diS-C_3(3) stained cell suspensions were measured using a FluoroMax-4 spectrofluorometer (Horiba Jobin Yvon) in intervals of 5-10 min. Excitation wavelength was 531 nm, fluorescence range 560–590 nm, duration of a single spectral scan ~20 s, scattered light was eliminated by orange glass filter with a cut-off wavelength of 540 nm. The time-course of the position of fluorescence emission maximum (λ_{max}) was recorded to obtain the so-called staining curves [19, 20]. The samples were kept at room temperature and gently stirred by turning upside down before acquiring their emission spectra.

Where appropriate, chemical stressors were introduced 10 minutes before (ODDC, DM-11 and BAC) or after the addition of the probe (glucose, CCCP). The Tok1p channel inhibitor TEA^+ was added 10 minutes before the probe.

It should be emphasized here that the equilibrium staining (λ_{max}^{eq}) values cannot be directly converted to underlying membrane potential values in mV [26]. Using our calibration-free method, only differences in plasma membrane potentials under two different conditions (e.g. presence of a stressor or absence of a gene) can be acquired using the difference in equilibrium staining values ($\Delta\lambda_{max}^{eq}$). The conversion of this difference to membrane potential changes in mV relies on the fact that λ_{max}^{eq} values are clearly linked to the B/A ratio of the fractions of bound dye spectra and free dye spectra in the final spectrum [21]. The difference of their logarithms, $\log(B/A)_2 - \log(B/A)_1$, assessed through $\Delta\lambda_{max}^{eq}$ can be used to calculate the difference of underlying membrane potentials: $\Delta\Psi_2 - \Delta\Psi_1 = (RT/F)[\log(B/A)_2 - \log(B/A)_1]$, where R, T and F are the universal gas constant, absolute temperature and Faraday constant, respectively.

2.5. Monitoring of cytosolic pH via synchronously scanned pHluorin fluorescence

Cells of the pHluorin-expressing strain (see "Yeast strains and plasmids") were cultivated and harvested as for fluorescence measurements and resuspended in the same buffer to a final cell density three times higher (i.e. $OD_{578} = 0.3$, corresponding to 7.5×10^6 cells/ml) to provide better signal-to-noise ratio (this change of cell concentration in the suspension does not affect the quantitative response of pHluorin fluorescence to the used concentrations of respective chemicals; data not shown). Cytosolic pH (pH_{cyt}) was measured using the method described by Plášek *et al* in 2015 [27].

Synchronously scanned fluorescence spectra (SSF) of the cell suspensions were measured in 1×1 cm UV-grade fluorometric cuvettes (Kartell, Italy) using a FluoroMax-3 spectrofluorometer (Horiba Jobin Yvon). For each sample two SSF spectra were recorded using excitation vs. emission offsets of 30 and 110 nm. Each of these spectra follows one of the two peaks normally found in the

standard excitation spectra of pHluorin fluorescence. Since the full width of half maximum of the peaks is considerably reduced in this way, the method provides higher resolution and precision. Furthermore, it enables for straightforward and simple subtraction of the cell autofluorescence which only has to be measured once for each sample type [27].

Calibration was carried out in the same buffer as the measurements, with the addition of 50 mM KCl and 50 mM NaCl, 10 mM sodium azide and 200 mM ammonium acetate, in accordance with previous studies [28, 29]. The buffer was then titrated with either HCl or NaOH to various pH values in the range of 4.6 to 8.2. The SSF spectra of cells resuspended in this set of buffers were measured over the course of one hour. From the obtained values, only those stable in time were used to obtain the calibration curve.

In the actual measurements, the SSF spectra were measured for ca. 120 minutes to follow the time course of pH_{cyt} changes. Where appropriate, the stressors were added ~15 minutes after the start of the assay. Each pH_{cyt} measurement included 3-4 extra samples with the studied cells resuspended in various calibration buffers to verify the coincidence with the calibration curve. These were measured both before and after the measurement of pH_{cyt}.

2.6. Monitoring of pHluorin localization and cell wall integrity using confocal microscopy

Cells for cytosolic pHluorin localization (pHluorin-expressing strain) measurements were cultivated, harvested and resuspended as for fluorescence measurements. The cells were then treated with respective chemicals (glucose and CCCP) and fixed with 1% agarose gel on microscopic slides to prevent their movement. The effect of the stressors on pHluorin localization was monitored using an Olympus IX83/FV1200 laser scanning microscope with a water immersion objective UPLSAPO 60x/1.2. The micrographs were cropped and their contrast digitally enhanced using the open source digiKam software (version 4.12.0) where appropriate.

2.7. Monitoring of drug susceptibility via plating tests

Cells were cultivated, harvested and resuspended as for the fluorescence spectra measurements, but to a final cell density two times higher (i.e. OD_{578}=0.2; 5×10^6 cells/ml). The cells were incubated with various concentrations of DM-11, ODDC or BAC at room temperature while being continuously gently stirring. At designated times aliquots of 100 µl were taken from the samples and diluted 10-fold three times (i.e. to the final 1000-fold dilution). Three replicates of 100 µl were then plated on 1% YPD agar plates (1% agar, 1% yeast extract, 1% peptone, 2% glucose) and incubated for 48 hours at 30°C. Colonies were counted and the survival rates for each time-point

were calculated relative to untreated controls. For control samples the number of colonies per plate was ~200.

2.8. Monitoring of cellular material release by measuring cell suspension absorbance

Cells were cultivated, harvested and resuspended as for the fluorescence spectra measurements. Aliquots of the cell suspension were incubated with various concentrations of BAC at room temperature while being continuously gently stirred. Aliquots of 3 ml were taken at various times, centrifuged and the supernatant was used for absorption measurements. The absorption spectra were acquired in 1×1 cm quartz cuvettes using a Varian Cary 50 UV spectrophotometer (200-350 nm scanning range of 1 nm steps; integration time of 0.2 s). The absorbance was determined as a mean over the interval of 260 ± 2 nm.

2.9. Monitoring of the extent of permeabilization by propidium iodide staining

Cells were cultivated, harvested and resuspended as for the fluorescence spectra measurements. Aliquots of 0.5 ml were then incubated in Eppendorf tubes with various BAC concentrations for the desired period of time and occasionally gently stirred. The aliquots were then stained by adding 1 µl of propidium iodide solution and incubated for 10 minutes. Consequently, 20 µl were transferred to a SD100 cell-counting chamber (Nexcelom Bioscience LLC) and the amount of permeabilized cells was measured in a Nexcelom Bioscience LLC Cellometer® Vision using the VB595-502 emission filter. The data were analysed using the Cellometer Vision software.

3. Results

To understand the contribution of Tok1p to membrane potential regulation under the conditions of chemical stress leading to plasma membrane depolarization, the protonophore CCCP was selected as the model depolarizing agent. This weak lipophilic acid mediates passive proton transport across cellular membranes [20, 30-32], which results not only in plasma membrane depolarization [28] but also cytosolic acidification [32, 33].

We expected the CCCP-induced plasma membrane depolarization to trigger Tok1p channel opening and potassium release, while the cytosolic acidification leads to activation of Pma1p. Pmap1 exports protons out of the cytosol both to keep the pH_{cyt} constant and to re-polarize the plasma membrane [16, 34-36]. The setting of the experimental window (i.e. experimental conditions under which there is a manifest contribution of Tok1 to the maintenance of plasma membrane potential) included following factors: **(1)** cell culture growth phase, **(2)** activation of

Pma1p by glucose, **(3)** time of stressor addition relative to the beginning of cell staining with diS-$C_3(3)$, **(4)** cytosolic acidification, **(5)** use of known inhibitors of Tok1p (TEA^+) and Pma1p (DM-11).

3.1. The effect of growth phase and glucose on the contribution of Tok1p channel to ΔΨ maintenance

The plasma membrane depolarization in the suspension of washed cells devoid of glucose represents a practical benchmark value for the contribution of Tok1p channel to ΔΨ maintenance under chemical stress.

Washed exponential cells exhibit significantly lower staining compared to the cells with added glucose, which indicates their relative depolarization, Fig. 1A. Furthermore, the cells of the *tok1* mutant are also significantly depolarized relative to the parental strain, as revealed by lower equilibrium staining value, λ_{max}^{eq}, consistent with previous research [14, 15]. The difference between the staining of the parental strain and the *tok1* mutant (grey area in Fig. 1A) displays the Tok1p channel contribution to ΔΨ maintenance in time. In equilibrium the difference in staining ($\Delta\lambda_{max}^{eq}$) is 1.6 ± 0.2 nm which corresponds to ΔΨ difference of 14.6 ± 2.8 mV, cf. [21]. This amounts to 48 ± 6% of ΔΨ change caused by glucose addition to *tok1* mutant cells. Furthermore, addition of even relatively low concentrations of glucose leads to merging of the staining curves of the strains, indicating Tok1p channel inactivation by high membrane potential, consistent with previous studies [15]. On the other hand, there is practically no difference in the membrane potential of the two strains in the post-diauxic phase regardless of the presence of glucose, Fig. 1B.

It should be noted here that under our experimental conditions, the pH_{cyt} of untreated exponential cells is almost lower than pH_{cyt} of post-diauxic cells by 0.30 ± 0.15 units, Fig. 1C. Nevertheless, addition of glucose to the cells of both growth phases leads to extensive and quite rapid alkalization and reaches the same final value. The rise in pH_{cyt} is in both cases preceded by a small transient acidification, which is consistent with previous research [37]. Correct cytosolic pHluorin localization in our strain is documented in Fig. 1D for post-diauxic cells, both untreated and treated with glucose.

3.2. Tok1p channel activity under chemical stress induced by a model depolarizing agent CCCP

Exponential (Fig. 2A) and post-diauxic (Fig. 2B) cells were subjected to a sublethal concentration of the protonophore CCCP at two different times relative to the probe addition (12 and 50 minutes). The differences in the staining curve profiles corresponding to various times of CCCP addition can be attributed to unequal amounts of fluorescent probe accumulated in the cells before depolarization is induced. The initial depolarization is followed by relatively slow redistribution of the probe

between the cytosol and external buffer. However, as already noted in the Introduction, not the ΔΨ transients, but steady-state ΔΨ values represent the physiologically relevant parameter to characterize the response of cells to chemical stress. Hence, the main information obtained from the staining curves measured in CCCP treated cell suspensions is revealed by their mean λ_{max}^{eq} and $\Delta\lambda_{max}^{eq}$ (indicating the extent of Tok1p channel activity) values, not by their whole time course. Regardless of the difference between staining profiles, the λ_{max}^{eq} values of both strains measured in the CCCP treated cell suspensions are independent of the time of CCCP addition, Fig. 2A and 2B. They therefore represent an unambiguous measure of plasma membrane depolarization induced by CCCP.

Despite the fact that the staining curves fail to precisely follow the fast changes of ΔΨ, they still report the existence of a pronounced temporary depolarization caused by the addition of CCCP to *tok1* mutant cells. Moreover, they also reveal that about 10 minutes after the initial depolarization, ΔΨ begins to rise again towards a new equilibrium value due to Pma1p activation. The initial depolarizing effect of CCCP in post-diauxic cells of both strains is considerably more pronounced than in the exponential cells. Note also that the CCCP-induced drop of pH_{cyt} is greater in post-diauxic cells (from 6.7 ± 0.2 to 5.0 ± 0.2 in about 60 min after CCCP addition) compared to exponential cells (from 6.3 ± 0.2 to 5.0 ± 0.3), Fig. 2C (Fig. 2D provides proof of the pH_{cyt} reporter's cytosolic localization and vacuolar membrane integrity after exposure of cells to CCCP). It should be emphasized that the response of pHluorin to immediate pH_{cyt} changes is faster than about 3 sec [33]. Therefore, the slow changes in pH following the initial very rapid drop after CCCP addition (Fig. 2C) are not due to methodological limitations, but represent real slow changes of pH_{cyt} occurring in washed cells devoid of glucose.

Observed λ_{max}^{eq} data report following relationships between steady-state ΔΨ values in CCCP-treated cells and untreated controls: **(1)** Exponential phase: In the cells of the parental strain, there is only a slight temporary CCCP-induced ΔΨ drop that is finally fully restored. The *tok1* mutant controls have lover ΔΨ relative to the parental strain. Moreover, the CCCP-induced temporary ΔΨ drop is more pronounced than in the parental strain, but it is still almost completely recovered, Fig. 2A. **(2)** Post-diauxic phase: For both strains, the CCCP-induced temporary ΔΨ drop is more pronounced than in the exponential phase. The final steady state depolarization induced by CCCP addition is therefore also deeper than in the exponential cells (Fig. 2B).

To clearly demonstrate that the difference between the staining of the parental strain and the *tok1* mutant ($\Delta\lambda_{max}$) corresponds to the Tok1p channel activity, we used TEA^+ (tetraethylammonium ion), the established inhibitor of Tok1p channel [10, 11]. In suspensions

treated solely with TEA^+ (of 100 mM concentration) the cells exhibited some depolarization relative to the control, regardless of strain and growth phase, as reported by λ_{max}^{eq} (Fig. 3A and 3B). This depolarization is accompanied by slight cytosolic alkalization ($\leq$ 0.1 pH units) in both growth phases (Fig. 3C and 3D), as found in the parallel experiment performed with the pHluorin-expressing strain.

In the exponential phase, the extent of TEA^+-induced depolarization (measured by the difference between corresponding λ_{max}^{eq} of controls and TEA^+-treated cells) in the parental strain is roughly twice that in the cells of the *tok1* mutant. On the other hand, there is no such difference in the size of TEA^+-induced depolarization in the post-diauxic phase, as the respective staining curves of the parental and *tok1* mutant and their λ_{max}^{eq} values overlapped nearly perfectly, both in the control and TEA^+-treated cells. Moreover, conversion of the $\Delta\lambda_{max}^{eq}$ values to changes of $\Delta\Psi$, cf. [21], indicates that the contribution of Tok1p channel to $\Delta\Psi$ maintenance after TEA^+ addition (amounting to 8.0 ± 0.9 mV) is significantly smaller than in the absence of the inhibitor (19.8 ± 0.3 mV). Furthermore, pretreatment of the cells with TEA^+ completely abolishes the Tok1p contribution to $\Delta\Psi$ in response to CCCP-mediated depolarization only in post-diauxic cells, as indicated by the coincidence of the staining curves in the latter, but not in the former (Fig. 3A and 3B).

To prove that the gradual $\Delta\Psi$ restoration in CCCP-treated cells is caused by Pma1p activation, we employed the lysosomotropic compound DM-11 (2-dodecanoyloxyethyl-dimethylammonium chloride), a known inhibitor of Pma1p [25]. When added to the cells in combination with CCCP (as CD cocktail containing 10 μM DM-11 and 10 μM CCCP) it completely depolarizes the plasma membrane due to rapid dissipation of the proton gradient [16]. As shown in Fig. 3A and 3B, the pronounced depolarization caused by CD cocktail is not followed by a significant $\Delta\Psi$ recovery, thus indicating that the rise in staining in the absence of the inhibitor is indeed the result of CCCP-induced Pma1p activation. The Tok1p channel activity in the cells treated with CD cocktail is somewhat lower than after the treatment with CCCP alone (by ~6 mV and ~1.7 mV in exponential and post-diauxic cells, respectively, see Table 1). In contrast, cytosolic acidification following CD cocktail addition is practically identical to that caused by the addition of CCCP alone (Fig. 3C).

Table 1: Contribution of Tok1p channel to $\Delta\Psi$ under chemically induced depolarization caused by protonophore CCCP (10 μM) alone and CD cocktail (10 μM CCCP + 10 μM DM-11), respectively. Means and SDs were calculated from ten independent repeats.

	Tok1p contribution (mV) in CCCP-treated cells	Tok1p contribution (mV) in CD cocktail-treated cells
Exponential cells	17.3 ± 1.6	11.3 ± 2.0
Post-diauxic cells	10.3 ± 2.5	8.6 ± 1.3

The results obtained with CCCP and TEA^+-treated cells show that it is more convenient to use post-diauxic cells for monitoring of Tok1p contribution to ΔΨ maintenance under the conditions of chemical stress. Their chemically-induced depolarization is, in contrast to exponential cells, not preceded by depolarization caused by down-regulation of Pma1p upon glucose removal. Furthermore, the channel expression is higher in this growth-phase [38-40], making post-diauxic cells even more favourable for assays to be carried out with other chemical stressors.

3.3. Tok1p channel activity increases in cells treated with Pma1p inhibitor DM-11

The Pma1p inhibitor DM-11 causes weak depolarization of not only the parental strain used in this study [16], but also of other strains [41]. We therefore tested the contribution of Tok1p to the ΔΨ maintenance in these cells. DM-11 belongs to the group of lysosomotropic compounds whose deprotonated form readily penetrates cellular membranes and their protonated form accumulates in acidic compartments such as lysosomes or vacuoles. Moreover, these lysosomotropic compounds can even cause disruption of membranes if used at high concentrations [42-44].

Increasing the concentration of DM-11 leads to lower λ_{max}, indicating depolarization, in the cells of both strains. For concentrations exceeding 10 μM, the depolarization in *tok1* mutant cells gradually becomes considerably deeper than that in the parental cells. On the other hand, the depolarization of the parental strain is constant in the range of 10 to 25 μM, Fig. 4A and 4B (higher concentrations lead to significantly affected viability, Fig. 4D). Hence, the difference in staining of the two strains, indicating Tok1p channel activity, becomes gradually more extensive with deeper depolarization, in a manner consistent with electrophysiological studies. The highest Tok1p channel activity after treatment of cells with DM-11 corresponds to 17.9 ± 1.4 mV, as indicated by the arrow in Fig. 4B.

When the cells are treated with DM-11 alone, the cytosolic acidification is much less extensive than that caused either by CCCP alone, Fig. 4C, or by the combination of DM-11 with CCCP in the CD cocktail, Fig. 3C and 3D.

3.4. Tok1p channel activity increases in cells treated with the surface active compound ODDC

Another compound with a known depolarizing effect is octenidine dihydrochloride (ODDC) [17]. ODDC readily binds to and disrupts microbial cell envelopes and eukaryotic cell membranes. Its action results in a broad antimicrobial spectrum [45] at very low concentrations [46-49] and short exposure times [17]. It was shown using the plating test that the exposure of cells to ODDC at concentration as high as 300 nM does not lead to a significant lowering of cell survival on the time scale of 90 minutes (higher than 80% for 300 nM ODDC after 90 min exposure; data not shown).

Raising the ODDC concentration is followed by gradual depolarization of the *tok1* mutant plasma membrane. The membrane potential of the parental strain, however, becomes only slightly lower than that of controls and remains constant in the range of 12.5 to 175 nM. The difference in staining of the two strains therefore becomes gradually more extensive with deeper depolarization, indicating elevated Tok1p channel activity, in a manner consistent with electrophysiological studies. The highest Tok1p channel activity after treatment of cells with ODDC corresponds to 29.9 ± 3.4 mV (in response to 175 nM ODDC), as indicated by the arrow in Fig. 5A. At concentrations of 200 nM and higher the equilibrium staining of the parental strain decreases. The λ_{max}^{eq} of the *tok1* strain also decreases with increasing ODDC concentration, but not as rapidly as in the case of the parental strain. This indicates concentration-dependent lowering of Tok1p channel contribution to $\Delta\Psi$ at concentrations above 200 nM, Fig. 5A. Simultaneously with the plasma membrane depolarization, ODDC causes relatively low, concentration-dependent, cytosolic acidification (0.6 ± 0.3 pH units after almost 2-hour exposure to 300 nM ODDC) compared to the effect of CCCP (1.7 ± 0.4 pH units), Fig. 5B.

3.5. Tok1p channel is inhibited by BAC in a concentration-dependent manner

To understand how much the different modes of stressor's action may affect the Tok1p channel activity we tested BAC (benzalkonium chloride) that belongs to the group of quaternary ammonium compounds. These chemicals induce plasma membrane disorganization leading to leakage of low molecular weight materials [50]. BAC causes not only membrane depolarization but also acts in an intracellular manner and affects cell metabolism. In fact, it was clearly shown that the dominant role in BAC toxicity lies within metabolic inhibition rather than plasma membrane damage [17].

The response of the Tok1p channel to the depolarizing action of BAC is considerably different from that following exposure to DM-11 and ODDC, as evidenced from Fig. 6A. In particular, the difference between respective λ_{max}^{eq} values found for the parental strain and the *tok1* mutant strain decreases for BAC concentrations over 2.5 μM. On the other hand, it gradually increased with increasing concentration of DM-11 (Fig. 4A and 4B) and ODDC (Fig. 5A). Besides depolarization, BAC also causes slight, concentration-dependent, acidification. The effect of BAC

on pH_{cyt} is almost equal to that caused by DM-11 and ODDC at concentrations causing the same extent of depolarization (Fig. 6B).

The ΔΨ decrease caused by BAC is associated with a leakage of intracellular molecules, including those absorbing light at 260 nm, such as ATP (Fig. 6C). For the range of BAC concentrations displayed in Fig. 6A this leakage of intracellular material increases only very slowly compared to the sharp rise following the increase of BAC concentration to 50 μM. Furthermore, we tested the BAC treated cells for membrane permeability by the means of propidium iodide staining. As shown in Fig. 6D, BAC concentrations ≤ 10 μM cause only a very limited fraction of the suspension to become permeabilized. Our results indicate that BAC-induced cell depolarization is not a trivial consequence of membrane permeabilization.

Since an electrophysiological study showed that the channel opening is dependent on cytosolic ATP [10], we also analysed the effect of ATP depletion. For this purpose, washed post-diauxic cells were incubated for 2 hours in C-P buffer with 5 mM 2-deoxy-D-glucose (2DG). As above, the indication of Tok1p activity is the difference between λ_{max}^{eq} values measured with the parental strain and its *tok1* mutant. As shown in Fig. 7, neither the depletion of ATP by incubating the cells with 2DG, nor the starvation of washed cells without glucose has any significant effect on the Tok1p channel activity.

3.6. Comparison of Tok1p channel activity in response to depolarization caused by ODDC, BAC and DM-11

In this work we present concentration dependencies of depolarization as observed in washed cells after the application of chemical stressors of different types. These were used to search for a hypothetical relationship between the extent of yeast cell depolarization and Tok1p channel activity, as assessed from the difference in staining of the parental strain and the *tok1* mutant. The dependence of the channel's activity in equilibrium on the respective depolarization of treated *tok1* mutant cells can be plotted either in terms of $\Delta\lambda_{max}^{eq}$ (Fig. 8A) or directly in mV (Fig. 8B). The latter provides the additional advantage of the possibility to compare the absolute values of Tok1p-mediated ΔΨ restoration in response to exposure of the cells to various stressors.

As evident from Figs. 8A and 8B, there is almost no difference between the stressors at concentrations leading to low depolarization. Deeper depolarization, however, reveals the differences in the Tok1p channel activity as a direct consequence of the distinct mode of action of the compounds. The most striking difference between the stressors can be observed when the depolarization lies within the range of 30-40 mV (Fig. 8B). While the channel is able to counterbalance astounding ~75% of the depolarization caused by ODDC within said range,

inducing equivalent depolarization by BAC enables the Tok1p channel to counterbalance only about 25% of the lost membrane potential.

4. Discussion

In this paper we attempt to clarify the contribution of the Tok1p channel to the maintenance and/or restoration of yeast plasma membrane potential under depolarizing action of several chemical stressors. These include CCCP as a model depolarizing agent, Pma1p inhibitor DM-11, and surface active compounds ODDC and BAC, the latter being capable of inducing plasma membrane disorganization. We monitored membrane potential changes induced by these drugs through the intracellular accumulation of the redistribution potentiometric fluorescent probe diS-C_3(3). The extent of probe accumulation is revealed by the spectral shifts of probe fluorescence emission maxima. We assessed the activity of Tok1p channel by comparing the extent of depolarization in a strain expressing the *TOK1* gene with that in a *tok1* mutant strain lacking it.

In our study we used cells of a multidrug resistance pump–deficient strain AD1-3 and its *tok1* mutant to avoid misleading artefacts in intracellular probe accumulation due to a possible efflux of diS-C_3(3) by the pumps. Furthermore, we performed the assays aimed at Tok1p performance with suspensions of washed cell devoid of glucose, because the role of Tok1p channel is masked by Pma1p activity in the presence of the sugar [15].

The above necessary condition for disclosing the contribution of Tok1p to plasma membrane potential maintenance is confirmed in Fig. 1A. The presented staining curves indicate that in exponential cells, the depolarization caused by glucose removal is less extensive in the parental strain than in the *tok1* mutant. The observed λ_{max}^{eq} difference between the depolarized cells of the parental strain and its *tok1* mutant corresponds to a $\Delta\Psi$ difference of ~15 mV. This amounts to ~50% of $\Delta\Psi$ change caused by glucose addition to *tok1* mutant cells. Thus, the results indicate considerable contribution of the Tok1p channel to $\Delta\Psi$ maintenance when Pma1p activity is reduced in the absence of glucose.

We analysed the role of Tok1p channel also in post-diauxic cells. It is known that the removal of glucose from the cells' surroundings leads to down-regulation of Pma1p activity [51] and consequently depolarization of the plasma membrane. On the other hand, cells of post-diauxic cultures are adapted to the absence of glucose in their growth medium. Their transfer to the glucose-free buffer therefore need not considerably affect Pma1p activity. Thus, even in the situation of higher Tok1p channel expression relative to exponential cells [38-40], there is practically no difference in the membrane potential of the two strains in post-diauxic cells (Fig. 1B).

However, the cytosolic alkalization of post-diauxic cells following glucose addition (Fig. 1C) indicates the possibility of Pma1p and V-ATPase activation by glucose not only in exponential [52, 53], but also in post-diauxic cells. Interestingly, the extensive and quite rapid alkalization following the addition of glucose (preceded by a small transient acidification, consistent with previous research [37]) reaches the same final value regardless of the strain. It should also be noted that under our experimental conditions, the pH_{cyt} of glucose-starving exponential cells is consistently about 0.2 pH units lower than pH_{cyt} of the post-diauxic cells. This difference can be readily explained by the known effect of Pma1p down-regulation [51] and V-ATPase disassembly [52, 53] upon glucose removal from exponential cells.

The protonophore CCCP was used as a model depolarizing agent. It caused a relatively deep transient depolarization followed by partial restoration of $\Delta\Psi$. Although the relatively slow response of diS-C_3(3) fluorescent probe does not allow for accurate tracking of rapid $\Delta\Psi$ changes, the staining curves shown in Fig. 2 still reliably prove the existence of the restoration phase. Furthermore, the equilibrium staining levels are reliable, as demonstrated by their equality regardless of the CCCP-addition time.

Addition of CCCP to glucose-starving exponential cells of the parental strain does not cause any significant change in the steady-state level of cell staining, i.e. in the steady-state $\Delta\Psi$ (Fig. 2A). This is consistent with our previous study in which we attributed the absence of any λ_{max} drop after the protonophore addition to Pma1p activation [16]. The addition of the protonophore to *tok1* mutant cells (which are already slightly depolarized compared to the cells of the parental strain) led to much more pronounced initial drop in staining, followed by large, but not complete $\Delta\Psi$ restoration. This means that the Tok1p channel plays a considerable role not only in the maintenance of high $\Delta\Psi$ in untreated cells, but also in $\Delta\Psi$ restoration following their CCCP-induced depolarization. The depolarizing effect of CCCP in post-diauxic cells of both strains is considerably more pronounced than in exponential cells (Fig. 2B). The apparent contribution of Tok1p channel to maintaining the membrane potential under CCCP-induced depolarization is also stronger in this case, which is consistent with elevated expression of the channel in post-diauxic cells [38-40]. Furthermore, the contribution of the channel to $\Delta\Psi$ maintenance gradually decreases in both exponential and post-diauxic cells after achieving maximum as a consequence of increasing membrane potential.

The conclusion that the above discussed differences between membrane potentials of the parental strain and its *tok1* mutant reflect the Tok1p channel activity, is further supported by the results of assays using the Tok1p channel inhibitor TEA^+ (Fig. 3). When using an established

inhibitor, one expects the difference between the staining of the two strains (corresponding to the Tok1p channel activity) to disappear completely. Indeed, in post-diauxic cells the extent of depolarization caused by the addition of TEA^+ is small and of the same extent in both strains, demonstrating the absence of any Tok1p channel contribution to $\Delta\Psi$ (Fig. 3B). In exponential cells, however, the use of the inhibitor does not result in complete merging of the staining curves of the two strains (Fig. 3A). However, it does make the difference between them less extensive. This difference in staining, and hence $\Delta\Psi$, originates in Tok1p channel opening and K^+ release in response to depolarization (due to glucose removal and Pma1p down-regulation) which precedes the addition of TEA^+ to the cells. Since the difference between $\Delta\Psi$ of the strains originates in K^+ redistribution, the fact that the inhibition of the efflux-oriented Tok1p channel leads to decrease of this difference points to the existence of a simultaneous influx and efflux of potassium across the plasma membrane, consistent with general belief [4, 54-56].

The $\Delta\Psi$ restoration after the transient CCCP-induced depolarization can be plausibly attributed to H^+ efflux resulting from Pma1p activation. We found that although the post-diauxic cells of the parental strain have higher pH_{cyt} than exponential cells, their acidification (the total change of pH_{cyt}) after exposure to CCCP is more extensive. Therefore, the overall response of Pma1p to CCCP appears less extensive in post-diauxic cells than in exponential cells. This notion is consistent with lower Pma1p expression in post-diauxic cells, as has been reported not only for the parental strain used in this study [57] but also for other strains [38-40, 59], suggesting it to be a general phenomenon. Considering also that the channel expression is higher in the post-diauxic phase [38-40], it is not surprising that the apparent contribution of Tok1p to the maintenance of $\Delta\Psi$ in CCCP treated cells is more pronounced in post-diauxic cells compared to exponential cells. Therefore, further assays using chemical stressors DM-11, ODDC and BAC were carried out with post-diauxic cells.

The use of the surface-active compounds ODDC and BAC yielded valuable information about the performance of Tok1p channel in cells depolarized by stressors of distinct chemical nature. The results obtained with gradually rising concentration of ODDC indicate that the Tok1p channel activity rises with more extensive depolarization, consistent with the studies of the channel's electrophysiology [6, 11]. They further show that the channel activity is sufficient to almost completely compensate the ODDC-induced depolarization up to 175 nM (Fig. 5A). At concentrations of 200 nM and higher the Tok1p channel contribution to $\Delta\Psi$ becomes less extensive. This might be caused by various effects of ODDC on cell surface structures, e.g. weakening of the cell envelope, as was shown to be the result of one-hour incubation with 240 nM ODDC [47]. Comparing the contribution of Tok1p to $\Delta\Psi$ at the corresponding level of depolarization of the *tok1*

mutant (572.3 nm) following the addition of ODDC (~30 mV; Fig. 5A) and CCCP (~16.5 mV; Fig. 2B) clearly demonstrates the effect of cytosolic acidification on the channel activity. In this case, deepening the acidification by 1 pH unit causes a loss of about 45% of the channel's activity. It is very curious that even at pH_{cyt} ~ 6.0, when the Tok1p opening probability is only about 15% [12], the channel is able to almost completely counterbalance the loss of $\Delta\Psi$ caused by the action of up to 175 nM ODDC.

Compared to DM-11, exposure of the parent strain to ODDC leads to less extensive depolarization, indicating higher contribution of the channel to $\Delta\Psi$ relative to that under the effect of DM-11 (by 11 mV). To bring an insight into the lower Tok1p channel activity after exposure to DM-11 compared to ODDC, one needs to consider the cytosolic acidification at concentrations leading to the same depolarization (Fig. 4A, 4C and 5A, 5C). However, since the compounds cause comparable acidification, the effect of pH_{cyt} on Tok1p channel activity after exposure to the compounds is also comparable.

Since DM-11 is known to interact with Pma1p [25], it is possible that it also interacts with the Tok1p channel, causing slight inactivation. This interaction can be either direct or mediated by affecting the immediate lipid environment of the channel after incorporation in the plasma membrane, a known action of the compound [44]. While the elucidation of the actual inactivation mechanism is beyond the scope of the present study, it is clear that not only cytosolic acidification (as was the case under CCCP-induced depolarization), but also other effects of the stressor may influence the Tok1p channel activity.

The surface-active compound BAC is capable of inducing plasma membrane disorganization leading to leakage of low molecular weight materials [49]. It is important to note that while lethal to microorganisms at higher concentrations and longer exposure times, the toxicity of BAC has been shown to originate in metabolic inhibition rather than plasma membrane damage [17]. The compound was chosen to gain insight into how much different modes of stressor's action may affect the depolarization-induced Tok1p channel activity.

The suitability of this choice became obvious by finding that the depolarizing action of BAC is considerably different from that following exposure to DM-11 and ODDC, as evidenced by Fig. 6. In particular, the Tok1p activity (revealed by the difference between probe accumulation in the parental strain and the *tok1* mutant) does not gradually increase with the stressor concentration, but decreases for BAC concentrations over 2.5 μM. Despite that the effect of BAC on pH_{cyt} is almost identical to that caused by DM-11 and ODDC at concentrations causing the same extent of depolarization, the same extent of depolarization leads to lower Tok1p activity in the cells treated

with BAC. This finding again indicates that the mode of action of the stressor is an important determinant of Tok1p channel activity.

Any acceptable explanation of the different BAC mode of action must first of all consider the way in which BAC induces depolarisation. In contrast to the action of DM-11, where membrane depolarization reflects the extent of H^+ entering the cytosol that is not counterbalanced by Pma1p due to its inhibition by the compound [41], BAC depolarises cells by inducing leakage of negatively charged cytosolic molecules, including ATP. Following the investigation of the effect of ATP depletion from BAC treated cells, neither the depletion of ATP (by incubating the cells with 2-deoxy-D-glucose for 2 hours) nor the starvation of washed cells without glucose has any significant effect on the Tok1p channel activity indicating that decreased level of intracellular ATP is not the reason of BAC-induced Tok1p inhibition. The latter finding challenges the conclusion based on whole-cell electrophysiological recording that the Tok1p opening is dependent on the presence of cytosolic ATP [10]. Our findings indicate that the negative effect exhibited by BAC on the Tok1p channel activity is mediated either by interaction with immediate lipid environment of the channel and/or direct interaction with the channel itself. These possibilities are supported by the mechanism of alcohol-induced inhibition of Pdr5p and Snq2p multidrug resistance pumps [18]. Furthermore, cells deficient in the multidrug resistance pump Pdr5p (such as those used in this study) accumulate BAC, since they are unable to mediate its efflux, as we have shown previously [17]. Therefore, we cannot exclude that BAC interacts with Tok1p from the intracellular side of the plasma membrane.

Fig. 8 conveniently displays and compares the efficiency of Tok1p channel-mediated $\Delta\Psi$ restoration after exposure of cells to different chemical stressors, namely the lysosomotropic compound DM-11 and the surface-active compounds ODDC and BAC. As discussed above, the selected stressors elicit similar degree of cytosolic acidification in the treated cells, making their direct comparison more straightforward. CCCP was not included into this analysis as it induces much greater pH_{cyt} change than the other stressors. Despite the comparable effect of DM-11, ODDC and BAC on pH_{cyt}, Fig. 8 clearly displays differences in Tok1p channel activity in response to each of these compounds. It is therefore clear that to make a qualified conclusion about the Tok1p channel contribution to $\Delta\Psi$ maintenance under the conditions of chemical stress, it is necessary to consider not only the extent of depolarization, but also the manner in which the depolarization is accomplished. However, even in the case when the exact molecular mechanism of the stressor's effects are not known, its influence on the Tok1p channel opening capacity can be directly compared with that of other stressors.

A complex set of data on Tok1p contribution to plasma membrane potential maintenance in yeast under chemically induced depolarization is presented in this paper. The study revealed that the

Tok1p channel activity can be affected by a range of effects originating in the mode of action of a specific stressor, as graphically summarised in Fig. 9. These include transfer of a hydrogen ion into the cell and acidification of the cytosol, direct interaction with the plasma membrane and influx of the compound into the cell leading to further effects either on metabolism or membrane structures within the cytoplasm. While the application of a stressor does not have to necessarily lead to all of them, we see that they are somewhat intertwined and not independent. Our results indicate that the most adverse effects of a stressor on the Tok1p channel activity are produced by its interaction with the plasma membrane, by affecting the protein from either extracellular or intracellular side, and/or by affecting its immediate lipid environment.

Acknowledgements

We gratefully acknowledge Zdena Palková (Department of Genetics and Microbiology, Charles University, Prague, Czech Republic) and Libuše Váchová (Institute of Microbiology, Academy of Sciences, Prague, Czech Republic) for valuable discussions. We further acknowledge Jan Malínský and Miroslava Opekarová (Institute of Experimental Medicine, Academy of Sciences, Prague, Czech Republic) for critical reading of the manuscript and valuable input.

This work was supported by the Grant Agency of Charles University [grant numbers 456213 and 1072313]; Charles University [grant numbers SVV 260 323 and UNCE 204013]; Grant Agency of the Czech Republic [grant number 15-08225S]; EU supported Operational Programme "Research and Development for Innovation" [OP VaVpI no. CZ.1.05/4.1.00/16.0340]; MŠMT [grant number LH 13049]; RVO [grant number 61388971] and the project BIOCEV [grant number CZ.1.05/1.1.00/02.0109].

Conflict of interest

The authors declare that they have no conflict of interest.

References

1. Gaber RF (1992) Molecular genetics of yeast ion transport. *Int Rev Cytol* 137A, 299-353.

2. Serrano R, Kiellandbrandt MC, Fink GR (1986) Yeast plasma membrane ATPase is essential for growth and has homology with (Na^++K^+), K^+- and Ca^{2+}-ATPases. *Nature* 319, 689-693.

3. Serrano R (1988) Structure and function of proton translocating ATPase in plasma membranes of plants and fungi. *Biochim Biophys Acta* 947, 1-28.

4. Ariño J, Ramos J, Sychrová H (2010) Alkali metal cation transport and homeostasis in yeasts. *Microbiol Mol Biol Rev* 74, 95-120.

5. Ketchum KA, Joiner WJ, Sellers AJ, Kaczmarek LK, Goldstein SAN (1995) A new family of outwardly rectifying potassium channel proteins with two pore domains in tandem. *Nature* 376, 690-695.

6. Bertl A, Slayman CL, Gradmann DJ (1993) Gating and conductance in an outward-rectifying K^+ channel from the plasma membrane of *Saccharomyces cerevisiae*. *Membr Biol* 132(3), 183-199.

7. Fairman C, Zhou XL, Kung C (1999) Potassium uptake through the TOK1 K^+ channel in the budding yeast. *J Membr Biol* 168, 149-157.

8. Vergani P, Miosga T, Jarvis SM, Blatt MR (1997) Extracellular K^+ and Ba^{2+} mediate voltage-dependent inactivation of the outward-rectifying K^+ channel encoded by the yeast gene *TOK1*. *FEBS Lett* 405, 337-344.

9. Loukin SH, Saimi Y (1999) K^+-dependent composite gating of the yeast K^+ channel, Tok1. *Biophys J* 77, 3060-3070.

10. Bertl A, Bihler H, Reid JD, Kettner C, Slayman CL (1998) Physiological characterization of the yeast plasma membrane outward rectifying K^+ channel, DUK1 (TOK1), *in situ*. *J Membr Biol* 162, 67-80.

11. Gustin MC, Martinac B, Saimi Y, Culbertson MR, Kung C (1986) Ion channels in yeast. *Science* 233(4769), 1195-1197.

12. Lesage F, Guillemare E, Fink M, Duprat F, Lazdunski M, Romey G, Barhanin J (1996) A pH-sensitive yeast outward rectifier K^+ channel with two pore domains and novel gating properties. *J Biol Chem* 271, 4183-4187.

13. Gustin MC, Zhou XL, Marinac B, Kung C (1988) A mechanosensitive ion channel in the yeast plasma membrane. *Science* 242(4879), 762-765.

14. Marešová L, Urbánková E, Gášková D, Sychrová H (2006) Measurements of plasma membrane potential changes in *Saccharomyces cerevisiae* cells reveal the importance of the Tok1 channel in membrane potential maintenance. *FEMS Yeast Res* 6, 1039-1046.

15. Marešová L, Muend S, Zhang YQ, Sychrová H, Rao R (2009) Membrane hyperpolarization drives cation influx and fungicidal activity of amiodarone. *J Biol Chem* 284, 2795-2802.

16. Hendrych T, Kodedová M, Sigler K, Gášková D (2009) Characterization of the kinetics and mechanisms of inhibition of drugs interacting with the *S. cerevisiae* multidrug resistance pumps Pdr5p and Snq2p. *Biochim Biophys Acta* 1788, 717-723.

17. Kodedová M, Sigler K, Lemire BD, Gášková D (2011) Fluorescence method for determining the mechanism and speed of action of surface-active drugs on yeast cells. *Biotechniques* 50(1), 58-63.

18. Gášková D, Plášek J, Zahumenský J, Benešová I, Buriánková L, Sigler K (2013) Alcohols are inhibitors of *Saccharomyces cerevisiae* multidrug-resistance pumps Pdr5p and Snq2p. *FEMS Yeast Res* 13(8), 782-795.

19. Denskteinová B, Gášková D, Heřman P, Večeř J, Malínský J, Plášek J, Sigler K (1997) Monitoring of membrane potential changes in *Saccharomyces cerevisiae* by diS-C_3(3) fluorescence. *Folia Microbiol* 42, 221–224.

20. Gášková D, Brodská B, Heřman P, Večeř J, Malínský J, Sigler K, Benada O, Plášek J (1998) Fluorescent probing of membrane potential in walled cells, diS-C_3(3) assay in *Saccharomyces cerevisiae*. *Yeast* 14, 1189–1197.

21. Plášek J, Gášková D (2014) Complementary methods of processing diS-C_3(3) fluorescence spectra used for monitoring the plasma membrane potential of yeast, their pros and cons. *J Fluoresc* 24, 541-547.

22. Decottignies A, Grant AM, Nichols JW, de Wet H, McIntosh DB, Goffeau A (1998) ATPase and multidrug transport activities of the overexpressed yeast ABC protein Yor1p. *J Biol Chem* 273, 12612-12622.

23. Goldstein AL, McCusker JH (1999) Three new dominant drug resistance cassettes for gene disruption in *Saccharomyces cerevisiae*. *Yeast* 15, 1541-1553.

24. Hegemann JH, Heick SB (2011) Delete and repeat: a comprehensive toolkit for sequential gene knockout in the budding yeast *Saccharomyces cerevisiae*. *Methods Mol Biol* 765, 189-206.

25. Witek S, Goffeau A, Nader J, Luczynski J, Lachowicz TM, Kuta B, Obłąk E (1997) Lysosomotropic aminoesters act as H^+-ATPase inhibitors in yeast. *Folia Microbiol* 42, 252-254.

26. Plášek J, Gášková D, Lichtenberg-Frate H, Ludwig J, Höfer M (2012) Monitoring of real changes of plasma membrane potential by diS-C_3(3) fluorescence in yeast cell suspensions. *J Bioenerg Biomembr.* 44(5), 559-569.

27. Plášek J, Melcrová A, Gášková D (2015) Enhanced sensitivity of pHluorin-based monitoring of intracellular pH changes achieved through synchronously scanned fluorescence spectra. *Anal Chem* 87(19), 9600-9604.

28. Preston RA, Murphy RF, Jones EW (1989) Assay of vacuolar pH in yeast and identification of acidification-defective mutants. *Proc Natl Acad Sci* 86, 7027-7031.

29. Ali R, Brett CL, Mukherjee S, Rao R (2004) Inhibition of sodium/proton exchange by a Rab-GTPase-activating protein regulates endosomal traffic in yeast. *J Biol Chem* 279(6), 4498-4506.

30. Heytler PG, Prichard WW (1962) A new class of uncoupling agents--carbonyl cyanide phenylhydrazones. *Biochem Biophys Res Commun* 7, 272-275.

31. Kasianowicz J, Benz R, McLaughlin S (1984) The kinetic mechanism by which CCCP (carbonyl cyanide *m*-chlorophenylhydrazone) transports protons across membranes. *J Membr Biol* 82(2), 179-190.

32. Purwin C, Nicolay K, Scheffers WA, Holzer H (1986) Mechanism of control of adenylate cyclase activity in yeast by fermentable sugars and carbonyl cyanide *m*-chlorophenylhydrazone. *J Biol Chem* 261(19), 8744-8749.

33. Plášek, J, Babuka D, Gášková D, Jančíková I, Zahumenský J, Hoefer M (2017) A novel method for assessment of local pH in periplasmic space and of cell surface potential in yeast. *J Bioenerg Biomembr* DOI:10.1007/s10863-017-9710-3.

34. dos Passos JB, Vanhalewyn M, Brandão RL, Castro IM, Nicoli JR, Thevelein JM (1992) Glucose-induced activation of plasma membrane H^+-ATPase in mutants of the yeast *Saccharomyces cerevisiae* affected in cAMP metabolism, cAMP-dependent protein phosphorylation and the initiation of glycolysis. *Biochim Biophys Acta* 1136, 57-67.

35. Brandão R, Castro IM, dos Passos JB, Nicoli JR, Thevelein JM (1992) Glucose-induced activation of the plasma membrane H^+-ATPase in *Fusarium oxysporum*. *J Gen Microbiol* 138, 1579-1586.

36. Pereira MB, Tisi R, Fietto LG, Cardoso AS, Franca MM, Carvalho FM, Tropia MJ, Martegani E, Castro IM, Brandão RL (2008) Carbonyl cyanide *m*-chlorophenylhydrazone induced calcium signalling and activation of plasma membrane H^+-ATPase in the yeast *Saccharomyces cerevisiae*. *FEMS Yeast Res* 8, 622-630.

37. Thevelein JM, Beullens M, Honshoven F, Hoebeeck G, Detremerie K, Griewel B, den Hollander JA, Jans AW (1987) Regulation of the cAMP level in the yeast *Saccharomyces*

cerevisiae: the glucose-induced cAMP signal is not mediated by a transient drop in the intracellular pH. *J Gen Microbiol,* 133(8), 2197-205.

38. DeRisi JL, Iyer VR, Brown PO (1997) Exploring the metabolic and genetic control of gene expression on a genomic scale. *Science* 278(5338), 680-686.

39. Gasch AP, Spellman PT, Kao CM, Carmel-Harel O, Eisen MB, Storz G, Botstein D, Brown PO (2000) Genomic expression programs in the response of yeast cells to environmental changes. *Mol Biol Cell* 11(12), 4241-4257.

40. Brauer MJ, Saldanha AJ, Dolinski K, Botstein D (2005) Homeostatic adjustment and metabolic remodeling in glucose-limited yeast cultures. *Mol Biol Cell* 16(5), 2503-2517.

41. Palková Z, Váchová L, Gášková D, Kučerová H (2009) Synchronous plasma membrane electrochemical potential oscillations during yeast colony development and aging. *Mol Membr Biol* 26(4), 228-235.

42. Miller DK, Griffiths E, Lenard J, Firestone RA (1983) Cell killing by lysosomotropic detergents. *J Cell Biol* 97(6), 1841-1851.

43. Dubowchik GM, Padilla L, Edinger K, Firestone RA (1994) Reversal of doxorubicin resistance and catalytic neutralization of lysosomes by a lipophilic imidazole. *Biochim Biophys Acta* 1191, 103-108.

44. Obłąk E & Krasowska A (2010) Biologiczna aktywność związków lizosomotropowych. *Postepy Hig Med Dosw* (online) 64, 459-465.

45. Kramer A, Müller G (2008) Octenidindihydrochlorid. In *Wallhausers Praxis der Sterilisation, Desinfektion, Antiseptik und Konservierung* (Kramer A, Assadian O, ed 1.) pp. 799-805. Georg Thieme Verlag KG, Stuttgart, Germany.

46. Harke HP (1989) Octenidine dihydrochloride, properties of a new antimicrobial agent. *Zentralbl Hyg Umweltmed* 188, 188-193.

47. Ghannoum MA, Abuelteen K, Ellabib M, Whittaker PA (1990) Antimycotic effects of octenidine and pirtenidine. *J Antimicrob Chemother* 25, 237-245.

48. Hübner NO, Siebert J, Kramer A (2009) Octenidine dihydrochloride, a modern antiseptic for skin, mucous membranes and wounds. *Skin Pharmacol Physiol* 23(5), 244-258.

49. Koburger T, Hübner NO, Braun M, Siebert J, Kramer A (2010) Standardized comparison of antiseptic efficacy of triclosan, PVP-iodine, octenidine dihydrochloride, polyhexanide and chlorhexidine digluconate. *J Antimicrob Chemother* 65(8), 1712-1719.

50. Salton MR (1968) Lytic agents, cell permeability, and monolayer penetrability. *J Gen Physiol* 52(1), 227-252.

51. Serrano R (1983) *In vivo* glucose activation of the yeast plasma membrane ATPase. *FEBS Lett* 156, 11-14.

52. Kane PM (1995) Disassembly and reassembly of the yeast vacuolar H^+-ATPase *in vivo*. *J Biol Chem* 270, 17025–17032.

53. Seol JH, Shevchenko A, Shevchenko A, Deshaies RJ (2001) Skp1 forms multiple protein complexes, including RAVE, a regulator of V-ATPase assembly. *Nat Cell Biol* 3(4), 384-391.

54. Ortega MD, Rodríguez-Navarro A (1985) Potassium and rubidium effluxes in *Saccharomyces cerevisiae*. *Z Naturforsch* 40C, 721–725.

55. Laphatitis G, Kotyk A (1998) Univalent cation fluxes in yeast. *Biochem and Mol Bio Int* 44(2), 371-380.

56. Volkov V (2015) Quantitative description of ion transport via plasma membrane of yeast and small cells. *Front Plant Sci* 6, 425.

57. Hlaváček O, Kučerová H, Harant K, Palková Z, Váchová L (2009) Putative role for ABC multidrug exporters in yeast quorum sensing. *FEBS Lett* 583(7), 1107-1113.

58. Segal E, Shapira M, Regev A, Pe'er D, Botstein D, Koller D (2003) Module networks: identifying regulatory modules and their condition-specific regulators from gene expression data. *Nat Genet* 34(2), 166-176.

59. Maris P (1995) Modes of action of disinfectants. *Rev Sci Tech* 14(1), 47-55.

Fig. 1. Contribution of Tok1p channel to ΔΨ maintenance depends on growth phase and presence of glucose. Staining curves of the parental strain and *tok1* mutant grown to **(A)** exponential and **(B)** post-diauxic phase; comparison of untreated and glucose-treated cells. Data are representative of ten independent repeats which were also used to calculate the means and SDs in the inserts: equilibrium staining levels (λ_{max}^{eq}) after 60 minutes of staining. "ns" and the asterisks indicate *P*-values obtained from the *t*-test: ns (not significant) – *t*-test *P* value ≥ 0.05; *** – *t*-test *P* value < 0.001. **(C)** Effect of glucose on cytosolic pH (pH_{cyt}) of exponential and post-diauxic cells of the pHluorin-expressing strain. Data are representative of five independent repeats. **(D)** Exclusively cytosolic localization of pHluorin in post-diauxic cells both in absence and presence of 5 mM glucose (~60-minute exposure). Representative figures.

Fig. 2. Contribution of Tok1p to post-CCCP ΔΨ restoration in equilibrium is independent of addition time. Staining curves of the parental strain and *tok1* mutant grown to **(A)** exponential and **(B)** post-diauxic phase; effect of CCCP added at three different times (12 and 50 min) relative to the diS-C_3(3) fluorescent probe. Data are representative of ten independent repeats. **(C)** Effect of CCCP on cytosolic pH (pH_{cyt}) of exponential and post-diauxic cells of the pHluorin-expressing strain. Data are representative of ten independent repeats. **(D)** Exclusively cytosolic localization of pHluorin in exponential and post-diauxic cells treated with 10 μM CCCP for ~60 minutes. Representative figures.

Fig. 3. Tok1p response to CCCP-induced depolarization in the presence of known inhibitors of Tok1p (TEA^+) and Pma1p (DM-11). Staining curves of the parental strain and *tok1* mutant grown to **(A)** exponential and **(B)** post-diauxic phase; effect of the Tok1p channel inhibitor TEA^+ added 10 minutes before the diS-C_3(3) fluorescent probe and Pma1p inhibitor DM-11 added simultaneously with CCCP (CD cocktail). Data are representative of ten independent repeats. Effect of CCCP, TEA^+, their combination and CD cocktail on cytosolic pH (pH_{cyt}) of **(C)** exponential and **(D)** post-diauxic cells of the pHluorin-expressing strain. TEA^+ was added 10 minutes before the start of the pH_{cyt} measurement and DM-11 simultaneously with CCCP (CD cocktail). Data are representative of five independent repeats.

Fig. 4. Tok1p contribution to ΔΨ restoration following exposure to DM-11. (A) Staining curves of the parental strain and *tok1* mutant grown to post-diauxic phase and treated with various concentrations of DM-11 added 10 minutes before the diS-C_3(3) fluorescent probe. Data are representative of ten independent repeats. **(B)** Dependence of equilibrium staining levels (λ_{max}^{eq}) of

post-diauxic cells on the used DM-11 concentrations. Means and SDs were calculated from ten independent repeats. **(C)** Effect of various concentrations of DM-11 on cytosolic pH (pH_{cyt}) of post-diauxic cells of the pHluorin-expressing strain; effect of CCCP for comparison. Data are representative of five independent repeats. **(D)** Time-dependent viability of post-diauxic cells of the parental strain exposed to various DM-11 concentrations. Means and SDs were calculated from three independent repeats.

Fig. 5. Tok1p contribution to ΔΨ restoration following exposure to ODDC. (A) Dependence of equilibrium staining levels (λ_{max}^{eq}) of post-diauxic cells treated with various concentrations of ODDC added 10 minutes before the diS-C_3(3) fluorescent probe. Means and SDs were calculated from ten independent repeats. **(B)** Effect of various concentrations of ODDC on cytosolic pH (pH_{cyt}) of post-diauxic cells of the pHluorin-expressing strain; effect of CCCP for comparison. Data are representative of five independent repeats.

Fig. 6. Tok1p is inhibited by BAC in a concentration-dependent manner. (A) Dependence of equilibrium staining levels (λ_{max}^{eq}) of post-diauxic cells treated with various concentrations of BAC added 10 minutes before the diS-C_3(3) fluorescent probe. Means and SDs were calculated from ten independent repeats. The arrow indicates the maximal Tok1p-mediated repolarization (12.6 ± 2.3 mV; corresponding depolarization of the *tok1* mutant was 27.4 ± 1.8 mV). **(B)** Effect of various concentrations of BAC on cytosolic pH (pH_{cyt}) of post-diauxic cells of the pHluorin-expressing strain; effect of CCCP for comparison. Data are representative of five independent repeats. **(C)** Effect of various concentrations of BAC on the release of low molecular-weight intracellular material absorbing light at 260 nm; measured in post-diauxic cells of the parental strain. Means and SDs were calculated from three independent repeats. **(D)** Concentration-dependent permeabilization of cells exposed to BAC in post-diauxic cells of the parental strain, measured by propidium iodide staining. Means and SDs were calculated from three independent repeats, each consisting of three biological replicates.

Fig. 7. Depletion of intracellular ATP by 2-hour incubation with 2-deoxy-D-glucose (2DG) does not affect Tok1p channel opening capacity. Concentration-dependent equilibrium staining levels (λ_{max}^{eq}) of BAC-treated post-diauxic cells incubated with 5 mM 2-deoxy-D-glucose (2DG) for 2 hours to deplete intracellular ATP; effect of 0-hour and 2-hour starvation in absence of 2DG for comparison. Means and SDs were calculated from three independent repeats.

Fig. 8. Mode of action of a stressor influences the Tok1p channel activity in response to depolarization in a concentration-dependent manner. Tok1p channel activity in response to depolarization caused by various concentrations of DM-11, ODDC and BAC expressed in **(A)** $\Delta\lambda_{max}^{eq}$ and **(B)** mV; measured in post-diauxic cells. Means and SDs were calculated from λ_{max}^{eq} from ten independent repeats. The DM-11 dependence is cut short compared to BAC and ODDC due to loss of membrane integrity after exposure to higher DM-11 concentrations. The repolarization efficiency denotes the ratio of Tok1p channel opening and the extent of respective *tok1* mutant depolarization.

Fig. 9. Schematic overview of possible effects following the addition of a stressor.

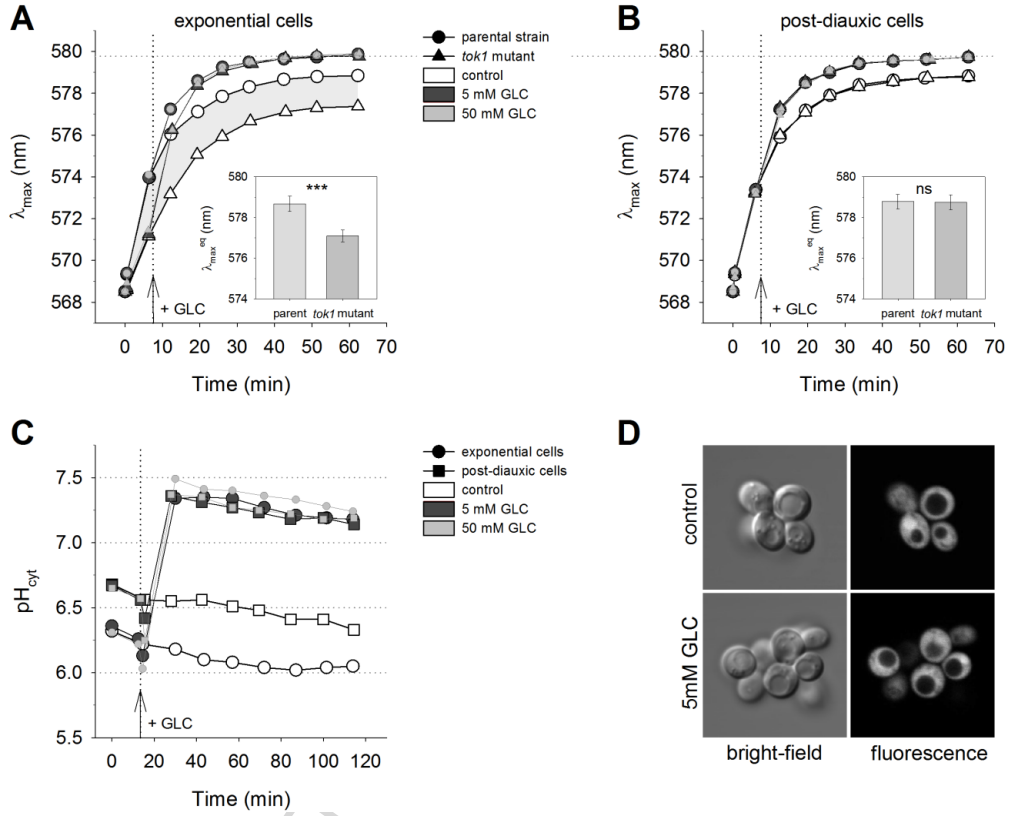

Fig. 1

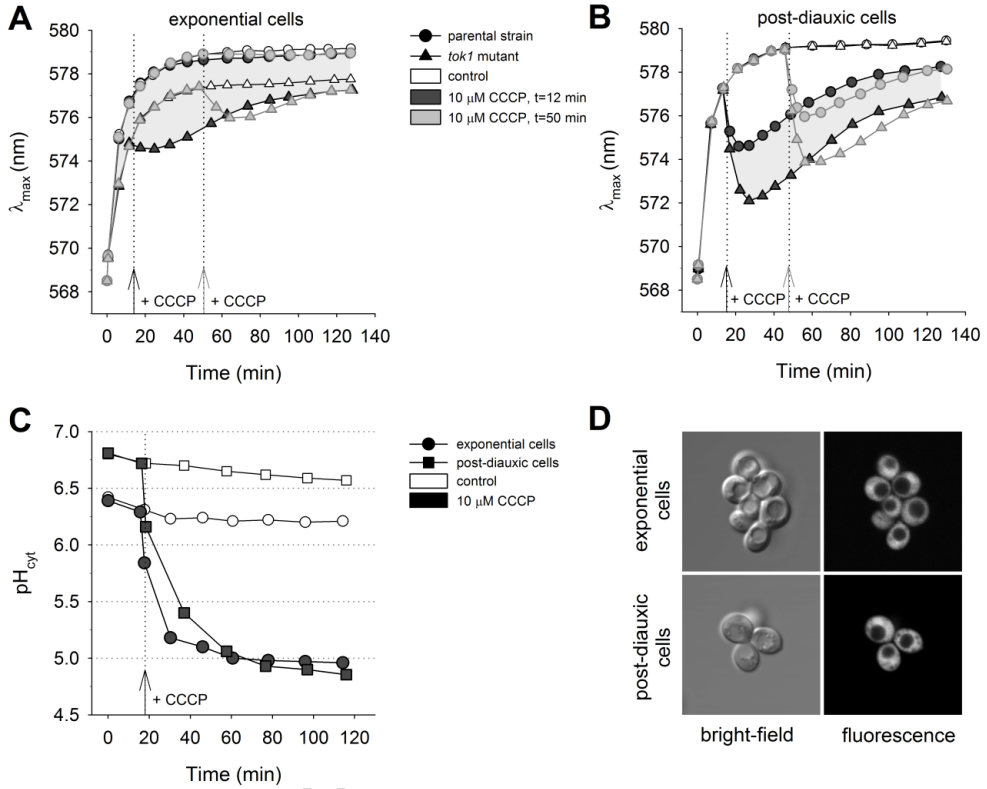

Fig. 2

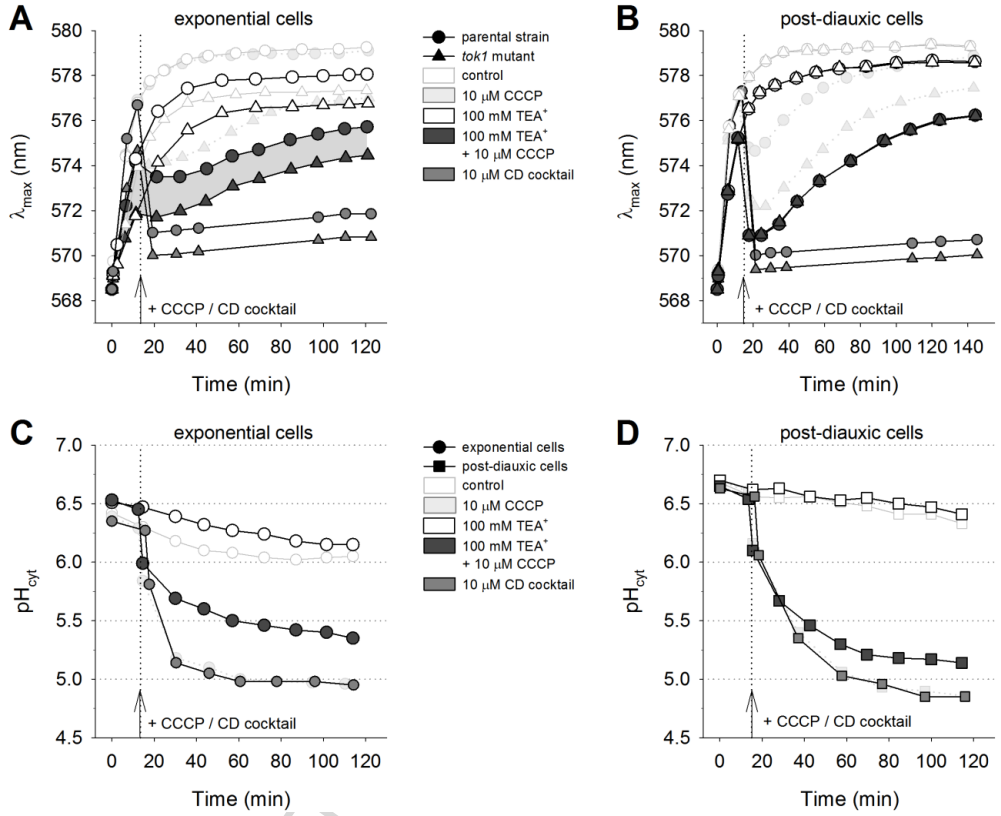

Fig. 3

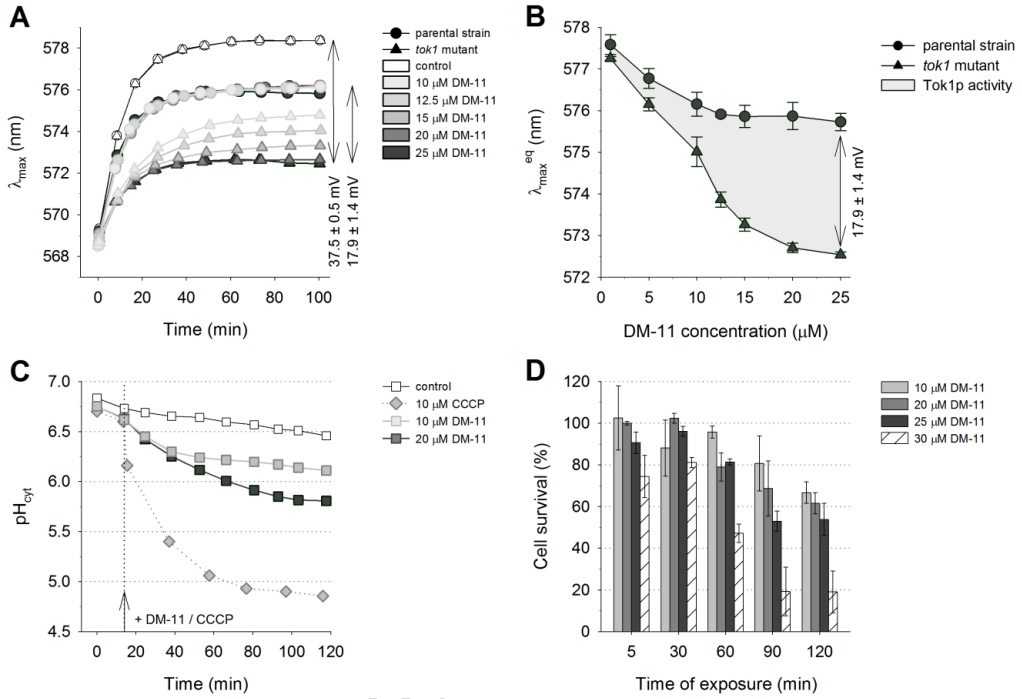

Fig. 4

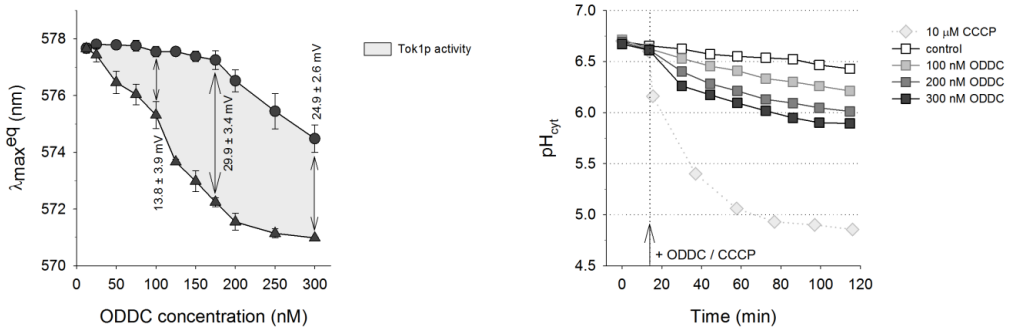

Fig. 5

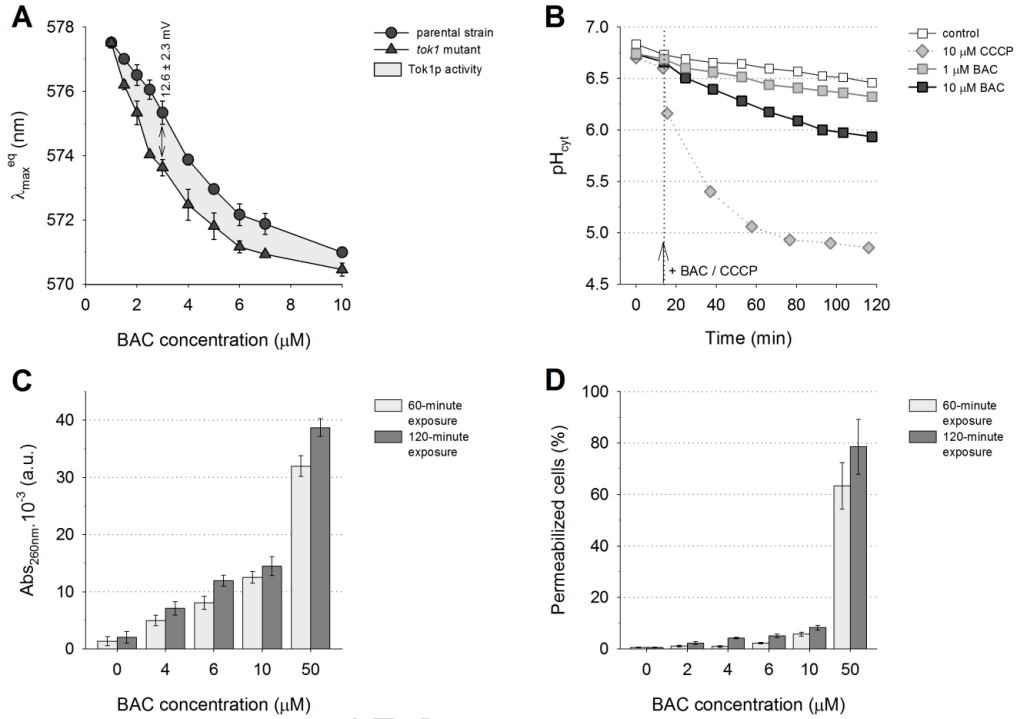

Fig. 6

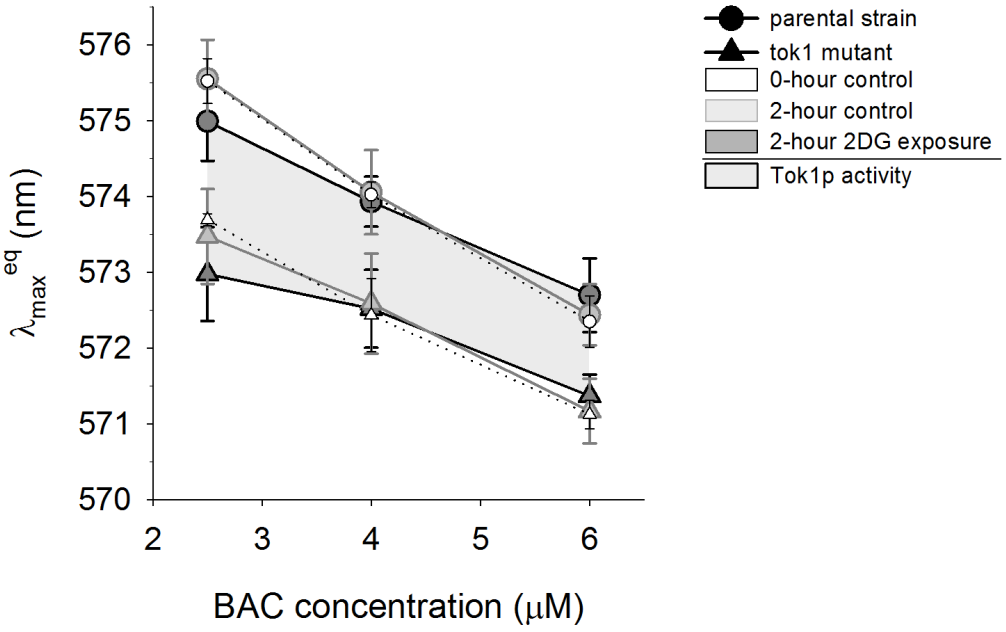

Fig. 7

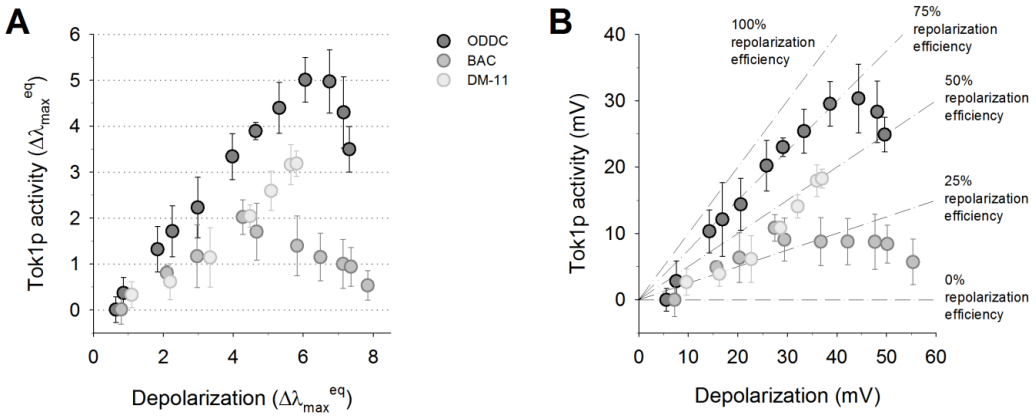

Fig. 8

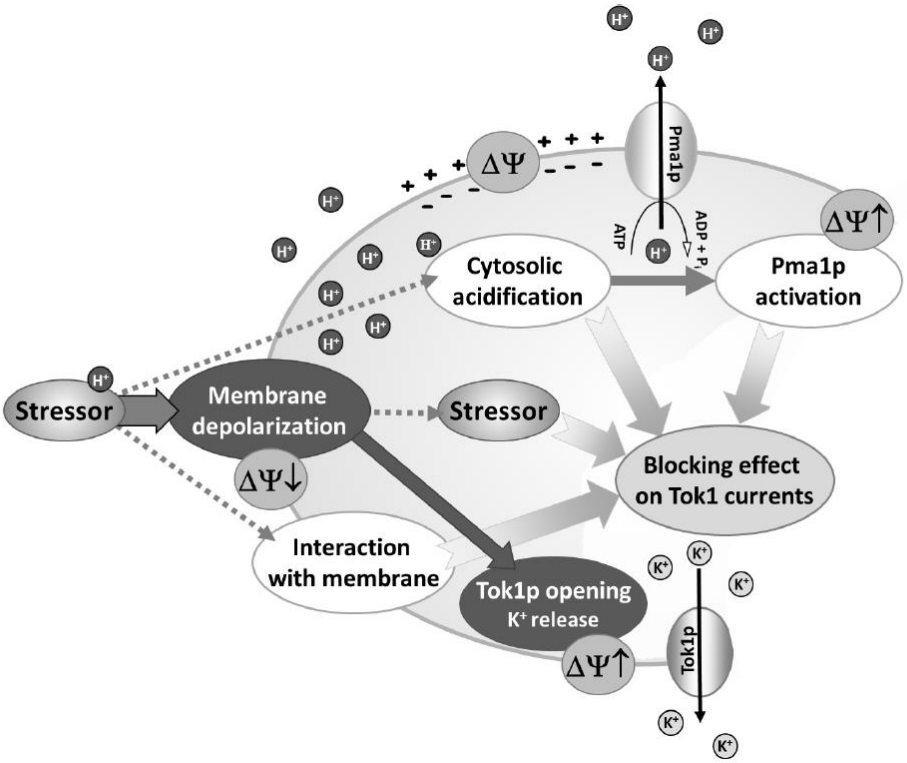

Fig. 9

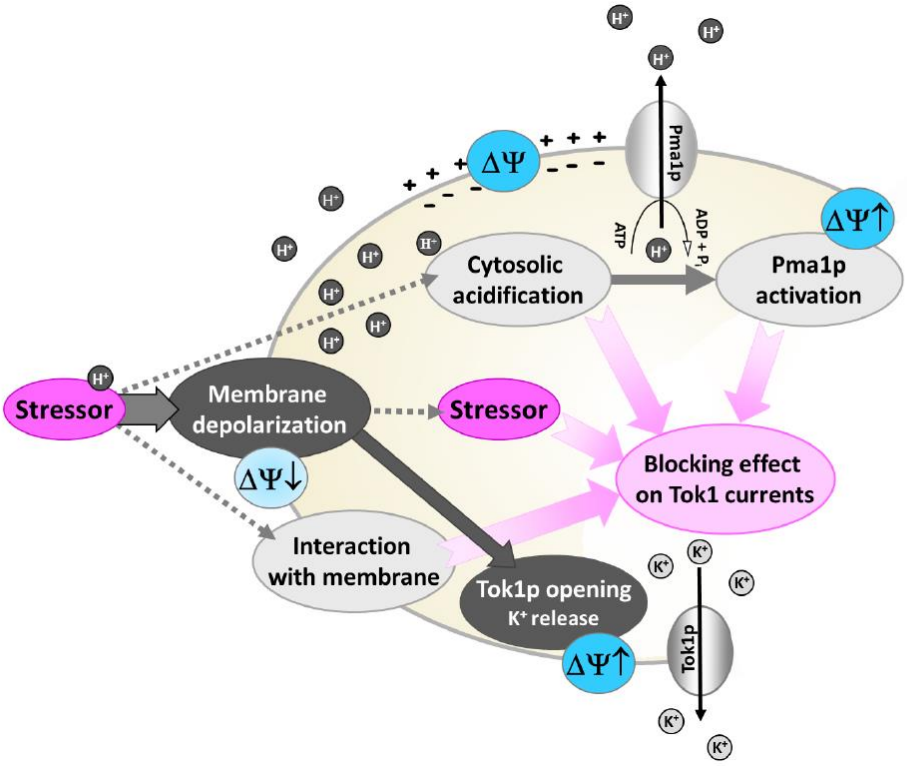

Graphical abstract

Highlights

- Tok1p channel plays an important role in the regulation of membrane potential
- It is able to counterbalance up to 75% of chemically-induced depolarization
- Effects of stressors beside depolarization may affect Tok1p channel activity

Attachment III

P9

Complex regulation of the yeast membrane potential in response to CCCP-induced depolarization and cell acidification

Jakub Zahumensky[1], Andrea Drietomská[1], Karel Sigler[2], Otakar Hlaváek[2], Jaromír Plášek[1], and Dana Gášková[1]

[1]Charles University, Faculty of Mathematics and Physics, Institute of Physics, Ke Karlovu 5, 121 16 Prague 2, Czech Republic

[2]Institute of Microbiology, CR Academy of Sciences, Videňská 1083, 142 20 Prague 4, Czech Republic

E-mail: jakub.zahumensky@gmail.com

Under non-stress conditions, the maintenance of yeast membrane potential is a highly regulated process. In Saccharomyces cerevisiae, the membrane potential is controlled mainly by the regulation of cation fluxes (H^+, K^+). Besides Pma1 H^+-ATPase, which actively extrudes protons from cells, several types of active and passive transporters mediating the K^+ influx and efflux, respectively, are believed to contribute to the maintenance of membrane potential. Under stress conditions, such as the presence of harmful agents, cells try to eliminate changes caused by the stressor via membrane proteins transporting (cat)ions, i.e. the transporters are activated to counteract the induced changes. Depending on the concentration, stressor-induced changes can overwhelm cellular homeostasis and lead to cell death. Fluorescent dye diS-C3(3) that responds to the plasma membrane potential can easily be used to monitor real time changes in the magnitude of the membrane potential of yeast cells. In preceding SMYTEs we showed that the addition of protonophore CCCP to exponential Pdr5p- and Snq2p-deficient cells AD1-3, in which the probe accumulates solely according to membrane potential, does not lead to any expected decrease in membrane potential, but triggers immediate concentration-dependent hyperpolarization. The increase in membrane potential caused by CCCP-induced activation of the H^+ATPase has been proposed as the most likely explanation. In this work, we concentrated on elucidating (1) how the "profile" of membrane hyperpolarization in response to CCCP-induced proton fluxes depends on the growth stage of the cells, and (2) whether the activation of the H^+ATPase is the only factor that is involved in the re-building of membrane potential in the presence of depolarizing agent CCCP.

This work was supported by Czech Science Foundation (grant no. 205/10/1121), Grant Agency of Charles University in Prague (grant no. 456213) and by Institutional Research Concept RVO61388971.

Attachment IV

S6/O26

Alcohols are inhibitors of *S. cerevisiae* multidrug resistance pumps Pdr5p and Snq2p

Dana Gášková [1], Jaromír Plášek[1], Jakub Zahumenský[1], Ivana Benešová[1], Ľuboslava Buriánková[1] and Karel Sigler[2]

[1]Charles University, Faculty of Mathematics and Physics, Institute of Physics, Ke Karlovu 5, 121 16 Prague 2, Czech Republic
[2]Institute of Microbiology, CR Academy of Sciences, Vídeňská 1083, 142 20 Prague 4, Czech Republic
E-mail: Dana.Gaskova@mff.cuni.cz

The effect of alcohols on cell membrane proteins has originally been assumed to be mediated by their primary action on membrane lipid matrix. Many studies carried out later on both animal and yeast cells have revealed that ethanol and other alcohols inhibit the functions of various membrane channels, receptors and solute transport proteins, and a direct interaction of alcohols with these membrane proteins was proposed. Using our fluorescence diS-C_3(3) diagnostic assay for multidrug-resistance pump inhibitors in a set of isogenic yeast Pdr5p and Snq2p mutants we found that n-alcohols (from ethanol to hexanol) variously affect the activity of both pumps. Beginning with propanol, these alcohols have an inhibitory effect that increases with increasing length of the alcohol acyl chain. While ethanol does not exert any inhibitory effect at any of the concentration used (from 0.1 to 3 %), hexanol exerts a strong inhibition at 0.1 %. The alcohol-induced inhibition of MDR pumps was detected even in cells whose membrane functional and structural integrity was not compromised. This supports a notion that the inhibitory action does not necessarily involve only changes in the lipid matrix of the membrane but may entail a direct interaction of the alcohols with the pump proteins.

This work was supported by Czech Science Foundation (grant no. 205/10/1121) and by Institutional Research Concept RVO61388971.

Attachment V

O20

In vivo monitoring of membrane potential changes in yeast under CCCP-induced stress: the respective roles of Tok1p and H^+-ATPase

Jakub Zahumenský[1], Andrea Drietomská[1], Andrea Švenkrtová[2,3], Otakar Hlaváček[2], Jaromír Plášek[1], Karel Sigler[2] and Dana Gášková[1]
[1]*Charles University, Faculty of Mathematics and Physics/Institute of Physics, Prague, Czech Republic;* [2]*Institute of Microbiology, CR Academy of Sciences, Prague, Czech Republic;* [3]*Faculty of Food and Biochemical Technology, Institute of Chemical Technology, Prague, Czech Republic*

Using the potentiometric fluorescent probe 3,3'-dipropylthiacarboxycyanine, diS-C3(3), we studied the regulation of *Saccharomyces cerevisiae* plasma membrane potential ($\Delta\Psi$) in the cells of AD1-3 strain deficient for multidrug resistance pumps (Pdr5p, Snq2p, Yor1p) and its isogenic mutant AD1-3--tok1, also lacking the Tok1p potassium channel. We followed the effects of the uncoupler CCCP mediating proton influx into the cytosol, H^+-ATPase inhibitor DM-11 and Tok1p inhibitor TEA^+. Here we show how Tok1p opening and H^+-ATPase activation work in synergy to restore $\Delta\Psi$ under CCCP-induced stress. Our results also reveal that the complex regulation of $\Delta\Psi$ in *S. cerevisiae* under CCCP-induced stress varies with the cell age, with the main alteration in relative contributions of Tok1p and H^+-ATPase being observed in relation to the diauxic transformation.

Attachment VI

SMYTE 33

OP31. Comparison of Tok1p and Pma1p roles in membrane potential maintenance of fermenting and respiring *S. cerevisiae* cells challenged with chemically induced acidification and depolarization

Jakub Zahumenský[1], Andrea Drietomská[1], Andrea Švenkrtová[2,3], Otakar Hlaváček[2], Tomáš Hendrych[4], Jaromír Plášek[1], Karel Sigler[2], Dana Gášková[1]

[1] Faculty of Mathematics and Physics, Institute of Physics, Charles University, Prague, Czech Republic; [2] Institute of Microbiology, CR Academy of Sciences, Prague, Czech Republic; [3] Faculty of Food and Biochemical Technology, Institute of Chemical Technology, Prague, Czech Republic; [4] Department of Genetics and Microbiology, Charles University, Faculty of Science, Prague, Czech Republic.

Yeast cells have an amazing capacity to counteract the effect of stress conditions by activating various proteins. Exposure of the cells to chemical stress mediated by ionophores tends to dissipate vital ion gradients across the plasma membrane triggering a rapid cellular response. Among the fastest responses to such conditions is opening of ion channels, such as Tok1p K^+ channel, followed closely by activation of ATP-dependent transporters of ionic species, such as Pma1p H^+-ATPase. These processes lead to partial or complete restoration of the lost electrical imbalance. The plasma membrane Tok1p channel is the major exporter of K^+ ions out of the *S. cerevisiae* cytosol. Previous studies have provided useful insights into its specificity, directionality and the dependence of its opening probability on both plasma membrane potential (DY) and intracellular pH, being almost fully inhibited by pH_{in} values lower than 5.5. Intracellular acidification also activates Pma1p H^+-ATPase, the main proton exporter of the yeast plasma membrane, which is known to be responsible for the build-up and maintenance of DY. The significance of the action of these proteins under various conditions has been studied *in vivo* by measurements of DY changes in the AD1-3 and AD1-3–*tok1 S. cerevisiae* mutant cells using the potentiometric fluorescent probe diS-C_3(3), supported by measurements of pH_{in} by the use of a AD1-3 mutant expressing pHluorin. We have found that the most important change in the activity and relative contribution of Tok1p and Pma1p to DY maintenance is related to the diauxic shift of the growing yeast culture. In this study, we therefore compare yeast growing under fermentative and oxidative conditions, challenged with nutritional (lack of glucose) and chemical stress, leading to cellular acidification and/or membrane depolarization.

This work was supported by the Grant Agency of Charles University in Prague (grant no. 456213) and by Institutional Research Concept RVO61388971.

Attachment VII

Tok1p channel plays an important role in membrane potential maintenance under chemical stress

Zahumenský Jakub[1], **Jančíková Iva**[1], **Švenkrtová Andrea**[2], **Gášková Dana**[1]

[1]Charles University, Faculty of Mathematics and Physics, Institute of Physics, Prague, Czech Republic
[2]Institute of Chemical Technology, Faculty of Food and Biochemical Technology, Prague, Czech Republic
Correspondence: jakub.zahumensky@gmail.com

Tok1p is a highly specific plasma membrane potassium channel with strong outward directionality. Its opening and K+ release is induced by membrane depolarization. Although the biophysical properties of the channel are well-described, its potentially important physiological role in vivo is currently largely unexplored. While in electrophysiological experiments the value of the desired plasma membrane potential ($\Delta\Psi$) can be set directly, it is not as straightforward in cell suspensions, either in natural niches or in the laboratory. Instead, the externally-induced changes of the plasma membrane potential are the result of the cell's interaction with various chemical species, above all those that affect the permeability of the plasma membrane. We were therefore interested in bringing insight into how the Tok1p channel responds to changes in plasma membrane potential brought about by chemical stressors with various modes of action, e.g. transport of ions according their electrochemical gradients or interaction with either plasma membrane or with the channel itself. Using the diS-C3(3) fluorescence assay and a tok1 deletion mutant we report that the activity of the Tok1p channel, and therefore its capacity to restore membrane potential, is indeed strongly dependent not only on the extent of depolarization, but also on the particular chemical stressor used. While some compounds may lead to partial inhibition of the channel, either by direct interaction, by affecting the lipid environment of the channel or by cytosolic acidification, other exhibit no significant negative influence. In such cases the Tok1p channel is able to counterbalance up to 75 % of the membrane potential lost due to the action of the compound. Our study is not only the first to show the physiological role of the Tok1p channel in membrane potential maintenance under chemical stress, but also the first to report the estimate of the extent of depolarization the channel is able to counterbalance.